MET and Epithelial to Mesenchymal Transition as novel targets in Small Cell Lung Cancer

Israel Cañadas Castillo

PhD THESIS UPF/2013

Thesis directors

Dr. Joan Albanell and Dr. Edurne Arriola

Molecular Therapeutics and Biomarkers in Cancer

Cancer Research Program

Hospital del Mar Medical Research Institute (IMIM)

A mis padres

If I have seen further than others, it is
by standing upon the shoulders of giants

Isaac Newton

ACKNOWLEDGEMENTS

Recuerdo como si fuera ayer la primera vez que tuve un microscopio en mis manos. Fue un regalo de Navidad de cuando era niño. Y aunque era un juguete más, para mí fue mucho más que eso. En ese momento empezaba mi interés por todo lo relacionado con la biología, la ciencia y los experimentos. Ahora puedo decir que aquel microscopio de juguete se ha convertido en una realidad gracias a esta tesis doctoral.

Ha sido un largo e intenso camino lleno de experiencias, aprendizaje e ilusión y ahora ha llegado el momento de dar las gracias. Creo que uno de los momentos más importantes, ya que sin todos/as vosotros/as esto no hubiera sido posible.

Primero de todo, me gustaría dar las gracias a mis directores de tesis: a Joan Albanell, por haberme dado la posibilidad de empezar haciendo prácticas en su grupo cuando sólo era un recién licenciado en Biología, sin prácticamente experiencia, y después formar parte de su equipo y poder hacer el doctorado. Gracias por tu confianza, tus consejos y correcciones y por inculcarnos la visión "traslacional" de la investigación, un punto que considero clave en mi formación. Y a Edurne Arriola, por ser mi directora de tesis, mi jefa y una compañera más. Me considero muy afortunado de haberme cruzado en tu camino. Para mi gran parte del mérito de esta tesis también es tuyo. Gracias por confiar en mí y haberme apoyado y animado siempre. Y por supervisarme en el día a día, por todos tus consejos y por enseñarme tantísimas cosas. Gracias por preocuparte por mí y tener ese tipo de detalles tan importantes en muchos momentos. ¡Y porque he disfrutado y me lo he pasado genial durante todo este tiempo trabajando juntos! Considero que eres una gran oncóloga, una gran científica, pero sobre todo una gran persona. Muchas gracias por todo, de verdad. También me gustaría agradecer a Ana Rovira, alguien muy importante en todo este recorrido desde el primer día en que llegué al IMIM. Para mí, mi tercera directora de tesis. Muchas gracias por haber apostado por mí desde el principio, por tu apoyo en todo momento y por acompañarnos a los "URTEC" en el día a día. Gracias por animarme siempre y por haberme ayudado y aconsejado con el diseño, realización e interpretación de prácticamente todos

los experimentos de esta tesis. Por otro lado, también agradecer a Fredi Rojo, alguien indispensable en todo este proyecto y en mi formación. Gracias por toda tu ayuda con las inmunos, el análisis de imagen y los análisis estadísticos. Y por encontrar siempre tiempo para nuestro proyecto y estar siempre dispuesto a ayudarme. Y también agradecer a Montse Arumí, por sus aportaciones en todo lo referente a anatomía patológica y sobre todo con las inmunohistoquímicas.

En especial, me gustaría agradecer a mis compañeros de lab, con los que he compartido muchísimos momentos durante estos años y han sido indispensables para la realización de esta tesis. ¡Ha sido un auténtico placer trabajar con vosotros! A Alba, por tu interés desde el principio en este proyecto, tu motivación muchas veces tan necesaria en este "mundillo" y porque me he lo he pasado muy bien contigo. A Oriol, por ser un gran compañero, aportar equilibrio y tranquilidad en el laboratorio y haber sido mi maestro con los in vivo. Y por todos esos coffees y conversaciones compartidas. Gràcies soci! A Jetzi, por ser tan maja y simpática, preocuparte por este proyecto y porque me he reído mucho contigo. A Irene, por haberme enseñado mejor que nadie como se trabaja en un laboratorio y por todos esos momentos tan divertidos que nos has regalado a todos. A Sílvia Menéndez, por ser tan eficaz y por haber hecho prácticamente todas las inmunos de esta tesis, ¡en el fondo has disfrutado! Jeje. Y por tu paciencia con las muestras de los ratoncitos cada vez que acabábamos un in vivo. A los nuevos fichajes, Anna y Ali, por haberos adaptado desde el principio al grupo y por vuestros consejos e interés por mi tesis. Y a Sílvia Geeraerd, por estar siempre dispuesta a ayudarme con cualquier tema, por tu eficiencia y por tu generosidad. También me gustaría dar las gracias a Cristina Oliva, por toda su ayuda en el laboratorio cuando casi no sabía ni lo que era un western. Y a las oncólogas que nos acompañaron en el lab durante una temporada, Cris Suárez y Laura Lema, porque me lo pasé realmente bien con vosotras y por ser tan divertidas. Agradecer también a los estudiantes que han pasado por nuestro grupo: Anna, Isart y Sandra, por la ilusión y el interés por lo que hacemos aquí.

Dentro de nuestro grupo, también quiero dar las gracias a los oncólogos: a Clara Montagut, por sus sugerencias y aportaciones que han hecho mejorar nuestro proyecto y esta tesis; a Álvaro Taus, por tener tan bien organizado el seguimiento clínico de todos los pacientes de nuestro proyecto y por hacer la tabla de Excel más grande y compleja jamás vista; y a Joaquim Bellmunt, por haber aceptado ser tutor de esta tesis. También quiero agradecer a los data managers del grupo, en especial a Xavi Villanueva, por su humor y amabilidad. ¡Qué hubiera hecho sin el vampiro del Hospital del Mar!. Y también a todas sus compañeras: Marta, Andrea, Gemma, Susana, Clara y Roser.

Por otro lado, me gustaría dar las gracias al Servicio de Anatomía Patológica del Hospital del Mar. En especial a Marta Salido, por su implicación casi desde el inicio en nuestro proyecto, por haberme ayudado y enseñado mejor que nadie el FISH y los cariotipos, y por su simpatía y amabilidad cada vez que he ido a pedirle algo. Y a Ana Belén y María, por ayudarme y enseñarme a hacer la técnica del FISH. Quiero agradecer también a Lara Pijuan, por estar siempre dispuesta a ayudar y ser tan eficiente, y a Bea Bellosillo, por su implicación y ayuda en este proyecto y explicarnos en los lab meetings los nuevos avances en el mundo de la genómica. Como no también agradecer a Silvia Pairet, por toda su ayuda cada vez que la he necesitado, sobre todo con lo referente al mundo de las extracciones de DNA, RNA, y PCRs.

Una aportación muy importante para esta tesis y para mi formación ha sido la de Antonio García de Herreros. Gracias por tu interés, por todas tus sugerencias y por habernos ayudado tan estrechamente con el desarrollo de todo el proyecto. Y por supuesto agradecer a todo su grupo, y especialmente a Raúl Peña, por ser tan amable conmigo y haberme resuelto infinidad de dudas; a Rosa Viñas, por estar siempre dispuesta a ayudarme con cualquier cosa, por tu paciencia y por esa vitalidad que desprendes y que tanto se agradece; y a Jelena, por resolverme dudas cada vez que la he necesitado. Dar las gracias también a Esther Barreiro y todos los miembros de su grupo, en especial a Siscu, Carme, Clara y Esther, por su ayuda sobre todo con los ELISAs.

También me gustaría agradecer a todos aquellos compañeros del IMIM externos a mi grupo que han compartido conmigo muchísimos momentos durante estos años y que no han tenido desperdicio. A Xavi, por todas esas conversaciones de todo tipo, desde ciencia a política, pasando por deportes (nuestro querido Barça) y, por supuesto, nuestra razón de ser, las series. También me acuerdo de tus nuevos compis, Sergi y Judith, gracias por todas esas risas que he compartido con vosotros estos últimos meses. Por supuesto también quiero dar las gracias a Rita y Teresa, por vuestra simpatía y vitalidad. Y como no, a Marc, mi primer maestro en esto de la ciencia. Gracias por tu Master Class en cultivo celular aquel "Passa l'estiu al Parc Científic", y por todas las divertidas conversaciones en el bar y durante los coffees estos años ya en el PRBB. Y no me olvido de mi equipo de Volley que, aunque todavía no hayamos conseguido la copa que nos merecemos, no tengo duda que llegará el día en que la levantaremos. Visca els VolleyBlots!

Quiero agradecer también a mis compañeros en el curso de experimentación animal, Sergi, Lorena y Eva, me lo pasé muy bien aquellas semanas con vosotros, y ahora por suerte nos podemos seguir viendo por el IMIM. Y a Neus Martínez, por ser tan maja y simpática, y a Lorena Tomás, por ser tan eficiente y ayudarme desde que empecé con cualquier trámite administrativo. Y por supuesto me acuerdo también de todos aquellos compañeros que ya no siguen por el PRBB, especialmente de Dani, Susana, Guy y Noe, ¡por todas las risas compartidas!

También me gustaría agradecer als Serveis Cientificotècnics de l'IMIM, a Nuria Somoza, Piedad Navarro, Xavier Mayol… Especialmente al Servei de Microarrays. Gracias Lara y Eulàlia por ser tan majas y resolvernos siempre cualquier duda o problema. Y lo más importante, siempre con una sonrisa. Y al Servei de Bioestadística, especialmente a Sergi Mojal, por su paciencia intentando entender mis experimentos antes de cualquier análisis. También agradecer als Serveis Generals de l'IMIM, a Patxi, y al Servicio de limpieza y de compras, por hacernos la vida en el lab más fácil. En especial a Carlos, que aunque seas merengón, ¡eres buen tío! jeje. Y

por supuesto dar las gracias a todo el personal del estabulario del PRBB, y especialmente a Marisol, por cuidar mejor que nadie de nuestros ratoncitos.

Quiero agradecer también a Roger Gomis y Marc Guiu por su colaboración y ayuda con los modelos in vivo de metástasis.

Agradecer también a todos los miembros de mi tribunal de tesis por haber aceptado formar parte.

Fuera del PRBB y de este mundillo científico son muchas las personas que me han acompañado durante estos años y que también se merecen un GRACIAS en mayúsculas.

Primero de todo, a los grandes, a los de toda la vida: mis amigos. A mi amiguísimo Anton, por regalar siempre tu sonrisa y por hacer que esta vida sea "cósmica", no cambies nunca; a Alexis, porque sé que siempre podré contar contigo y eres un amigo de verdad; a Albertini, por ser mi amigo desde que tengo uso de razón; y a Jose, por nuestras innumerables e interesantes conversaciones sobre cualquier tema y por interesarte siempre por lo que hago. Y a Andrea, Esther, Sandra y Lluís, por haberos interesado siempre por mí y por esta tesis. También quiero agradecer a Adri, mi compañero inseparable de la uni, con el que he compartido estudios, aficiones, gustos y fiestas, por tu interés por todo lo que hago y por ser un gran amigo. Por supuesto agradecer a todos mis amigos de Sant Joan Despí, y especialmente a Cris, mi "helmana", por entenderme siempre tan bien y por tener tantas cosas en común conmigo (normal, somos "helmanos"). Y, como no, a Lidia, Mònica, Nacho, Esther, Manu, Sonia, Dani, Miriam y Javi. ¡Sois geniales!

También me gustaría agradecer a todos los profes que he tenido a lo largo de mi vida académica: a los del cole Nuestra Señora del Mar, del Instituto Salvador Dalí, y de la facultad de Biología de la UB.

Dicho esto, ahora me gustaría dar las gracias a toda mi familia por todo el interés, cariño y apoyo recibido durante todos estos años. Primero de todo a mi abuelo y abuela y yayo y yaya, que sé que estarían orgullosos de mi. Y a todos mis tíos, tías, primos y primas (que no son pocos…jeje.). Especialmente me gustaría dar las gracias a mis

primos Poti y Ester, porque además de mi familia sois mis mejores amigos. Hemos vivido tantos momentos juntos que, sin saberlo, sois una parte esencial de mí y, por lo tanto, de esta tesis. También a mi primo Joan por preocuparse siempre por mí, y a mi prima Alba por hacerme reír. Y por supuesto, a mi primo y compañero de gremio, Sergi, por todos sus consejos durante este tiempo y ayudarme con la portada de este librito.

También agradecer a Manolo, Paqui y Laura por hacerme sentir como uno más de la familia, cuidarme y preocuparse siempre por mí. ¡Sois únicos!

Y ahora me gustaría dar las gracias a mi hermano Mario, por tu humor tan necesario en muchos momentos, tu vitalidad constante y hacer que la vida pueda ser maravillosa. Y no me olvido de tu inseparable Neo, ¡la mejor mascota que se pueda tener! Y por supuesto, a los auténticos responsables de todo esto: mis padres. Muchas gracias por vuestro cariño y apoyo incondicional, sin vosotros nada de todo esto hubiera sido posible y nunca hubiera llegado hasta aquí. Gracias por vuestros consejos y por todas las cosas que me habéis enseñado, no tienen precio. Os lo debo prácticamente todo. Para mí, esta tesis es tan vuestra como mía.

Y por último, quiero agradecer a la persona que me ha acompañado y ha estado a mi lado durante toda esta aventura, desde el principio. Muchas gracias Noe, por hacer que todo haya sido más fácil, por entenderme en todo momento y por tu gran apoyo en el día a día. Gracias por tu paciencia y tus ánimos y por ayudarme la primera y cada una de las veces que he tenido que hacer presentaciones en inglés. Esta tesis también es tuya. Gracias por hacerme reír como tú sólo sabes y por darme luz cada mañana.

This work has been financed by the following research projects:

- PS09/1285 from Instituto de Salud Carlos III (ISCIII)-Fondo de Investigación Sanitaria, Spanish Health Ministry.
- PS09/01594 from ISCIII-Fondo de Investigación Sanitaria, Spanish Health Ministry.
- PS09/01296 from ISCIII-Fondo de Investigación Sanitaria, Spanish Health Ministry.
- RD06/0020/0109 from "Red Temática de Investigación Cooperativa en Cáncer" (RTICC), ISCIII/FEDER.
- 2009 SGR 321, from Agència de Gestió Ajuts Universitaris de Recerca, Generalitat de Catalunya.

For the publication (printing) of this PhD Thesis this work has received funding from IMIM (Institut Hospital del Mar d'Investigacions Mèdiques).

We thank Fundació Cellex (Barcelona) for a generous donation to the Hospital del Mar Medical Oncology Service. We are also grateful to Pfizer Inc. for generously providing PHA-665752 and PF-2341066. We also thank the Tumour Bank of the Pathology Department of Hospital del Mar and the Xarxa de Bancs de Tumors de Catalunya for providing tissue samples (Biobank grants from ISCIII FEDER (RD09/0076/00036; RD09/0076/0101)).

And finally, we thank all the patients participating in the study for their cooperation.

ABSTRACT

Small cell lung carcinoma (SCLC) is a highly lethal disease due to its chemorefractory nature after first line treatment. The mechanisms to overcome this resistance have remained elusive to tackle up to date. MET is a transmembrane tyrosine kinase receptor and its activation is associated with increased motility, migration and invasion in cancer cells. MET is activated in several tumour types and has been linked to patient prognosis. MET activation by its natural ligand Hepatocyte Growth Factor (HGF) has been involved in Epithelial to Mesenchymal Transition (EMT), a process by which cells decrease adhesion, lose polarity, acquire the ability to migrate and invade surrounding tissue. EMT is also associated with resistance to anticancer agents. We hypothesized that HGF-induced EMT would explain resistance to chemotherapy in SCLC and that MET inhibitors could revert this phenomenon.

In our work we demonstrated that HGF-induced MET activation in SCLC cells resulted in a more aggressive phenotype. In human SCLC we demonstrated in two independent series that MET phosphorylation was associated with poor prognosis. In preclinical models we observed that MET activation by HGF induced EMT that resulted in chemoresistance *in vitro* and *in vivo*. MET inhibition was able to block or reverse this process and resensitized cells to chemotherapy. Mesenchymal markers in human SCLC specimens were associated with MET activation, predicted a worse survival and were upregulated in chemorefractory disease. Finally, increased HGF serum levels in SCLC patients correlated with higher risk of death. These results suggest that the use of MET inhibitors in combination with chemotherapy as a therapeutic approach in the MET-activated subpopulation of SCLC merits further investigation.

RESUMEN

El Cáncer de Pulmón de Célula Pequeña (CPCP) es una enfermedad altamente letal debido a su naturaleza quimiorefractaria después del tratamiento de primera línea. Los mecanismos para derrotar estar quimioresistencia han fracasado hasta la fecha. MET es un receptor de membrana tirosina cinasa y su activación está asociada a una incrementada motilidad, migración e invasión en células tumorales. MET está activado en diversos tipos tumorales y está asociado al pronóstico de los pacientes. La activación de MET mediante su ligando natural "Factor de Crecimiento Hepatocitario" (HGF) ha estado involucrado en la Transición Epitelio-Mesenquimal (EMT), un proceso mediante el cual las células disminuyen su adhesión, pierden la polaridad, adquieren la habilidad de migrar e invaden los tejidos adyacentes. La EMT está también asociada a la resistencia a agentes antitumorales. Nuestra hipótesis es que la EMT inducida por HGF explicaría la resistencia a la quimioterapia en el CPCP y que los inhibidores de MET podrían revertir este fenómeno.

En nuestro trabajo demostramos que la activación de MET inducida por HGF en líneas celulares de CPCP dio lugar a un fenotipo más agresivo. En dos series independientes de CPCP humano demostramos que la fosforilación de MET estaba asociada a un peor pronóstico. En modelos preclínicos observamos que la activación de MET mediante HGF indujo la EMT, dando lugar a quimioresistencia *in vitro* e *in vivo*. La inhibición de MET fue capaz de bloquear o revertir este proceso, sensibilizando las células tumorales a la quimioterapia. Los marcadores mesenquimales en muestras humanas de CPCP se asociaron a activación de MET, prediciendo una peor supervivencia. Además, la expresión de estos marcadores estaba incrementada en la enfermedad quimiorefractaria.

Estos resultados sugieren que el uso de inhibidores de MET en combinación con quimioterapia como una aproximación terapéutica en la subpoblación de pacientes de CPCP con activación de MET merece una investigación más extensa.

PREFACE

The work presented in this PhD thesis has been conducted in the Molecular Therapeutics and Biomarkers in Cancer laboratory from the IMIM Cancer Research Program. The group, led by Dr. Joan Albanell, is divided in two different areas: the preclinical laboratory, coordinated by Dr. Ana Rovira, and the Biomarker research laboratory, coordinated by Dr. Federico Rojo. Both laboratories together comprise a multidisciplinary team composed by oncologists, pathologists and biologists and joint the knowledge of the different disciplines to work in traslational projects with clinical relevant interest.

Along the years as a predoctoral student in this group, since 2007, I have been working in a FIS project leaded by Dr. Edurne Arriola. The results presented in this PhD thesis are derived from this project and have been published in different scientific journals. The work was done in close collaboration with the Oncology and Pathology departments of Hospital del Mar and we have also counted on the valuable collaboration of Dr. Antonio García de Herreros, from IMIM Cancer Researh Program.

The work of this PhD Thesis has been based on the study of the SCLC biology to find novel therapeutic strategies to improve patient outcome. SCLC is a highly lethal disease due to its chemorefractory nature and the mechanisms to overcome this resistance are unknown. We have worked to thoroughly characterize the role of HGF/MET pathway in SCLC chemoresistance and progression. As a result of this study a novel therapeutic strategy in SCLC has been proposed.

The translational model of our group has been essential for this PhD thesis because we have answered, by preclinical tools, questions derived from the clinical practice, with the aim of improving personalized cancer medicine.

INDEX

ABBREVIATIONS AND ACRONYMS

%: Percentage

aCGH: Comparative Genomic Hybridization Array

ADAM: A Disintegrin And Metalloproteinase

ALK: Anaplastic Lymphoma Kinase

ATP: Adenosine Triphosphate

BCL-2: B-Cell Lymphoma-2

bHLH: Basic Helix-Loop-Helix

BMP: Bone Morphogenic Protein

CBL: Casitas B-Lineage Lymphoma

CD-31: Platelet/Endothelial cell adhesion molecule 1

CDC42: Cell Division Cycle 42

CDDP: Cisplatin

ECM: Extracellular Matrix

EGF: Epidermal Growth Factor

EGFR: Epidermal Growth Factor Receptor

ELISA: Enzyme-Linked ImmunoSorbent Assay

EML4: Echinoderm Microtubule Associated Protein Like 4

EMT: Epithelial to Mesenchymal Transition

ERK1/2: Extracellular Regulated Kinase

ED: Extensive-Disease

FAK: Focal Adhesion Kinase

FAS: TNF receptor superfamily, member 6

FFPE: Formalin-Fixed, Paraffin-Embedded

FGF: Fibroblast Growth Factor

FGFR: Fibroblast Growth Factor Receptor

FISH: Fluorescence In Situ Hybridization assay

GAB1: GRB2-Associated Binding protein 1

GPCR: G-Protein Coupled Receptor

GRB2: Growth Factor Receptor-Bound Protein 2

H&E: Hematoxylin & Eosin

HER2: Human Epidermal Growth Factor Receptor 2

HGF: Hepatocyte Growth Factor

HIF: Hypoxia Inducible Factor

HNSCC: Head and Neck Squamous Cell Carcinoma

IF: Immunofluorescence

IGF: Insulin Growth Factor

IGFR: Insulin Growth Factor Receptor

IHC: Immunohistochemistry

IPT: Integrin-Plexin-Transcription factor

JNK: Mitogen-activated protein kinase 8

LC: Lung cancer

LD: Limited-Disease

MAPK: Mitogen Activated Protein Kinase

miRNA: microRNA

MMP: Matrix Metalloproteinase

mRNA: Messenger Ribonucleic Acid

MYC: Myelocytomatosis viral oncogene homolog

NCAM: Neural Cell Adhesion Molecule CD56

NF-kB: Nuclear Factor Kappa Light polypeptide gene enhancer in B-cells

NSCLC: Non-Small Cell Lung Cancer

OS: Overall Survival

PCR: Polymerase Chain Reaction

PDGF: Platelet-Derived Growth Factor

PDGFR: Platelet-Derived Growth Factor Receptor

PI3K: Phosphatidylinositol 3-Kinase

PKC: Protein Kinase C

PLC: Phopholipase C

PS: Performance Status

PSI: Plexin-Semaphorin-Integrin

PTEN: Phosphatase and Tensin homolog

qRT-PCR: Quantitative Reverse Transcription real-time PCR

ROC: Receiver Operator Curve

RON: Macrophage stimulating 1 receptor

ROS: Reactive Oxygen Species

RTK: Tyrosine Kinase Receptor

SCLC: Small Cell Lung Cancer

Ser: Serine

SF: Scatter Factor

SHC: SRC Homology 2 domain Containing

SHIP1: Inositol Polyphosphate-5-phosphatase

SHP2: Protein tyrosine phosphatase, non-receptor type 11

SOS1: Son Of Sevenless homolog 1

SPARC: Secreted protein, acidic, cystein-rich (osteonectin)

SPH: Serine Proteinase Homology

SRC: Sarcoma (Schmidt-Ruppin A-2) viral oncogene homolog

STAT: Signal Transducer and Activator of Transcription

TEK: Endothelial-specific receptor tyrosine kinase

TGFβ: Transforming Growth Factor β

Thr: Threonine

TNF-α: Tumour Necrosis Factor α

TNM: Tumour Node Metastasis

TP53: Tumour protein p53

TPR: Translocated Promoter Region

TSG: Tumour Suppressor Gene

Tyr: Tyrosine

VEGF: Vascular Endothelial Growth Factor

VEGFR: Vascular Endothelial Growth Factor Receptor

VP-16: Etoposide

WB: Western Blot

WNT: Wingless-type MMTV integration site family, member 1

WT: Wild-Type

ZEB: Zinc Finger E-Box binding homeobox

INTRODUCTION

I.1. SMALL CELL LUNG CANCER

I.1.1. The paradigm of SCLC

Lung cancer (LC) is the most common cause of cancer-related deaths and the second most common type of cancer for both genders[1]. Small Cell Lung Cancer (SCLC) represents approximately 15% of all lung carcinomas and this histological subtype of lung cancer is strongly associated with tobacco smoking. The incidence of SCLC has decreased slightly in recent years, probably related to the decrease of the number of smokers and to changes in the characteristics of cigarettes[2,3]. This refers to the use of filtered cigarettes that leads to the decrease in the size of aerosols, since filters appear to be less effective in the elimination of smaller particles. Whereas long-term smokers of cigarettes with high nicotine and no filter have the highest deposition of particles in the bifurcation zone of the tracheobronchial tree, and were more prone to present histologies derived from these locations such as SCLC and squamous cell carcinomas, the deeper inhalation of smaller particles with filtered cigarettes the distal distribution of particles typical of adenocarcinomas (the most frequent histology currently).

The behaviour of SCLC is also unique within solid tumours and clearly distinct from NSCLC. It is characterized by its aggressive clinical course, with rapid growth and early dissemination. The uniqueness of this tumour consists of an initial exquisite response to chemotherapy or radiotherapy. However, at relapse, which occurs early in the majority of cases, the tumour is resistant to all available therapy and will eventually cause a premature death of the patient. These results in an overall 5-year survival of approximately 5% for the whole population of patients

diagnosed with SCLC. This dismal prognosis has not significantly changed in past years[4,5] (**Figure I.1.**).

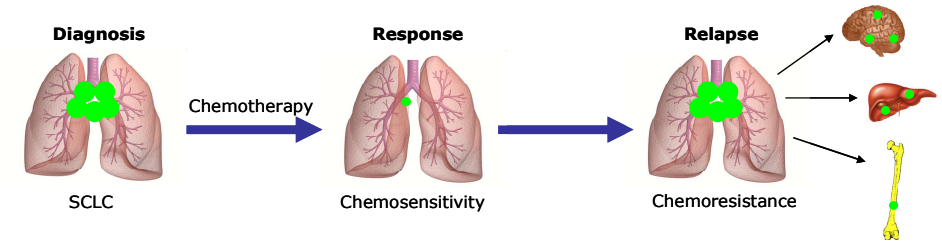

Figure I.1. Natural history of SCLC. Overview of SCLC behaviour upon chemotherapy treatment.

For more than 50 years, SCLC has been staged mainly as either limited-disease (LD-SCLC) or extensive-disease (ED-SCLC). LD-SCLC is characterized by tumours confined to one hemithorax, that could be encompassed in the same radiation portal as the primary tumour. All other patients are classified as ED-SCLC. From the time of diagnosis, the median ranges of survival for LD-SCLC and ED-SCLC are 15-20 months and 8-13 months, respectively. Approximately 10-13% for LD-SCLC and 1-2% of ED-SCLC patients survive 5-year[6,7].

However, since 1982 several authors suggest the importance of TNM (tumour, node, metastasis) staging system in SCLC.

Recently, in small published series of patients with SCLC, the TNM staging system has been shown to be prognostic of outcome. In fact, several studies have confirmed that TNM staging clearly identifies patients with different prognosis and is applicable to the staging of SCLC[8,9].

The extent of disease is the most important tumour-related prognostic factor[7,9,10]. However, in terms of prognosis there are other factors that

predict improved survival. One of the most relevant is initial performance status (PS) greater than or equal to 70 (Karnofsky index). Others include serum lactate dehydrogenase, serum sodium concentration, serum alkaline phosphatase, serum bicarbonate, Haemoglobin level, total White Cell Count (WCC) and neurone-specific enolase [2,6].

I.1.2. Treatment

As previously stated, SCLC is extremely sensitive to chemotherapy and radiotherapy at diagnosis. Overall response rates range from 73% to 93% of patients with LD-SCLC and 50% to 85% of those with ED-SCLC[6,11]. Chemotherapy is the cornerstone of treatment for SCLC. Concurrent chemotherapy and radical thoracic radiotherapy is the current accepted standard treatment for patients with less than stage IV SCLC. Platinum-based chemotherapy (Cisplatin or Carboplatin) in combination with Etoposide is the treatment of choice in fit patients with good organic function. Anthracycline-containing regimens represent a viable alternative for patients where platinum-based chemotherapy is contraindicated[4,6]. Patients who relapsed or progress after first-line chemotherapy have a very poor prognosis. Second-line therapy may produce a modest clinical benefit. Topotecan, a Topoisomerase I inhibitor, is currently the only approved single-agent for second-line therapy and recent data with oral Topotecan show significant anti-tumour activity and symptom palliation in relapsed SCLC[12,13]. A number of other chemotherapeutic agents, including Irinotecan, Paclitaxel and Amrubicin, have shown some activity in small Phase II/III trials when used as monotherapy or in combination with other cytotoxic agents[14-16]. Maintenance chemotherapy has not been shown to convincingly improve outcomes for SCLC[5]. On the other hand,

prophylactic cranial irradiation has been shown to reduce the incidence of brain metastases and prolong survival for responder patients at any stage without negative impact on quality of life and cognitive function[17]. A number of targeted agents have been investigated in SCLC, mostly in unselected populations, with disappointing results.

I.1.3. Genetic alterations in SCLC

In an attempt to better understand the biology of this disease and to find potentially relevant alterations to be targeted by new agents, many studies focusing on genetic alterations of these tumours have been performed. As a result, multiple genetic changes have been implicated in the development of SCLC, but unfortunately, to date, these findings have not been translated into a clinical benefit for patients.

I.1.3.1. Cytogenetic changes and genomic copy number variations

The analysis of karyotypic changes in SCLC has revealed a number of recurrent copy number alterations that are implicated in the development of this tumour[18,19]. These changes are usually numerous and involve regions encompassing genes described as oncogenes and tumour suppressor genes (TSGs)[20,21]. The use of comparative genomic hibridisation (CGH), arrayCGH technology and allelotyping studies have further refined the regions of loss and gain in these tumours and interesting genes have emerged in these studies as potential therapeutic targets[22-26].

Several studies have evaluated fresh SCLC tumour samples in some cases, cell lines in others or both sample types and consistent genetic gains and

loses are found irrespective of the sample type. It is interesting to note that regions containing *TP53* and *RB* genes known to act as TSGs in many tumours are often lost in SCLC[18,21]. Moreover, these alterations are exclusive to cancer cells, when compared to other tumours. Thus, they can be used as tumour specific "markers".

Furthermore, amplification of several members of the *MYC* family is quite common in SCLC, particularly in chemorefractory disease[26,27].

In addition to the genetic alterations present at diagnosis of SCLC, treatment with chemotherapy and radiotherapy may also induce genetic changes, which provide a survival advantage for subclones of the tumour. This has been demonstrated in SCLC cell line studies[28-30]. Specific approaches against these genetic alterations might represent an additional tool in the treatment of chemorefractory disease.

I.1.3.2. Gene expression profiles

Several works evaluating the expression profiles of SCLC have been reported[31-34].

One common finding is that SCLC samples (tumours and cell lines) cluster together in hierarchical clustering analysis and can clearly be distinguished from NSCLC samples. Therefore, SCLC can be considered a distinct entity reproducing the currently used histopathological classification.

In these studies[33,34] overlapping overexpressed genes were reported. Interestingly, the achaete scute homologous protein (*ASCL1*) and the insulinoma associated 1 (*INSM1* or *IA-1*) genes are upregulated in several studies. These genes could be used for diagnostic purposes as they are neuroendocrine markers[35], but there are data showing that they may also play a role in the progression of tumours, and therefore could also be

used as therapeutic targets[36]. SCLC is also characterised by overexpression of neuroendocrine genes, such as gastrin-releasing peptide (GRP), certain chromogranins and CD56 (NCAM)[31].

I.1.3.3. MicroRNAs

Mutations or misexpressions of miRNA have recently been associated with cancer and its prognosis[37]. These studies indicate that miRNAs can act as oncogenes or TSGs. Few publications have addressed the role of miRNAs in SCLCs yet. It is demonstrated that overexpression of specific miRNAs may play a role in the development of SCLC[38]. Other reports[39,40] have suggested a potential oncogenic role of miRNAs in SCLC, but this remains to be validated in the clinic.

I.1.3.4. Genomic instability

In addition to the specific genetic changes, there is also evidence to suggest that there may be genomic instability in SCLC, including changes to the number of short-tandem microsatellite repeats. Although microsatellite instability is not common in SCLC, another form of microsatellite alteration has been reported, in which the incorrect replication of a single microsatellite marker is observed, and is clonally preserved as the tumour develops[41].

I.1.3.5. Oncogenic pathways

Finally, the study of the key features in malignant transformation and the associated signalling pathways has resulted in the characterization of genes with a relevant oncogenic role in SCLC. Whether targeting these

pathways will result in clinical benefit is now being evaluated. The most relevant pathways that are dysregulated in SCLC include different members of tyrosine kinase receptors (RTKs) like EGFR[42], IGFR[43], VEGFR[44], FGFR[45], MET[46,47] and c-KIT[48], neuroendocrine markers such as NCAM[49], tumour suppressor genes like TP53[50] and RB[51], antiapoptotic proteins such as BCL-2[52], signalling pathways like PI3K/AKT/mTOR and PTEN[53,54] and other molecules such as Gastring-releasing peptide (GBR)[55,56] and DNA-Topoisomerase II α[57].

We have focused our work in the study of one of this oncogenic pathways and its role on the behaviour and response to the treatment of SCLC, the HGF/MET pathway.

I.2. THE HGF/MET PATHWAY

I.2.1. The structure of MET and its ligand HGF/SF

MET is a proto-oncogene located on chromosome 7q31.1. It is constituted of 21 exons encoding a heterodimeric transmembrane receptor tyrosine kinase (RTK) composed of an extracellular α chain (50kDa) disulfide bonded to a membrane-spanning β (145 kDa) chain originated from the proteolytic cleavage of a single chain precursor (170kDa).

The extracellular region of MET includes three functional domains (Figure I.2.):

- Sema domain (which is also found in the semaphorins and plexins): comprises the first 500 residues at the N terminus, encompassing the whole α-subunit and part of the β–subunit. It is involved in ligand-receptor interaction.

- Plexin-Semaphorin-Integrin (PSI) domain (which is also present in the plexins, semaphorins and integrins): covers approximately 50 residues and contains four conserved disulphide bonds.

- A protein-protein interaction domain that covers the residual 400 residues connecting the PSI domain to the transmembrane helix. It is made of four immunoglobulin-like structures (integrin, plexin, transcription factor (IPT) domain).

The intracellular portion of MET receptor is formed by a juxtamembrane section followed by a catalytic site and a C-terminal regulatory tail. The juxtamembrane segment plays a role in receptor downregulation[58]. It contains a serine residue (Ser 975) that upon HGF-induced phosphorylation inhibits the receptor kinase activity, and a tyrosine (Tyr 1003) capable of binding CBL. *CBL* proto-oncogene is a ubiquitin ligase that promotes receptor polyubiquitination resulting in MET degradation[59,60]. The catalytic site positively modulates kinase activity following trans-phosphorylation of Tyr1234 and Tyr1235. Carboxy-terminal multifunctional docking site contains two docking tyrosines (Tyr1349 and Tyr1356) that are involved in the recruitment of several transducers and adaptors and is essential in downstream signalling[61,62] (**Figure I.2.**)

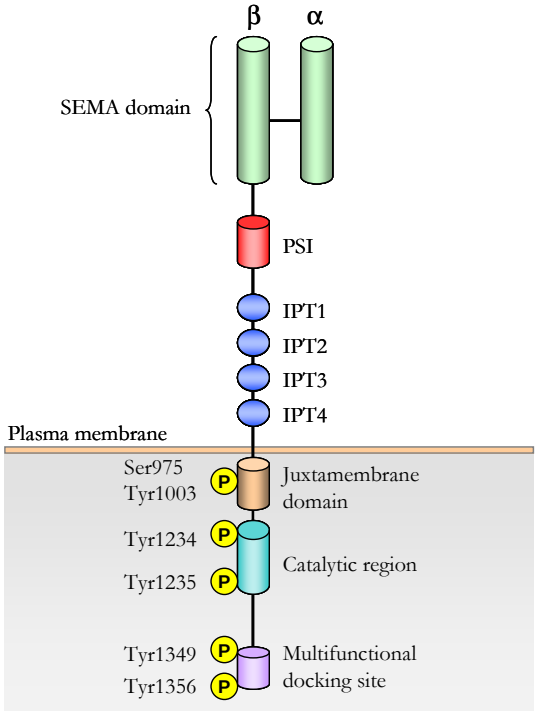

Figure I.2. Schematic structure of MET. MET receptor is a single-pass heterodimer comprising an entirely extracellular α-subunit that is linked by a disulphide bond to a transmembrane β-subunit, which contains the intracellular catalytic activity. The extracellular region of MET includes three functional domains: the SEMA, PSI and protein-protein interaction domains. The intracellular segment is composed of three portions: a juxtamembrane sequence (Ser975, Tyr1003), a catalytic region (Tyr1234, Tyr1235) and a carboxy-terminal multifunctional docking site (Tyr1349, Tyr1356).

MET high affinity ligand is known as Scatter Factor (SF) or Hepatocyte Growth Factor (HGF). SF and HGF were identified independently as a factor capable of inducing scatter of epithelial cells[63,64] and as a potent growth inductor for primary hepatocytes in culture[65], respectively. Both SF and HGF were proved to be identical molecules[66]. HGF belongs to the plasminogen family. It is secreted as a single-chain, biologically inert

precursor (pro-HGF) and converted into its mature form by site-specific, extracellular proteinases matriptase, pepsin and HGF-activator. The active form consists of disulphide bonded α - and a β- chain. The α-chain contains an N-terminal hairpin loop followed by four copies of the kringle domain (K1-4) (80 amino acid double-looped structures formed by three internal disulphide bridges). The β- chain contains the C-terminal serine proteinase homology (SPH) domain, that is structurally related to the catalytic domain of serine proteinases but that is enzimatically inactive[67-69] (**Figure I.3.**).

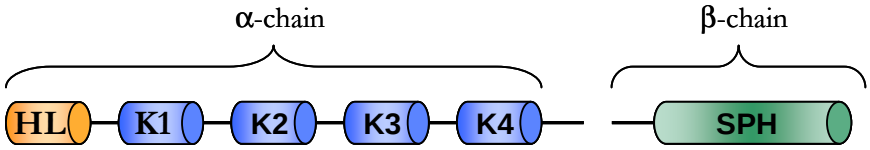

Figure I.3. Schematic structure of HGF. The HGF mature form consists of an α and β chain that are held together by a disulphide bond. The α-chain contains an N-terminal hairpin loop (HL) followed by four copies of the kringle domain (K1-4). The β-chain contains a C-terminal serine proteinase homology (SPH) domain that is structurally related to the catalytic domain of serine proteinases but that is enzymatically inactive. HGF contains two MET-binding sites: one in the NK1 fragment and one in the SPH domain.

The HGF high-affinity site is located in the α-chain and recognizes the IPT3 and IPT4 domains of MET independently of HGF processing and maturation. Nevertheless, the low-affinity site lies within the β-chain of HGF and is exposed only after HGF activation and interacts with the SEMA domain of MET[68].

This growth factor is widely distributed in the extracellular matrix of most tissues, where it is sequestered, mainly in its inactive form, by

heparin-like proteoglycans[70]. Cells of mesenchymal origin are the major HGF source, which acts in a paracrine manner on epithelial cells that express the MET receptor[71]. During tissue repair several cytokines that are abundant in the reactive intersticial compartment induce transcriptional upregulation of both HGF (in fibroblast and resident macrophages) and MET (in epithelial cells)[72]. The inflammatory stroma also overexpresses proteases that are involved in pro-HGF activation[73]. Therefore, this transcriptional and post-translational regulation of HGF leads to an optimal MET activation on target cells, considered the general mechanism of physiological defence to tissue damage.

I.2.2. MET signalling pathway

Following HGF binding, MET is autophosphorylated on the tyrosine residues Tyr1230, Tyr1234 and Tyr1235 within the activation loop of the tyrosine kinase domain. These regulate kinase activity through phosphorylation of the Y1349 and Y1356 tyrosine residues near the COOH terminus, which forms a multifunctional docking site that recruits intracellular adapters. This occurs via Src homology-2 domains and other recognition motifs, leading to downstream signalling[74-76]. Among the most widely studied adapter proteins and direct substrates in this pathway are growth factor receptor-bound protein 2 (Grb2), GAB1, phosphatidylinositol 3-kinase (PI3K), phospholipase C-γ, Shc, Src, Shp2, Ship1, and signal transducer and activator of transcription 3 (STAT3)[74,75]. These cytoplasmic effectors are directly recruited to the multifunctional docking site of MET receptor and these proteins become frequently phosphorylated on tyrosine residues. GAB1 and Grb2 are considered critical effectors and interact directly with the receptor. These recruit a network of adaptor proteins that are involved in the activation of various

downstream signalling cascades, contributing to the pleiotropic biological effects induced upon HGF binding.

MET-dependent signals are organized in several pathways that transmit biochemical information from the cell membrane (where MET resides) to the nucleus (where modulation of gene expression occurs). Signalling by the RAS-MAPK and PI3K-AKT pathways reaches the nucleus to affect gene expression and cell cycle progression. Cytoplasmic signalling cascades that are mediated by CDC42-RAC1 or FAK-Paxillin pathway elicit cytoskeletal changes. Signalling to membrane-bound lipids and PKC, STAT pathway and IKK-NF-κB complex are also activated. These signalling pathways control important functions such as cell proliferation and cell survival (**Figure I.4.**).

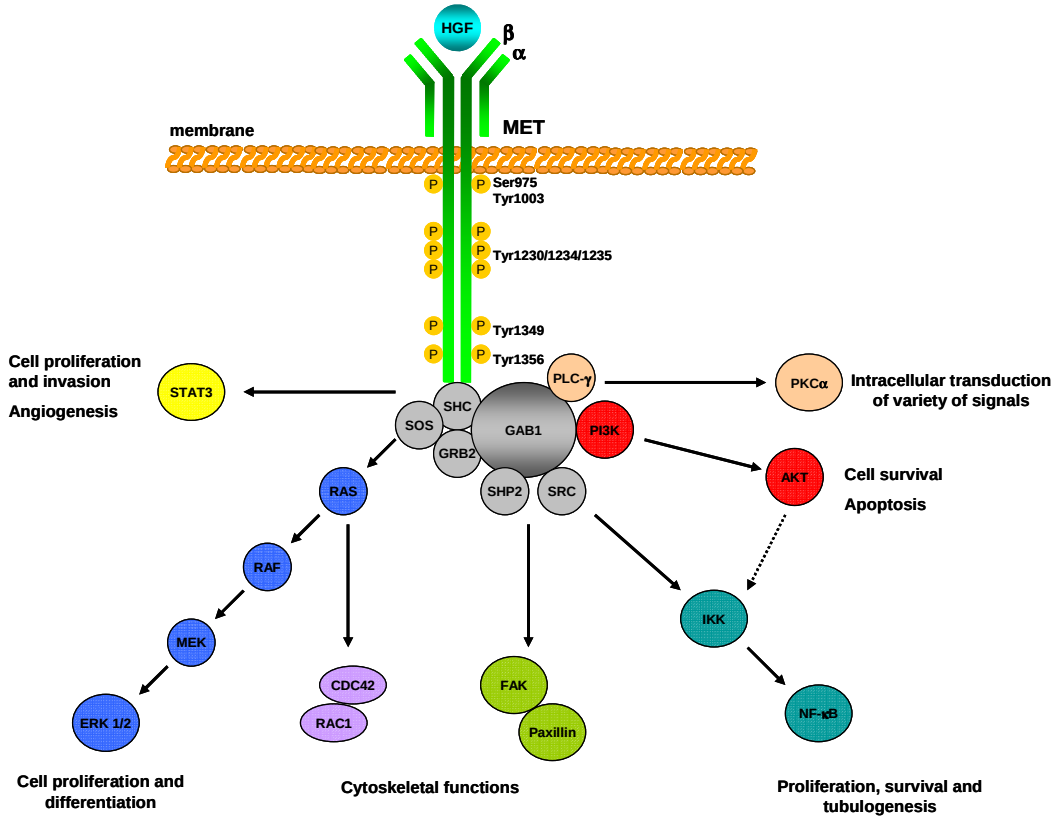

Figure I.4. MET-dependent signalling pathways. HGF induces dimerisation and activation of MET at the plasma membrane. The cytoplasmic phosphorylation (P) sites of MET are indicated: Ser975 and Tyr1003 are in the juxtamembrane domain, Tyr1230/1234/1235 are in the active site of the kinase, and Tyr1349 and Tyr1356 are in the bidentate docking site. Various cytoplasmic effector molecules such as GRB2, GAB1 and SRC are recruited to the bidentate docking site. Tyrosine-phosphorylated GAB1 that is bound to MET can attract further docking proteins, including SHP2, PI3K and others, which together with the direct MET binders, activate various downstream signalling cascades: Ras-MAPK pathway, PI3K-AKT axis, signalling to membrane-bound lipids and PKC, RAC1-cell division control protein 42 (CDC42) cascade, FAK-Paxillin signalling, the STAT pathway and the IκBα-NFκB complex.

I.2.3. Regulation of physiologic MET signalling

MET signalling must be regulated to avoid a pathway overstimulation that might lead to cell transformation. Moreover, MET expression at the cell surface is regulated by different spatially restricted events, such as extracellular shedding, intracellular cleavage and ubiquitin-mediated degradation.

I.2.3.1. Ligand-dependent regulation

HGF represents the MET-high affinity ligand. On ligand activation, MET is internalized through clathrin-mediated endocytosis. The internalized receptor is delivered to endosomal compartments and remains capable of signalling during vesicle trafficking. MET is recruited into early endosomes through protein kinase Cε (PKCε) and allows the delivery of active ERK to focal adhesions, where it can mediate HGF-induced cell migration[77]. From the peripheral endosomes, MET traffics

along the microtubule network and accumulates in a nondegradative perinuclear endomembrane compartment through a process promoted by PKCα. This post-endocytic trafficking brings active MET into close proximity to the nucleus, which protect STAT3 against phosphatase activity and allows its efficient phosphorylation and translocation to the nucleus[78,79]. Subsequently, the receptor is degraded in the lysosomal compartment, the major determinant of receptor desensitization and signal restriction. Trafficking to the lysosomes is triggered by ligand-induced activation of MET, and requires the function of CBL, an E3 ubiquitin ligase that is recruited to a juxtramembrane phosphotyrosine residue in the active MET receptor (Tyr1003). CBL leads to MET ubiquitylation at multiple sites, which enables its recognition by endocytic adaptors that contain ubiquitin-binding domains, its sorting into clathrin-coated areas at the cell surface and its delivery to the endosomal network. From these sorting endosomes, MET accumulates on multivesicular bodies, which fuse with the lysosomes and MET undergoes proteolytic degradation [80,81]. CBL also contains a RING finger domain that engages E2 protein ubiquitin ligases to mediate ubiquitylation of MET, which might occur at the cell membrane or in the early endocytic compartment. Ubiquitylated MET is degraded in a late endosomal or lysosomal compartment in a proteasome-dependent manner[76,80].

Furthermore, MET receptor can also interact with Semaphorins and Plexins (low affinity ligands), a broad family of ligand-receptor pairs whose signalling is critical for many cellular aspects of organogenesis, including cell migration, proliferation and survival. Members of the class B Plexins family associate with MET and transactivate it in response to their Semaphorins low affinity ligands, even in the absence of HGF, providing an alternative way to stimulate MET biological responses[82].

I.2.3.2. Ligand-independent regulation

Another mechanism that leads to downregulation of MET is regulated proteolysis and shedding of the extracellular domain. Shedding is mediated by members of the disintegrin and metalloproteinase (ADAM) family and results in the formation of a soluble MET ectodomain and a membrane-anchored cytoplasmic tail. The surface-associated cytoplasmic tail undergoes proteolysis by γ-secretase and is rapidly cleared by proteasome-mediated degradation. Unlike CBL-mediated endosomal degradation, regulated proteolysis of MET is ligand- and ubiquitin-independent and does not require the kinase activity of the receptor[83].

I.2.4. Physiologic role of HGF and MET

MET and its ligand HGF play an essential role in normal physiological conditions during embryonic development and organ formation. In adult life this pathway regulates inflammatory responses and wound healing processes as part of the acute injury repair.

During development, HGF and MET are essential for embryonic formation coordinating muscle development, nervous system organization, bone remodelling and angiogenesis[84-86].

In adult life MET has also an active and important role in the cell proliferation and migration during acute injury repair[87-89].

I.2.5. Deregulation of MET in cancer

The regulation of HGF/MET pathway that is observed during embryonic development and organ regeneration is lost in cancer at multiple levels.

Deregulation of the HGF/MET pathway has been observed in many human malignancies, and the effects of sustained MET activation have been extensively characterized in preclinical models[90]. A variety of mechanisms that lead to aberrant MET signalling have been characterised, including overexpression of MET, *MET* gene amplification, mutations, structural rearrangements or ligand-dependent autocrine or paracrine mechanisms[58]. In addition, a number of other mechanisms, including inadequate degradation, receptor crosstalk or synergies in downstream signalling, have also been observed[91,92].

Oncogenic MET was first identified as the protein product of a transforming oncogene called Translocated Promoter Region (TPR)-MET, derived from a chromosomal rearrangement in an osteosarcoma cell line treated with a chemical carcinogen[93]. The oncogenic TPR-MET fusion protein is constitutively active. In animal models, transgenic expression of TPR-MET leads to the development of mammary tumours and other malignancies[94]. Moreover, the TPR-MET rearrangement has been detected in human gastric cancer, in precursor lesions and in the adjacent normal mucosa, suggesting that this genetic translocation can predispose to the development of gastric carcinomas[95].

Since then, other mechanisms of MET aberrant activation have been identified.

I.2.5.1. *MET* gene amplification

One well characterised MET deregulation mechanism is *MET* gene amplification that causes, in the majority of cases, protein overexpression and constitutive activation of the kinase domain[96]. *MET* gene amplification, although is not a frequent event, has been observed in primary tumours or as a secondary event that alters the sensitivity of

cancer cells to therapy[97-99]. Cancer cell lines displaying *MET* gene amplification are dependent on MET for growth and survival. In such cells MET inhibition results in a proliferative block or massive cell death. This MET-addicted phenotype has been consistently described in cultured cells from gastric carcinomas and non-small cell lung carcinomas (NSCLCs)[96]. This 'oncogene addiction' has been further confirmed in *in vivo* models of alveolar and embryonal rhabdomyoscarcoma[100]. *MET* amplification has been reported in a number of human primary tumours, like gastric and oesophageal carcinomas[101], colorectal cancers[102], NSCLC with acquired resistance to epidermal growth factor receptor (EGFR) inhibitors[103], medulloblastomas[104] and glioblastomas[105]. A number of studies suggest that the increased *MET* gene copy number is an independent negative prognostic factor in different tumours, such as surgically resected NSCLC patients[106,107] and has also been associated with advanced stage and the presence of liver metastases in patients with colorectal cancer[108].

I.2.5.2. *MET* activating mutations

Another mechanism that causes an inappropriate activation of MET is the presence of activating mutations. Missense germ-line mutations in the tyrosine kinase domain have been described in patients with hereditary papillary renal carcinoma[85]. However, sporadic mutations are more pervasive and can involve the tyrosine kinase, juxtamembrane, or semaphorin domains. These sporadic mutations have been detected in sporadic papillary renal carcinoma[85], childhood hepatocellular carcinoma[109], gastric carcinoma[110], head and neck cancer[111], glioblastomas[112], SCLC[47], NSCLC[113], mesothelioma[114], melanoma[115] and pancreatic cancer[47,116]. Interestingly only some of these mutant alleles

(P1009S, T1010I, M1268T) have been shown to have a role in malignant transformation as a result of constitutive receptor activation, thus offering the potential of therapeutic inhibition[110,117]. These oncogenic mutations were found to be predominantly located in the non-kinase domain, such as on the SEMA domain or juxtamembrane domain[47]. In some cell line models from lung cancer (H1437 and H596 NSCLC cell lines) the presence of MET oncogenic mutations was associated with increased MET phosphorylation and downstream signalling resulting in enhanced tumorigenicity, increased cell motility and altered cellular architecture and. Moreover, strong response to therapeutic inhibition with MET small molecule inhibitors has been demonstrated in these cell line models[113,117-119]. The presence of MET mutations in lymph nodes and metastatic sites suggests the existence of a selection of these mutated cells during metastatic progression[120]. The prognostic role of MET mutations has not been explored in many tumour types. Follow-up studies in HNSCC indicate that MET mutations could be associated with resistance to radiotherapy and poor progression free survival[121,122].

I.2.5.3. MET overexpression

Although the above genetic alterations on the MET gene could be potentially relevant therapeutic targets in these tumours, these cases are rare in the general population of cancer patients. The most frequent cause of constitutive MET activation in human tumours is increased protein expression due to a transcriptional upregulation, in the absence of gene aberrations. This is often induced by negative microenvironmental conditions, such as low oxygen tension (hypoxia) in the stroma surrounding the tumour. Hypoxia stimulates MET transcription, resulting in higher levels of protein expression, enhances HGF signalling and

promotes tumour invasion by sensitizing cells to HGF stimulation. Consistent with this, an increased MET expression in hypoxic regions or human tumours has been reported[123].

In *in vitro* assays with cell lines, receptor overexpression can lead to local receptor oligomerization and reciprocal activation, rendering cells responsive to sub-threshold ligand concentrations. In addition, in an animal model, the overexpression of wild-type MET in hepatocytes is sufficient to cause hepatocarcinomas that regress following transgene inactivation[124].

Many studies have been conducted in the past years to examine expression/overexpression of MET in a number of tumour tissues. The identification of different neoplasms with MET overexpression is constantly increasing and, at least for carcinomas, cases of excessive levels of MET expression have been found in all types of these malignancies[125]. MET has been shown to be overexpressed in neoplastic tissue relative to normal surrounding tissue, and the extent of overexpression correlates with disease severity and outcome in several tumour types[126-128]. Studies in lung cancer demonstrate MET expression in the vast majority of cases, with strong expression found in up to 60% of cases[113]. When assessing for functional activity with p-MET staining, MET activation was observed between 40-100% of cases depending on the specific lung cancer tissue[113,126,129-131]. High rates (>80%) of MET overexpression have also been observed in malignant pleural mesothelioma and renal cell carcinoma studies[114,132]. Similarly, MET overexpression has been observed in ovarian cancers[133,134] and breast cancers[135]. The prognostic significance of MET overexpression and/or activation has been evaluated in several tumour types and globally, it seems to be associated with more advanced disease stage and impaired outcome. This is the case for lung cancer studies where MET

overexpression was associated with higher pathological tumour stage and worse outcome[126,130]. In colon cancer, MET expression level has also been correlated with advanced stage disease/liver metastases and seems to predict tumour invasion and lymph node metastases[108,136]. This association with unfavourable outcome has also been demonstrated in patients with ovarian and breast tumours[128,137,138].

Despite these results, the exact cut off for MET overexpression has not been defined in these works and this makes it difficult to categorize MET expression in clinically meaningful levels by different techniques, especially immunohistochemistry.

I.2.5.4. HGF-dependent MET oncogenic activation

Paracrine activation

Most often in cancer, MET activation occurs via a ligand-dependent mechanism. HGF itself is able to activate the transcription of MET[139,140]. It is expressed throughout the body and it is particularly active in the reactive stroma of tumours[141]. These observations suggest that this cytokine allows paracrine positive feedback loops to support the dissemination of cancer cells. In fact, MET activation could be mediated by HGF production by tumour invading fibroblast-like cells[142]. Moreover, it is described that tumour cells could secrete factors that induce HGF secretion, which in turn activates MET in a paracrine fashion and might trigger the tumour cells to invade the surrounding stroma[143]. This is in agreement with the observation that MET activating mutations require HGF to boost their catalytic efficiency[144].

Autocrine activation

HGF can also aberrantly activate MET in an autocrine manner, as described for various human tumours like glioblastomas[145], breast carcinomas[146], rhabdomyosarcomas[147] and osteosarcomas[148]. In experimental systems, exogenous co-expression of MET and HGF in several human and mouse cell lines leads to the formation of invasive tumours upon implantation in nude mice[149].

I.2.5.5. MET defective degradation

In addition to the enhanced MET signalling observed with MET overexpression, oncogenic MET receptor mutants or ligand dependent activation, loss of negative regulation also contributes to oncogenic activation of MET. It has been shown that MET receptor mutated at the CBL juxtamembrane binding site Tyr1003, which acts as a negative regulator of MET biological activity, can induce constitutive scattering of epithelial cells and transformation of fibroblast. These constitutive responses are the consequence of the decrease of receptor ubiquitination, which prevents its degradation[59]. The oncogenic fusion protein TPR-MET, characterize by an absence of the CBL-binding site, can also escape lysosomal degradation[150]. Furthermore, it is described that MET receptor mutants uncoupled from CBL-dependent ubiquitination, are transforming and tumorigenic, through enhanced stability of MET and sustained signalling of downstream pathways[59,60].

I.2.5.6. Crosstalk between MET and other membrane proteins

Crosstalk between MET and membrane partners collaborates in the modulation of the activation of MET and leads to the integration of signals in the extracellular environment[97].

Crosstalk between MET and EGFR receptor has been described in different biological contexts, such as during kidney development, providing evidence for the role of MET and EGFR cooperation in kidney-branching morphogenesis[151], or in various cancers, which HGF mediated MET activation can induce resistance to EGFR inhibition[152,153]. Moreover, studies in cancer cell lines demonstrate that amplified MET drives the activity of EGFR family members and, conversely, that mutated and amplified EGFR can drive MET activity[154]. *MET* amplification can activate ERBB3-PI3K-AKT signalling in EGFR mutant lung cancer cells, inducing gefitinib resistance. Moreover, inhibition of MET signaling in these cells restored their sensitivity to gefitinib[98].

MET receptor can be also activated in response to G-protein coupled receptor (GPCR) agonists. Both EGFR and GPCR ligands are known to increase the intracellular level of reactive oxygen species that inhibit phosphatases, inducing the activation of MET[155].

It is also well established that MET cooperates with ErbB2 receptor to support the invasive growth, the biological program that defines the ability of neoplastic cells to invade the adjacent tissues, survive in foreign compartments, and proliferate and settle at distant sites. MET and ErbB2 receptors synergise to enhance the malignant phenotype, promoting the break-down of cell-cell junctions and enhancing cell invasion, particularly in cancers where ErbB2 is overexpressed and HGF is a growth factor physiologically present in the stroma[156].

MET also interacts with a membrane receptor called RON. The *RON* gene displays 25% homology with *MET* in the extracellular region and 63% homology in the tyrosine kinase domain. Moreover, the RON ligand MSP has a 45% homology with HGF. It is known that MET activation by HGF binding results in RON transphosphorylation and vice-versa. This transphosphorylation occurs in a direct way and does not require the C-terminal docking site of either receptor, whereas a tyrosine kinase inactive RON is sufficient to block MET transforming activity[157]. In addition, it is described that this RON transphosphorylation sustains MET oncogene addiction[158].

Another protein that cooperates with MET in normal and transformed epithelial cells is CD44, a transmembrane cell adhesion molecule that functions as a linker between the extracellular matrix and the intracellular actin cytoskeleton. The extracellular domain of the v6 splice variant of the CD44 (CD44v6) forms a ternary complex with MET and HGF, an event that is necessary for MET activation. The intracellular portion of CD44v6 links the MET cytoplasmic domain to actin microfilaments through GRB2 and intermediate ezrin, radixin and moesin (ERM) proteins, which facilitates MET-induced activation of RAS through SOS[159,160].

Interaction between MET and $\alpha 6\beta 4$ integrin is also described. Upon MET activation, the $\beta 4$-subunit cytoplasmic domain of the integrin is phosphorylated, inducing the recruitment of transducers like SHC, PI3K and SHP2. Thus, the $\alpha 6\beta 4$ integrin acts as a supplementary docking platform for the recruitment of additional transducers that allow the signal amplification of MET pathway[161].

MET can also associate with FAS, the death receptor. The extracellular domain of MET interacts with FAS, which prevents the FAS receptor-

FAS ligand recognition and FAS self-aggregation and ultimately results in protection for apoptosis[162].

Crosstalk between MET and developmental signalling pathways, such as WNT-β-catenin and TGF-β-bone morphogenic protein (BMP), has also been identified in cancer models. On the one hand, it has been shown that the presence of mutation or overexpression of key components of the WNT-β-catenin pathway can cause cancer[163]. Studies in colon cancer and other tissues demonstrate that *MET* is a direct transcriptional target of WNT-β-catenin[164]. It is also described that MET and integrin α3β1 signalling regulate the WNT7B transcription in the kidney[165]. In addition, HGF is able to induce the nuclear translocation of β-catenin-TCF and the transcription of their target genes in liver and bladder cancer cells, as well as the tyrosine phosphorylation of BCL92, a β-catenin binding protein, in colon cancer cells[166,167]. On the other hand, genetic experiments in mice show an important interaction between TFGβ and MET signalling. Following mutation of TGFβ receptor II in mesenchymal cells, the presence of stomach and mammary-gland epithelial tumours are observed as a result of the upregulation of stromal HGF and MET activation in epithelial cells[168].

Another protein receptor that cooperates with MET in endothelial cells is the vascular endothelial growth factor receptor (VEGFR). MET and VEGFR do not physically associate or trans-phosphorylate each other but they synergistically activate common signalling intermediates: ERK-MAPK, AKT and focal adhesion kinase (FAK)[169]. Angiogenesis and lymphangiogenesis are important processes in tumour formation and metastasis. VEGF and VEGFR families have an important role in both processes, but HGF/MET signalling is also a potent inducer of endothelial cell growth and promotes angiogenesis and

lymphangiogenesis *in vitro* and *in vivo*[170,171]. HGF has been found to stimulate VEGF-A production in non-endothelial cells[172,173] and to increase the expression of VEGFRs and MET in endothelial cells[174]. MET signalling can induce VEGF-A expression and angiogenesis through common signalling intermediates such as SRC homology 2 domain-containing proteins (SHCs). A gene expression profiling study suggested that VEGF-A and HGF cooperate by inducing a number of pathways, leading to a more robust proliferative response[175]. Under angiogenic *in vitro* conditions, it is described that the combination of VEGF-A and HGF can promote vascularization of endothelial cells by enhancing intracellular signalling pathways involved in the regulation of the cytoskeleton and cellular migration and morphogenesis[169].

I.2.6. MET and lung cancer

A number studies have been carried out in the past years studying the role of MET in lung cancer. MET receptor dysregulation has been described in both SCLC and NSCLC[46,113,129].

I.2.6.1. NSCLC

Several works have reported MET receptor overexpression to be in the range of 25-60%, in NSCLC lung adenocarcinomas, showing increased MET expression when compared with adjacent normal tissue. These studies found 25, 40 and 60% of MET overexpression in 42, 40 and 32 NSCLC tumour samples, respectively[113,129,176].

Moreover, a number of studies have assayed the expression of p-MET in NSCLC, showing MET phosphorylation in a range of 33-72% in 32 and 40 NCLC tumour samples, respectively[113,176]. In addition, it was detected

a preferential expression of p-MET staining in the tumour cells in the invasive front of the NSCLC specimens[113].

Another study characterized tyrosine kinase signalling across 41 NSCLC cell lines and more than 150 NSCLC tumour samples and established that MET was one of the highly tyrosine-phosphorylated receptor in NSCLC tumour samples[177].

MET gene mutations and copy number variations have also been reported in lung cancer[47,113,176,178-181]. *MET* receptor mutations in lung cancer are mainly found in the nontyrosine kinase domain, specifically in the juxtamembrane and SEMA domain. *MET* mutations in the kinase domain have been found to be somatically selected in the metastatic tissues, compared with the primary solid cancers[120]. *MET* missense mutations within the SEMA (E1689D, L229F, S323G and N375S) and juxtamembrane domain (R988C, T1010I and S1058P) of a NSCLC cell line and adenocarcinoma tissues have also been described. In addition, in a lung tumour specimen the investigators detected an alternative splice variant affecting the juxtamembrane domain[113]. Another study reported the identification of somatic intronic mutations of *MET* kinase in NSCLC. These somatic mutations lead to an alternatively spliced transcript which encodes a deletion of the juxtamembrane domain, resulting in a delayed down-regulation of the receptor. As a consequence, elevated MET expression in primary lung tumours was observed compared with normal tissue[118].

Several studies have reported primary *MET* amplification to be in the wide range of 2% to 21%, in NSCLC lung adenocarcinomas[178,179,181]. A study in a collection of 106 NSCLC specimens found *MET* amplification in the 21% of the samples (22 of 106)[178]. Other works in NSCLC samples from Japanese patients found *MET* gene amplification in 4% (n=183)[180] and 1.4% (n=148)[181] of the specimens. In addition, this *MET*

amplification was associated with MET activation by immunohistochemistry. Furthermore, the Lung Cancer Mutation Consortium, by using the FISH assay, reported that 4.1% of adenocarcinomas (n=295) had *MET* amplification[182]. *MET* amplification was associated with poor survival. The largest study of MET (n=447 NSCLC) found high *MET* gene copy number in 48 cases (11.1%), including 18 cases with true gene amplification (4.1%). Interestingly, this increased *MET* gene copy number was negatively associated with survival in this study[106].

I.2.6.2. SCLC

Previous studies have also reported MET expression in SCLC cell lines and human SCLC. In an *in vitro* study MET expression has been found in 10 SCLC cell lines, and MET was highly expressed in four of the lines and moderately expressed in two[47]. In a small study 25% of SCLC tumour tissues examined (n=4) showed strong expression of MET receptor, 100% of the samples showed phosphorylation at the Tyr1003 site, and 50% were phosphorylated at Tyr1230/1234/1235[113].

In another study, several *MET* mutations were identified in one collection of SCLC samples and cell lines. These *MET* alterations were identified among 3 of 10 SCLC cell lines and 4 of 32 SCLC paired-SCLC/normal tissues. Two SCLC cell lines presented a novel missense mutation (R988C) in the juxtamembrane domain, one SCLC sample had another novel juxtamembrane missense mutation (T1010I), and one more had a missense mutation (E168D) in the SEMA domain. Two SCLC samples also presented two-base-pair insertional mutations within the MET juxtamembrane domain and an alternative spliced *MET* transcript skipping the entire exon 10 was observed in other SCLC cell

line. Studies where the juxtamembrane mutations R988C and T1010I and the alternative spliced juxtamembrane-deleting variant were characterized demonstrated that these were oncogenic activating variants with increased oncogenic signalling, tumorigenecity, cell motility and migration[47,118]. Nevertheless, a recent study defined these *MET* receptor sequence variants (R988C and T1010I) as rare single-nucleotide polymorphisms without transforming capacity. In this work different cancer patients and healthy subjects were screened and found these *MET* sequence variants at low frequencies in most cohorts, including normal individuals. In addition, no evidence of increased phosphorylation or transformative capacity by either sequence variant was found[183].

I.2.7. HGF/MET signalling inhibition

Due to the pleiotropic role in cellular processes important in oncogenesis and cancer progression, HGF and MET are considered to be important therapeutic targets in several tumour types. The inhibition of the HGF/MET signalling pathway can be addressed using different strategies targeting either the binding of the ligand or the receptor activation. In this part of the introduction we discuss the most relevant drugs that target HGF/MET pathway whose clinical development seems more promising (**Figure I.5.**, **Table I.1.**).

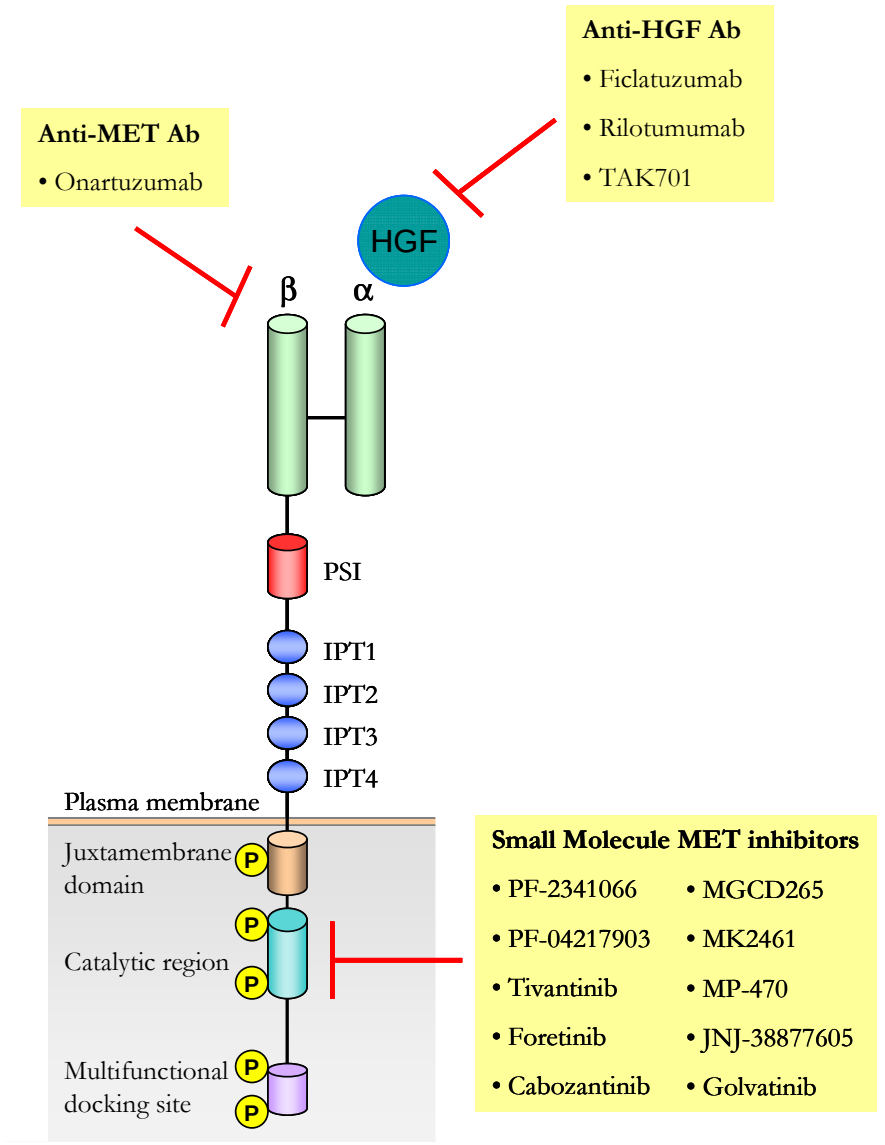

Figure I.5. MET signalling inhibition strategies. Therapeutic intervention strategies to block and inhibit MET receptor oncogenic signalling cascade include blocking ligand-receptor interaction through anti-HGF antibodies, preventing receptor dimerization by anti-MET antibodies and blocking MET kinase intrinsic activity with small molecule MET inhibitors.

Table I.1. Ongoing trials on MET inhibitors

Molecule	Targets	Type	Phase	Treatment	Drug associated	Patient population
Tivantinib	MET	TKI	I	Combination	Topotecan	SCLC
			II	Combination	Erlotinib	EGFR positive NSCLC
			III	Combination	Erlotinib	KRAS positive NSCLC
Cabozantinib	MET, VEGFR2, RET, Kit, AXL, FLT3	TKI	II	Monotherapy	-	Solid tumours
			II	Monotherapy	-	KIF5B/RET NSCLC
			II	Combination	Erlotinib	EGFR negative NSCLC
Foretinib	MET, VEGFR, PDGFRb, Tie-2, RON, Kit, FLT3	TKI	I-II	Combination	Erlotinib	NSCLC
Golvatinib	MET, VEGFR	TKI	I	Monotherapy	-	Solid tumours
MGCD265	MET, VEGFR, RON, Tie2	TKI	I-II	Combination	Erlotinib/Docetaxel	NSCLC
Onartuzumab	MET	Monoclonal antibody	II randomised	Combination	Carboplatin-Paclitaxel	Squamous NSCLC
			III	Combination	Erlotinib	MET positive NSCLC
			II randomised	Combination	Platinum+Pemetrexed; Platinum+Paclitaxel+Bevacizumab	Non-squamous NSCLC
Rilotumumab	HGF	Monoclonal antibody	I-II	Combination	Erlotinib	NSCLC

I.2.7.1. HGF and MET biological antagonists

There are molecules created to specifically prevent the interaction between the ligand and the receptor but unable to activate the downstream signalling.

HGF contains two MET binding sites with different receptor affinities: the high-affinity binding site can recognize MET independently of HGF processing and maturation but does not activate HGF/MET pathway[184,185]; the low-affinity site becomes accessible only upon pro-HGF conversion and is essential for MET dimerization and activation[186,187]. Therefore, an inactive precursor of HGF, or HGF fragments that retain only the high-affinity site, can interact with MET but do not induce MET signalling because they cannot induce MET dimerization.

In addition, the Sema domain of MET, either *per se* or as a full-length, soluble MET extracellular portion, might competitively displace HGF and impair dimerization of the endogenous receptor[67].

All these HGF and MET variants have been validated *in vitro* and *in vivo* models as powerful antagonists.

Clinical development of these approaches is at this point immature, so we will not explain these further.

I.2.7.2. Antibodies against MET

Another type of MET-targeted agent is monoclonal antibodies against the MET extracellular domain, which have displayed promising results in tumours with high MET levels.

- **OA-5D5** (MetMAb) (Onartuzumab) (Genentech): it is a recombinant, humanized, monovalent monoclonal antibody antagonist of the MET receptor to achieve targeted inhibition of the ligand HGF-induced MET signalling. It is a monovalent Fab fragment with murine variable domains for the heavy and light chains fused to human IgG1 constant domains. MetMAb binds the SEMA domain of MET and displays potent antagonistic activity. It acts as a classic receptor antagonist by competing for the binding of HGF to MET. In preclinical models, this antibody inhibits intracerebral growth of HGF-expressing glioblastoma cells when delivered locally[188]. Similar results were seen with pancreatic cancer models[189].

A recent phase II clinical trial using MetMAb in combination with erlotinib to treat NSCLC patients resulted in a doubling of patient survival from 6.4 to 12.4 months. However, patients with MET negative tumours treated with MetMAb and erlotinib had a worse overall survival when compared with the erlotinib plus placebo arm, indicating that only MET-expressing patients benefited from the combinational treatment. These results lend support for further investigation of MetMAb as potential personalized MET-targeting cancer therapeutics for NSCLC patients, and a phase III study is being recruiting patients currently[190].

MetMAb is also now under clinical evaluation in randomized double-blinded phase II trials in combination with paclitaxel and bevacizumab in triple-negative breast cancer or in combination with Oxaliplatin and Fluorouracil and bevacizumab in colorectal carcinoma[191].

I.2.7.3. Antibodies against HGF

Several monoclonal antibodies against HGF have also been developed for targeting the pathway.

- **Rilotumumab** (AMG102) (Amgen): a fully human neutralizing monoclonal antibody (IgG2) that specifically targets HGF and it is recombinantly produced in mammalian cells. The antitumor activity and mechanism of action of AMG102 have been evaluated in preclinical studies. It inhibits tumour growth, induce tumour regression, increase apoptosis and decrease cell proliferation in human xenograft models of cancer. Previous studies have shown that rilotumumab inhibits HGF-mediated MET phosphorylation and downstream signalling in paracrine stimulated prostate cancer cells and in autocrine stimulated glioblastoma cells. The antibody is able to inhibit proliferation of glioblastoma cells and HUVECs, and breast cancer cell invasion. Rilotumumab alone is shown to inhibit the growth and survival of glioblastoma xenografts and more so when AMG102 is used in combination with temozolomide or docetaxel. This molecule has also been tested in kidney carcinomas and clinical trials are ongoing against malignant pleural mesotheliomas and ovarian and primary peritoneal cancers. Rilotumumab is also currently evaluated in clinical phase I/II studies alone or in combination with the EGFR-blocking antibody Panitumumab, and in phase II clinical trials for glioblastoma multiforme and metastatic renal cell carcinoma. It is under evaluation in combination with avastin in glioma, erlotinib in NSCLC, and platinum-based chemotherapy in SCLC, mesothelioma, gastric cancer as well as mitoxantrone in prostate cancer[192-196].

- **TAK-701** (Millennium Pharmaceuticals, Inc): it is a humanized anti-HGF neutralizing antibody. *In vitro*, TAK-701 binds preferably to the mature two-chain form of HGF, blocking HGF-MET binding. In addition, TAK-701 inhibits the intracellular phosphorylation of MET and shows antitumour activities against various cancer cells with an autocrine

dependence on HGF *in vivo*. TAK-701 is currently in phase I clinical trials in adult patients with advanced non-hematological malignacies[197,198].

- **AV-299** (Ficlatuzumab) (AVEO Pharmaceuticals): it is a humanizad anti-HGF IgG1 monoclonal antibody that inhibits the activation of the MET receptor by neutralizing its only known natural ligand, HGF.
In preclinical studies, Ficlatuzumab demonstrated additive activity when given in combination with Erlotinib, Cetuximab and Temozolomide.
Clinical data from phase I studies of Ficlatuzumab indicated a favourable tolerability profile and good combinability with EGFR inhibitors such as Erlotinib and Gefitinib[199,200].
It is currently evaluated in a phase II study in combination with gefitinib in previously untreated Asian patients with NSCLC[201].

I.2.7.4. Small-molecule MET inhibitors

These small-molecule MET inhibitors are low molecular weight molecules able to compete for the ATP binding site in the tyrosine kinase domain of MET and prevent receptor transactivation and recruitment of the downstream effectors.

- **PF-2341066** (Crizotinib) (Pfizer): It is an orally available 2-amino-3-benzyloxy-5-arylpyridine compound that selectively targets MET and anaplastic lymphoma kinase (ALK). This compound shows efficacy at well-tolerated doses. It has cytoreductive anti-tumour activity and anti-angiogenic activity in several neoplastic models featuring constitutively activated forms of MET or ALK. Interestingly, the drug was initially developed intending as a MET inhibitor preclinically and subsequently in a phase 1 trial[202-204]. It potently inhibited MET phosphorylation and

MET-dependent proliferation, migration or invasion of human tumour cells in vitro. In addition, it also potently inhibited HGF-stimulated endothelial cell survival or invasion and serum-stimulated tubulogenesis *in vitro*, indicating that its cytoreductive antitumor efficacy may be mediated by direct effects on tumour cell growth or survival as well as antiangiogenic mechanisms[205]. Crizotinib also shows a marked antitumour action in MET amplification-positive lung cancer cells but not in cells without MET amplification, including those with a MET mutation[206]. Moreover, in a xenograft model of ovarian cancer metastasis it is demonstrated that Crizotinib-MET inhibition effectively reduces tumour burden and increases mice survival[207].

Preclinical and clinical studies have shown that cancer cells harbouring EML4-ALK and other ALK abnormalities are exquisitely sensitive to ALK inhibition. The clinical development of Crizotinib is focused primarily on NSCLC patients whose tumour harbours EML4-ALK gene fusion. Data from the phase I and phase II clinical trials of Crizotinib in ALK+ NSCLC has led to the approval of Crizotinib by the FDA (US Food and Drug Administration). Given the confirmation of the efficacy of Crizotinib in a second line trial versus chemotherapy in the same population the European Medicines Agency (EMA) has also approved this drug in second line setting[208,209].

More recently, a NSCLC patient with the novo MET amplification but not ALK rearrangement achieved a rapid and durable response to Crizotinib, indicating that it is also a good MET inhibitor clinically[210]. Dramatic clinical improvement and radiographic regression were also observed in patients with MET-amplified esophagogastric adenocarcinoma[204] and glioblastoma multiforme[211] upon treatment with Crizotinib.

- **PF-04217903** (Pfizer): it is a novel ATP-competitive small molecule inhibitor of MET kinase. This drug demonstrated >1000 fold selectivity for MET compared with more than 150 kinases, making it one of the most selective MET inhibitors described to date. PF-04217903 inhibits tumour cell proliferation, survival, migration/invasion in MET amplified cells *in vitro*, and demonstrates marked antitumor activity in tumour models harbouring MET gene amplification or HGF/MET autocrine loop at well-tolerated dose levels *in vivo*. The antitumor efficacy of this compound is dose-dependent and correlates with the inhibition of MET phosphorylation, downstream signalling and tumour cell proliferation and survival[212].

- **ARQ197** (Tivantinib) (ArQule): it is a non ATP competitive drug that was identified as a selective MET inhibitor in a screen that assessed the biochemical profile of 230 kinases. It is uniquely the first non-ATP-competitive small molecule that selectively targets MET receptor tyrosine kinase, with the mechanism of action as locking the kinase in a "closed" and "inactive" conformation when bound to the drug. In vivo study demonstrated its antitumor activity in various cancers (colon, gastric, and breast cancers)[213]. A number of phase 2 trials have been performed to investigate the effects of ARQ197 in various malignancies. It has demonstrated clinical benefit (in terms of prolonged stable disease) in phase II clinical testing among patients with several types of solid tumours, including NSCLC, sarcomas, pancreatic cancer, hepatocellular carcinoma, germ cell tumours and colorectal cancer[214,215]. It has recently completed a phase II clinical trial (ARQ197-209) in advanced NSCLC patients to analyse ARQ197 effects in combination with Erlotinib[216]. First reports shown an increased response rate and overall survival when ARQ197 is combined with Erlotinib. Interestingly, ARQ197 combined

with Erlotinib was also found to delay tumour metastases in this phase 2 study. Based on these results, ARQ197 has entered a randomized, double-bind, placebo-controlled phase III study in previously treated patients with metastatic NSCLC[216,217]. Unfortunately, the lack of molecular selection in this study has lead to a lack of benefit of this approach.

- **XL-880** (Foretinib) (Exelixis): it is a multitargeted small-molecule kinase inhibitor that targets MET and members of the VEGF receptor kinase families, with additional inhibitory activity toward KIT, FLT-3, PDGFR β, Tie-2, RON, and AXL. In vivo, these effects produce significant dose-dependent inhibition of tumour burden in an experimental model of lung metastasis[218]. A phase I study of Foretinib has been conducted in metastatic or unresectable solid tumour patients and a stabilization of the disease in 55% of the treated patients was found[219]. It is undergoing phase II trials in patients with poorly differentiated diffuse gastric cancer, head and neck squamous-cell carcinomas, and papillary renal cell carcinoma. It is currently ongoing a phase 1/2 clinical trial that considers the combination of this inhibitor with Erlotinib in locally advanced or metastatic NSCLC. Moreover, a phase 1/2 study of XL880 in combination with lapatinib in patients HER2 overexpressing metastatic breast cancer is now recruiting patients[220,221].

- **XL-184** (Cabozantinib) (Exelixis): it is a tyrosine kinase inhibitor for the potential oral treatment of medullary thyroid cancer, glioblastoma multiforme and NSCLC. The principal targets of XL-184 are MET, VEGFR-2 and RET, but the drug is also reported to display inhibitory activity against KIT, FLT3 and TEK. Treatment with cabozantinib

inhibits MET and VEGFR2 phosphorylation *in vitro* and in tumour models *in vivo* and reduces cell invasion *in vitro*. In mouse models, cabozantinib dramatically alters tumour pathology, resulting in decreased tumour and endothelial cell proliferation coupled with increased apoptosis and dose-dependent inhibition of tumour growth in breast, lung, and glioma tumour models. Importantly, treatment with cabozantinib does not increase lung tumour burden in an experimental model of metastasis[222].

The drug exhibits significant oral bioavailability and blood-brain barrier penetration. It is undergoing phase I trial in patients with advanced solid malignancies, phase II trial in patients with progressive or recurrent glioblastoma and NSCLC, and phase III trial in patients with medullary thyroid cancer[223].

- **MGCD265** (Methylgene): It is a tyrosine kinase inhibitor that targets the MET, VEGFR1, VEGFR2, VEGFR3, Ron and Tie-2 receptor tyrosine kinases, which appear to play key roles in tumour development and blood vessel formation (angiogenesis) and tumour survival. *In vivo* antitumour activity of MGCD265 has been reported in combination with docetaxel, paclitaxel or erlotinib in multiple xenograft models including NSCLC models that express an EGFR mutant resistant to erlotinib (T790M). The combination *in vivo* of MGCD265 with either a taxane or erlotinib resulted in improved antitumour activities when compared to treatments with either agent alone. MGCD265 has completed a phase 1 single agent study for solid tumour cancers, and is nearing completion of a phase I single agent clinical trial and two phase 1/2 combinations, one with docetaxel and one with erlotinib in solid tumours[224,225].

- **MK2461** (Merck): it is an ATP-competitive multitargeted inhibitor of activated MET. It is currently in Phase I/II clinical trials in patients with advanced solid tumours[182,225].

- **Golvatinib** (Eisai Co., LTD.): it is a novel small molecule ATP-competitive inhibitor of MET receptor that potently and selectively inhibits the autophosphorylation of MET and VEGF-induced phosphorylation of VEGFR. Golvatinib also circumvents resistance to reversible, irreversible and mutant-selective EGFR-TKIs induced by exogenous and/or endogenous HGF in EGFR mutant lung cancer cell lines, by blocking the MET/Gab1/PI3K/AKT pathway in vitro and also prevents the emergence of gefitinib-resistant cells, induced by continous exposure to HGF[226]. A phase 1 study with oral daily Golvatinib administered continuously once a day in patients with advanced solid tumours was performed[227].

- **MP-470** (SuperGen): it is an orally bioavailable small-molecule tyrosine kinase inhibitor of MET, although it also inhibits other protein tyrosine kinase targets, including mutant forms of c-Kit receptor, PDGFRα and Flt-3. It is shown that MP-470 radiosensitizes several Glioblastoma multiforme (GBM) cell lines both *in vitro* and *in vivo*, and may help to improve outcomes for patients with GBM[228]. It is undergoing Phase I/II trials in unspecified adult solid tumour. Furthermore, tumour responses in SCLC are observed in a phase Ib clinical study in combination with VP-16 and carboplatin. A phase II clinical trial is recruiting SCLC subjects who have not responded to standard treatment or relapsed after standard treatment[225].

- **JNJ-38877605** (Johnson & Johnson): it is an orally bioavaiable, small-molecule inhibitor of the MET receptor with potential antineoplastic activity. It potently inhibits HGF-stimulated and constitutively activated MET phosphorylation *in vitro*. It is undergoing Phase I trials in neoplasm[225,229].

In summary, the HGF/MET signalling pathway is implicated in development and progression of many tumour types. Aberrant activation of the MET receptor is found in many human cancers and seems to define a distinct clinical behaviour for this patient population. Moreover, preclinical and early clinical evidence support the role of MET as a promising therapeutic target for patients with MET activated tumours. Upcoming clinical data will define the patients and clinical scenarios that will benefit from MET inhibition as part of their therapeutic strategies.
SCLC is a disease characterized by high invasive and metastatic capacity, a typical feature of MET-activated tumour models. Preliminary evidence suggests that MET could be an interesting target in SCLC[46,230,231]. The aim of our work was to evaluate its relevance for SCLC patient outcome and the potential role of MET inhibitors for the treatment of this disease.

I.3. EPITHELIAL TO MESENCHYMAL TRANSITION (EMT)

One of the effects that have been described as a result of MET activation is EMT. MET activation displays the so called invasive growth program, first step of EMT. The invasive growth is a program of epithelial motility and morphogenesis that comprises several steps that occur at a particular time and place. All these events are required during embryiogenesis and in adult tissues to overcome injuries, but contribute to tumorigenesis and metastasis when aberrantly regulated. In cancer, the ability of neoplastic cells to invade the adjacent tissues, survive in foreign compartments and proliferate to settle at distant sites defines the invasive growth program.
EMT is a coordinated molecular and cellular process defined as a reduction in cell-cell adhesion, apical-basolateral polarity and epithelial markers, as well as an acquisition of motility, spindle-like morphology and mesenchymal markers. EMT was first recognized as a fundamental differentiation process in early embryogenic morphogenesis[232]. However, accumulating evidence suggests a critical role in cancer progression, as a potent mechanism that enhances the detachment of cancer cells from primary tumours and the invasion to other tissues[233,234].

I.3.1. Morphologic features and molecular markers of epithelial and mesenchymal cells

Epithelial cells present a highly apical-basolateral polarization essential for their biological functions. The epithelial cell basolateral surface is closely associated with neighbouring cells through keratin filaments and regularly

spaced membrane-associated specialised junctions, composed of desmosomes, adherens junctions and tight junctions[235].

The best characterized molecular marker expressed in epithelial cells is the transmembrane glycoprotein E-cadherin, localized in the adherens junctions and basolateral plasma membrane. The extracellular domain of E-cadherin mediates calcium-dependent homotypic interactions with adjacent cells, while the intracellular domain binds cytosolic catenins and provides a link to the actin cytoskeleton. This creates the communication between cell contact, regulation of cytoskeleton and cell shape, necessary for keeping the epithelial cells immobile and physically linked in the epithelial layer[236]. Early contacts between two cells are also mediated by E-cadherin molecules, which cluster into small complexes to form stable adherens junctions and promote the formation of desmosomes below them[237,238].

In contrast to well-differentiated epithelial cells, mesenchymal cells do not establish stable intercellular junctions. Mesenchymal cells present a reduced E-cadherin expression that causes adherens junction breakdown. Dissolution of adherens junctions imparts mesenchymal cells with a higher capacity to detach from the epithelial layer[239]. Mesenchymal cells lack the apical-basolateral polarity and posses and elongated morphology with front-back asymmetry that facilitates motility and locomotion. Filapodial extensions at the leading edge of the mesenchymal cells are enriched with integrin family receptors that interact with the extracellular matrix and also contain matrix metalloproteinases (MMP) that digest basement membranes and promote invasion[240,241]. Progression to a mesenchymal phenotype is also accompanied by increased expression of mesenchymal proteins, such as the intermediate filament protein Vimentin, highly associated with an invasive cellular phenotype[242]. Other cytoskeleton proteins or extracellular matrix components such as

Fibronectin are up-regulated in mesenchymal cells and can facilitate pseudopod formation and cytoskeletal remodelling[243]. Several transcription factors that strongly repress E-cadherin expression, such as members of the Snail, Zeb and bHLH families, are also up-regulated in mesenchymal cells and involved in tumour progression[244].

I.3.2. EMT in development and homeostasis

The basic point for the formation of a multicellular organism is the generation of an epithelium which consists of layer of continuous and polarized cells along the apical-basal axis. These structures contain closely associated cells that ensure the integrity of a tissue and establish a permeability barrier necessary to separate different tissues and create an embryo. However, during morphogenic events of the early stage of metazoan development, cells from early embryonic epithelium are internalised to form the mesodermal tissue. At this stage cells must be able to detach from the junctions that connect them to the neighbouring ones, change their shape and polarity, delaminate and migrate. The event responsible for such important changes is EMT. Furthermore, morphogenic movements during gastrulation and formation of organs depend on EMT [232]. In adults, during wound healing or tissue inflammation, new fibroblasts are formed by EMT and appear and retain a permanent mesenchymal state resulting in fibrosis[245].

I.3.3. EMT and cancer

Deregulation of EMT can also disturb normal epithelial homeostasis, contributing to cancer cell metastases.

During the progression of carcinomas, advanced tumour cells frequently exhibit downregulation of epithelial markers and a loss of intercellular junctions, resulting in a loss of epithelial polarity and reduced intercellular adhesion. This decrease in adhesive force facilitates the dispersion of carcinoma cells from the primary tumour mass. The decrease of epithelial features is often accompanied by expression of mesenchymal genes, loss of contact inhibition, degradation of extracellular matrix (ECM), altered growth control and increased cell motility and invasiveness. Furthermore, these tumour cells can acquire the ability to survive outside the epithelium in a relatively poorly structured and variable tissue environment. These molecular and morphologic features indicative of EMT often correlate with poor histologic differentiation, destruction of tissue integrity and metastasis. Therefore, EMT is often considered an indispensable process for tumour invasion and metastasis. However, it is important to consider the remarkable heterogeneity and plasticity present in cancer cells. Tumours encompass a highly diverse population of cells with different phenotypes. Although some carcinoma cells may undergo a complete transition to a mesenchymal phenotype, many of the defining characteristics of EMT are not present in all invasive or metastatic tumour cells. In fact, cancer metastases are often histopathologically similar to the primary tumours from which they are derived. To resolve this apparent contradiction, Mesenchymal-Epithelial Transition has been postulated as the process that explain the establishment and stabilization of distant metastasis and the histopathological similarity between primary and metastatic tumours. Such observations suggest that transitions between epithelial and mesenchymal-like states play an important role in tumour progression. Interestingly, these changes in cellular phenotype associated to tumour progression are frequently associated with molecular events described during development[233,246-248].

I.3.4. Molecular mechanisms involved in EMT and prognostic role

A variety of molecular pathways have been shown to contribute to EMT during embryogenesis and in tumorigenesis. The signalling pathways that can initiate the EMT are numerous, involving TGFβ and Tyrosine Kinase Receptors (RTKs) signalling, and Wnt-, Notch-, Hedgehog- and NF-κB-dependent pathways. Many of these mechanisms interact at multiple levels and regulate important cellular processes that can activate or repress EMT during development, homeostasis or disease[248]. EMT-inducing signalling pathways have many common endpoints: repression of E-cadherin by transcriptional regulators such as Snail1 or Twist emerges as one critical step driving EMT[249].

I.3.4.1. Epithelial markers

Some epithelial markers, such as E-cadherin and Neural Cell Adhesion Molecule CD56 (NCAM), are downregulated in many human tumours.
The gene encoding the adherens junctions E-cadherin is considered to be the paradigmatic epithelial gene. It mediates intercellular interactions and is important for the maintenance of tissue architecture[250]. Many experiments *in vitro* and *in vivo* have found an association between E-cadherin repression and higher cell invasion and metastasis[251,252]. E-cadherin downregulation is sufficient to trigger EMT in mammalian cell systems[253-255]. Therefore, loss of E-cadherin in an epithelial cell is normally considered the main hallmark of EMT.
E-cadherin has been found inactivated in human cancer[256]. It is described that the loss of E-cadherin can lead to tumour progression, metastasis

and poor prognosis in various human carcinomas[257-263]. During tumour progression, E-cadherin can be functionally inactivated or silenced by different mechanisms including somatic mutations, down-regulation of gene expression and transcriptional repression[264].

NCAM is another epithelial marker downregulated in cancer and associated with tumour metastasis. NCAM belongs to the immunoglobulin superfamily and is involved in cell adhesion regulating mechanisms, intracellular signalling and cytoskeleton dynamics[265,266].

Some observations suggest that this molecule is implicated in tumour metastasis[267]. A correlation between reduced NCAM expression and poor prognosis has been reported for a few cancer types[268-270].

I.3.4.2. Mesenchymal markers

Many mesenchymal markers have been found overexpressed and associated with chemoresistance and poor survival in different human tumours. The expression of the mesenchymal marker Vimentin in breast and gastric cancer and NSCLC associated with a malignant phenotype and poor survival has been reported[271-273]. Another important mesenchymal marker, the glycoprotein Fibronectin, is also expressed in several human tumours such as bladder, colorectal and ovarian carcinomas. Furthermore, Fibronectin correlates with higher histologic grade, liver metastasis and prognosis in colorectal cancer and it is associated with poor survival in ovarian carcinoma[274-276]. The expression of the mesenchymal marker N-cadherin is also associated with tumour aggressiveness in esophageal carcinoma and correlates with angiogenesis in NSCLC. It is also a novel prognostic factor of progression in superficial urothelial tumours[277-279].

I.3.4.3. E-cadherin transcriptional repressors

The most important E-cadherin transcriptional repressors associated to EMT belong to the Snail-related zinc-finger transcription factors (Snail1 and Slug), the Zeb family (Zeb1 and Zeb2) and the bHLH family (Twist)[249].

SNAIL family

SNAIL transcriptional repressors, and particularly Snail (Snail1), are the most widely studied effectors of EMT and E-cadherin expression. The three members belonging to the SNAIL family have been called Snail (Snail1), Slug (Snail2) and the less characterized Scratch (Snail3). All the family members encode transcription factors of the zing-finger type. They present a similar organization with a highly conserved C-terminal domain (which contains from four to six zinc fingers) and a quite divergent amino-terminal region. Zinc fingers function as sequence-specific DNA binding motifs.

Snail1 is the most well-characterized homolog of the family and is expressed during mesoderm formation, gastrulation and neural crest development, as well as in most developmental processes in which EMT is required[249]. Snail1 appears to be the major E-cadherin repressor in most studies focusing on tumour progression. Different reports demonstrate that Snail1 is capable of binding E-cadherin E-boxes and repressing its transcription, consequently inducing EMT. This transcription factor is sufficient to downregulate E-cadherin expression and induces EMT *in vitro*. Furthermore, forced EMT in cultured cells correlates with induction of Snail1[280,281].

SNAIL transcriptional repressors, in particular Snail1, have been associated with tumour progression, chemoresistance and poor prognosis in many cancer types[282-287].

Snail1 is associated with downregulation of E-cadherin, tumour recurrence and poor prognosis in various human carcinomas, including breast, colorectal, ovarian, sarcoma, squamous-cell, oesophageal and hepatocellular carcinoma[282-290]

The expression of the transcription factor Slug is also an indicative of metastasis and poor prognosis in cancer[291-295].

I.3.5. EMT-associated resistance to cancer therapies

Emerging data suggests that EMT is also associated with drug resistance and tumour relapses, representing an escape mechanism from apoptosis. Therefore, the acquisition of a mesenchymal phenotype induces a multifaceted capacity to proliferate, migrate and avoid death and permanent arrest in tumour cells, as well as protection from extracellular signals and drug effects. There is growing evidence that demonstrates the association between EMT and chemoresistance in cancer. **Table I.2**. summarises EMT-associated resistance to cancer therapies found in several studies. One common finding is that EMT is a determinant of sensitivity to different biological and chemotherapy agents *in vitro* and *in vivo* in cancer models. It is described that cancer cell lines undergone EMT present resistance to EGFR inhibitors, such as Erlotinib, Gefitinib or Cetuximab in lung, hepatocellular, urothelial and head and neck squamous cell carcinomas[296-300]. As shown in **Table I.2.**, EMT-related transcription factors, such as Snail1 or Twist, are also associated with drug resistance in several cancer models[301-306]. In other studies represented in **Table I.2**. are reported that cancer epithelial cell lines

made resistant to different chemotherapy agents (Oxaliplatin, Paclitaxel, Gemcitabine) exhibit a mesenchymal morphology and express several markers of EMT. Finally, few publications have addressed the role of EMT in the chemoresistance of cancer patients[307-310].

Table I.2. EMT-associated resistance to cancer therapies

Tumour type	EMT markers	Drug Resistance	Description	Reference
Lung Cancer	Vimentin, N-cadherin, E-cadherin	Erlotinib in combination with chemotherapy	Epithelial versus mesenchymal phenotype determines in vitro sensitivity and predicts clinical activity of Erlotinib in lung cancer patients	296
NSCLC	E-cadherin, Vimentin, Fibronectin	Erlotinib	EMT is a determinant of sensitivity of NSCLC cell lines and xenografts to EGFR inhibition	297
HNSCC and NSCLC	E-cadherin, Claudin7, Claudin4, Vimentin	Gefitinib	EMT predicts gefitinib resistance in cell lines of HNSCC and NSCLC	298
Hepatocellular carcinoma	E-cadherin, Vimentin	EGFR inhibitors	EMT and integrin-linked kinase mediate sensitivity to EGFR inhibition in human hepatoma cells	299
Urothelial Carcinoma	E-cadherin, beta-catenin, Vimentin	Cetuximab	Sensitivity to EGFR inhibitor requires E-Cadherin expression in urothelial carcinoma cells	300
Nasopharyngeal, bladder, ovarian, and prostate carcinoma	Twist	Taxol	Identification of a novel function of TWIST, a bHLH protein, in the development of acquired taxol resistance in human cancer cells.	301
Breast Cancer	Twist, Vimentin, Fibronectin, E-cadherin, beta-catenin	Paclitaxel	Twist transcriptionally up-regulates AKT2 in breast cancer cells leading to increased migration, invasion, and resistance to paclitaxel	302
Breast Cancer	Twist, Vimentin, E-cadherin	Doxorubicin	Twist1-mediated adriamycin-induced EMT relates to multidrug resistance and invasive potential in breast cancer cells	303
Ovarian Cancer	Snail, Slug	Paclitaxel, g-radiation	Snail and Slug mediate radioresistance and chemoresistance by antagonizing p53-mediated apoptosis and acquiring a stem-like phenotype in ovarian cancer cells	304
Breast Cancer	E-cadherin, Occludin, Claudin, Snail, Slug	Doxorubicin	Aberrant expression of the transcription factors snail and slug alters the response to genotoxic stress.	305
Colorectal Cancer	Vimentin, Snail, E-cadherin	5-fluorouracil (5-FU)	EMT with expression of SNAI1-induced chemoresistance in colorectal cancer	306

Tumour type	EMT markers	Drug Resistance	Description	Reference
Colorectal Cancer	Snail, Slug, Vimentin, Twist, E-cadherin, beta-catenin	Oxaliplatin	Chronic oxaliplatin resistance induces EMT in colorectal cancer cell lines	307
Ovarian Cancer	E-cadherin, Fibronectin, Vimentin	Paclitaxel	Chemoresistance to paclitaxel induces EMT and enhances metastatic potential for epithelial ovarian carcinoma cells.	308
Pancreatic Cancer	E-cadherin, beta-catenin	Gemcitabine	Development and characterization of gemcitabine-resistant pancreatic tumor cells	309
Pancreatic Cancer	Vimentin, ZEB1, Twist, Fibronectin, beta-catenin, E-cadherin	Gemcitabine	Acquisition of EMT phenotype of gemcitabine-resistant pancreatic cancer cells is linked with activation of the Notch signaling pathway	310

I.3.6. EMT-inducing signalling pathways

Several inductors of EMT have been described such as Wnt/β-catenin signalling, Notch and Hedgehog signalling and NFκB-dependent pathways. The classical inductor of EMT is TGFβ.

I.3.6.1. TGFβ

Transforming Growth Factor β (TGFβ) family of cytokines, which binds to transmembrane receptor serine/threonine kinases, are involved in cell growth, proliferation, differentiation, deposition of ECM and migration. Moreover, signalling through TGFβ is a potent mechanism to promote the phenotypic changes of EMT. TGFβ-dependent EMT in cancer cells coincides with loss of E-cadherin expression, mediated by the ability of TGFβ to induce the expression of the transcriptional repressors Slug, Snail1 or Zeb1[311,312]. TGFβ is frequently present in the tumour microenvironment, initially as a signal to prevent premalignant progression, but eventually as a factor that malignant cells may use to their own advantage. The presence of TGFβ has been documented in

many human tumours, indicating that this cytokine is associated with cancer. The accumulation of TGFβ at the invasive front of the tumour, and its association with tumour progression have been described[313,314].

I.3.6.2. Tyrosine Kinase Receptors (RTKs)

Many of the mechanisms that contribute to EMT involve growth factors that promote various signalling cascades through their cognate receptor tyrosine kinases (RTKs), such as Fibroblast Growth Factor (FGF), Insulin-like Growth Factor (IGF), Epidermal Growth Factor (EGF), Platelet-derived Growth Factor (PDGF) or Hepatocyte Growth Factor (HGF). Downstream kinases, including Ras, Src, PI3K and MAPK, have all been implicated in promoting a malignant phenotype. Activation of Src can increase invasiveness and promote the degradation of E-cadherin, whereas downstream targets of Ras and MAPK include Snail1 and the related protein Slug. The activation of RTKs signalling pathways also result in a disassembly of junctional complexes and important changes in the cytoskeletal organization that occur during EMT[248,315,316].

I.3.7. Role of HGF/MET pathway in EMT

As mentioned above, HGF is a multifunctional molecule that induces mitogenic and morphonenic activities in developmental as well as in many pathophysiological processes. Multiple lines of evidence exist indicating that HGF and MET play a critical role in the invasive growth of tumour cells, a hallmark of metastatic cancers. Malignant tumour progression involves multiple steps as loss of cell-cell adhesion, cell migration or invasion, survival in the bloodstream and colonization of distant tissues. HGF-induced signalling could contribute to these steps by

its pleiotropic effects on cell scattering, production of metalloproteinases, induction of anti-apoptotic signals and induction of cellular proliferation and angiogenesis[317]. HGF is well known for its ability to induce cell motility and a scattered phenotype in various epithelial cell types, where loss of tight and adherent junctions is a requirement. It has been shown that the scattered phenotype induced by HGF is equivalent to an EMT, at least in defined cellular models[318]. In fact, extensive experimental studies in various cancer models provide convincing evidence that HGF/MET pathway activation can induce EMT. It is reported in several cancer cell lines that HGF-induced cell scattering correlates with E-cadherin downregulation, activation of some EMT-related transcription factors such as Snail1 or Slug, and transcriptional activation of matrix metalloproteinases. In human hepatocarcinoma cell lines HGF induces scattering and EMT by upregulating the expression of Snail1 through the Ras/Raf/MAPK signal transduction pathway (**Figure I.6.**). Moreover, this Snail1 upregulation was required for HGF-induced cell scattering in this model[318]. Other studies in hepatocellular carcinoma also demonstrate that HGF/MET signalling can induce EMT in cell lines, whereas the pharmacological inhibition of MET activity with a small molecule inhibitor reversed the HGF/MET induced- fibroblast-like morphology[319,320]. Another work reports that HGF stimulation of hepatocellular carcinoma cell lines induced downregulation of E-cadherin and cell scattering through the activation of the Wnt/β-catenin signalling pathway and the transcriptional activation of matrix metalloproteinases. The results obtained suggest that blocking the HGF/MET pathway might present a practical therapeutic target for interference with hepatocellular carcinoma metastasis[321]. It is also described that HGF induces EMT-like morphologic changes that correlate with the downregulation of E-cadherin and the upregulation of Snail1 and N-

cadherin expression in hepatocellular carcinoma cell lines. Interestingly, knockdown of Snail1 or pharmacological inhibition of MAPK pathway cancelled the HGF-mediated EMT[320]. HGF is also reported to induce EMT in bladder carcinoma cells, and suppression of the transcription repressor Slug is able to inhibit the HGF-induced EMT in this model[322]. In addition, it is described that Slug is highly and transiently upregulated during the HGF-induced partial-EMT phase of canine kidney epithelial cells tubulogenesis[323]. Other studies demonstrate that HGF-induced MET activation can modulate the expression of E-cadherin in gastric carcinoma, which is accompanied by a more aggressive phenotype[324]. Furthermore, in ovarian carcinoma, an important mesenchymal marker, Fibronectin, promotes cancer invasion and metastasis through the interaction with $\alpha 5\beta 1$-integrin and the specific activation of the MET signalling pathway[325].

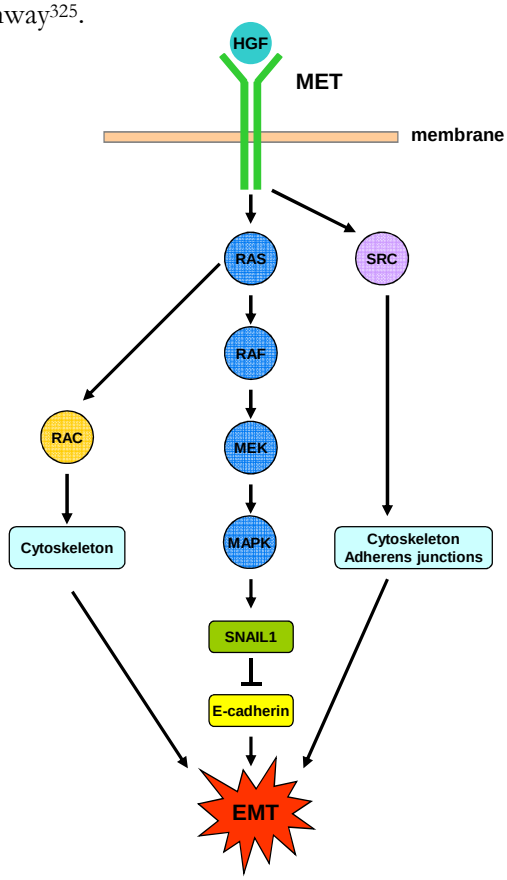

Figure I.6. Molecular mechanisms underlying HGF-induced EMT. Binding of HGF to its receptor leads to autophosphorylation of MET and the activation of the RAS/RAF/MAPK pathway. Activated MAPK then phosphorylates and activates immediate early transcription factors, which bind the Snail1 promoter and induce Snail1 expression. Snail1 then binds the promoter of its target genes, such as E-cadherin, repressing its transcription and inducing EMT. HGF/MET pathway also activates other intracellular effectors molecules, such as RAC or SRC, effectors that orchestrate the disassembly of junctional complexes and the changes in cytoskeletal organization that occur during EMT.

I.3.8. EMT in lung cancer

Several studies exist indicating that EMT may occur during lung cancer development. The loss or switch of adhesion molecules and the expression of classically mesenchymal markers have been associated with the induction of mesenchymal changes and carcinoma aggressiveness in lung cancer. A number of studies have reported that expression of molecules involved in EMT correlate with clinicopathological features in lung cancer patients[295,326-329].

In general, several studies report the expression of epithelial markers in the central region of lung tumours adjacent to a region with mesenchymal features near the invasive front[326,329-331].

Table I.3. summarizes the relevance of EMT molecules expression in lung cancer and its correlation with clinicopathological features. Numerous reports have found that loss of E-cadherin function or expression is quite common in NSCLC. However, high E-cadherin expression correlates with increasing histological differentiation in these tumours[332]. It is described that lung cancer patients who have tumours with reduced expression of E-cadherin have a significantly poorer prognosis compared with patients with E-cadherin positive

tumours[272,332,333]. It is also reported that NSCLC specimens present higher levels of mesenchymal markers compared with normal bronchial epithelium[329]. Overexpression of mesenchymal markers such as Vimentin predicts poor outcome in NSCLC patients[272]. In addition, several studies report expression of EMT-related transcription factors (Snail1, Slug, Twist) and correlation with tumour progression, invasion and decreased survival in NSCLC patients[295,327,331,334]. The classical EMT inductor TGFβ is also associated with angiogenesis, tumour progression and prognosis in patients with NSCLC[335]. In fact, several lung cancer cell lines undergo EMT upon TGFβ treatment [336,337]. Focusing on SCLC, it is also observed a correlation between β-catenin cytoplasmic overexpression with a shorter time to progression as well as with a shorter overall survival[332].

Emerging evidence suggests that EMT is also associated with drug resistance and tumour relapses in lung cancer. Lung cancer cell lines having undergone EMT are insensitive to the growth inhibitory effects of EGFR kinase inhibitors (Erlotinib, Gefitinib, Cetuximab) *in vitro* and in xenografts. Epithelial but not mesenchymal gene signature has been associated with sensitivity to Erlotinib. Further clinical trials confirmed a clinical benefit in patients with NSCLC with high expression of E-cadherin and who received Erlotinib[296,297]. In addition, several studies have reported that treatment with EGFR specific inhibitors on patients with EGFR mutant lung cancer induces EMT, which may account for the acquired resistance to EGFR inhibitors[338].

Table I.3. Relevance of EMT-molecules expression in lung cancer

Molecules	Histological Lung cancer subtype	Relevance	References
E-cadherin	NSCLC	Expression in the central region of lung tumours Common loss of its expression or function in lung cancer Increased expression correlates with histological differentiation Reduced expression correlates with poor patient survival High expression is a positive prognostic indicator for disease-specific survival	272, 332, 333
Vimentin	NSCLC	High expression is a negative prognostic factor	272
Snail	NSCLC	Common upregulation in NSCLC tissue Expression near the invasive front High expression correlates with decreased survival	327, 334
Slug	NSCLC	Promotes carcinoma invasion Expression near the invasive front Predicts outcome of patients	295, 331
Twist	NSCLC	Predicts outcome of patients	327
TGFβ	NSCLC	Promotes angiogenesis and tumour progression Increased levels correlate with poor prognosis Induce EMT in some lung cancer cell lines	335, 336, 337
β-catenin	NSCLC SCLC	Reduced expression is significantly associated with a poor prognosis Cytoplasmic overexpression correlates with a shorter time to progression and shorter overall survival	328, 332

In summary, activation of the HGF/MET axis is able to induce EMT in different tumour models. The aim of our work was to confirm this hypothesis in our SCLC cell line models and to validate it in human samples.

HYPOTHESIS

HYPOTHESIS

We hypothesised that the HGF/MET pathway activation as an inducer of EMT would be a mechanism of progression and chemoresistance in SCLC. Therefore, HGF/MET inhibition could be a plausible therapeutic strategy for SCLC patients with activation of this pathway.

OBJECTIVES

OBJECTIVES

The general objective of this PhD thesis was to evaluate the role of HGF/MET pathway in SCLC, the relationship with EMT and its potential therapeutic interest in this disease.

The specific objectives were:

1. **To Characterize the HGF/MET pathway in SCLC**
    - To analyse MET status (mutation, amplification or activation) in SCLC cell lines.
    - To assess MET expression and phosphorylation in clinical SCLC specimens.
    - To study HGF levels in SCLC serum samples from patients at diagnosis and relapses.

2. **To evaluate whether HGF-mediated EMT has a role in the biological behaviour of SCLC**
    - To evaluate whether HGF-induced MET activation is able to result in EMT in SCLC cell lines.
    - To assess the biological effects of the HGF-induced EMT in SCLC cell lines *in vitro* and *in vivo*.

3. **To study the role of MET inhibitors in SCLC**
    - To analyse cellular and molecular effects of MET inhibitors as monotherapy or in combination with chemotherapy in SCLC cell lines *in vitro* and *in vivo*.

- To test *in vitro* and *in vivo* whether MET inhibition is able to prevent or revert HGF-induced EMT in SCLC cell lines.

4. To analyse EMT biomarkers in SCLC samples

- To analyse EMT markers in clinical SCLC specimens and their correlation with MET status.
- To study the association of EMT biomarkers with the prognosis of SCLC patients.

RESULTS

R.1. SCLC CELL LINES CHARACTERIZATION

For our preclinical work and in order to characterize thoroughly SCLC behaviour we worked with 11 SCLC cell lines in an initial approach. **Table R.1.** and **Figure R.1.** summarize the characteristics of these cells lines. Globally, we observed two patterns of growth: cells that can grow as cultures in suspension (i.e.H69) and cells that can grow as adherent cultures (anchorage dependent) (i.e.H865). Cells in suspension presented a rounded small morphology and grew as floating aggregates. Adherent cells were larger in size and more elongated than the rounded suspension cells.

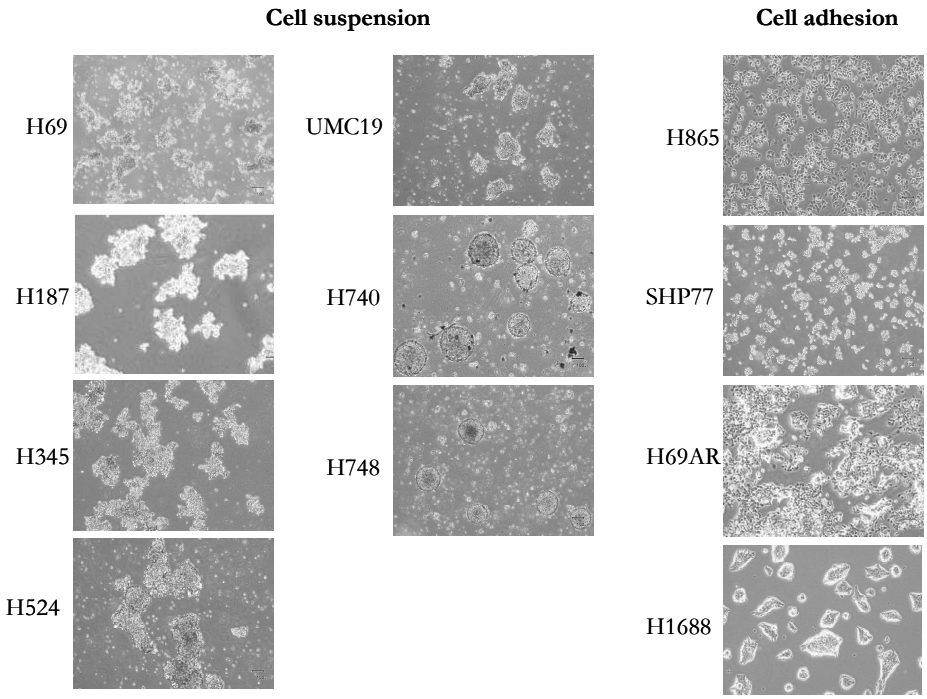

Figure R.1. Cell morphology of SCLC cell lines. Light microscopy images showing different growth patterns of SCLC cell lines.

Table R.1. Characteristics of SCLC cell lines

Cell line	Origin	Cell type	Growth properties
NCI-H69	Primary small cell lung carcinoma	Classic SCLC	Cell aggregates in suspension
H69AR	Small cell lung carcinoma. Derived from H69 cell line treated with increasing concentrations of Doxorubicin during 14 months	Chemoresistant SCLC	Cell adhesion
NCI-H187	Small cell lung carcinoma. Derived from metastatic site: pleural effusion	Classic SCLC	Cell aggregates in suspension
NCI-H345	Small cell lung carcinoma. Derived from metastatic site: bone marrow	Classic SCLC	Cell aggregates in suspension
NCI-H524	Small cell lung carcinoma. Derived from metastatic site: lymph node. The patient received prior chemotherapy and radiation therapy	Classic SCLC	Cell aggregates in suspension
UMC19	No ATCC information	Classic SCLC	Cell aggregates in suspension
NCI-H865	Small cell lung carcinoma. Derived from metastatic site: pleural effusion. The patient received prior chemotherapy and radiation therapy.	Chemoresistant SCLC	Cell adhesion
SHP-77	Small cell lung carcinoma. Derived from a non-encapsulated primary lung tumour from the apical portion of the upper lobe of the left lung	Large cell variant	Cell suspension and loosely adherent
NCI-H1688	Small cell lung carcinoma. Derived from a liver metastasis taken from a patient prior to therapy	Epithelial	Cell adhesion
NCI-H740	Small cell lung carcinoma. Derived from metastatic site: lymph node.	Classic SCLC	Cell aggregates in suspension
NCI-H748	Small cell lung carcinoma. Derived from metastatic site: lymph node. The patient received prior chemotherapy and radiation therapy	Classic SCLC	Cell aggregates in suspension

R.1.1. Chemotherapy effects on viability in SCLC cell lines

As chemotherapy is the standard treatment for SCLC patients, cell viability was analysed by MTS assay. First of all we evaluate tumour cell sensitivity to standard first line chemotherapy used in SCLC patients: cisplatin and etoposide (**Figure R.2**). To this objective we selected 5 SCLC cell lines: H69, H69AR, H524, H865 and SHP77. We did not evaluate the sensitivity to chemotherapy in the remaining SCLC cell lines for technical reasons.

Figure R.2 shows different chemosensitivity of our panel of SCLC cell lines. Cell lines obtained from SCLC patients that had received chemotherapy or radiation therapy (H865 and SHP77 cell lines) presented partial resistance to cisplatin or etoposide in comparison with cell lines obtained from patients prior to therapy (H69 and H524 cell lines). Interestingly, cells that grew in suspension were in general more sensitive to chemotherapy that cells growing adhered to the plate. This could suggest that the changes that provide the ability to adhere can also be related to chemoresistance.

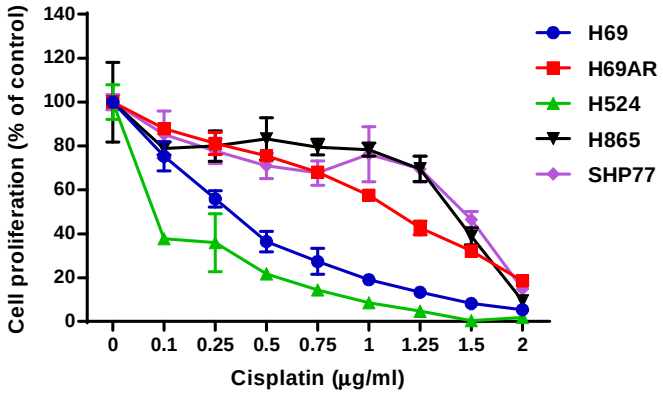

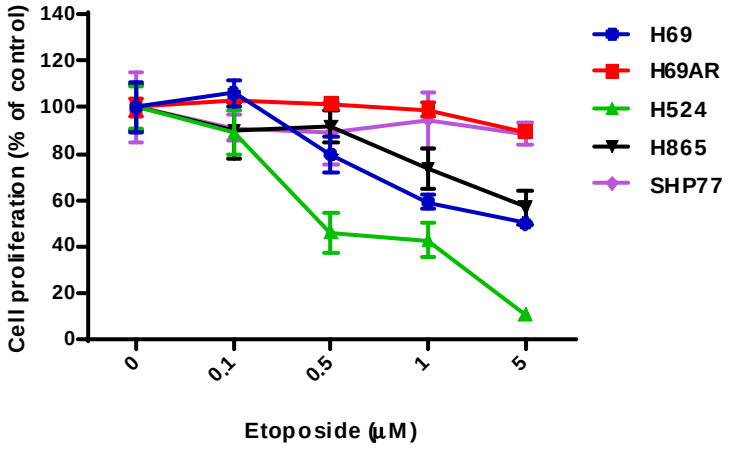

Figure R.2. Sensitivity of SCLC cell lines to chemotherapy. Sensitivity of H69, H69AR, H524, H865 and SHP77 cells to continous Cisplatin or Etoposide exposure for 72 hours, assessed by MTS assay. Each data point represents the mean ± s.d. percent cell growth of three independent experiments. Data are reported as percentage in relation to the control group (set at 100%).

R.1.1.1. H69AR cells present a more aberrant karyotype when compared to H69

To evaluate potential causes of chemoresistance in SCLC we analysed the chromosomal differences in one isogenic cell line pair within our panel: H69 and H69AR (chemoresistant cells derived from H69 subjected to prolonged exposure to doxorubicin)[339]. First of all, we confirmed that H69AR cells were highly resistant (10-fold) to doxorubicin when compared to H69, as previously reported[340] (**Figure R.3A**).

Then, we performed spectral karyotyping (SKY) analysis of both cell lines to screen for the overall pattern of chromosomal changes that could explain chemoresistance and to explore the MET containing region.

H69AR cells presented a more aberrant karyotype than that of parental cells. SKY analysis of H69 cell line revealed three new alterations not

previously defined by G-banding and confirmed seven, as previously reported[339,341]. H69AR SKY karyotype confirmed 10 new structural abnormalities not observed in the parental H69 karyotype and identified new breakpoints. Of note, these chromosomal alterations did not affect the region that codifies *MET* gene (**Figure R.3B**).

A

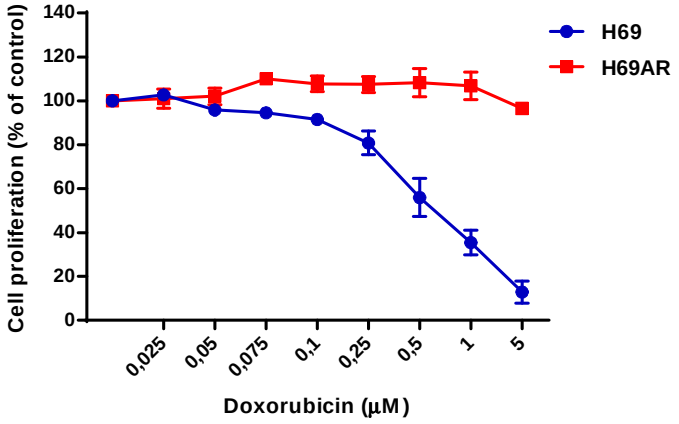

B

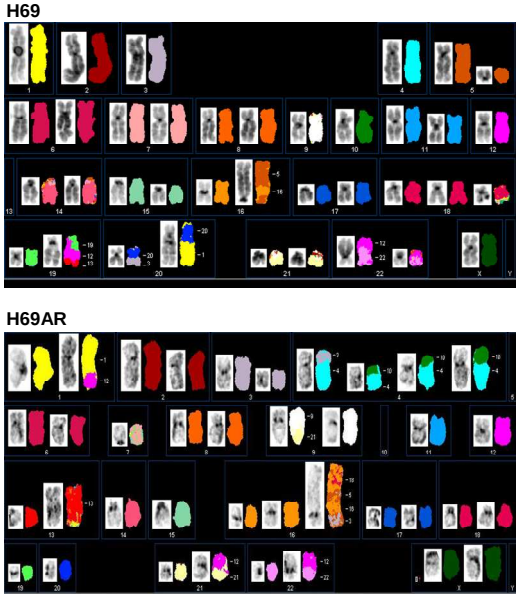

H69	H69AR
der(16)t(5;16)(q11;p13)	der(16)t(3;16;18;5;18)
del(11)(q23)	del(11)(q23)
add(12)(p13)	der(1)t(1;12)(p12;q11)
del(17)(p13)	del(17)(p13)
der(18)	der(18)
der(19)t(12;13;19)	der(19)t(12;13;19)
der(20)t(1;20)(q21;p13)	der(20)t(1;20)(q21;p13)
der(22)t(12;22)(p11;q11)	der(22)t(12;22)(p11;q11)
der(20)t(3;20)	--
del(15)(q22)	der(15)t(X;15)(q11;p11)
--	der(5)t(5;15)
--	der(3)t(3;4)(p21;?)
--	der(4)t(3;4)(?;p15)
--	der(7)t(1;7)(q25;q22)
--	der(9)t(9;21)(q34;?)
--	der(7)t(7;14)(p22;?)
--	der(10)t(4;10)(q21;p11)x2
--	der(13)t(13;18)(q?;q?)
--	der(21)t(12;21)

Figure R.3. H69AR cells are resistant to Doxorubicin and present a more aberrant karyotype when compared to H69.

A. Sensitivity of H69 and H69AR cells to Doxorubicin treatment for 72 hours, measured by MTS assay. Each data point represents the mean ± s.d. percent cell growth of three independent experiments. Data are reported as percentage in relation to the control group (set at 100%). **B.** SKY karyotyping showing chromosomal aberrations of H69 and H69AR SCLC cells using the SKY technique.

R.2. HGF/MET PATHWAY CHARACTERIZATION IN SCLC CELL LINES

R.2.1 MET status in SCLC cell lines

To investigate the role of MET in our panel of SCLC cells, we first characterized *MET* gene mutational status, gene copy number and protein expression. **Table R.2.** illustrates results of MET evaluation by sequencing, FISH and Western Blot.

(Next page)

Table R.2. MET status in SCLC cell lines

Name	FISH MET		Previously described mutations *	MET protein expression
NCI-H69	95% 2O2G	Disomic	R988C	Yes
H69AR	77% 4O3G	MET gain (chromosome 7 trisomy)	R988C	Yes
NCI-H187	56% 3O4G, 23% 3O3G	MET relative loss	No	Yes
NCI-H345	65% 3O3G, 20% 2O2G, 12% 2O3G	65 % chromosome 7 trisomy 12% MET relative loss	No	Yes
NCI-H524	48% 2O2G, 25% 3O2G, 10% 3O3G	MET gain (chromosome 7 trisomy)	No	Undetectable
UMC19	58% 3O4G, 15% 4O5G, 17% 3O3G	MET relative loss	No	Undetectable
NCI-H865	77% 3O3G, 8% 4O4G, 12% 2O2G	3-4 copies of chromosome 7	No	Yes
SHP-77	47,5% 2O3G, 44,5% 2O4G	MET relative loss	No	Undetectable
NCI-H1688	95% 2O2G, 5% 4 4O4G	Disomic	No	Yes
NCI-H740	62% 4O4G, 14% 3O3G, 4% 5O5G	62% 4 copies chromosome 7 4 % 5 copies chromosome 7	No	Undetectable
NCI-H748	76% 3O2G, 17% 3O3G, 7% 2O2G	MET relative loss	No	Undetectable

Abbreviations: O = orange probe (MET); G = green probe (chromosome 7 centromere)
* R988C, T1010I, E168C (MET mutations)

Interestingly, we observed that the H69 cell line harboured a previously described juxtamembrane polymorphism of MET (R988C)[47,231]. The H69 is a classical model of chemosensitive SCLC. We also observed that H69AR (chemoresistant cell derived from H69) also preserved the R988C polymorphism.

We could not detect the previously described *MET* polymorphisms (R988C, T1010I, E168C) in the rest of the cell lines. FISH analysis revealed different *MET* copy number changes with cases of losses (H187, SHP-77, H345 and UMC19 cell lines) and gains (H69AR, H524 and H748 cell lines), but no case with clear gene amplification. In addition, chromosome 7 gain was observed in our SCLC cell lines[342]. MET protein expression by WB also showed variable results with cell lines with high expression levels (H69, H69AR and H345 cells) and others with lower levels of total MET (H187, H865 and H1688 cells). Two bands of 170 kD and 145 kD were observed corresponding to the unprocessed and mature proteins, respectively (**Figure R.4**). No clear association was found between copy number state and protein expression levels.

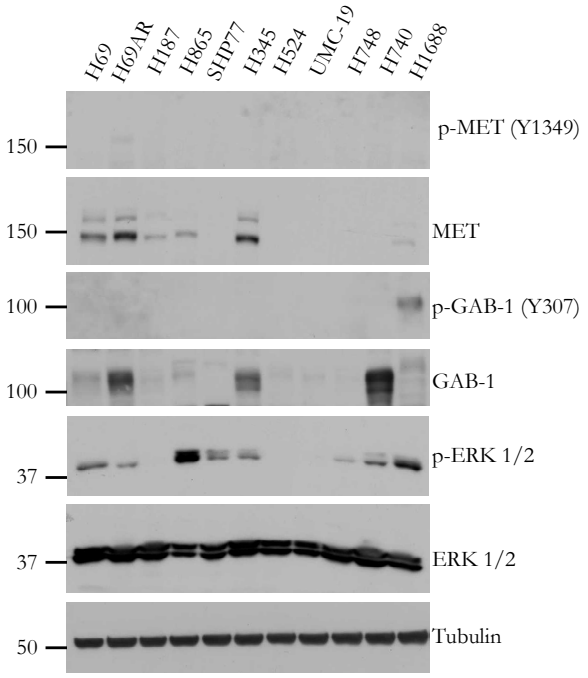

Figure R.4. Expression of HGF/MET pathway molecules levels in SCLC cell lines. Whole cell lysates from all SCLC cell lines were prepared and subjected to Western Blot analysis with the indicated antibodies.

R.3. EFFECTS OF HGF/MET MODULATION IN SMALL CELL LUNG CANCER

Based on the above findings we selected SCLC cells with distinct MET status as a potential surrogate variable that may identify differential effects of HGF stimulation or specific MET inhibition. H69 and H69AR were selected based on the previous literature as cell lines sensitive to MET modulation. In addition, we used H524 as a cell line with undetectable expression of MET protein, and H345 and H187 as cell models with different levels of MET protein expression. As a positive control we included the H1993 NSCLC cell line, known to harbour MET amplification and to be sensitive to MET inhibition[343].

R.3.1. HGF/PHA-665752 molecular effects in SCLC cell lines

To study the molecular effects of the MET pathway modulation in our selected cell lines we evaluated by Western Blot total and phosphorylated protein levels of MET and downstream relevant molecules ERK and GAB-1 upon MET stimulation and/or inhibition. To analyse MET pathway activation we stimulate SCLC cells with HGF (40 ng/ml) during 15'. To study HGF/MET pathway inhibition we used PHA-665752 (Pfizer Inc), a potent selective small molecule MET inhibitor that prevents MET phosphorylation at concentration in the nanomolar range[344].

Specifically cell lines were treated with PHA-665752 at 0.05 μM during 3 hours, and then stimulated with HGF (40 ng/ml) 15'. As in **Figure R.4.**, we again observed basal expression of total MET in H69, H69AR, H187 and H345 but not in the H524 SCLC cell line. As expected, MET-amplified H1993 cells showed high-levels of total MET. MET phosphorylation was undetectable in H69, H187, H345 and H524 at basal conditions. However, when we stimulated with HGF 15' we detected a clearly upregulated MET phosphorylation in H69, H69AR and H187 cell lines. H345 cells showed a slight increase in MET phosphorylation after HGF stimulation and H524 cells showed no change. The MET-amplified H1993 cells showed high levels of basal and phosphorylated MET and absence of MET modulation by HGF, as expected. Two MET phosphorylation sites (Tyr1234/1235 and Tyr1349) were evaluated, obtaining similar results. Absence of basal and phosphorylated GAB-1 was observed in H1993 cells, as this activation is ligand independent. We also observed GAB-1 and ERK phosphorylation after HGF addition in H69, H69AR, H187 and H345 cells (**Figure R.5A**).

Then, we found that PHA-665752 treatment (3 hours) was able to inhibit MET and downstream molecules phosphorylation in a dose dependent manner in H69, H69AR, H187, H345 and H1993 cells, obtaining a complete inhibition at 0.5 μM (**Figure R.5A** and **Figure R.5B**).

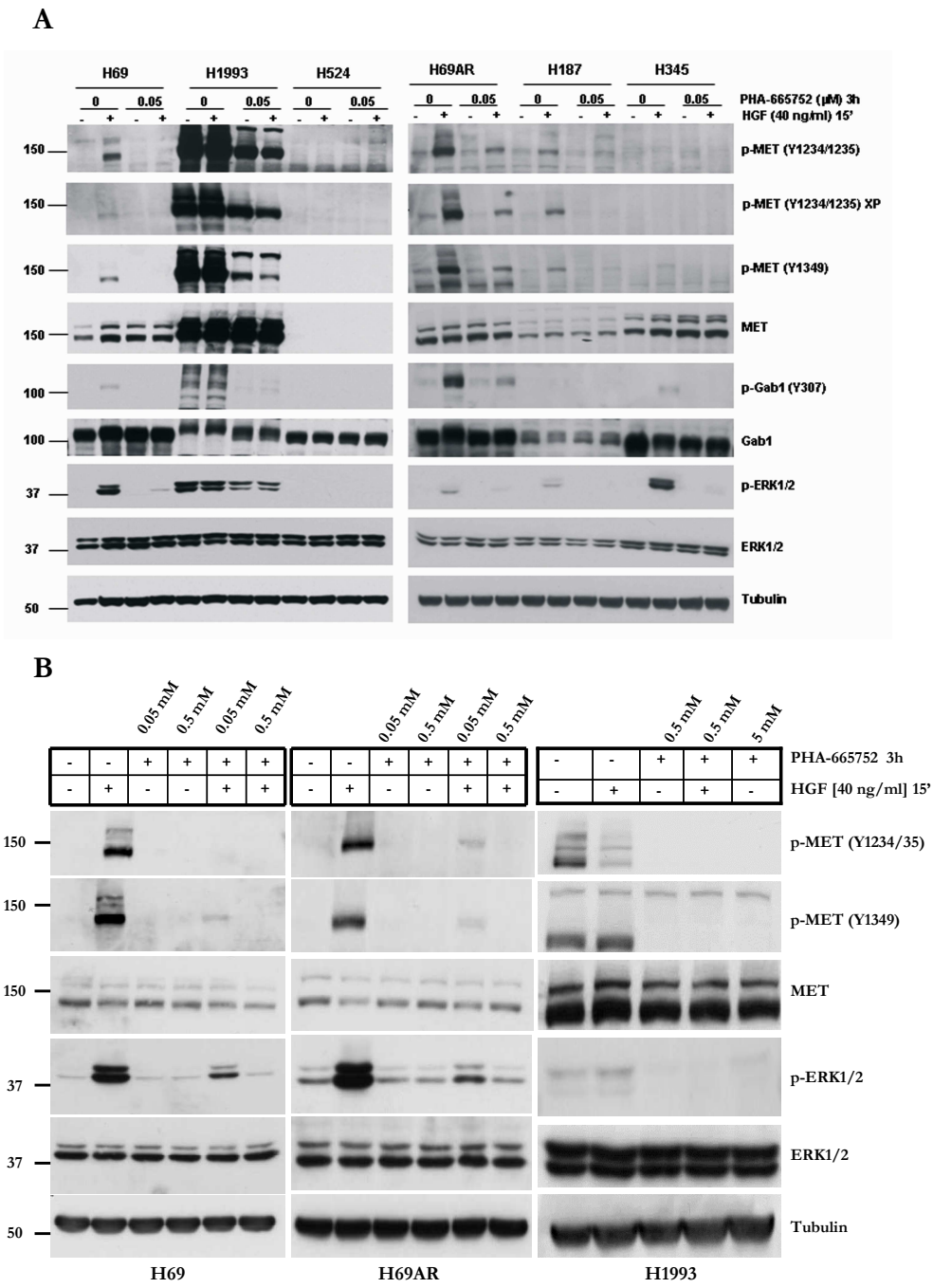

Figure R.5. HGF activates MET and downstream molecules in SCLC cells and PHA-665752 inhibits these effects. A. Cells were serum-starved for 24h and

then treated with PHA-665752 (0.05 μM) 3h and stimulated with HGF (40 ng/ml) during 15'. Whole cell lysates were purified and subjected to Western Blot to asses the expression of the indicated proteins. **B.** Cells were serum-starved for 24h and then treated with PHA-665752 (0.05 or 0.5 μM) 3h and stimulated with HGF (40 ng/ml) during 15'. Whole cell lysates were purified and subjected to Western Blot to asses the expression of the indicated proteins.

R.3.2. HGF/PHA-665752 cellular effects in SCLC cell lines

To analyze the cellular effects of MET pathway activation and inhibition in SCLC cell lines, we evaluated if cell proliferation, clonogenic capacity and cell invasion were modulated by HGF stimulation or blocked by PHA-665752 treatment. To this aim, we selected H1993 cells as a MET-addicted model, with known sensitivity to MET inhibition as a positive control[343].

R.3.2.1. PHA-665752 inhibits HGF induced proliferation in *MET* mutant SCLC cells

HGF increased cell proliferation by 60 and 30% in H69 and H69AR cells, respectively, within 72 hours of incubation. No effect in cell proliferation was found in H187, H524, H345 or H1993 cells upon continous exposure to HGF for 72 hours. Next, we analysed PHA-665752 effects in control and HGF-treated cells and we confirmed that MET inhibition decreased cell growth by 50% in H1993 MET amplified cells. However, PHA-665752 treatment alone did not affect SCLC cell proliferation. Notably, HGF-induced cell proliferation was prevented by PHA-665752 treatment in both H69 and H69AR cells **(Figure R.6.)**.

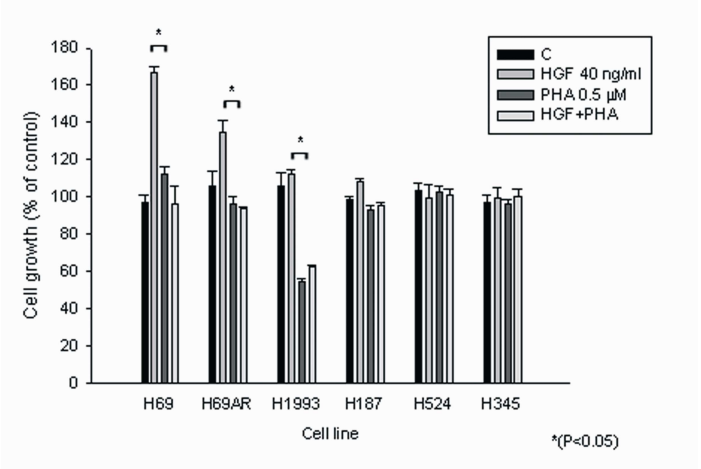

Figure R.6. PHA-665752 inhibits cell proliferation induced by HGF stimulation in H69 and H69AR SCLC cells. Cells were treated for 72 hours with HGF (40 ng/ml), PHA-665752 (0.5 μM) or the combination of both treatments. Cell number was assessed by the trypan blue exclusion method. Each data point represents the mean ± s.d. percent cell growth of three independent experiments. Data are reported as percentage in relation to the control group (set at 100%).

R.3.2.2. PHA-665752 inhibits HGF induced colony formation in *MET* mutant SCLC cells

Soft agar colony formation capacity is a surrogate of metastatic potential of cells in adverse 3D culture conditions. We evaluated if the colony formation capacity was stimulated by the addition of HGF and if PHA-665752 treatment would be able to inhibit this cellular effect alone or in the presence of HGF stimulation using the soft agar colony formation assay. SCLC cells were grown in soft agar in the presence and absence of HGF (40ng/ml) and PHA-665752 (0.5μM) during 21 days. We observed that continous HGF treatment increased colony formation by 50% only in H69 cell line, whereas we did not observe any change in clonogenic capacity of H187, H524 and H345 in these experimental conditions. We

also observed that MET inhibition (PHA-665752 at 0.5 μM) reduced colony formation in H69 cells in basal and HGF-stimulated conditions. In contrast, colony formation capacity in H187, H524 and H345 cells was not modulated by PHA-665752 treatment under the conditions used in these experiments **(Figure R.7)**.

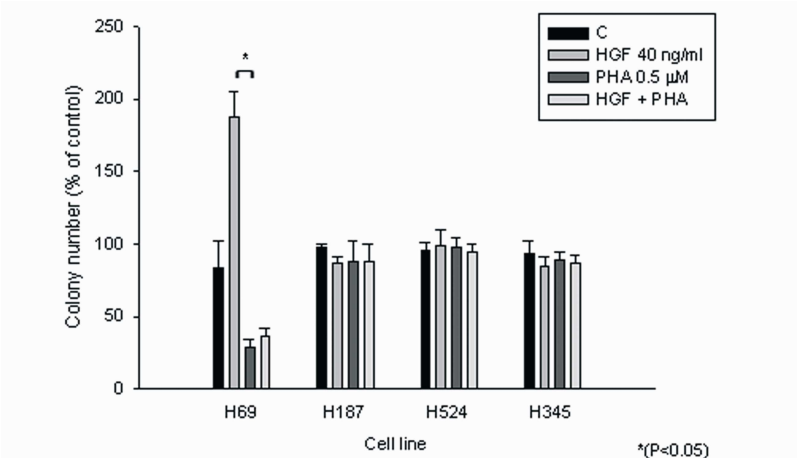

Figure R.7. PHA-665752 inhibits colony formation induced by HGF stimulation in H69 SCLC cells. Cells were plated in 0.3% soft agar (as described in Material and Methods) in the presence of HGF (40 ng/ml) and PHA-665752 (0.5 μM) for 21 days. Each data point represents the mean ± s.d. colony number of three independent experiments. Data are reported as percentage in relation to the control group (set at 100%).

R.3.2.3. PHA-665752 decreased invasion capacity in *MET* mutant SCLC cells

SCLC cells were treated with PHA-665752 at 0.5 μM and incubated for 24 h to analyse the effects on cell invasion capacity. We observed that treatment with PHA-665752 decreased invasion capacity of H69 by 52%, H69AR by 50% and H1993 by 47%. Nonetheless, the invasion capacity

of H524, H187 and H345 cells was not affected by PHA-665752 treatment **(Figure R.8.)**.

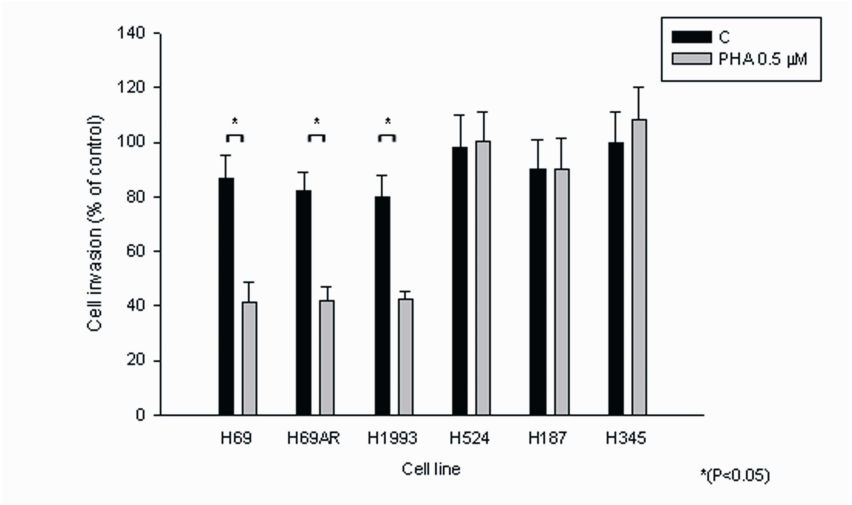

Figure R.8. PHA-665752 decreases cell invasion in H69 and H69AR SCLC cells. Cells were grown in serum-free media and seeded into the upper chamber of cell culture inserts of 24-well (8 µm pore size) CHEMICON Invasion Chamber in the presence of PHA-665752 (0.5 µM). Inserts were placed into 24-well plates containing 10% FBS and 40ng/ml HGF as chemoattractant. Cells were allowed to invade for 24 h. The number of invading cells on the underside of the membrane was determined using Crystal Violet staining. Each data point represents the mean ± s.d. cell invasion of three independent experiments. Data are reported as percentage in relation to the control group (set at 100%).

R.4. MET STATUS IN HUMAN SCLC

R.4.1. MET and p-MET protein expression show different patterns in human SCLC

As preclinical data suggested a potential role for MET inhibitors in the treatment of SCLC, our next step was to study the implication of total MET expression and its activation (phospho-MET) in human tumour

samples. We evaluated the pattern and prevalence of total MET and p-MET expression by immunohistochemistry in a series of 77 human SCLC samples. The majority of the specimens were from primary tumours (n=72), four samples were from regional lymph nodes and one from a distant site. Patients' characteristics are listed in **Table R.3.**

Table R.3. Clinical characteristics of SCLC patients

Characteristic		Number of patients
Median age (range)		65 (41-85)
Gender	Female	9 (12%)
	Male	68 (88%)
Smoking history	Never	1 (1%)
	Former	22 (29%)
	Current	54 (70%)
Performance status	0-1	48 (62%)
	2-3	13 (17%)
	Unknown	16 (21%)
Clinical stage	Limited	32 (42%)
	Extensive	42 (54%)
	Unknown	3 (4%)

As MET and p-MET antibodies have been criticized for the lack of specificity, we performed a thorough work of validation of these antibodies and used two for each marker.

Total MET expression in SCLC samples was consistent using two different primary antibodies (3D4 and SP44) that recognise the carboxylic region of MET receptor (P=0.009, R^2=0.85). MET phosphorylation was evaluated using the antibodies: Y1234/35 (D26) (MET autophosphorylation site) and Y1349 (130H2) (MET docking site). Results in **Figure R.9.** show a high correlation of the staining results (P<0.001, R^2=0.73) between each pair of antibodies.

A

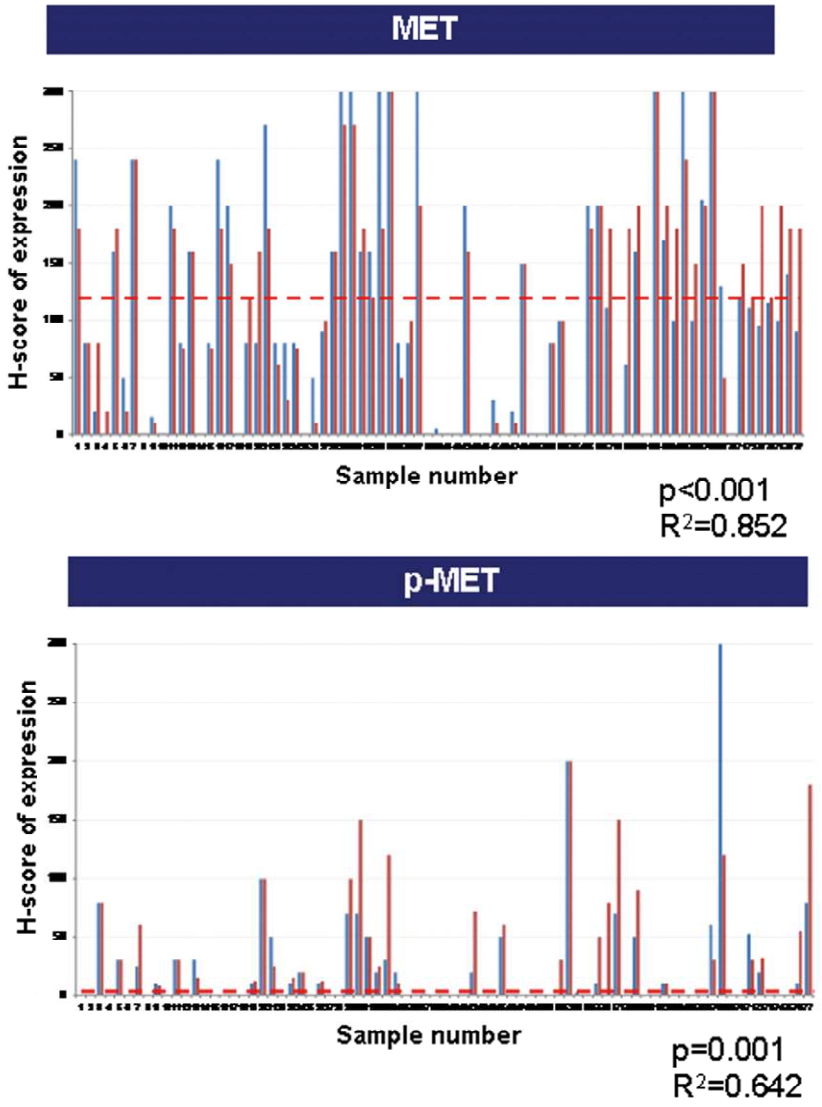

B

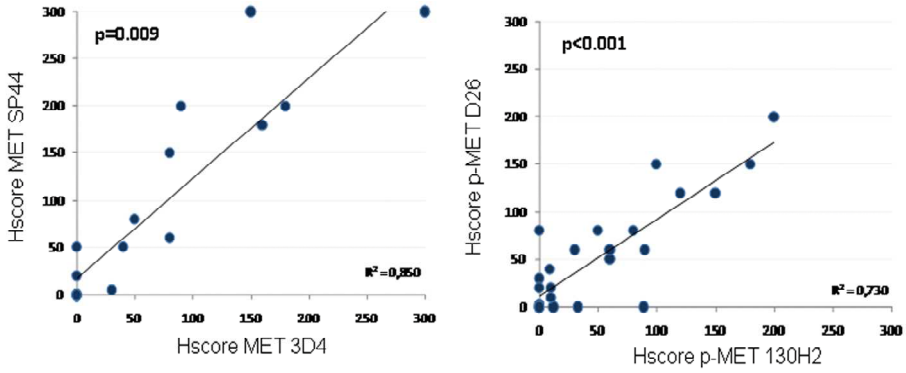

Figure R.9. Correlation of MET and p-MET Hscores between observers and antibodies. A. Hscores from two observers were displayed for MET and p-MET assays, showing a strong correlation in expression values ($p<0.001$; $R^2=0.852$ for MET, and $p=0.001$; $R^2=0.642$ for p-MET). **B.** Significant correlations between MET ($p=0.009$; $R^2=0.850$) and p-MET ($p<0.001$; $R^2=0.730$) Hscores, using two different antibodies (3D4 and SP44 for MET; 130H2 and D26 for p-MET) in a subset of SCLC samples.

Strong agreement was detected in MET and p-MET scores between two observers (MET $P<0.001$, $R^2=0.852$ and p-MET $P=0.001$, $R^2=0.642$) and mean of values were considered for statistical analysis. Receiver-operator curve (ROC) curves were used to determine the optimal cutoff points for MET and p-MET overexpression, which were calculated at Hscore of 120 and Hscore of 5, respectively. At this value, the sensitivity of the test for MET was 57.1%, with a specificity of 62.7%, and the sensitivity for p-MET was 46.3%, with a specificity of 85.7%. These scores were used to define overexpression (**Figure R.10.**).

A

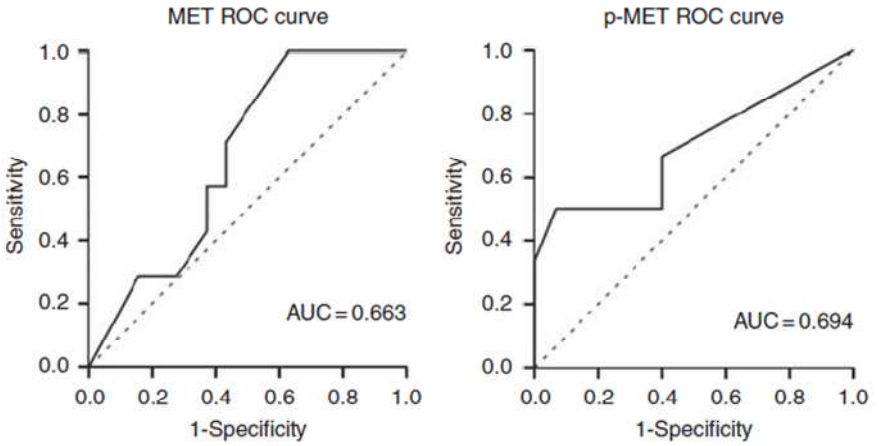

B

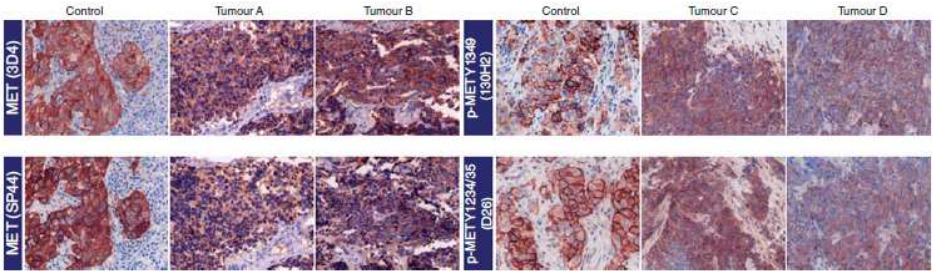

Figure R.10. MET and p-MET overexpression threshold in the cohort of SCLC patients. A. ROC was used to determine the optimal cut-off point for MET and p-MET expression. **B.** Immunohistochemistry for MET and p-MET in consecutive tissue sections from FFPE lung cancer specimens. A NSCLC (control) sample with well-known levels of MET and p-MET was used in 3D4 and SP44 (MET) and 130H2 and D26 (p-MET) assays. In SCLC samples, comparable intensity and pattern of staining were observed for MET expression (Tumors A and B) and for p-MET (Tumors C and D) between each pair of antibodies.

Given the high correlation obtained between each pair of antibodies used for total and phosphorylated MET, we selected MET (3D4) and p-MET

Y1349 (130H2) antibodies to analyse MET and p-MET expression in SCLC human tumours due to better performance. A total of 58 (75.3%) specimens did not show any MET expression and 42 (54.5 %) cases were considered as tumours with MET overexpression. MET staining was consistently observed in the plasma membrane of tumour cells, and the expression pattern of immunostaining was diffuse in the tumour. Interestingly, 33 (42.9%) cases showed p-MET overexpression following the ROC criteria. All p-MET positive cases also expressed the total form of the receptor. The pattern of p-MET staining was membranous and varied from a few cells showing positivity to diffuse staining in other tumours. Sixty-eight cases had also histologically normal bronchial epithelium representation in the section, and MET staining was detected in non-tumour epithelial cells in 67 (98%) specimens and p-MET staining in 16 (24%) (**Figure R.11.**).

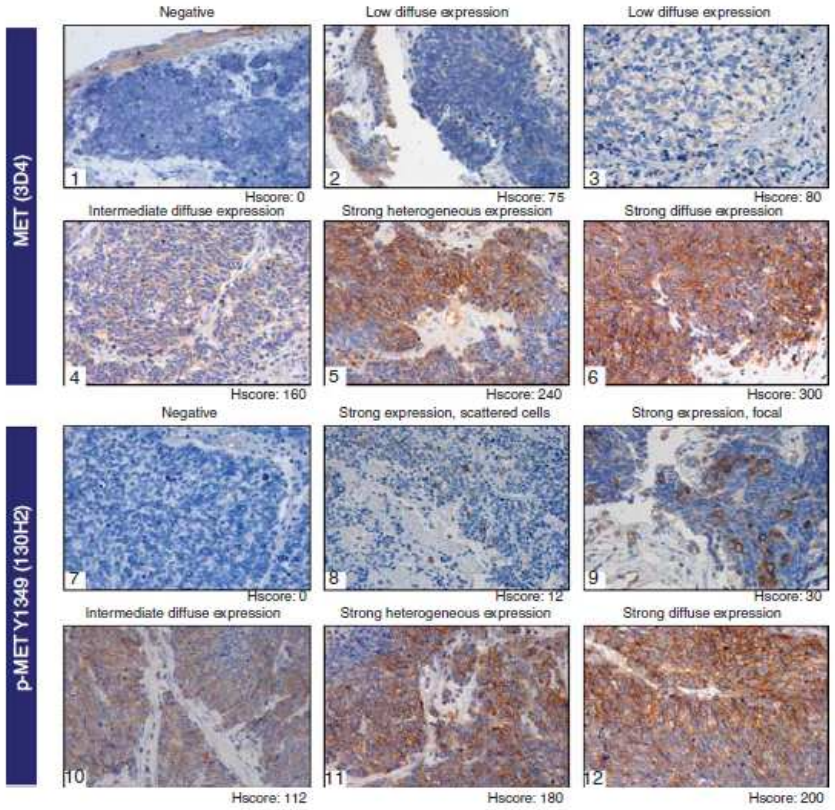

Figure R.11. MET and p-MET expression patterns in SCLC. (1–6) Different patterns of total MET expression in human SCLC (normal epithelia and tumour), assayed by immunohistochemistry. (7–12) Different patterns of p-MET (Y1349) expression in human SCLC. Negative expression observed in tumour 7. Strong expression of p-MET in scattered cells (tumour 8), focal (tumour 9) or diffuse (tumour 12). Intermediate or combined strong and intermediate expression patterns were observed in tumours 10 and 11, respectively. Diffuse: staining of a majority or all tumour cells; heterogeneous: presence of positive tumour areas while others negative.

Next association of MET and p-MET with clinical variables status was evaluated, and the only significant association we found was between p-MET positivity and extensive stage (P=0.048) (**Table R.4.**).

Table R.4. Association between MET and p-MET expression and clinical variables

		Total MET expression			p-MET expression		
		POS	NEG	p-value	POS	NEG	p-value
Gender	Female	5	4	0.948	3	6	0.539
	Male	37	31		30	38	
Smoking history	Previous/Never	16	8	0.253	8	16	0.453
	Current	25	27		24	28	
PS	0-1	29	19	0.544	21	27	0.855
	2-3	8	5		5	8	
Stage	Limited	15	17	0.381	9	23	0.048
	Extensive	24	18		21	21	

Abbreviations: NEG=negative; POS=positive; p-MET=phosphorylated MET; PS= performance status

R.4.2. MET activation is associated with decreased survival in MET-positive SCLC

Next we sought to evaluate the prognostic impact of MET and p-MET markers in SCLC. To this aim we performed a survival analysis of our series of patients stratified by the status of these markers. We first evaluated the association of clinical variables with overall survival (OS) and observed that patients with limited stage had a significantly better survival than patients with advanced disease (P<0.001). Next, we found that MET expression in SCLC patients was not significantly associated with prognosis (median OS: 270 days in MET overexpression; median OS: 203 days in low/negative MET expression (P=0.163). In contrast, p-MET overexpression in SCLC was significantly associated with a worse clinical outcome (P=0.001). Those patients with p-MET overexpression had worse prognosis (OS: 132 days) compared with p-MET negative/low expression cases (OS: 287 days). Moreover, an inverse significant correlation was detected between time of survival and levels of p-MET expression (P=0.022) (**Figure R.12.**).

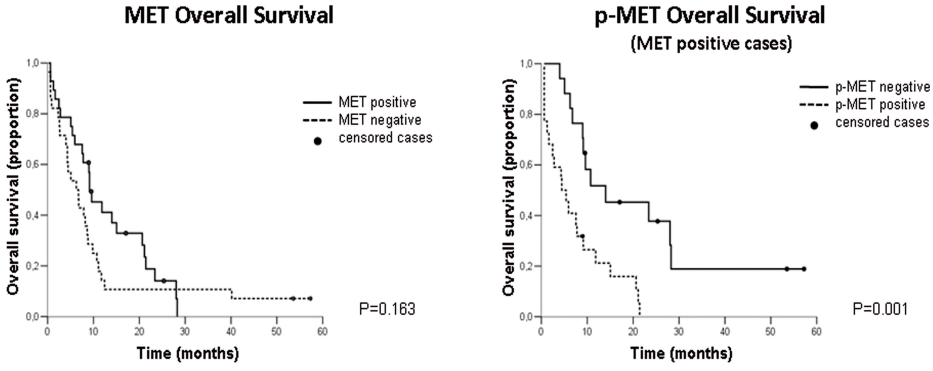

Figure R.12. Prognostic significance of MET and p-MET expression in the cohort of SCLC patients. Association between MET/p-MET expression and

overall survival. P-values were calculated using the log-rank test and survival curves by Kaplan–Meier analysis.

P-MET Hscore ranges were from 0 to 150. There was a trend towards an association between higher score and worse outcome (P=0.091). We performed an additional analysis selecting the 10 cases with highest p-MET expression compared with the rest of the group and observed that median survival was extremely poor in this p-MET high expression patients group (80.5 days vs 270 days) (**Figure R. 13.**). This suggests that the level of p-MET expression may influence patient outcome, albeit much larger series would be needed to confirm this hypothesis.

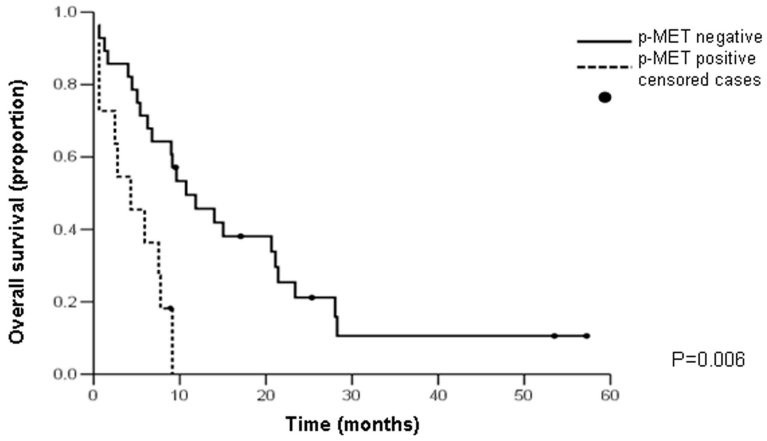

Figure R.13. Top-ten p-MET overexpressors overall survival. Kaplan-Meier overall survival curves for patients with the highest expression of p-MET compared with the rest of the group.

Finally, in a multivariate analysis including disease stage and p-MET status, both parameters remained as independent variables associated with OS (P<0.05) (**Table R.5.**).

Table R.5. Cox multivariate model for overall survival in SCLC

Prognostic variable	HR (95% CI)	P-value
Stage (extensive vs limited)	2.96 (1.58-5.54)	0.001
p-MET overexpression (no vs yes)	1.93 (1.07-3.48)	0.028

Abbreviations: CI= confidence interval; HR= hazard ratio

R.4.3. *MET* mutations in SCLC

MET mutations have been described in small series of SCLC: R988C, T1010I and E168C. Therefore, we explored whether these mutations were present in our sample set. DNA samples were extracted from FFPE tissue sections. Thirty-seven, 20 and 33 patients had enough remaining tumour tissue and were evaluated for each mutation respectively. Neither of these mutations were found in any of the patients tested, thus precluding further analysis of their potential relationship with p-MET or prognosis.

R.4.4. *MET* amplification in SCLC

In order to analyse *MET* gene copy number in our human SCLC sample set, we performed *MET* FISH analysis at Cytogenetics Laboratory of our Institution. Unfortunately, the small size of SCLC biopsies and the "crushing phenomenon" made impossible to make a definitive diagnosis by using FISH. Crush artefact is a common morphologic feature of human SCLC that causes smearing or streaming of nuclear chromatin [345].

R.4.5. HGF serum levels in SCLC patients

Our previous results strongly suggest a potential role of MET on SCLC biology. Therefore, we decided to conduct a prospective study to analyse the potential implication of its ligand HGF in SCLC behaviour.
We collected, after ethics committee approval and patient's signature on the informed consent form, serum samples during the different disease stages: diagnosis, chemotherapy best response and relapses. The patient's characteristics of these series are summarized in **Table R.6.**

Table R.6. Clinical characteristics of SCLC patients with at least one serum sample available

Characteristic		Number
N		67
Median age (range)		66 (60-72)
Gender	Female	12 (17,9%)
	Male	55 (82,1%)
Smoking history	Never	0 (0%)
	Former	17 (25,4%)
	Current	49 (73,1%)
	Unknown	1 (1,5%)
Performance status	0 - 1	45 (67,2%)
	>=2	22 (32,8%)
Clinical stage	1 - 3	19 (28,4%)
	4	48 (71,6%)
Liver Metastasis	Presence	18 (26,9%)
	Absence	30 (44,8%)

First of all we analysed the HGF serum levels in 67 SCLC patients at the time of diagnosis in comparison with 30 healthy subjects (a control population with similar age and gender). Levels of HGF detected in serum samples of SCLC patients were in the range of 1424-2259 pg/ml. The median HGF level in the 67 SCLC patients was 1680 pg/ml. HGF serum levels in healthy volunteers were in the range of 792-1618 pg/ml, with the median being 1131 pg/ml. Interestingly, HGF serum levels in healthy volunteers were significantly lower than SCLC patients (P<0.001) (**Figure R.14.**).

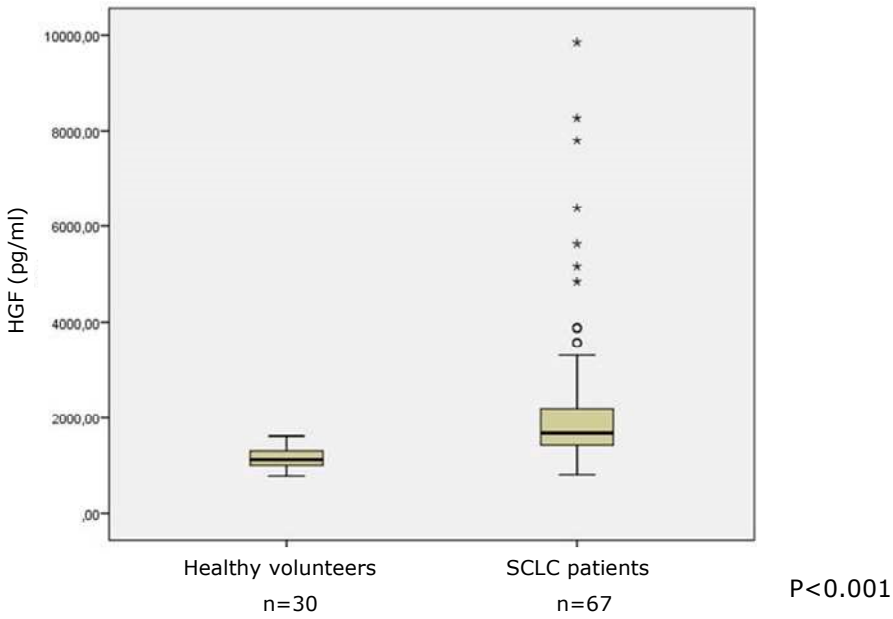

Figure R.14. Basal HGF serum levels in SCLC patients and healthy subjects. Blood samples from SCLC patients at diagnosis and healthy volunteers were centrifuged and serum was removed and stored at -20ºC. Serum HGF levels were determined using the ELISA kit manufactured by R&D Systems, Inc.

We then evaluated the HGF serum levels during the different stages of the disease (diagnosis, chemotherapy response and relapses) in SCLC

patients. Intriguingly, a significant decrease in HGF serum levels was observed during chemotherapy response (P=0.001). At progression, 50% of patients presented an increase in the levels of HGF and 50% a decrease. Although number of patients was probably too low (**Figure R.15.**).

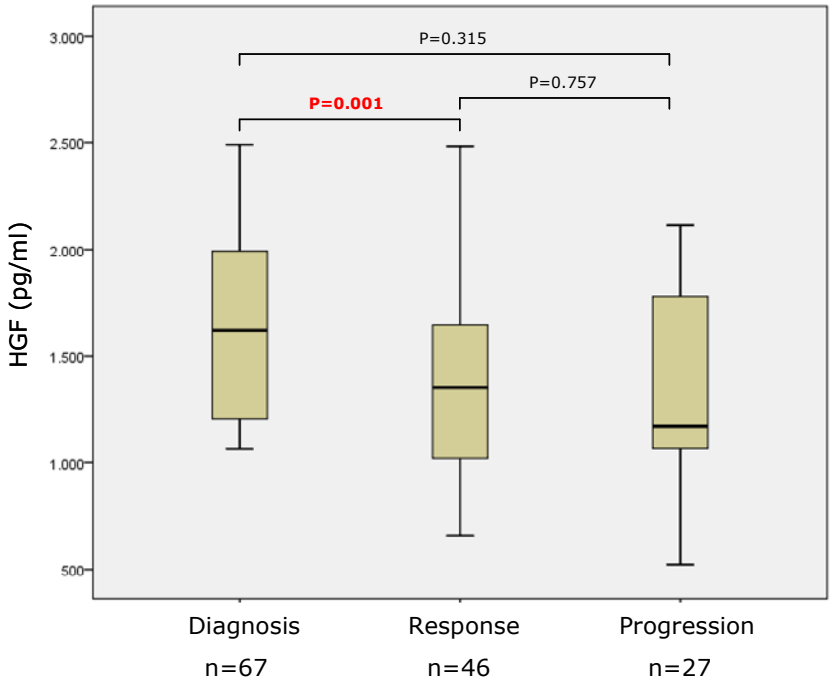

Figure R.15. HGF serum levels during the different stages of SCLC. Whole-blood samples were obtained from each SCLC patient during different disease stages (diagnosis, chemotherapy response and progression). Blood samples were centrifuged and serum was removed and stored at -20ºC. HGF serum levels were determined by ELISA kit.

For the analysis of overall survival of the SCLC patients (n=67), the median HGF basal level (1680 pg/ml) was used as the cut-off. As shown in **Figure R.16.**, patients with low HGF basal levels (HGF<=1680

pg/ml) had a significantly better overall survival than ones with elevated HGF levels (HGF>1680 pg/ml) (P=0.049).

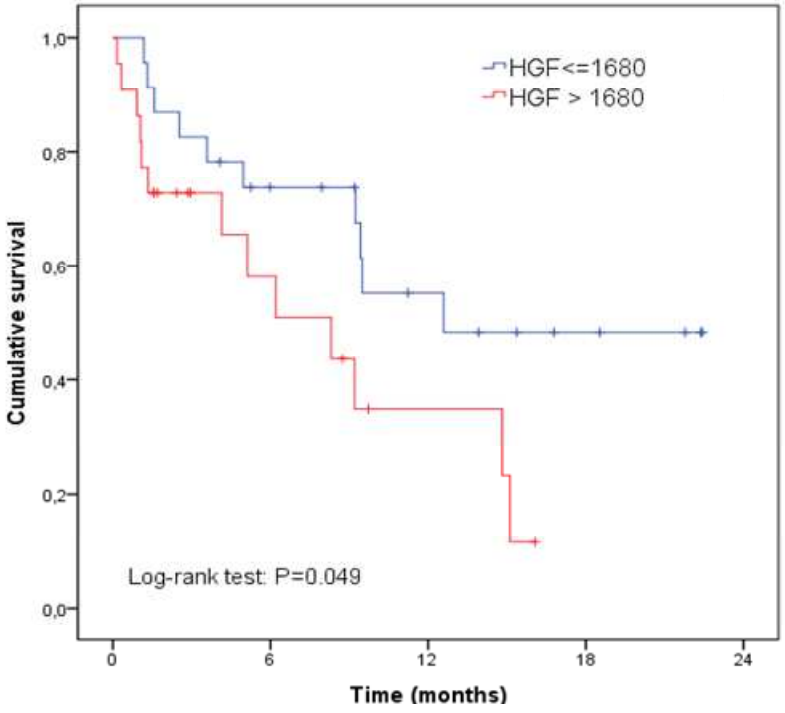

Figure R.16. Basal HGF serum levels show association with overall survival in SCLC patients. Association between overall survival and HGF serum levels in SCLC patients. The median HGF basal level (1680 pg/ml) was used as the cut-off. P-values were calculated using the log-rank test and survival curves by Kaplan-Meyer analysis.

We also performed the analysis using HGF as a continuous variable. We observed a significant increase in the risk of death (45%) for each increase of 1000 units in HGF serum levels.

The role of classical prognostic factors was also assessed in these series (performance status, liver metastasis, gender, smoking status…) for performance status and overall survival.

We finally evaluated the association of clinical variables with basal HGF serum levels in a Cox multivariate model for overall survival. Performance Status (PS) and HGF basal serum levels were the two only independent factors statistically significant (independently predictive of worse overall survival) (**Table R.7.**).

Table R.7. Cox multivariate model for overall survival in SCLC patients

Prognostic variables	**HR (95% CI)**	**P-value**
Performance status	3,71 (1.38-9,99)	0.009
HGF serum levels	1.45 (1.15-1.82)	0.002

Abbreviations: CI= confidence interval; HR= hazard ratio

R.5. ROLE OF HGF/MET PATHWAY IN THE INDUCTION OF EPITHELIAL TO MESENCHYMAL TRANSITION IN SMALL CELL LUNG CANCER

Based on the relevance of MET activation in SCLC showed by our previous work and the evidence of HGF as an inductor of EMT, we focused on the role of HGF induced-EMT in SCLC.
We hypothesised that HGF would be able to induce EMT in SCLC and that this could affect chemosensitivity.

R.5.1. HGF-induced EMT in SCLC cell lines

R.5.1.1. MET activation by HGF stimulation induces Snail upregulation in H69 SCLC cell line

Firstly, we wanted to evaluate the effects of HGF stimulation on the epithelial/mesenchymal phenotype in SCLC cells. First we selected the chemosensitive SCLC cell line H69 and its isogenic chemoresistant cells H69AR. We evaluated the protein levels of the epithelial and mesenchymal biomarkers E-Cadherin and Fibronectin, respectively, and the EMT inducers Snail1 and Zeb1. Significant differences in the epithelial/mesenchymal phenotype were observed in both cell lines at basal conditions (**Figure R.17A**). We observed that doxorubicin-resistant cells H69AR presented a mesenchymal phenotype when compared to H69. Absence of E-Cadherin expression but high levels of Fibronectin was detected in H69AR cells. Moreover, H69AR cells expressed higher levels of Snail1 and Zeb1 in comparison with H69. In addition, H69 and

H69AR cells were stimulated with HGF (40 ng/ml) during 15'. HGF stimulation did not modulate any biomarker in both cell lines at this time (**Figure R.17A**). We then exposed these cell line models to HGF stimulation for longer times. Thus, H69 and H69AR cells were treated with HGF (40 ng/ml) at 1, 6, 24 and 72 hours. MET phosphorylation was observed in all HGF-stimulated conditions in both cell lines but no change in E-Cadherin or Fibronectin protein levels were detected. However, upregulation of Snail1, the classical EMT inducer, was detected when we stimulated H69 cells with HGF during 6 and 24 hours (**Figure R.17B**). Due to an absence of E-Cadherin repression upon Snail1 upregulation at these time points, we wanted to check the effects of HGF stimulation after a more prolonged exposure.

A

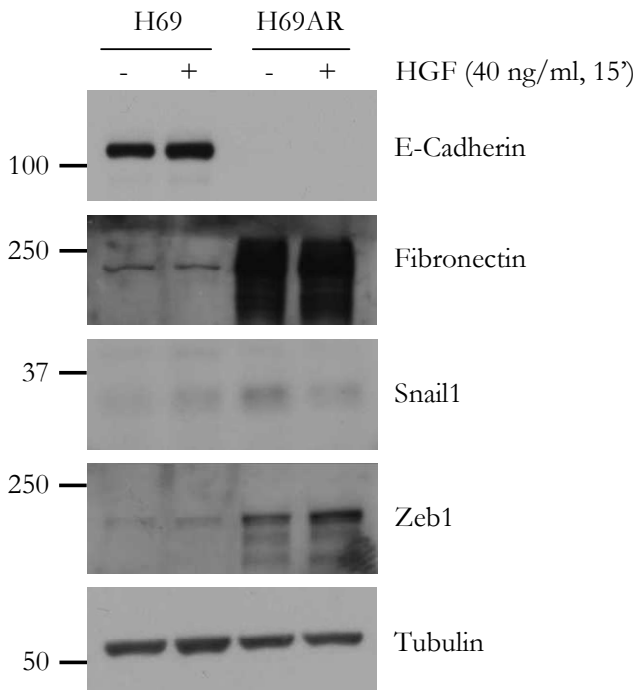

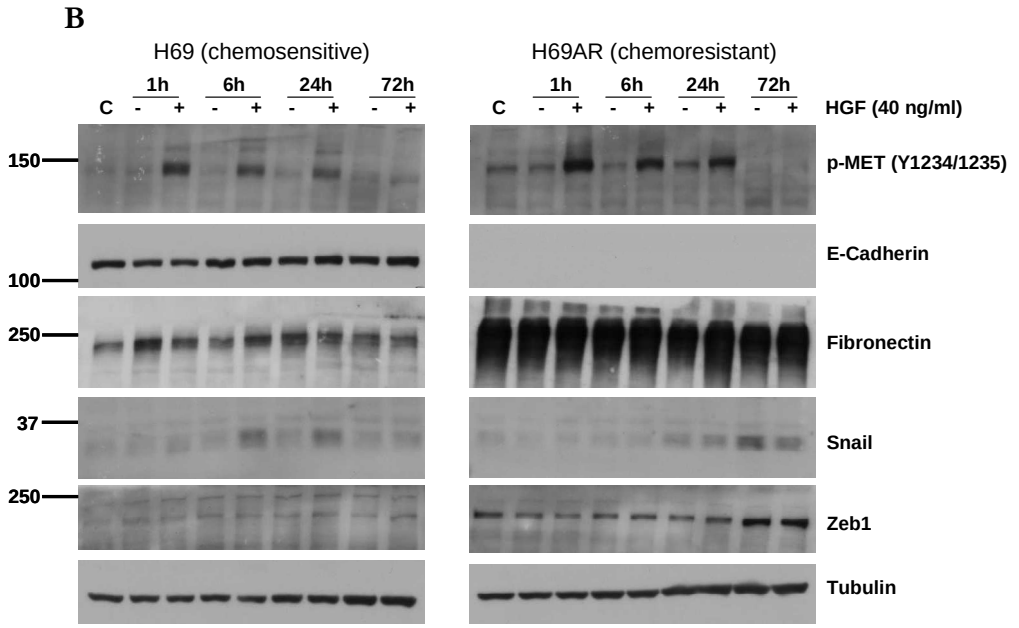

Figure R.17. HGF stimulation induces Snail1 upregulation in H69 SCLC cell line. A. H69AR cells present a mesenchymal phenotype when compared to H69. Cells were serum-starved for 24 hours and then treated with HGF (40 ng/ml) during 15'. Whole cell lysates were purified and subjected to Western Blot to analyse E-cadherin, Fibronectin, Snail1 and Zeb1 protein expression levels. **B.** Snail1 upregulation after HGF stimulation in H69 SCLC cell line. Cells were serum-starved for 24 hours and then treated with HGF (40 ng/ml) during 1, 6, 24 and 72 hours. Total cell lysates were obtained and Western Blot was performed to determine p-MET (Y1234/1235), E-cadherin, Fibronectin, Snail1 and Zeb1 protein expression levels.

R.5.1.2. Prolonged HGF stimulation induces a mesenchymal phenotype in H69 cell line

We previously observed that HGF stimulation within 6 to 24 hours was able to induce a Snail upregulation in H69 cell line. However, these effects did not correlate with E-Cadherin repression at the same time

points (**Figure R.17.**). In view of these results we tested the cellular and molecular effects of HGF stimulation after a prolonged exposure in H69, H69AR and H187. In addition, H69 cells were treated in parallel with TGFβ–1 (5 ng/ml), a well known inducer of EMT [246,346] (**Figure R.18.**).

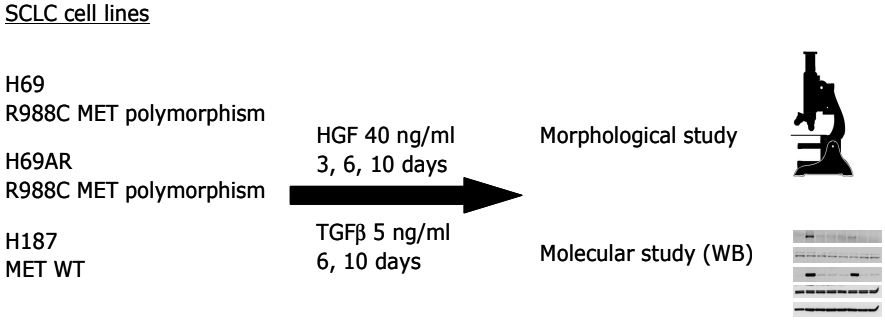

Figure R.18. Experimental model to study HGF effects on EMT in SCLC cell lines. H69, H69AR and H187 SCLC cells were treated with HGF (40 ng/ml) or TGFβ (5 ng/ml) during 3, 6, and 10 days or 6 and 10 days, respectively. A morphological study by light microscopy or molecular study by Western Blot was performed.

We observed in H69 cells a morphological change as judged by the appearance of cells with a spindle-like morphology in the HGF-treated experimental conditions. We also found scattering of cells as well as the presence of adherent population of cells by day 6 (**Figure R.19A**). In contrast, TGFβ exposure did not result in any morphological change in H69 cell line (**Figure R.19B**).

A

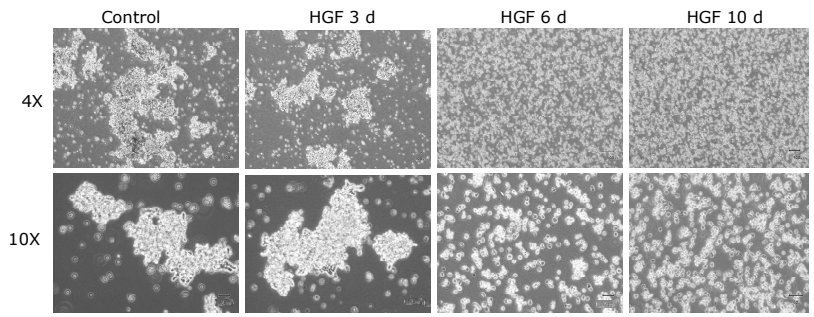

B

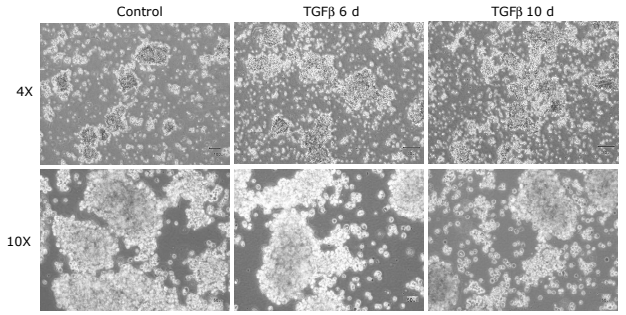

Figure R.19. Cell morphology effects after HGF or TGFβ prolonged exposure in H69 cell line. A. HGF stimulation induces cell scattering and spindle cell morphology in H69 cells. H69 cells were treated with HGF at 40 ng/ml during 10 days. Cell morphology was examined by light microscopy observation. Photomicrographs were taken at days 3, 6 and 10. **B.** TGFβ exposure does not induce morphological changes in H69 cells. H69 cells were treated with TGFβ at 5 ng/ml during 10 days. Cell morphology was examined by light microscopy observation. Photomicrographs were taken at days 6 and 10.

MET phosphorylation and total MET downmodulation was observed upon HGF prolonged exposure in H69 cell line. As we observed previously at shorter times, this MET activation after 3 days of HGF addition resulted in upregulation of Snail1. A decrease in E-Cadherin protein levels and increase of Fibronectin expression were observed upon HGF stimulation during 6 or 10 days. These results suggested that the repression of the epithelial marker E-Cadherin could be induced though HGF-dependent Snail upregulation. We detected that Zeb1 levels decreased upon 6 and 10 days of HGF exposure in H69 cells, contrary to what we expected. TGFβ-1 did not induce any relevant changes in H69 cells in the studied markers (**Figure R.20.**). These results correlated with the absence of morphological changes after TGFβ-1 treatment observed previously by light microscopy.

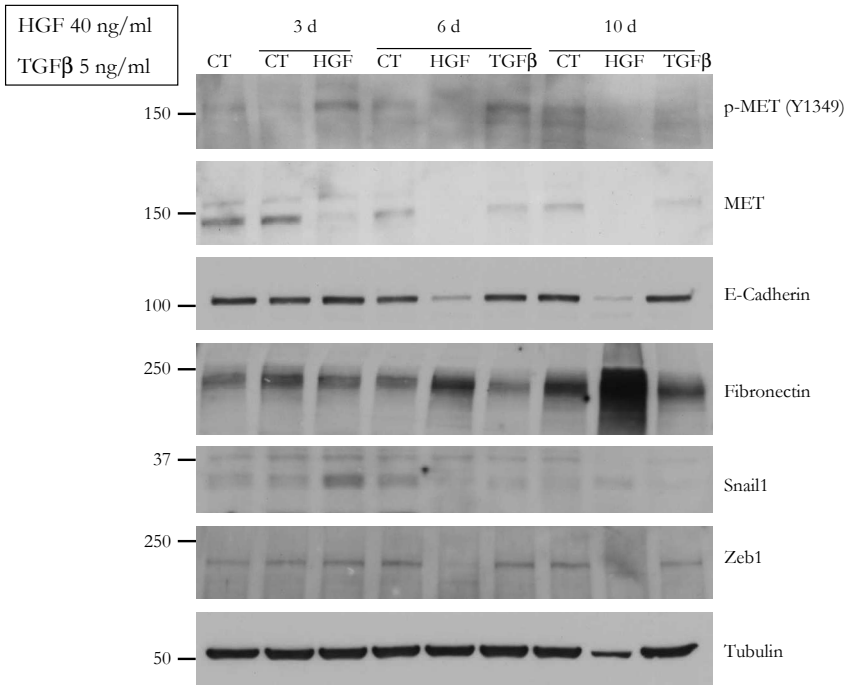

Figure R.20. HGF prolonged exposure induces a mesenchymal phenotype in H69 cells. H69 cells were treated with HGF (40 ng/ml) during 3, 6 and 10 days or TGFβ (5 ng/ml) during 6 and 10 days. Whole cell lysates were purified and subjected to Western Blot to analyse total and phosphorylated MET protein levels and E-cadherin, Fibronectin, Snail1 and Zeb1 protein expression levels.

The same analysis (after a prolonged HGF exposure) was performed with the doxorubicin resistant cell line H69AR, already a mesenchymal cell line. No cellular or molecular effects were observed after HGF exposure (data not shown).

Next, H187 cells were subjected to the same experiment. We did not found any morphological change by light microscopy upon HGF prolonged exposure in H187 cells (**Figure R.21A**). Western Blot analysis demonstrated that despite MET phosphorylation detected upon HGF addition during 3, 6 and 10 days, this MET activation did not correlate

with any relevant change in E-Cadherin and NCAM, Fibronectin and N-Cadherin, or Snail1 and Zeb1 (**Figure R.21B**).

Together, these results suggest that a prolonged HGF exposure was able to induce a mesenchymal phenotype only in H69 cell line. Therefore, the R988C MET polymorphism could have a role in the HGF capacity to induce such effects.

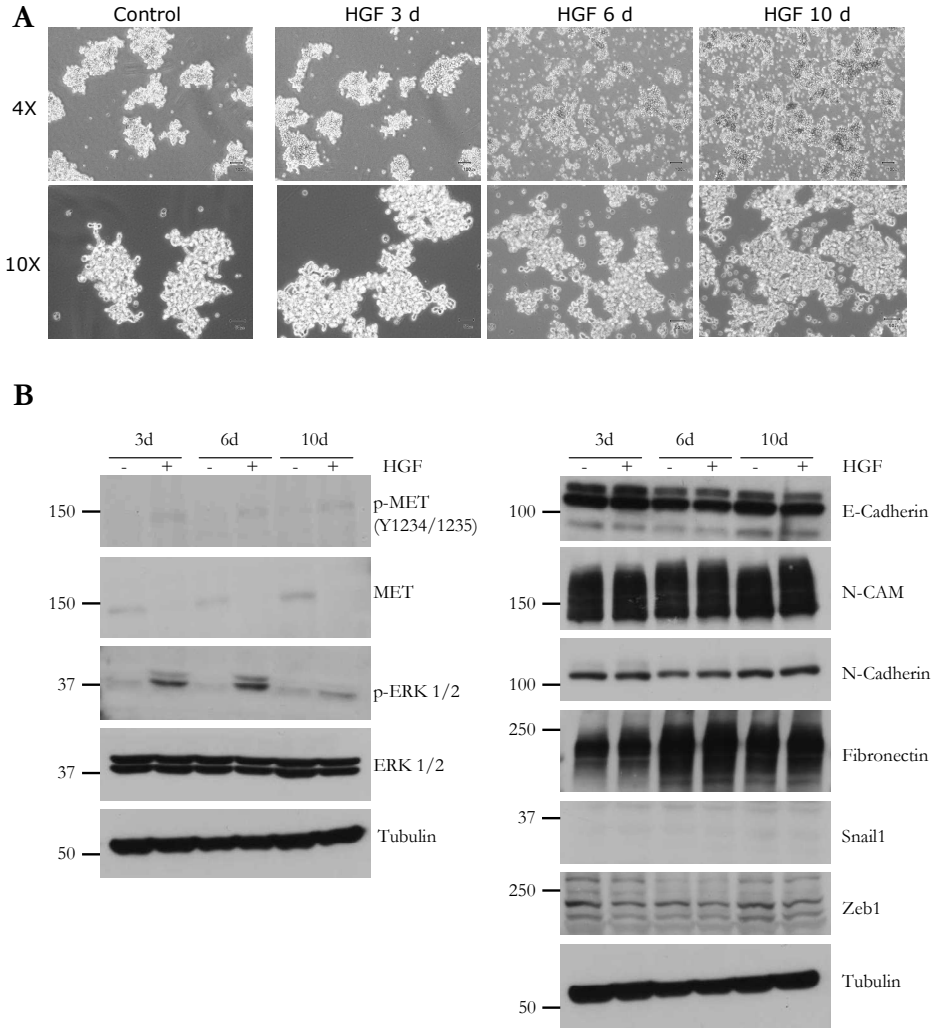

Figure R.21. HGF effects after a prolonged exposure in H187 cells. A. HGF exposure does not induce morphological changes in H187 cells. H187 cells were

treated with HGF at 40 ng/ml during 10 days. Cell morphology was examined by light microscopy observation. Photomicrographs were taken at days 3, 6 and 10. **B.** HGF exposure does not induce molecular changes on EMT markers in H187 cells. H187 cells were treated with HGF (40 ng/ml) during 3, 6 and 10 days. Whole cell lysates were purified and subjected to Western Blot to analyse total and phosphorylated MET and ERK1/2 protein levels and E-cadherin, N-CAM, N-cadherin, Fibronectin, Snail1 and Zeb1 protein expression levels.

R.5.2. PF-2341066 effects on HGF-induced EMT in a SCLC cell model

R.5.2.1. PF-2341066 prevents and reverts the HGF-induced EMT in H69 cell line

Given our previous results that indicated that HGF prolonged exposure was able to induce EMT in H69 SCLC cells, we sought to investigate the cellular and molecular effects of MET pathway inhibition on HGF-induced EMT. To this end we used a specific MET inhibitor (PF2341066) (Pfizer Inc.). PF-2341066 is a novel orally available ATP-competitive small-molecule inhibitor highly specific against MET and anaplastic lymphoma kinase (ALK). It has antitumor efficacy in tumour models at well-tolerated doses *in vivo* through antiproliferative and antiangiogenic mechanisms. Its therapeutic role is currently being evaluated in clinical studies with cancer patients [205,207,347,348].

Given that we used the dual MET/ALK inhibitor PF-2341066 in our experiments to inhibit HGF/MET pathway, we wanted to discard possible ALK alterations in our SCLC cell lines. Thus, ALK gene copy number and its oncogenic translocation were evaluated by FISH, but

neither ALK amplification nor translocation was found in the SCLC cell lines of our lab (data not shown).

To test the effects of MET inhibition by PF-2341066 on HGF-induced EMT in H69 we established two different cell experiments (**Figure R.22.**).

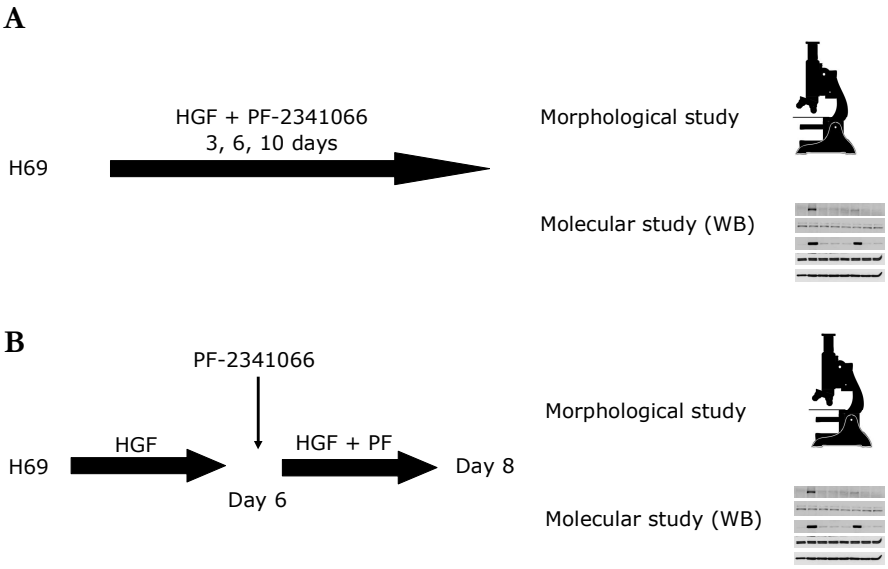

Figure R.22. Experimental model to study PF-2341066 effects on HGF-induced EMT in H69 cell line. A. PF-2341066 prevents the HGF-induced EMT in H69 cell line. H69 cells were treated with HGF (40 ng/ml) and PF-2341066 (200 nM) during 3, 6, and 10 days. A morphological study by light microscopy or molecular study by Western Blot was performed. **B**. PF-2341066 reverts the HGF-induced EMT in H69 cell line. H69 cells were treated with HGF (40 ng/ml) during 6 days. Then, PF-2341066 (200 nM) was added in combination with HGF since day 8. A morphological study by light microscopy or molecular study by Western Blot was performed.

In our first experimental model, H69 cells were treated with HGF (40 ng/ml) and the combination with PF-2341066 (200 nM) during 3, 6 and

10 days to know if the MET inhibitor PF-2341066 was able to prevent the HGF-induced EMT. The previously observed morphological changes in H69 cells were detected upon 6 days of HGF addition. Nevertheless, H69 cells treated with HGF and PF-2341066 showed no changes in cell morphology (cells grow as aggregates in suspension, similar to control cells) (**Figure R.23A**). By Western Blot we detected that HGF exposure in H69 cells induced a MET phosphorylation that correlated with a Snail upregulation and E-cadherin downmodulation. However the addition of PF-2341066 in the presence of HGF prevented this MET activation, the increase of Snail1 and the decrease of E-cadherin protein levels. No relevant changes in Fibronectin expression were observed (**Figure R.23B**). These results suggested that the specific MET inhibitor PF-2341066 was able to prevent the HGF-induced EMT in H69 cells through Snail1 modulation.

A

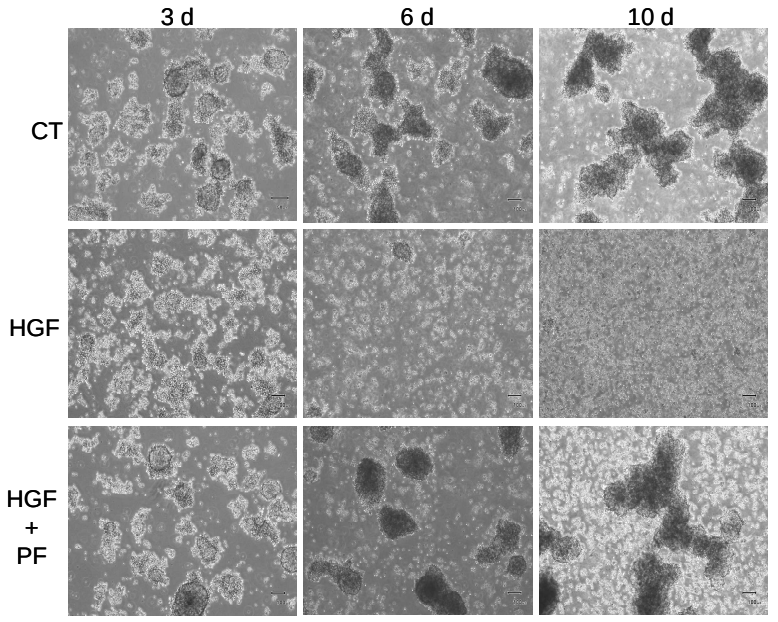

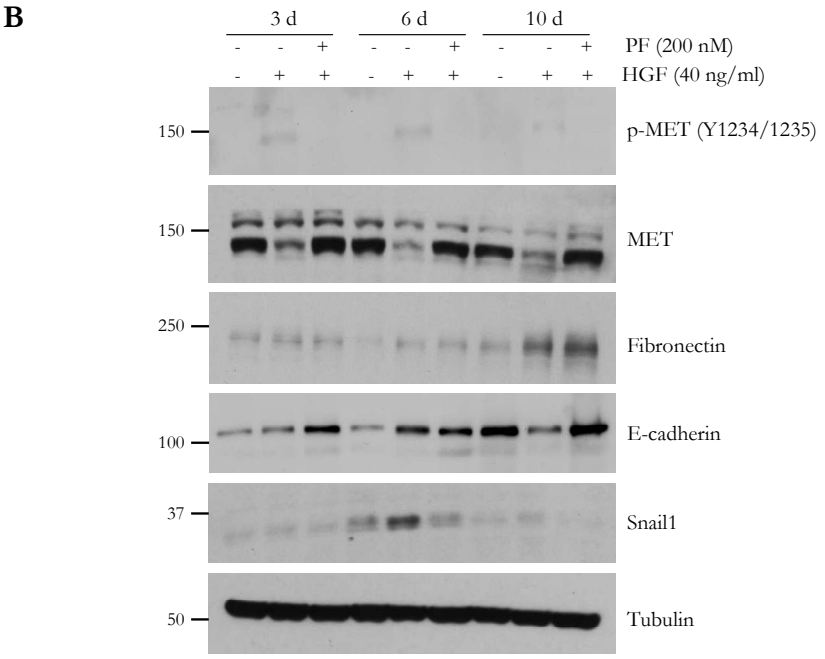

Figure R.23. PF-2341066 prevents the HGF-induced EMT in H69 cell line. A. PF-2341066 prevents the morphological changes induced by HGF in H69 cells. H69 cells were treated with HGF (40 ng/ml), PF-2341066 (200nM) or the combination of both treatments during 10 days. Cell morphology was examined by light microscopy observation. Photomicrographs were taken at days 3, 6 and 10. **B.** PF-2341066 prevents the molecular changes induced by HGF in H69 cells. H69 cells were treated with HGF (40 ng/ml), PF-2341066 (200 nM) or the combination of both treatments during 10 days. Whole cell lysates were purified and subjected to Western Blot to analyse total and phosphorylated MET protein levels and E-cadherin, Fibronectin and Snail1 protein expression levels.

In our second experimental model, H69 cells were treated with HGF (40 ng/ml) and PF-2341066 (200 nM) was added at day 6 (when HGF-induced morphological changes were detected by light microscopy). Consistent with previous experiments, the morphological study by light microscopy indicated that HGF addition during 6 days induced a spindle-like morphology and cell scattering. Interestingly, PF-2341066 treatment

during 48 hours (in the presence of HGF exposure) was able to revert the HGF-induced morphological changes, as indicated the presence of the H69 classical aggregates in suspension, similar to the control cells. HGF addition during 6 days induced MET pathway activation and Snail1 upregulation and PF-2341066 treatment resulted in an inhibition of the MET pathway but also an important downregulation of Snail1 protein levels (**Figure R.24.**).

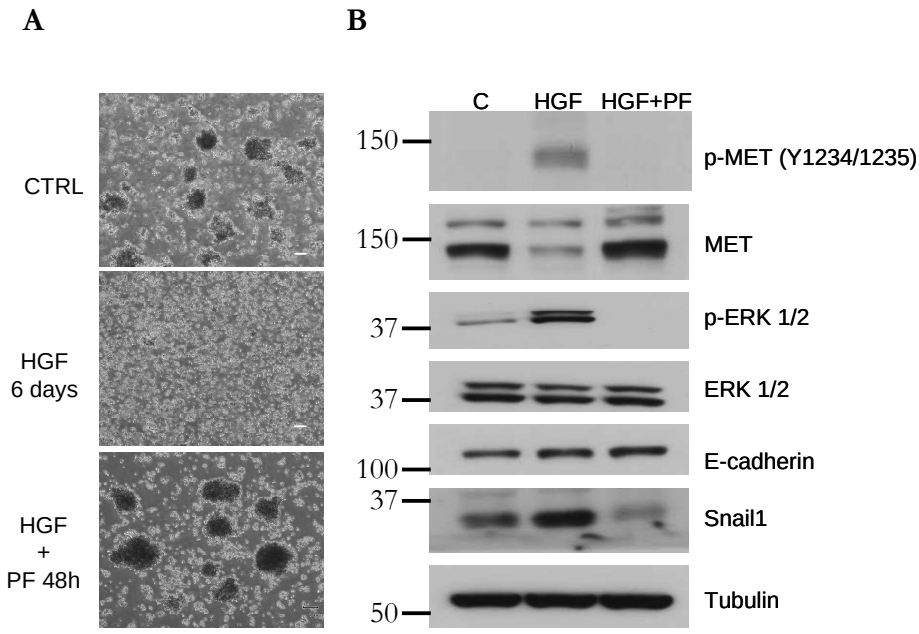

Figure R.24. PF-2341066 reverts the HGF-induced EMT in H69 cell line. A. PF-2341066 reverts the morphological changes induced by HGF in H69 cells. H69 cells were treated with HGF (40 ng/ml) during 6 days and then PF-2341066 (200nM) was added since day 8. Cell morphology was examined by light microscopy observation. Photomicrographs were taken at days 6 and 8. **B.** PF-2341066 reverts the molecular changes induced by HGF in H69 cells. H69 cells were treated with HGF (40 ng/ml) during 6 days and then PF-2341066 (200nM) was added since day 8. Whole cell lysates were purified and subjected to Western Blot to analyse total and

phosphorylated MET and ERK1/2 protein levels and E-cadherin, Fibronectin and Snail1 protein expression levels.

R.5.2.2. PHA-665752 prevents and reverts the HGF-induced EMT in H69 cell line

Due to the use of the dual MET/ALK inhibitor PF-2341066 to block the HGF-induced EMT, and to rule out these effects being associated with ALK inhibition, we wanted to confirm these results using the specific MET inhibitor PHA-665752. Therefore, we performed the same experimental model of the **Figure R.22.** but using PHA-665752.

H69 cells were treated with HGF (40 ng/ml) and the combination with PHA-665752 (0.5 μM) during 6 and 10 days to know if the MET inhibitor was able to prevent the HGF-induced EMT. As observed in **Figure R.25** PHA-665752 treatment prevented the HGF-induced effects on cell morphology in H69 cells.

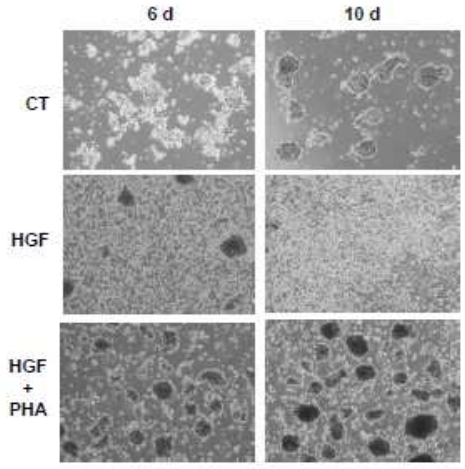

Figure R.25. PHA-665752 prevents the HGF-induced EMT in H69 cell line. A. PHA-665752 prevents the morphological changes induced by HGF in H69 cells. H69 cells were treated with HGF (40 ng/ml), PHA-665752 (0.5μM) or the

combination of both treatments during 10 days. Cell morphology was examined by light microscopy observation. Photomicrographs were taken at days 6 and 10.

In addition, we performed the experiment adding the MET inhibitor once morphological changes had occurred (day 6). We found that the addition of PHA-665752 reversed the HGF-induced effects, both morphological (**Figure R.26A**) and molecular. PHA-665752 was able to revert the Snail upregulation detected upon HGF stimulation (**Figure R.26B**).

A

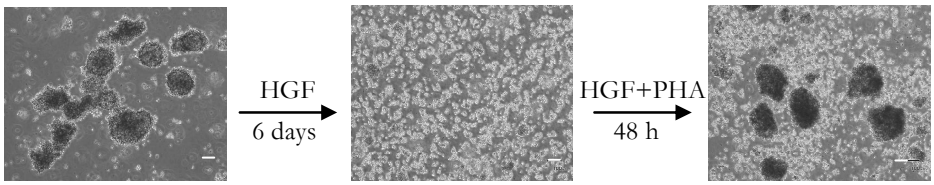

B

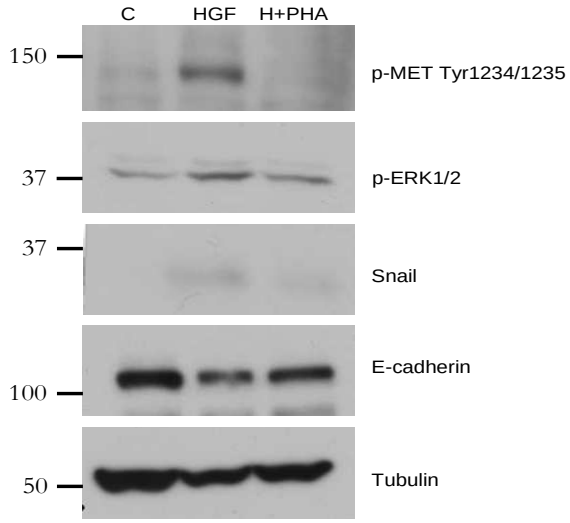

Figure R.26. PHA-665752 reverts the HGF-induced EMT in H69 cell line. A. PHA-665752 reverts the morphological changes induced by HGF in H69 cells. H69

cells were treated with HGF (40 ng/ml) during 6 days and then PHA-665752 (0.5μM) was added since day 8. Cell morphology was examined by light microscopy observation. Photomicrographs were taken at days 6 and 8. **B.** PHA-665752 reverts the molecular changes induced by HGF in H69 cells. H69 cells were treated with HGF (40 ng/ml) during 6 days and then PHA-665752 (0.5μM) was added since day 8. Whole cell lysates were purified and subjected to Western Blot to analyse p-MET p-ERK1/2, E-cadherin and Snail1 protein expression levels.

R.5.2.3. Snail1 knockdown prevents HGF-induced EMT

Snail1 is one of the key players in EMT. In our previous model we observed that MET activation through HGF resulted in upregulation of Snail1 and this was reverted and prevented by PF-2341066. To confirm the role of Snail expression in this transition we knocked down Snail in H69 cells. We observed downregulation of the protein compared to the empty vector infected cells (**Figure R.27A.**). We then treated H69shCT and H69shSnail with HGF for 10 days. At day 6 we observed scattering of the H69shCT cells that grew partially attached to the plate. In contrast, the KO Snail1 cells did not present this phenomenon and no morphological changes were observed under HGF treatment during 10 days (**Figure R.27B.**).

A

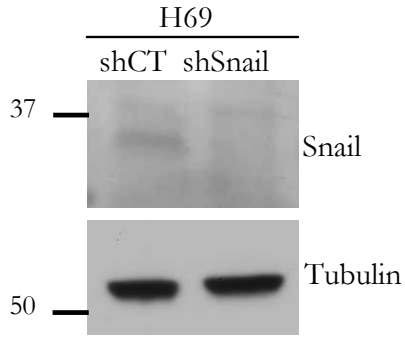

B

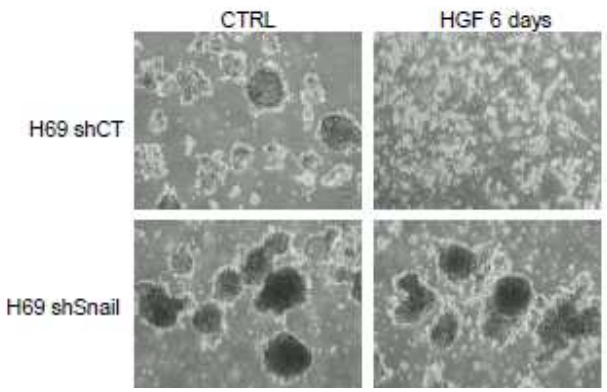

Figure R.27. Snail1 knockdown prevents HGF induced EMT. A. Western Blot analysis showing stable knockdown of Snail1 in H69shSnail cells. Whole cell lysates of H69shCT and H69shSnail were purified and subjected to Western Blot to analyse Snail1 protein levels. **B.** Snail1 knockdown prevents the morphological changes induced by HGF in H69 cells. H69shCT and H69shSnail cells were treated with HGF (40 ng/ml) during 6 days. Cell morphology was examined by light microscopy observation. Photomicrographs were taken at days 6.

R.5.3. Isolation of a mesenchymal subpopulation within H69 cells

As we showed before, upon 6 days of HGF addition to H69 cells media we observed the appearance of a phenotypically mesenchymal and adherent cell subpopulation that coexisted with cells that were morphologically similar to suspension cultures of parental cells with round cell morphology. From this mixed populations, we were able to isolate and maintain these "more mesenchymal" cells in culture. These cells displayed a spindle or fibroblast-like cellular morphology. We called this cell subpopulation "mesenchymal-H69" (H69M hereon) (**Figure**

R.28.). This adherent subpopulation remained stably mesenchymal even after elimination of HGF exposure.

Our aims were 1) to characterize the newly-established H69M cells 2) to evaluate cellular and molecular profile differences between this cell type and the parental cells and 3) to examine the response of H69M cells to PF-2341066 treatment.

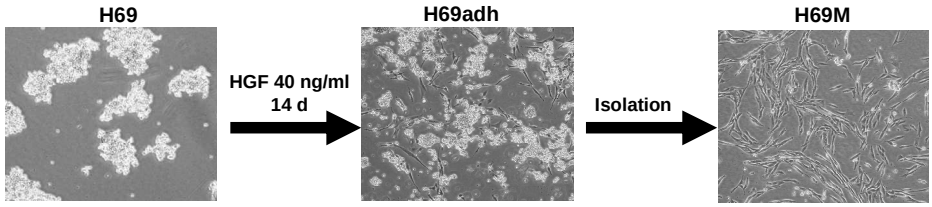

Figure R.28. HGF prolonged exposure induces the appearance of a mesenchymal subpopulation in H69 cell line. H69 cells were treated with HGF (40 ng/ml) until the appearance of a mesenchymal and adherent cell subpopulation that coexisted with H69 parental cells, that grow as a cell aggregates in suspension. Cell floating aggregates were manually removed until isolated the mesenchymal subpopulation, called H69M cells. H69M subpopulation was maintained in culture without the presence of HGF.

R.5.3.1. Karyotype studies show the authenticity of the H69M cell line excluding cross-contamination with other cells

In order to confirm that H69M cells derived from H69 cell line and to exclude this mesenchymal subpopulation as a possible contaminant cell line, we compared the karyotype of H69 and H69M cells. Karyotype analysis was performed at the Cytogenetics Laboratory of our Institution. The same chromosomal alterations were observed in both cases, ruling out contamination as a cause of the H69M detection (**Figure R.29.**).

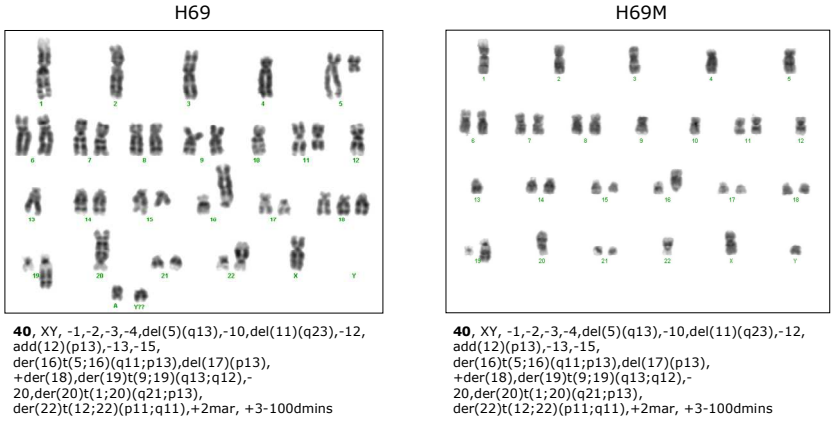

Figure R.29. H69 and H69M G-banding karyogram showing the chromosomal aberrations detected in both cell lines.

R.5.3.2. H69M presents higher growth rate when compared to H69 cells

Our next step was to determine H69 and H69M growth kinetics. We observed that H69M cells presented an increase about 40% of cell proliferation after 8 days of cell culture compared to the parental cells (H69) (**Figure R.30.**).

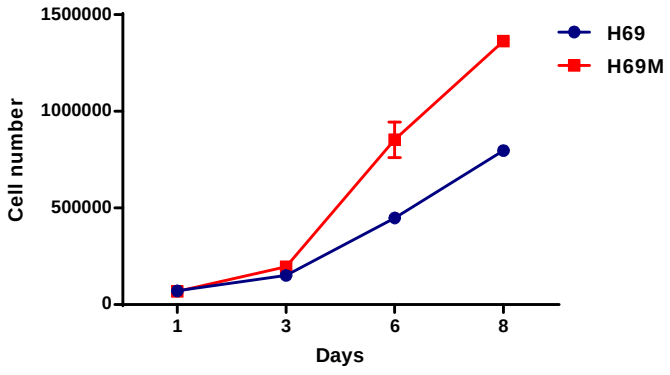

Figure R.30. H69M presents higher growth rate in comparison with H69 cells. H69 and H69M cells were grown during 1, 3, 6 and 8 days. Cell number was assessed by the trypan blue exclusion method. Each data point represents the mean ± s.d. cell number of three independent experiments.

R.5.3.3. H69M presents resistance to various chemotherapeutic agents

Due to the described association between EMT and chemotherapy resistance in several cancer models[349-353], we evaluated chemotherapy sensitivity of H69M in comparison with H69 cells. We found that H69M cells presented and increased chemoresistance to standard chemotherapeutic agents used in the treatment of SCLC (Cisplatin and Etoposide) (**Figure R.31.**).

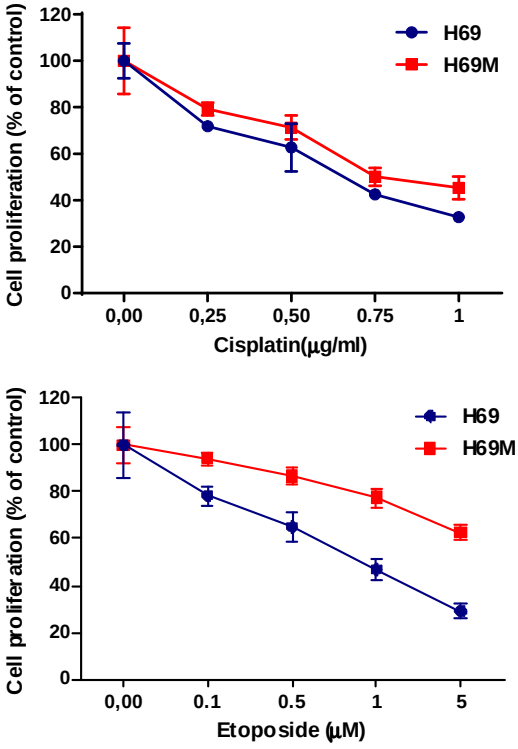

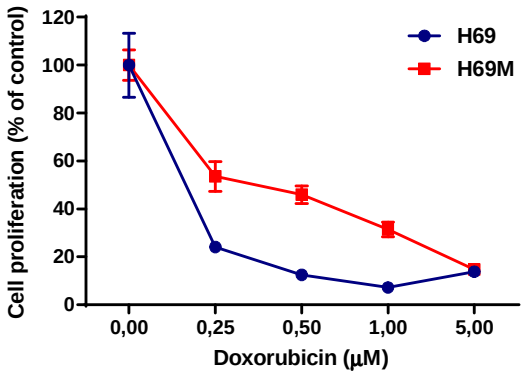

Figure R.31. Sensitivity of H69 and H69M cells to chemotherapy. Sensitivity of H69 and H69M cells to Cisplatin, Etoposide and Doxorubicin for 72 hours, assessed by MTS assay. Each data point represents the mean ± s.d. percent growth of three independent experiments. Each data point represents the mean ± s.d. percent cell growth of three independent experiments. Data are reported as percentage in relation to the control group (set at 100%).

R.5.3.4. Identification of genes differentially expressed in H69 versus H69M cells

We analyzed the changes in expression of 28869 genes in H69 compared to H69M cells. Genes with an adjusted p-value less than 0.05 were selected as significant. We found 9712 genes that were differentially expressed in H69M compared to H69 cells. All the significant differentially expressed genes were represented in a heatmap (**Figure R.32.**). **Table R.8.** shows the top ten up-regulated and down-regulated genes.

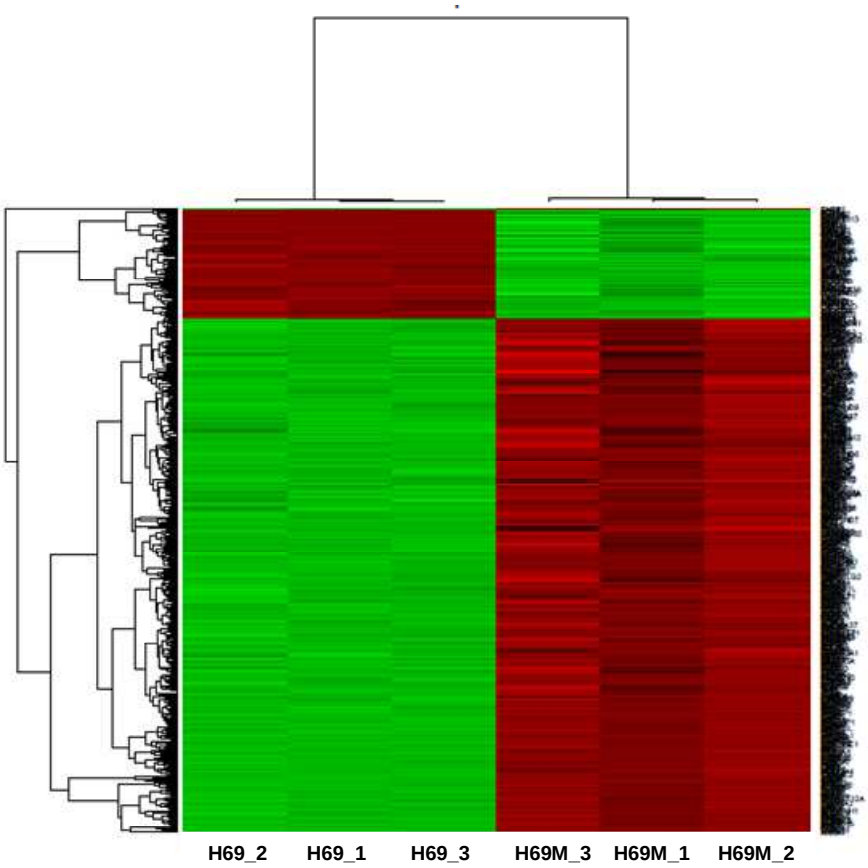

Figure R.32. Heatmap of expression changes in 28869 genes in H69M cells compared to H69. Horizontal rows show individual genes; vertical columns represent individual samples (3 samples from H69 on the left and 3 samples from H69M on the right). Color intensity means degree of gene expression modulation. Red indicates up-regulation and green down-regulation. Black indicates no change. The dendogram at the left site indicates the degree of similarity among the selected genes according to their expression patterns.

Table R.8. Top ten up-regulated and down-regulated genes in H69M cells compared to H69

Log Ratio up-regulated genes		
Symbol	**Description**	**Exp. Value**
SPARC	Secreted protein, acidic, cystein-rich (osteonectin)	7,928
CAV1	Caveolin 1	7,881
ITGA5	Integrin alpha-5 (fibronectin receptor)	6,869
FN1	Fibronectin 1	6,808
ACTA2	Actin alpha 2	6,769
IL6ST	Interleukin 6 signal transducer	6,657
LUM	Lumican	6,476
DCBLD2	Discoidin, CUB and LCCL domain containing-2	6,413
EDNRA	Endothelin receptor type A	6,408
VIM	Vimentin	6,255
Log Ratio down-regulated		
Symbol	**Description**	**Exp. Value**
ADH1C	Alcohol dehydrogenase 1C (class I)	-4,905
MCOLN3	Mucolipin 3	-4,21
MEP1B	Meprin A beta	-3,863
CDH20	Cadherin 20 type 2	-3,769
GPR116	G protein-coupled receptor 116	-3,765
RXRG	Retinoid X receptor gamma	-3,714
PTPRM	Protein tyrosine phosphatase, receptor type, M	-3,4
ENPP2	Ectonucleotide pyrophosphatase/phosphodiesterase 2	-3,062
SNAP91	Synaptosomal-associated protein	-3,053
PIP5K1B	Phospatidyl inositol-4-phosphate 5-kinase type I beta	-2,995

Ingenuity pathway analysis (IPA) was used to analyse the most significant signalling pathways and functions that were altered in H69M compared to H69 cells. Among the alterations in molecular and cellular functions, "Cellular movement", "Cell morphology", "Cell development", "Cellular growth and proliferation", and "Cell Signalling" were the top altered functions in H69M cells compared to H69. Interestingly, among the top altered signalling pathways, we found that H69M cells presented upregulated several genes associated with HGF/MET pathway and EMT. Moreover, changes in DNA repair and survival genes were observed in H69M cells compared to H69 (**Table R.9.**). The most relevant differentially expressed genes of these pathways were also represented in a heatmap (**Figure R.33.**).

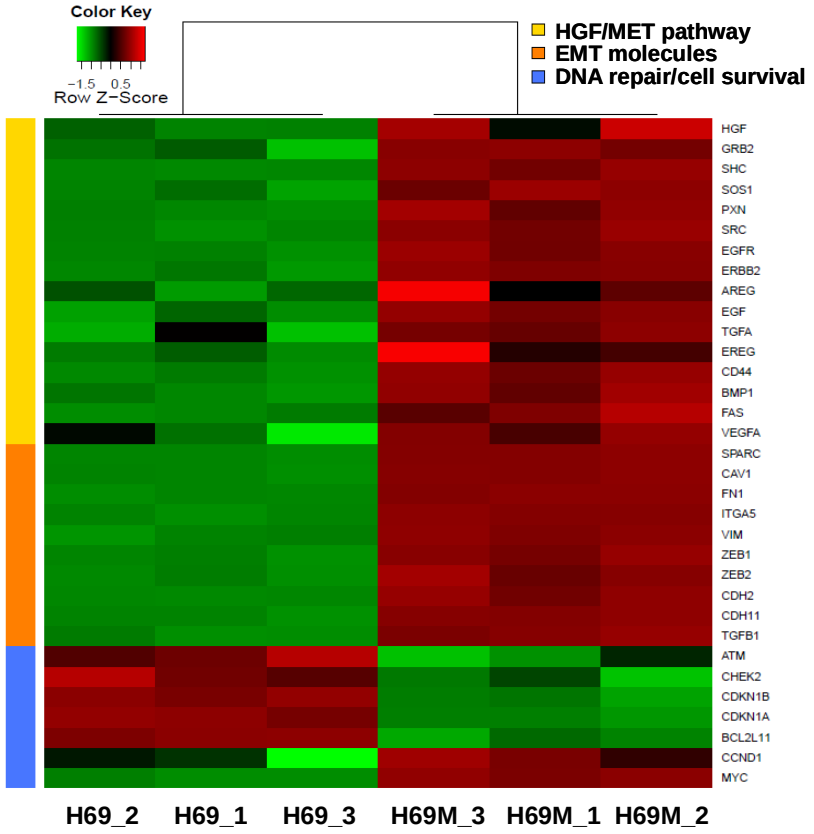

Figure R.33. Heatmap of altered genes of HGF/MET pathway, EMT, DNA repair and cell survival in H69M cells compared to H69. Horizontal rows show individual genes; vertical columns represent individual samples (3 samples from H69 on the left and 3 samples from H69M on the right). Color intensity means degree of gene expression modulation. Red indicates up-regulation and green down-regulation. Black indicates no change. The colours at the left site (yellow, orange, blue) indicates the three groups which belong the different genes.

Table R.9. The most **r**elevant differentially expressed genes of HGF/MET pathway, EMT, DNA repair and cell survival in H69M cells compared to H69.

HGF/MET pathway Molecules		
Gene	**Description**	**Exp. Value**
HGF	Hepatocyte Growth Factor	0,339
GRB2	Growth factor receptor-bound protein 2	0,406
SHC	Src homology 2 domain containing	1,873
SOS1	Son of Sevenless homolog 1	0,463
PXN	Paxillin	0,716
SRC	SRC	0,372
EGFR	Epidermal Growth Factor Receptor	3,152
ERBB2	HER2/neu	1,486
AREG	Amphiregulin	0,743
EGF	Epidermal Growth Factor	1,597
TGFA	Transforming growth factor alpha	0,487
EREG	Epiregulin	0,825
CD44	CD44	1,499
BMP1	Bone morphogenetic protein 1	0,979
FAS	TNF receptor superfamily, member 6	1,883
VEGFA	Vascular Endothelial Growth Factor A	0,603

Epithelial to Mesenchymal Transition (EMT) molecules		
Gene	**Description**	**Exp. Value**
SPARC	Osteonectin	7,928
CAV1	Caveolin1	7,881
FN1	Fibronectin	6,808
ITGA5	Integrin a5 (ITGA5)	6,869
VIM	Vimentin	6,255
ZEB1	Zinc finger E-Box binding homeobox 1	1,9
ZEB2	Zinc finger E-Box binding homeobox 2	2,688
CDH2	N-cadherin	1,723
CDH11	b-catenin	4,788
TGFB1	Transforming growth factor beta 1	3,61
DNA repair and survival molecules		
Gene	**Description**	**Exp. Value**
ATM	Ataxia Telangiectasia Mutated	-0,275
CHEK2	Chk2 (Checkpoint kinase 2)	-0,554
CDKN1B	p27Kip1 (cyclin-dependent kinase inhibitor 1B)	-0,56
CDKN1A	p21Cip1(cyclin-dependent kinase inhibitor 1A)	-1,292
BCL2L11	BIM	-1,443
CCND1	Cyclin D	0,353
MYC	MYC	1,98

To validate the microarray we further analysed by real-time RT-PCR the expression of HGF, SPARC, Fibronectin and Vimentin, genes upregulated in H69M cells (**Figure R.34.**). Increase in HGF, SPARC, Fibronectin and Vimentin expression was detected in H69M cells by qRT-PCR, which resembled the results of the microarrays.

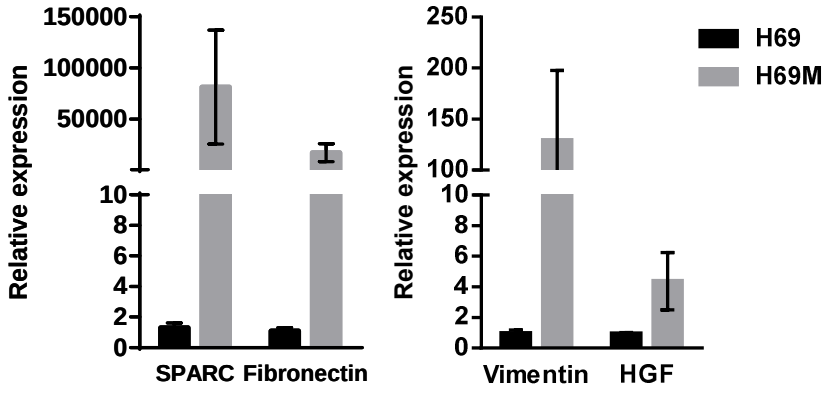

Figure R.34. qRT-PCR validation of HGF, SPARC and Fibronectin. Levels of HGF, SPARC, Fibronectin and Vimentin mRNA of H69 and H69M cells were assayed by quantitative real-time RT-PCR. cDNA was synthesized from RNA samples from H69 and H69M cells. Expression values were normalized to the levels of a control RNA (RPLP0). Relative mRNA levels were normalized to the expression of the control sample.

R.5.3.5. H69M cells secrete higher levels of HGF than H69

Given the increase of HGF mRNA expression in H69M compared to H69 cells, our next step was to measure in both cell lines the HGF released into the culture medium by ELISA. We found that H69M cells produced higher levels of HGF than H69, result that correlated with our previous finding of higher mRNA expression (**Figure R.35.**).

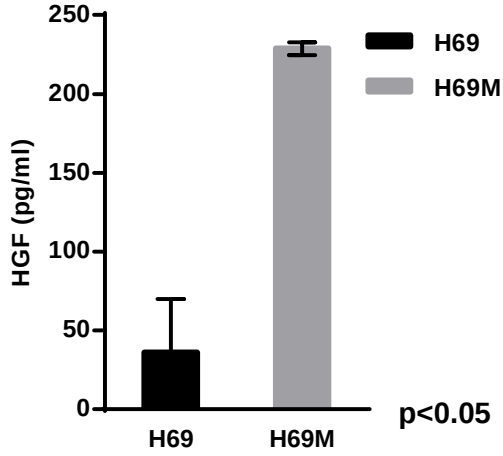

Figure R.35. HGF production in H69 and H69M cells analysed by ELISA technique. Cells were incubated in medium for 48 hours, culture supernatants were harvested and HGF concentrations were determined by ELISA. Each data point represents the mean ± s.d. HGF levels (pg/ml) of three independent experiments.

R.5.3.6. PF-2341066 is able to inhibit HGF-induced MET phosphorylation in the mesenchymal H69M cells

As HGF is and inductor of EMT in our cell line model, we assessed the expression of EMT-related markers in H69M cells as well as MET pathway. As shown in **Figure R.36.** H69M cells presented a mesenchymal phenotype when compared to H69. H69M cells showed mesenchymal features characterized by the upregulation of Snail1 and Fibronectin, and downregulation of NCAM and E-cadherin. In addition, MET basal activation demonstrated by phorphorylation of Tyr1349 was detected in H69M cells when compared to H69.

We then treated H69M cells with HGF for 15 minutes to asses if they were still sensitive to HGF stimulation. We observed a higher increase in MET phosphorylation when compared to the increase observed in H69 cells, and in the downstream molecules p-GAB-1 (Tyr307) and p-ERK1/2, indicating that these cells were more sensitive to exogenous HGF stimulation than parental H69.

Next, to study the molecular effects of the MET inhibitor PF-2341066, H69M cells were treated with PF (200 nM) for 3 hours and then stimulated with HGF (40 ng/ml) during 15 minutes. We found that PF-2341066 treatment was able to inhibit HGF-induced MET phosphorylation and downstream molecules in H69M cells (**Figure R.36.**).

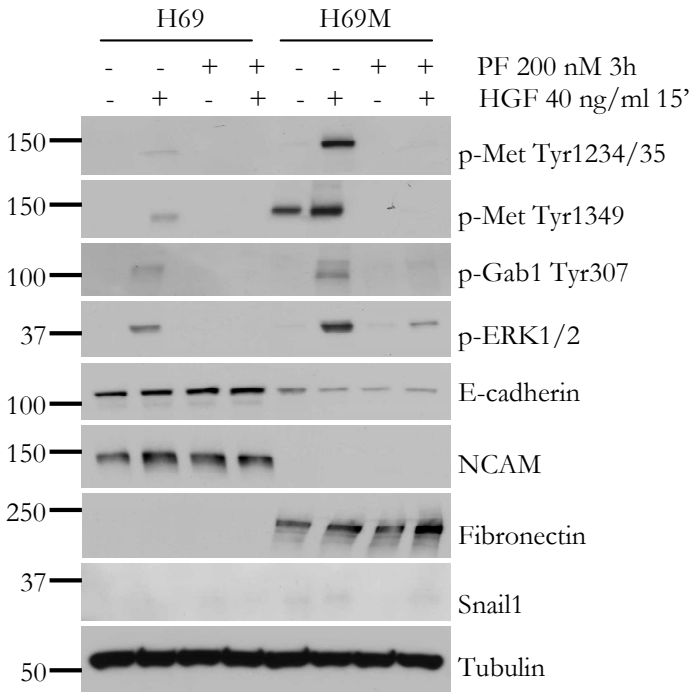

Figure R.36. H69M cells present a mesenchymal phenotype that correlate with HGF/MET pathway activation and PF-2341066 is able to inhibit HGF-induced MET phosphorylation in these cells. Cells were serum-starved for 24 hours and then treated with PF-2341066 (200 nM) for 3 hours and stimulated with HGF (40 ng/ml) during 15 minutes. Whole cell lysates were purified and subjected to Western Blot to asses phosphorylated MET, GAB-1 and ERK1/2 protein levels, and total levels of E-cadherin, NCAM, Fibronectin, and Snail1.

R.5.3.7. PF-2341066 decreases clonogenic capacity in H69M cells

Given our previous results that indicated that PF-2341066 treatment was able to inhibit basal and HGF-induced MET activation in H69M cells, we wanted to examine cellular effects of MET specific inhibition. First of all we analysed PF-2341066 effects on clonogenic capacity in H69M cells.. After 14 days of PF-2341066 treatment we found a significant dose-dependent reduction of anchorage-dependent growth in this

mesenchymal subpopulation. Treatment with PF-2341066 at 200 nM decreased anchorage-dependent growth of H69M by 50% ($P<0.05$) (**Figure R.37.**).

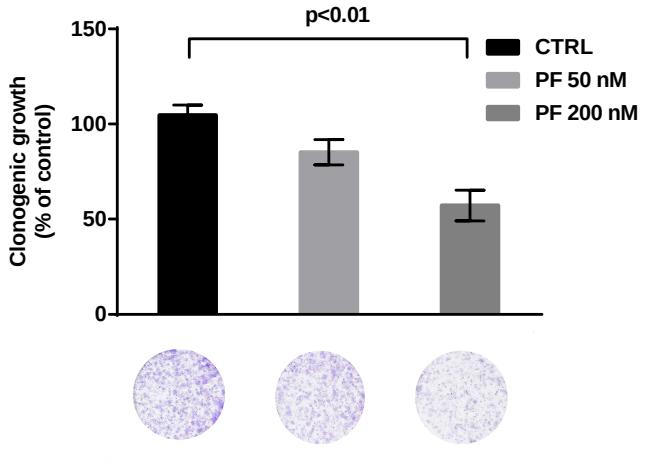

Figure R.37. PF-2341066 decreases anchorage-dependent growth in H69M cells. Cells were seeded at low density, treated during 14 days with PF-2341066 at 50 or 200 nM and the resultant colonies were stained with Crystal Violet and scanned. Image analysis was carried out using ImageJ software and results were plotted as arbitrary units. Each data point represents the mean ± s.d. percent clonogenic growth of three independent experiments. Data are reported as percentage in relation to the control group (set at 100%).

R.5.3.8. H69M cells present higher invasion capacity than H69 and PF-2341066 is able to inhibit this effect

It is described that mesenchymal cells presented an increased invasiveness [302,354,355]. Moreover, MET activation has been associated with this cellular feature [122,123,317,356]. We therefore compared invasive capacity between H69 and H69M cells and the cellular effects of PF-2341066. We observed that H69M presented an increase about 50 % of

cell invasion compared to H69 cells (P<0.05). Moreover, PF-2341066 treatment significantly diminished cell invasion in both cell lines (P<0.05) (**Figure R.38.**).

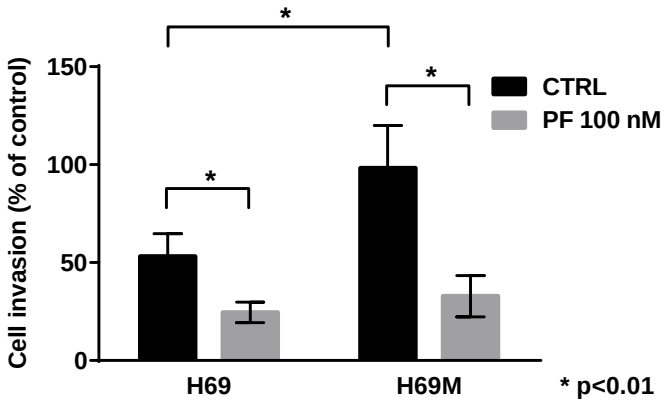

Figure R.38. PF-2341066 decreases cell invasion in H69 and H69M cells. Cells were grown in serum-free media and seeded into the inserts of 24-well (8 μm pore size) CHEMICON Invasion Chamber in the presence of PF-2341066 (200 nM). Inserts were placed into Falcon companion plates containing 10% FBS and 40 ng/ml HGF and incubated for 24 h. The number of invading cells on the underside of the membrane was determined using Crystal Violet staining. Each data point represents the mean ± s.d. percent cell invasion of three independent experiments. Data are reported as percentage in relation to the control group (set at 100%).

R.5.3.9. Mesenchymal cells are more tumorigenic *in vivo* than epithelial SCLC cells

To confirm our *in vitro* data that demonstrate that H69M cells presented higher growth kinetics and invasion capacity when compared to H69, we wanted to test the *in vivo* xenograft growh of both cell lines. Tumourigenicity of H69 and H69M cells were determined by subcutaneous injection of $10*10^6$ viable cells embedded in Matrigel into

the right flank (H69) and left flank (H69M) of ten 5-weeks-old male BALB/c nude mice (**Figure R.39.**).

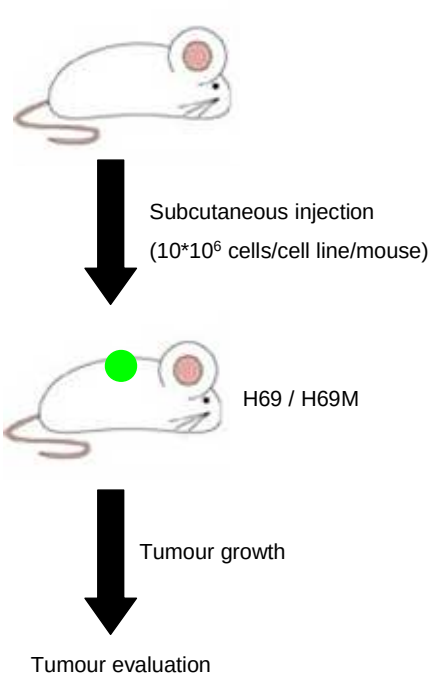

Figure R.39. Xenograft model with H69 versus H69M cells. Cells were subcutaneously injected into the right flank (H69) and left flank (H69M) of ten 5-week-old male BALB/c nude mice. Tumour volume was monitored using a calliper three times a week. At the end of the experiment, mice were euthanized and a portion of tumours were rapidly fixed in 4% formalin and embedded in paraffin for immunohistochemical study. Another portion of tumour was embedded in OCT compound for DNA, RNA or protein extraction.

Tumours were allowed to grow and tumour volumes were measured with a digital caliper three times a week. After 22 days, mice were euthanized and tumours were removed. A portion of tumour was formalin fixed and paraffin-embedded for the H&E staining and immunohistochemical study. In all mice we observed that tumours generated from H69M were significantly larger (median volume: 1511 mm^3) compared to the tumours

generated from H69 (median volume: 566 mm^3) ($P<0.05$) (**Figure R.40.**).

A

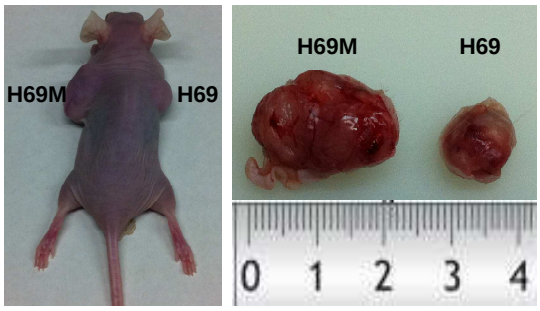

B

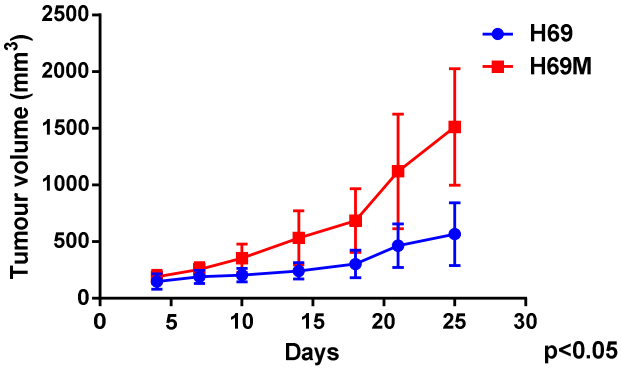

Figure R.40. H69M cells are more tumorigenic *in vivo* than H69. A. Photograph of a representative mouse with H69 and H69M cells subcutaneously inoculated at right and left flanks respectively (Top) and photograph of the excised tumours from the same animal (Bottom). **B.** Tumour growth curves obtained by plotting mean ± s.d. tumour volumes (mm^3) from H69 and H69M xenograft against time.

Histological examination revealed that both tumours shared very similar characteristics, suggesting that H69M were able to recapitulate the original round small cell morphology of the parental H69 (**Figure R.41.**).

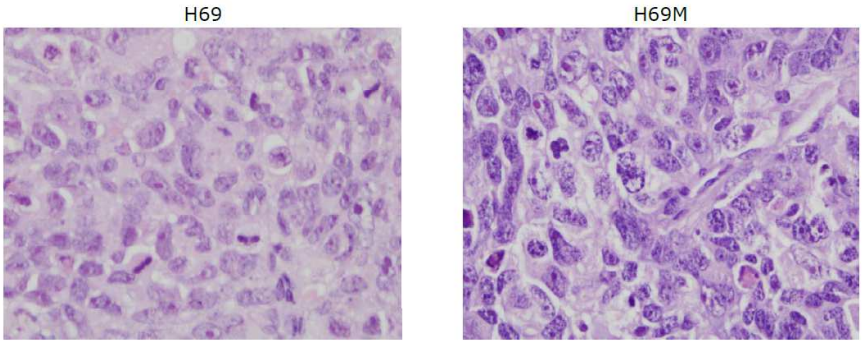

Figure R.41. H69M-derived tumours are able to recapitulate the original round small cell morphology of the parental H69. Representative H&E images showing the histological morphology of H69 and H69M-derived tumours.

Local invasiveness was also assessed by analysing invasive tumour foci in surrounding soft tissues. We found significant differences in local infiltration of surrounding tissues (muscle): H69M cells were more invasive locally showing foci of infiltrating cells in 9/10 mice compared to 1/10 for H69 cells ($P<0.001$) (**Figure R.42.**).

A

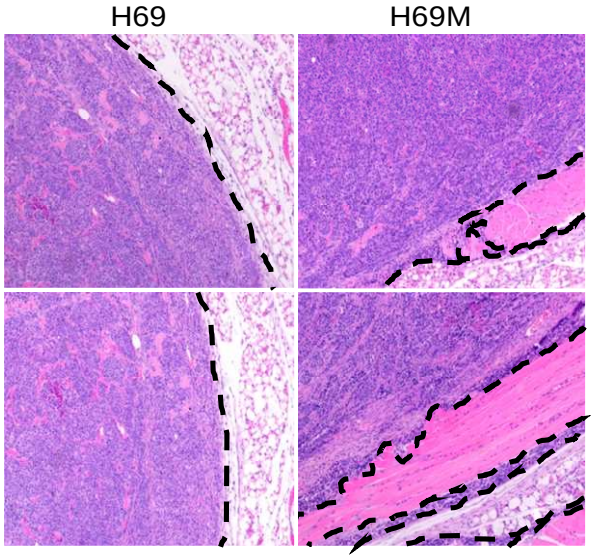

B

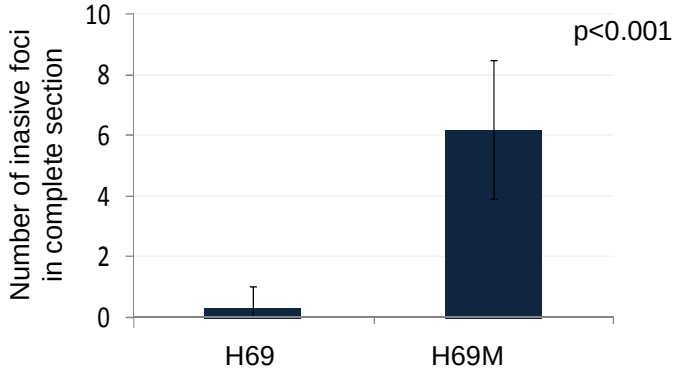

Figure R.42. H69M cells are more invasive locally in xenograft tumours. A. Representative H&E images of H69 and H69M-derived tumours showing the invasive tumour foci in surrounding soft tissues. **B.** Quantification of number of invasive tumour foci in complete H&E stained section for H69 and H69M xenograft tumours. Data are represented as mean ± SEM and significance level is displayed.

Then we studied proliferation according to Ki-67 marker, apoptosis (Cleaved-caspase 3) and angiogenesis (CD31) in these tumours. Representative images of the IHC markers used and graphs with the quantification of stained cells are shown in **Figure R.43.** No significant differences were found in Ki-67 and Cleaved-caspase 3 staining of H69 and H69M-derived tumours. Nevertheless, the presence of CD31-stained tubular structures was significantly increased in H69M-derived tumours (P=0.012), suggesting a possible role of angiogenesis in the greater tumorigenic capacity of H69M cells in comparison to parental cells.

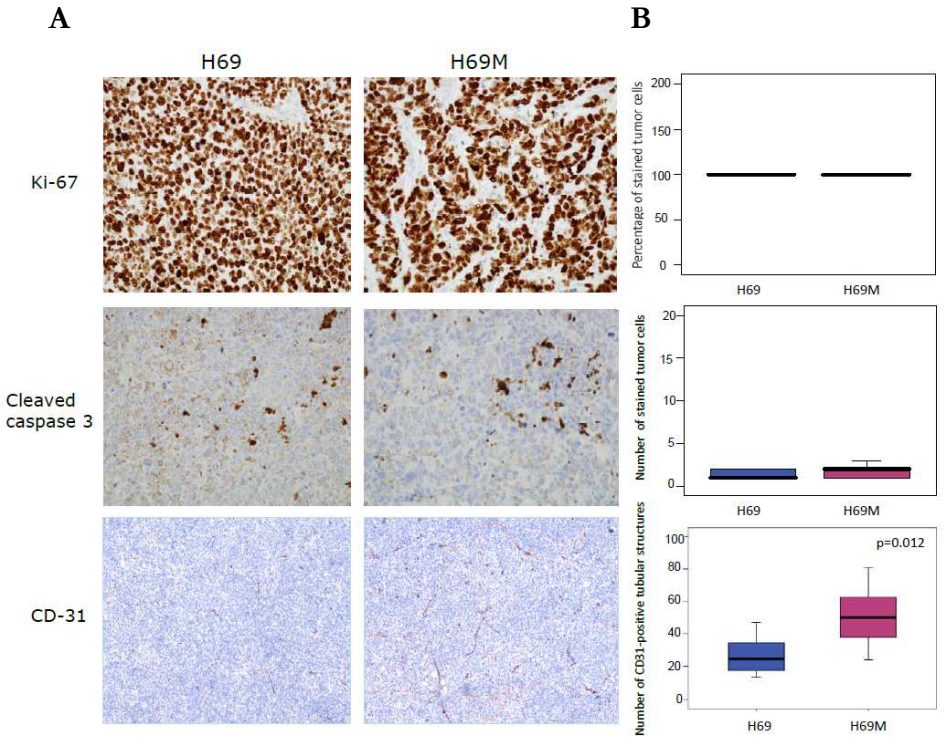

Figure R.43. H69M cells present increased vascularization in xenograft tumours. A. Representative IHC images of Ki-67, Cleaved-caspase 3 and CD-31 staining of H69 and H69M-derived tumours. **B.** Box plot graphs indicating the IHC results (mean ± SEM) for Ki-67, Cleaved-caspase 3 and CD-31 staining in H69 and H69M xenograft tumours.

In addition, phosphorylated MET levels and EMT markers were evaluated by immunohistochemistry in the same tumours. Representative images of the IHC markers used and graphs with the quantification of staining by Hscore are shown in **Figure R.44.** Interestingly, a significant MET activation was observed in H69M when compared to H69-derived tumours. Moreover, H69M showed lower levels of the epithelial markers NCAM and E-cadherin and higher levels of the mesenchymal markers Snail1, Vimentin and SPARC in comparison with H69-derived tumours.

All these differences were statistically significant. Therefore, H69M cells maintained the mesenchymal phenotype *in vivo*.

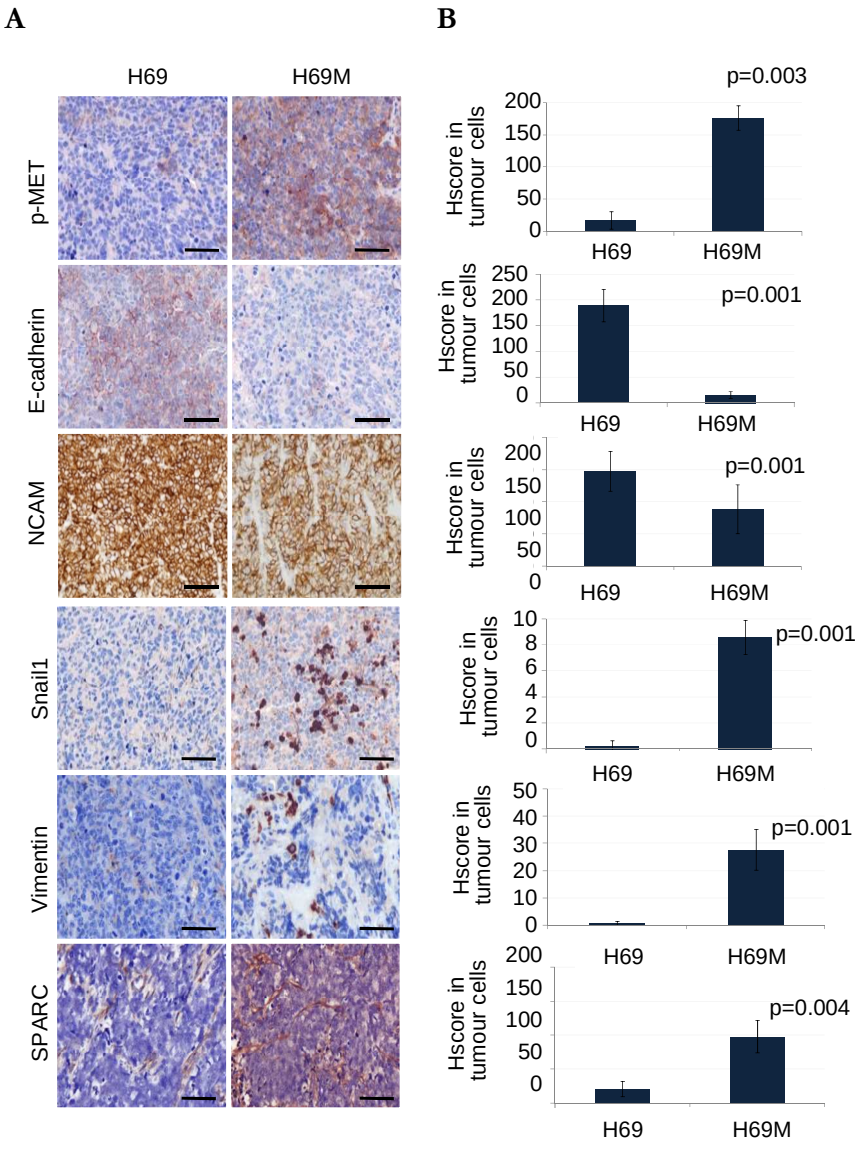

Figure R.44. H69M-derived tumours present a mesenchymal phenotype that correlate with MET activation. A. Representative IHC images of p-MET, E-cadherin, Snail1, SPARC, Vimentin and NCAM staining of H69 and H69M-derived tumours. **B.** Quantification of the IHC results for p-MET, E-cadherin, Snail1,

SPARC, Vimentin and NCAM staining (mean HSCORE ± SEM) in H69 and H69M xenograft tumours. Significance level is displayed.

Furthermore, we performed multiplexing assays with Snail1 and p-MET antibodies to evaluate if both proteins colocalize in H69M-derived tumours. As shown in multiplexing images of **Figure R.45.**, Snail1 was expressed in cells with up-regulated MET activity.

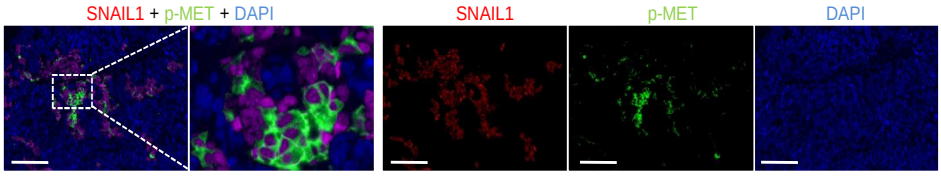

Figure R.45. Snail1 is expressed in cells with up-regulated MET activity in H69M-derived tumours. Representative image of immunofluorescence staining in H69M tumour for Snail1 (red), p-MET (green) and DAPI (blue). Boxes represent the region of magnification shown in adjacent image, indicating co-localization of Snail1 and p-MET. Scale bars, 75 μm.

R.5.3.10. Mesenchymal cells are more tumourigenic *in vivo* than H69 using a lower number of cells

Globally, higher local aggressiveness and a mesenchymal phenotype were observed in H69M-derived tumours. However, histological appearance was similar to H69, demonstrating the capacity of H69M to recapitulate the original SCLC histology. As these could be due to tumour initiating capacity (stemness), we subsequently performed an experiment with subcutaneous injection of 100 or 500 cells of H69 and H69M cells into the right and left flanks respectively of 5 mice. In the case of injection of 100 cells we observed tumour formation in 5/5 cases of H69M cells and

3/5 cases of H69. Moreover, the H69M tumours were larger (median volume= 165 mm^3) compared to the tumours generated by H69 cells (median volume= 79 mm^3). In the case of injection of 500 cells we found rapid tumour formation in 5/5 cases of H69M cells and slower tumour formation in 3/5 cases in H69. We found that tumours generated by H69M appeared 43 days after cell inoculation, whereas the H69 tumours did not appear until 51 days after cell inoculation. In addition, the H69M tumours were larger (median volume= 384 mm^3) compared to the tumours generated by H69 cells (median volume= 82 mm^3) (**Table R.10.**).

Table R.10. Tumour incidence related to the number of H69 and H69M cells injected into the flanks of nude mice

Cell type	Cell dose	Tumour incidence	Median tumour volume (mm3)
H69	100	3/5	79
	500	3/5	82
H69M	100	5/5	165
	500	5/5	384

R.5.3.11. PF-2341066 increases chemosensitivity of Etoposide in chemorefractory H69M cells *in vitro* and in xenograft model

Our next step was to evaluate whether MET inhibition was able to sensitize H69M cells to chemotherapy *in vitro*. Therefore, we analysed the

effects of PF-2341066, Etoposide and the combination of both treatments on clonogenic capacity of H69M cells. After 14 days of treatment we observed the strongest inhibition of clonogenicity with the combination of Etoposide and PF-2341066, suggesting that MET inhibition by PF-2341066 reversed chemoresistance ($p<0.05$) (**Figure R.46.**).

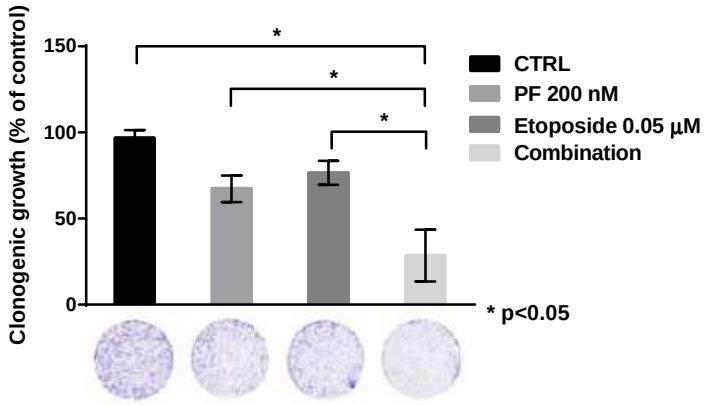

Figure R.46. PF-2341066 sensitizes H69M cells to chemotherapy. Cells were seeded at low density, treated during 14 days with PF-2341066 (200 nM), Etoposide (0.05 μM) or the combination of both drugs and the resultant colonies were stained with Crystal Violet and scanned. Image analysis was carried out using ImageJ software and results were plotted as arbitrary units. Each data point represents the mean ± s.d. percent clonogenic growth of three independent experiments. Data are reported as percentage in relation to the control group (set at 100%).

We confirmed this conclusion in tumour xenografts grown in immunodeficient mice. To this aim, $10x10^6$ H69M cells embedded in Matrigel were inoculated subcutaneously into the right flank of forty 5-weeks-old male BALB/c nude mice. Tumours were allowed to grow for one week and tumour volumes were measured with a digital caliper three times a week. When tumour volume reached approximately 200-300 mm^3 mice were randomized into 4 experimental groups with 10 mice in each

group: 1) no therapy, 2) Etoposide alone, 3) PF alone, 4) Etoposide+PF. Etoposide, PF-2341066 and respectives vehicles were administered at doses and schedules indicated in **Table R.11**.

Table R.11. Drug dosing and treatment schedule of H69M subcutaneous xenograft model

Group	Doses	Schedule
Control n=10	Etoposide vehicle PF-2341066 vehicle	i.p. day 1, 2, 3 oral gavage daily
Etoposide n=10	Etoposide 12 mg/kg PF-2341066 vehicle	i.p. day 1, 2, 3 oral gavage every day
PF-2341066 n=10	PF-2341066 100 mg/kg Etoposide vehicle	oral gavage every day i.p. day 1, 2, 3
Combination n=10	Etoposide 12 mg/kg PF-2341066 100 mg/kg	i.p. day 1, 2, 3 oral gavage every day

Focusing on tumour volume measurements, we observed that PF-2341066 alone at a dose of 100 mg/kg and Etoposide alone at a dose of 12 mg/kg had not significant effect on inhibiting tumour xenograft growth compared to the control group. However, the combination therapy produced a significant decrease in tumour growth compared with either group alone ($p<0.05$), suggesting that MET inhibition increases sensitivity of Etoposide in chemorefractory H69M-derived tumours (**Figure R.47.**).

A

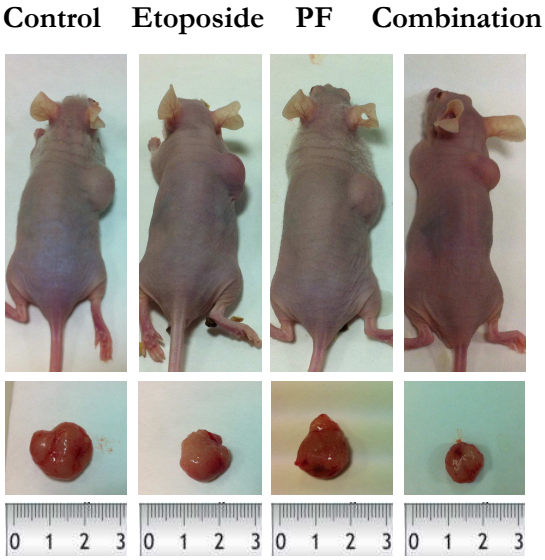

B

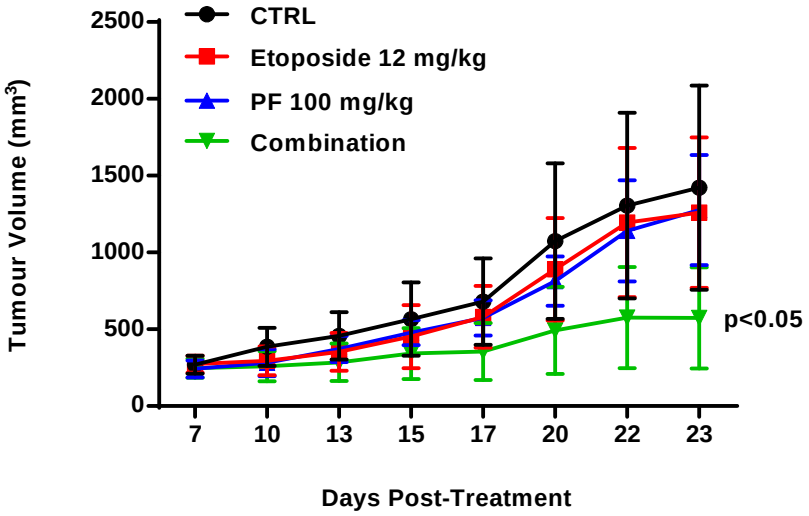

Figure R.47. PF-2341066 effects in combination with Etoposide in H69M xenograft model. A. Photograph of a representative mice of each group of treatment (Top) and photograph of the excised H69M-derived tumours from the same animals (Bottom). **B.** Tumour growth curves obtained by plotting the mean ± s.d. H69M xenograft tumour volume (mm^3) of each group of mice against time.

R.5.3.12. PF-2341066 in combination with Etoposide decreases mesenchymal markers and increases epithelial markers expression in mesenchymal derived tumours

After two weeks of treatment, tumour-bearing mice were sacrificed and tumours were prepared for IHC. Two subsets of markers were used to assess EMT: Snail1, Vimentin and SPARC, widely used as mesenchymal markers, and NCAM and E-cadherin as traditional epithelial markers. p-MET and CD31 were also evaluated. Representative images of the IHC markers used and graphs with the quantification of immunohistochemistry staining are shown in **Figure R.48.** No significant changes in the expression of the seven markers analysed were observed in the tumours from mice treated with Etoposide alone compared to controls. However, PF-2341066 treated tumours showed a significant increase of epithelial markers (NCAM and E-cadherin) and a significant decrease of mesenchymal markers (Snail1, Vimentin and SPARC), angiogenesis (CD31) and MET phosphorylation, when compared with expression levels of these markers in the control conditions. Interestingly, these effects were even more pronounced in the combination therapy group compared with those treated with PF alone.

Figure R.48. PF-2341066 in combination with Etoposide decreases mesenchymal markers and increases epithelial markers in H69M-derived tumours. A. Representative IHC images of E-cadherin, NCAM and CD31 staining and quantification (mean HSCORE ± SEM) in H69M xenograft tumours of each therapy group. **B**. Representative IHC images of p-MET, Snail, Vimentin and SPARC staining and quantification (mean HSCORE ± SEM) in H69M xenograft tumours of each therapy group.

Significance level is displayed. Scale bars, 75 μm.

(Next page)

A

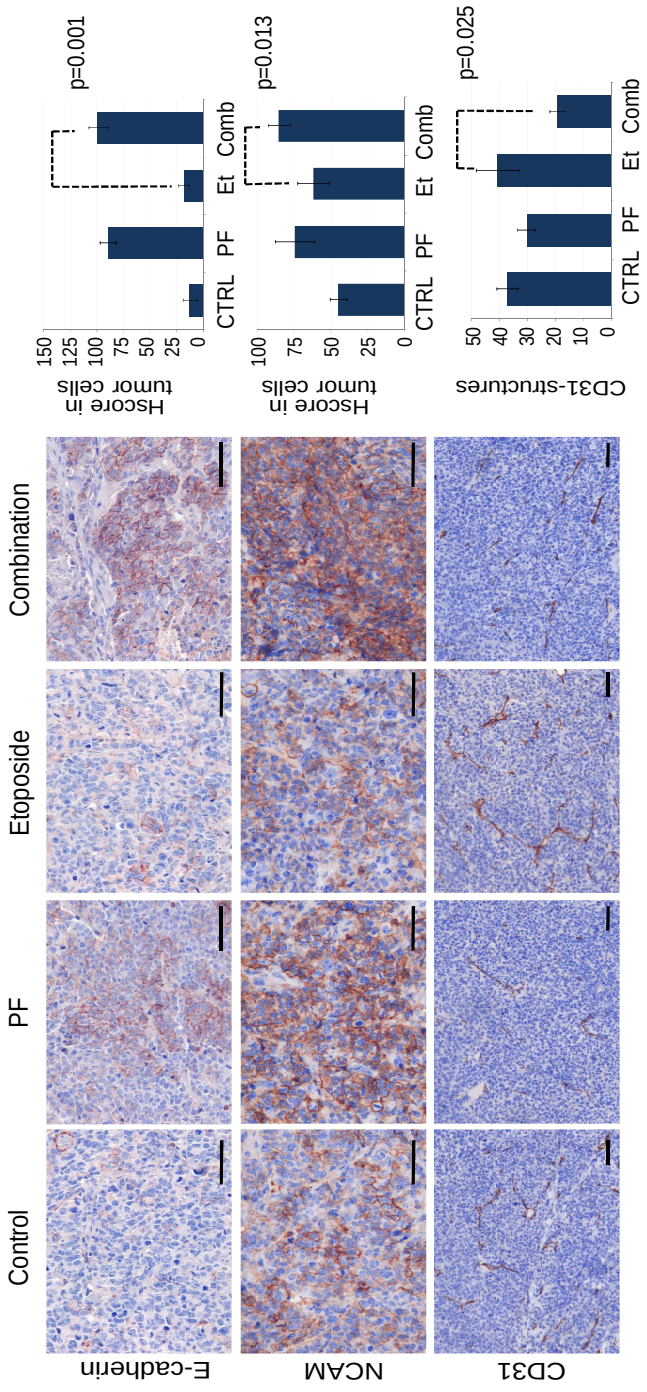
E-cadherin
NCAM
CD31
Control
PF
Etoposide
Combination
Hscore in tumor cells
CD31-structures
p=0.001
p=0.013
p=0.025
CTRL
PF
Et
Comb

B

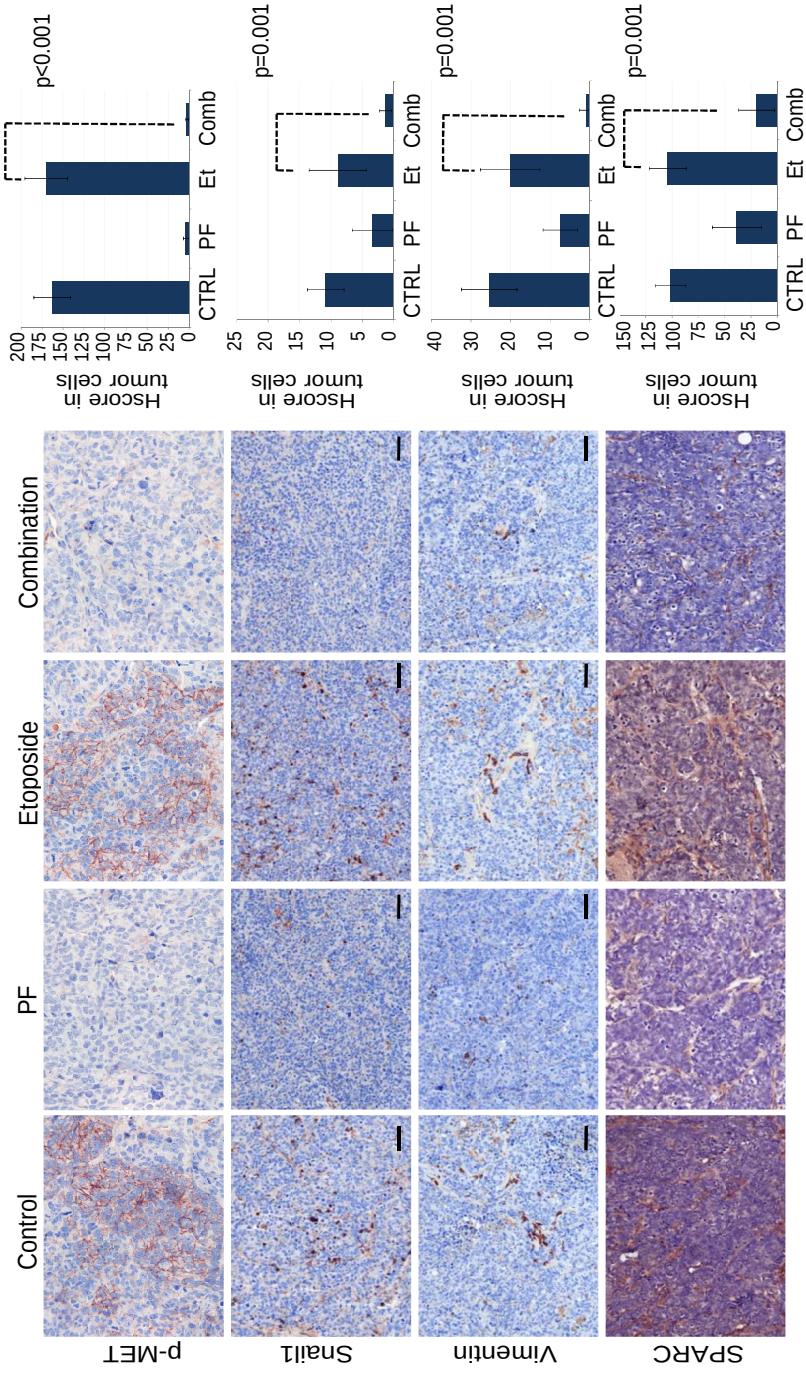
p-MET
Snail1
Vimentin
SPARC
Control
PF
Etoposide
Combination
Hscore in tumor cells
p<0.001
p=0.001
p=0.001
p=0.001
CTRL
PF
Et
Comb

R.5.3.13. PF-2341066 increases chemosensitivity of Etoposide in chemosensitive H69 derived tumours

Given the previous results, we wanted to know if PF-2341066 was able to increase chemosensitivity of Etoposide in the chemosensitive H69 cells. In this case, both Etoposide alone and the combination of Etoposide and PF-2341066 decreased the tumour size significantly when compared to the control group and PF alone ($p<0.05$) (**Figure R.49.**).

A

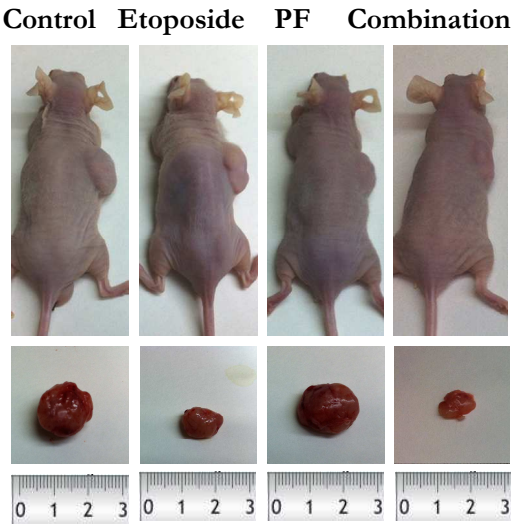

B

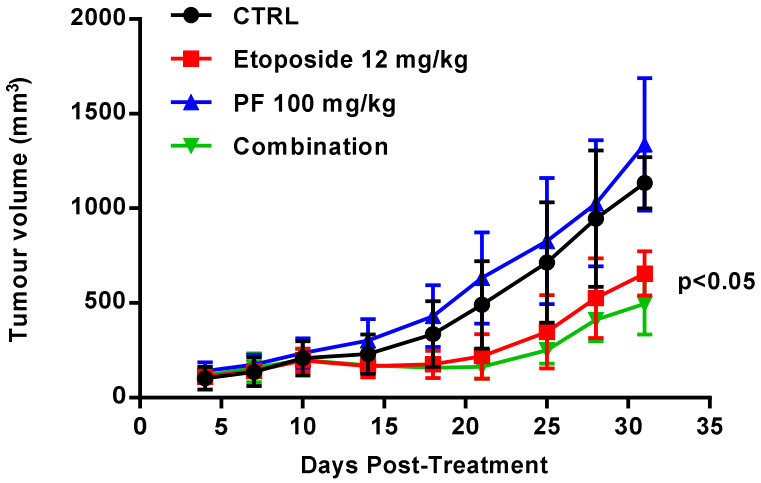

Figure R.49. PF-2341066 effects in combination with Etoposide in H69 xenograft model. A. Photograph of a representative mice of each group of treatment (Top) and photograph of the excised H69-derived tumours from the same animals (Bottom). **B.** Tumour growth curves obtained by plotting the mean ± s.d. H69 xenograft tumour volume (mm^3) of each group of mice against time.

R.5.3.14. PF-2341066 increases chemosensitivity of Etoposide in chemorefractory H865 derived tumours

To further explore the above hypothesis we decided to use the same experimental *in vivo* model with another SCLC cell line, H865. This cell line was derived from a SCLC patient treated with chemotherapy. We selected this cell line because it was sensitive to HGF stimulation showing increased expression of p-MET and PF-2341066 was able to inhibit these HGF-induced effects (**Figure R.50A**). In addition, H865 cells secreted higher levels of HGF when compared to H69 by ELISA (**Figure R.50B**) and presented resistance to Etoposide *in vitro* (**Figure R.50C**).

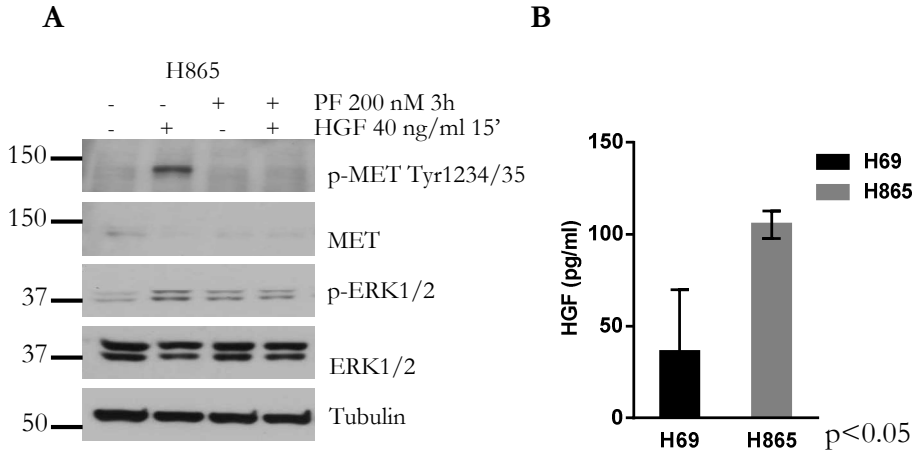

C

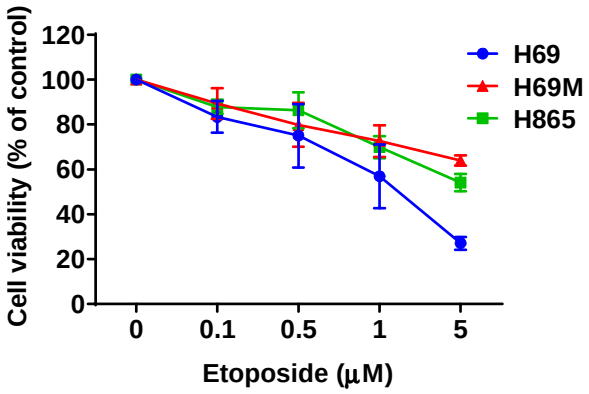

Figure R.50. H865 cells characterization. A. PF-2341066 inhibits HGF-induced MET phosphorylation in chemoresistant H865 cells. Cells were serum-starved for 24 hours and then treated with PF-2341066 (200 nM) for 3 hours and stimulated with HGF (40 ng/ml) during 15 minutes. Whole cell lysates were purified and subjected to Western Blot to asses total and phosphorylated MET, GAB-1 and ERK1/2 protein levels. **B.** H865 cells secrete higher levels of HGF than H69. Cells were incubated without change of medium for 72 hours. Culture supernatants were harvested and HGF concentration was determined by ELISA. Each data point represents the mean ± s.d. HGF levels (pg/ml) of three independent experiments. **C.** Sensitivity of H865 and H69 cells to Etoposide treatment for 72 hours, measured by MTS assay. Each data point represents the mean ± s.d. percent cell growth of three independent experiments. Data are reported as percentage in relation to the control group (set at 100%).

To elucidate if MET inhibition could revert chemoresistance in H865 cell line, we performed a clonogenic assay with Etoposide, PF-2341066 and the combination of both treatments. After 14 days of treatment we observed the highest inhibition rate with the combination of Etoposide and PF-2341066, suggesting that MET inhibition by PF-2341066 reversed chemoresistance in these cells ($p<0.05$) (**Figure R.51**).

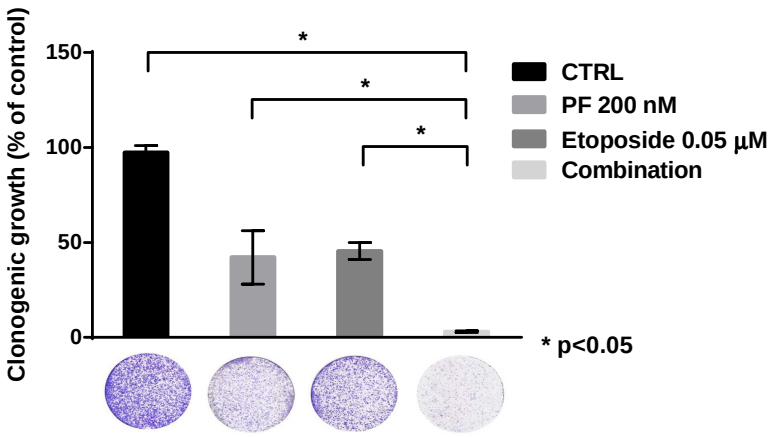

Figure R.51. PF-2341066 sensitizes H865 cells to chemotherapy. Cells were seeded at low density, treated during 14 days with PF-2341066 (200 nM), Etoposide (0.05 µM) or the combination of both treatments and the resultant colonies were stained with Crystal Violet and scanned. Image analysis was carried out using ImageJ software and results were plotted as arbitrary units. Each data point represents the mean ± s.d. percent cell growth of three independent experiments, compared to controls at 100%.

We next confirmed this conclusion *in vivo* following the same experimental model than in H69M. As above, PF-2341066 alone at a dose of 100 mg/kg and Etoposide alone at a dose of 12 mg/kg had not significant effect on inhibiting tumour xenograft growth compared to the control group. However, the combination therapy produced a significant decrease in tumour growth compared with either group alone ($p<0.01$), suggesting that MET inhibition was also able to increase sensitivity of Etoposide in chemorefractory H865-derived tumours (**Figure R.52.**).

A

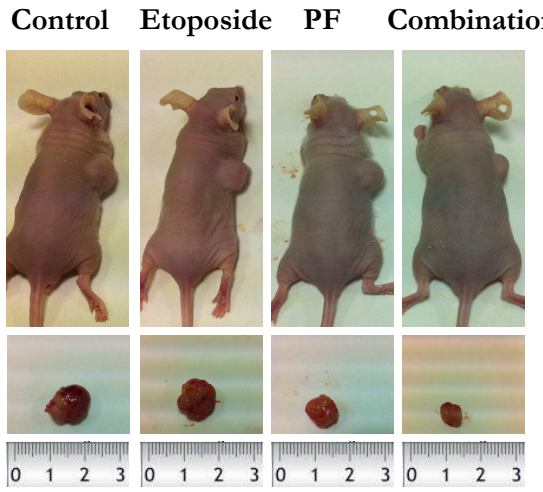

B

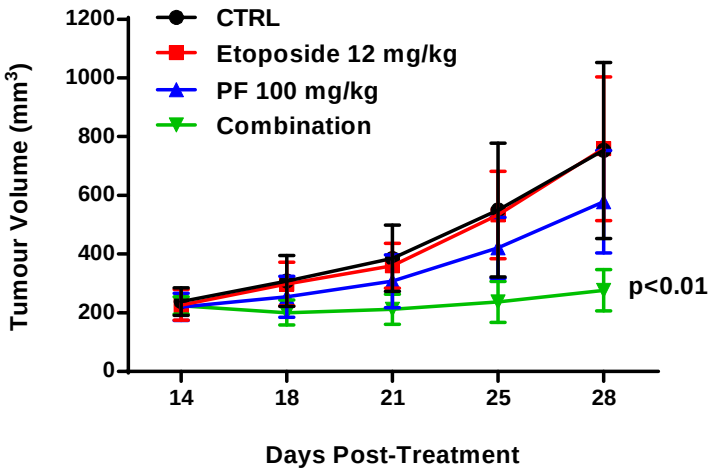

Figure R.52. PF-2341066 effects in combination with Etoposide in H865 xenograft model. A. Photograph of a representative mice of each group of treatment (Top) and photograph of the excised H865-derived tumours from the same animal (Bottom). **B.** Tumour volume (mm^3) of H865 xenograft tumours from each group of mice. Each data point represents the mean ± s.d. tumour volume of each group of mice compared to control

Then, we sacrificed three mice per group and the remaining six mice continued the experiment. The objective of this second approach was to study the behaviour of H865-derived tumours upon treatment discontinuation. Thus, we maintained three mice per group that were not treated (vehicle) and the remaining three mice were treated again following the same treatment conditions of the previous model (**Table R.12.**).

Table R.12. Treatment schedule for the study of the H865 tumour growth after treatment discontinuation

Group	Treatment
Control	Vehicle (n=6)
Etoposide	Vehicle (n=3) Etoposide (n=3)
PF-2341066	Vehicle (n=3) PF-2341066 (n=3)
Combination	Vehicle (n=3) Combination (n=3)

After 11 days of treatment (day 40), mice were ethically sacrificed. Focusing on tumour volumes, we did not observe significant differences in mice treated with Etoposide or PF-2341066 as monotherapy compared with mice without treatment (**Figure R.53B**, **Figure R.53C**). Nevertheless, in the combination therapy group, in mice without

treatment, H865-derived tumours showed a significant regrowth in comparison with treated mice (**Figure R.53D.**).

A

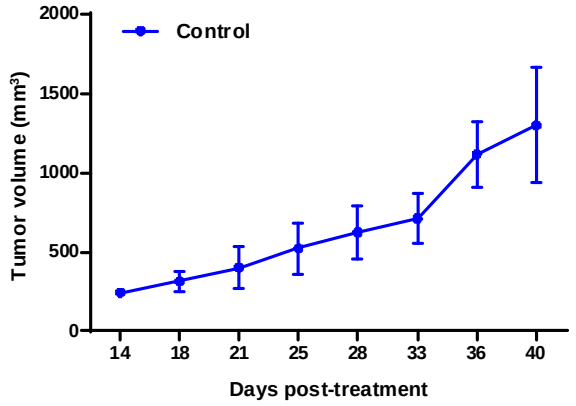

B

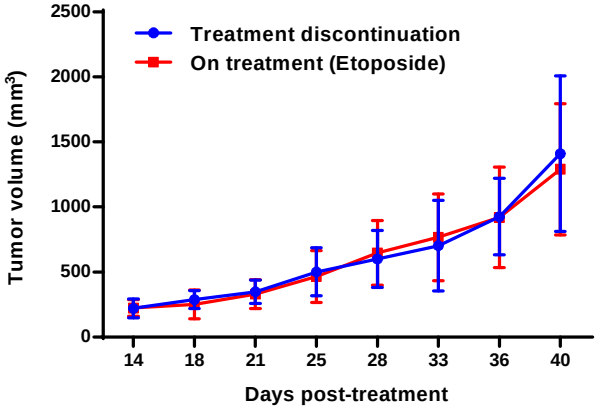

C

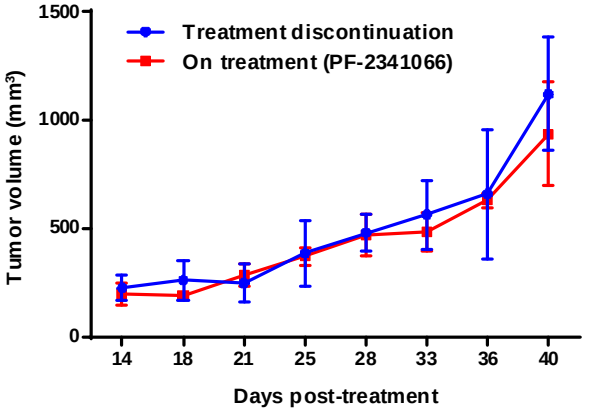

D

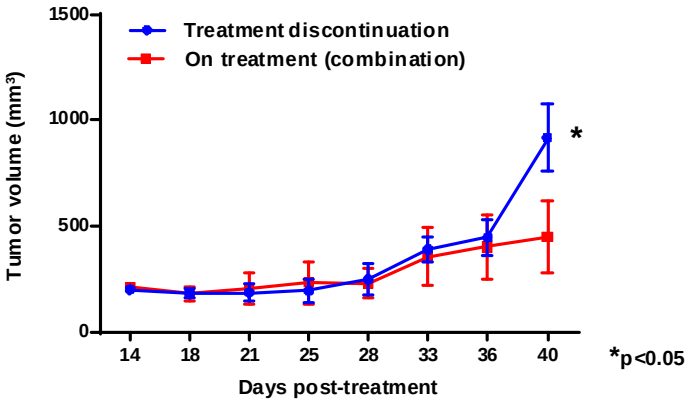

Figure R.53. H865-derived tumours from combination group regrow significantly upon treatment discontinuation. Tumour volume (mm^3) of H865 xenograft model from each group (on treatment or upon treatment discontinuation). Each data point represents the mean ± s.d. tumour volume of each group of mice.

R.5.4. Mesenchymal markers are associated with a worse prognosis in SCLC patients

The data presented above supports a potential role of MET inhibition in the treatment of SCLC. To validate this hypothesis in human samples, we evaluated an independent serie of 87 SCLC cases with routine diagnostic formalin fixed paraffin embedded (FFPE) tissue material by immunohistochemistry. **Table R.13.** shows the patients' characteristics. All these patients receive standard first-line chemotherapy with Platinum and Etoposide and concomitant radiotherapy in cases where indicated.

Table R.13. Selected SCLC patients' characteristics (N=87)

		Number	Percentage
Age	Median (range)	6 (29-87)	
Gender	Male	71	82
	Female	16	18
Smoking history	Current smoker	60	69
	Ex-smoker	27	31
ECOG PS*	0-1	65	75
	≥2	21	24
Stage	I	2	2
	II	1	1
	III	28	32
	IV	56	64
Liver metastases**	Present	18	21
	Absent	38	44

Abbreviations: PS: Performance status

* 1 patient PS not registered

** Only patients with metastatic disease

We analysed Snail1, Vimentin, SPARC, NCAM, MET, p-MET and E-cadherin expression in these specimens. **Figure R.54.** and **Table R.14.** show the intensity and pattern of expression of each biomarker.

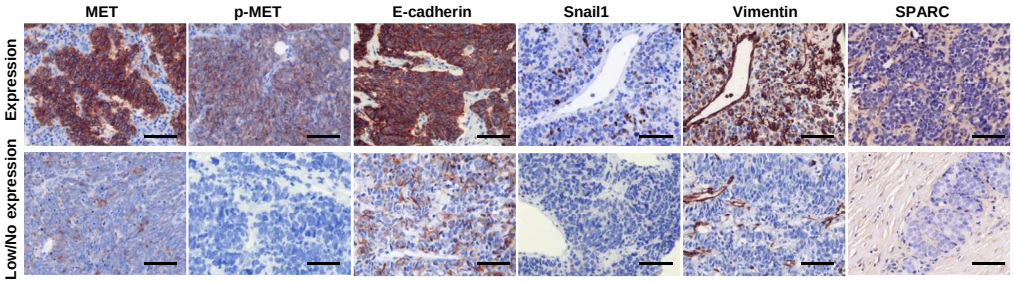

Figure R.54. MET status and EMT markers expression in SCLC specimens. Representative images from positive and negative human SCLC cases for MET, p-MET, E-cadherin, Snail1, Vimentin and SPARC markers. Scale bars, 75 μm.

Table R.14. Biomarker expression in SCLC human tumours

Biomarker	Negatives (%)	Positives (%)	x(+/-SD)	Med [p25-p75]	Min-max
Snail1	71	29	31 (27.6)	20 [10-50]	5-90
Vimentin	73	26	43.8 (28.5)	50 [10-60]	5-90
SPARC	56	43	50.5 (34.4)	50 [30-65]	10-130
p-MET	65	34	68.8 (48.3)	60 [30-100]	5-200
MET	18	82	128.3 (73.3)	100 [60-200]	10-300
NCAM	6	94	269.8 (47.5)	300 [255-300]	100-300
E-cadherin	0	100	174.9 (66.9)	200 [115-202]	30-300

Abbreviations: p-MET: phosphorylated MET; x: mean; SD: standard deviation; Med: median; p25:percentile 25; p75:percentile 75; Min: minimun value; max: maximun value

We had previously analysed Met and p-Met expression in a sample set of 77 SCLC specimens. For the current study we use an independent SCLC biopsy collection (N.87) where we assays Met and p-Met and EMT markers. As observed, there was a majority of negative (no expression) for Snail1, Vimentin, SPARC and p-MET (**Table R.14.**). For these parameters, in the cases with any expression, the magnitude of positivity was not correlated (**Table R.15.**).

Table R.15. Spearman correlation between biomarkers' expression

		VIM	SPARC	MET	p-MET	NCAM	E-cad
Snail1	Rho p-value N	.391** .04 28	.155 .345 39	.033 .786 70	.101 .557 36	-.068 .560 76	-.443** .000 83
VIM	Rho p-value N		.358** .023 40	.045 .713 70	.073 .672 36	.045 .706 74	-.430** .000 83
SPARC	Rho p-value N			.203 .085 73	-.094 .543 44	.006 .957 78	-.285** .008 85
MET	Rho p-value N				.166 .167 71	.088 .435 81	-.098 .370 86
p-MET	Rho p-value N					-.109 .347 77	-.531** .000 84
NCAM	Rho p-value N						-.073 .512 82

Abbreviations: p-MET: phosphorylated MET; E-Cad: E-cadherin; VIM: Vimentin

** statistically significant

Recommended cut-off scores with clinical validity have not been established for these biomarkers in SCLC. Therefore, we used the median as an arbitrary cut-off point. p-MET was expressed in 34% of patients, confirming the results of our previous serie of SCLC human tumours (**Table R.14.**). In a test of association between dichotomous variables, we found a direct association of p-MET expression with Snail1, Vimentin, SPARC and MET. An inverse correlation was found between p-MET and E-cadherin (all p-values <0.001) (**Table R.16.**). There was also a significant positive association between Snail, Vimentin and SPARC and

an inverse correlation between each of these variables and E-cadherin (data not shown).

Table R.16. Association of MET and p-MET with other biomarkers

	MET			P-MET		
	Positive	**Negative**	**p-value**	**Positive**	**Negative**	**p-value**
Snail1 +	15 (33%)	9 (24%)	0.367	17 (59%)	7 (13%)	<0.001
Vimentin +	14 (31%)	8 (21%)	0.301	15 (52%)	7 (13%)	<0.001
SPARC +	25 (54%)	12 (31%)	0.029	22 (76%)	15(27%)	<0.001
NCAM +	29 (64%)	19 (50%)	0.184	15 (54%)	30 (58%)	0.723
E-cadh +	22 (48%)	25 (62%)	0.173	7 (24%)	39 (71%)	<0.001

We found no association between MET or p-MET and clinical characteristics (Performance Status, stage).

For survival analysis, we first evaluated the association of classical prognostic factors for SCLC patients. As expected, poor performance status (PS) (>=2) and stage IV disease were associated with worse outcome ($p<0.001$). We then evaluated the impact of each biomarker in survival adjusted for PS and stage using Cox regression multivariate analysis. P-MET expression, but not total MET, was associated with decreased survival. Snail1, Vimentin and SPARC expression also correlated with poor prognosis (all p-values <0.05). In contrast, E-cadherin expression was a marker of better outcome ($p<0.05$), but not NCAM (**Figure R.55** and **Table R.17.**).

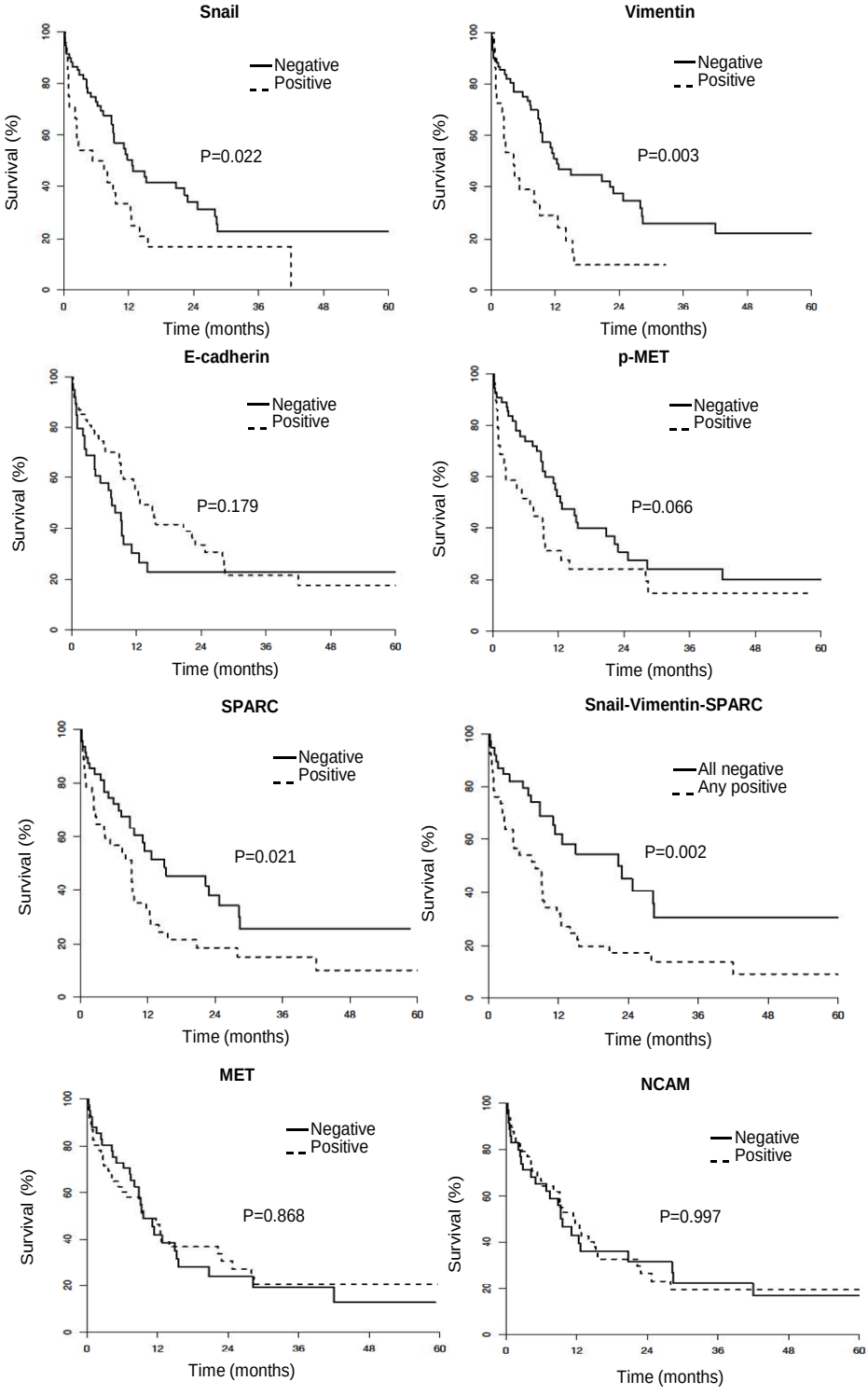
Snail
Negative
Positive
P=0.022
Survival (%)
Time (months)
Vimentin
Negative
Positive
P=0.003
Survival (%)
Time (months)
E-cadherin
Negative
Positive
P=0.179
Survival (%)
Time (months)
p-MET
Negative
Positive
P=0.066
Survival (%)
Time (months)
SPARC
Negative
Positive
P=0.021
Survival (%)
Time (months)
Snail-Vimentin-SPARC
All negative
Any positive
P=0.002
Survival (%)
Time (months)
MET
Negative
Positive
P=0.868
Survival (%)
Time (months)
NCAM
Negative
Positive
P=0.997
Survival (%)
Time (months)

Figure R.55. Kaplan-Meier curves for overall survival univariate analysis according to biomarker status. Association between the expression of the indicated biomarkers and overall survival. P-values were calculated using the long-rank test and survival curves by Kaplan-Meier analysis.

Table R.17. Cox regression analysis for overall survival for each variable adjusted for Performance Status (PS) and stage

Biomarker	OR (95%CI)*	P-value
Snail	2.5 (1.4-4.4)	0.002
Vimentin	2.9 (1.6-5.5)	<0.001
SPARC	3.0 (1.7-5.5)	<0.001
p-MET	2.1 (1.2-3.7)	0.009
MET	0.9 (0.6-1.6)	0.86
NCAM	1.0 (0.6-1.7)	0.92
E-cadherin	0.5 (0.3-0.9)	0.042
Snail, vim, SPARC neg	4.1 (2.2-7.7)	<0.001

Abbreviations: p-MET: phosphorylated; OR: odds ratio; CI: confidence interval
* Adjusted for stage and PS

Finally we evaluated colocalization for each p-MET, Snail and Vimentin stain by immunofluorescence in human SCLC samples. **Figure R.56.** demonstrates that tumour cells with MET phosphorylation present Snail1 and Vimentin expression.

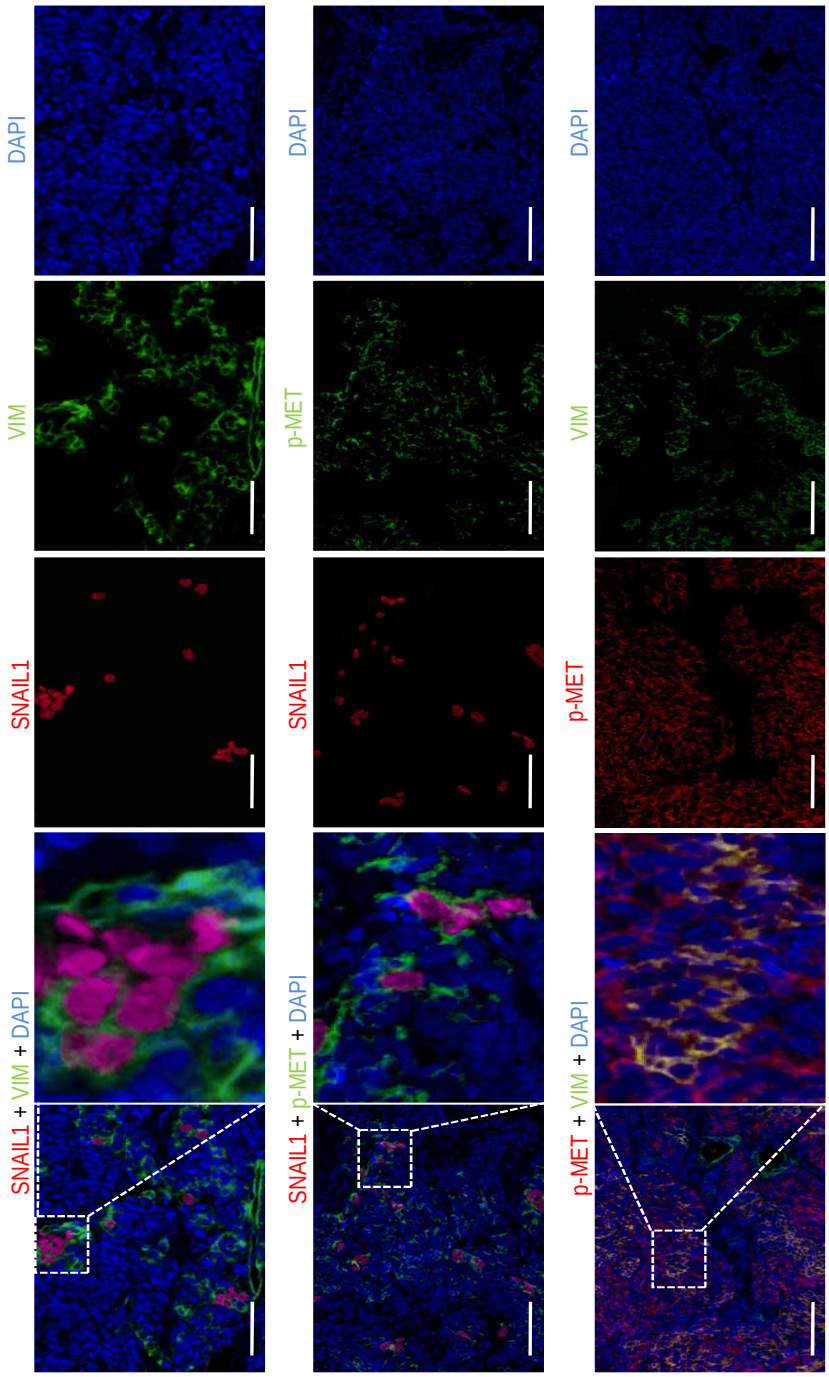
DAPI
VIM
SNAIL1
SNAIL1 + VIM + DAPI
DAPI
p-MET
SNAIL1
SNAIL1 + p-MET + DAPI
DAPI
VIM
p-MET
p-MET + VIM + DAPI

Figure R.56. Colocalization of p-MET, Snail1 and Vimentin in human SCLC samples. Representative images of immunofluorescence staining in three SCLC human tumours for Snail (red), Vimentin (green) and DAPI (blue); Snail (red), p-MET (green) and DAPI (blue); and p-MET (red), Vimentin (green) and DAPI (blue). Boxes represent the region of magnification shown in adjacent image, indicating co-localization of Snail1 and Vimentin; Snail1 and p-MET and p-MET and Vimentin. Scale bars, 75 μm.

R.5.5. Relapsed human SCLC shows mesenchymal features when compared to initial chemosensitive disease

For this project we prospectively obtained rebiopsy specimens from a number of patients. We obtained paired samples (biopsies or cytology block) from 11 patients before first-line treatment and at first relapse/progression. We sought to compare EMT markers and MET status in these samples to validate our preclinical hypothesis. Due to lack of material only five cases were evaluable for all markers in the pretreatment and relapse biopsies. Globally, we observed upregulation of mesenchymal features and MET phosphorylation on specimens obtained at relapse and these correlated with lack of response to chemotherapy in contrast to 100% of responders at first line treatment with a more epithelial phenotype (**Table R.18., Figure R.57.**).

Table R.18. Biomarker status in biopsies pre-treatment and at relapsed disease

Pacient #	Biopsy	MET	p-MET	Snail	Vim	SPARC	E-Cad	Response
1	**Pre**	210	10	30	50	90	180	PR
	Post	300	100	30	90	80	150	PD
2	**Pre**	180	10	90	0	0	200	CR
	Post*	60	50	60	100	80	NV	PR
3	**Pre**	200	150	50	0	80	210	PR
	Post*	200	50	90	90	60	90	PR
4	**Pre**	100	0	0	0	0	200	PR
	Post	120	50	10	30	50	100	PD
5	**Pre**	200	30	0	0	0	100	PR
	Post	200	120	20	50	80	30	PD

Abbreviations:

Pre: biopsy obtained at diagnosis, previous to any treatment

Post: biopsy obtained at progression after first line therapy with chemotherapy +/- radiotherapy*

p-MET: phosphorylated MET; E-Cad: E-cadherin; Vim: Vimentin

PR: Partial response; CR: complete response; PD: progressive disease

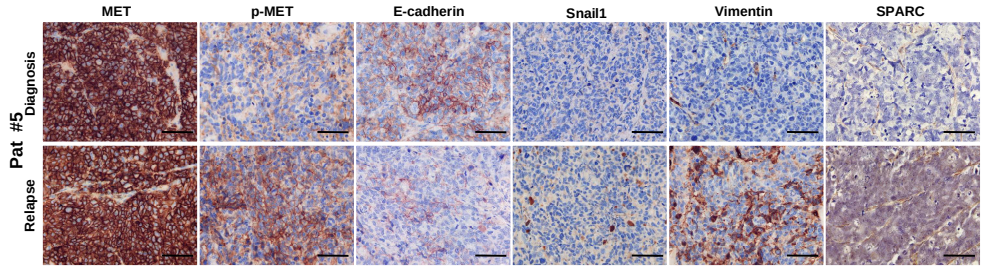

Figure R.57. Upregulation of mesenchymal markers and downregulation of E-cadherin expression in relapse human SCLC. Paired samples from SCLC patient #5 at diagnosis and relapse time-points, stained for MET, p-MET, E-cadherin, Snail1, Vimentin and SPARC. Scale bars, 75 μm.

DISCUSSION

DISCUSSION

The work presented here, demonstrates in two independent series the activation of MET in approximately one third of patients with SCLC. Importantly, this activation is associated with poor outcome independently of other classical prognostic factors. We also show that MET activation is associated with mesenchymal features in human SCLC. In preclinical SCLC models, we observe that MET activation by HGF is associated with EMT and results in increased tumorogenesis and chemoresistance. Of translational relevance, MET inhibition is able to prevent and revert HGF induced EMT. This blockade of EMT increases chemosensitivity in resistant tumours and arrests tumour growth in animal models.

The SCLC scenario

SCLC is a devastating disease. Patients with advanced SCLC have a median overall survival of 9 months with the best available treatment. SCLC presents an exquisite chemo/radiosensitivity at diagnosis that results in dramatic and rapid tumour responses in up to 80% of patients with first line chemotherapy (platinum+etoposide) similar to germ cell tumours[357]. However, and contrary to what happens in germ cell tumour, at relapse or progression, that occurs early (2-6 months from the end of first line treatment), disease is highly chemoresistant with a response rate of about 10% with standard second-line therapy (topotecan).

The mechanisms underlying this chemoresistance and that lead to the early death of patients have remained elusive to date. Many genetic alterations have been described in this tumour, mainly related to the high mutation rate due to its tight association with tobacco exposure (virtually

all patients have an important smoking history)[358]. Unfortunately, all targeted treatments tested in SCLC have been unsuccessful in improving patient outcome. This is potentially due to several reasons:

1. Intrinsic genetic complexity of this tumour[359,360] that makes difficult to discriminate which genetic alterations are drivers of the disease and which are passenger mutations.
2. Little information available of whole genome studies in large tumour sets. This is due to the extreme difficulty in obtaining sufficient tumour material in a disease that is almost never cured with surgery and from which we usually have small biopsies or cytology specimens. Moreover, rebiopsies are also challenging due to procedural feasibility in patients that rapidly deteriorate and may not be in optimal conditions.
3. The unselected population participating in clinical trials testing targeted agents. Lessons learned from NSCLC have shown us the importance of patient selection according to the molecular features of their tumours for the success of these treatments[361].

Taking all these factors into account and based on previous literature[47,113,176,230], our group decided to focus in the HGF/MET signalling pathway and to try to characterize thoroughly the implications of its activation in preclinical models and human SCLC. All this, having in mind the potential of MET as a target as many pharmaceutical companies were developing agents that block this pathway.

MET is a relevant biomarker in SCLC

Our first approach was to retrospectively assess MET expression by IHC in a series of tumour samples with clinical follow up. We observed total MET expression in the majority of samples evaluated (75%) (n=72), but

interestingly, activation of the receptor, identified by phospho antibodies was present in 43% of these samples. And most importantly, MET phosphorylation was associated with worse outcome in the multivariate analysis[362]. One of the main issues raised at this point was the specificity and sensitivity of MET and p-MET antibodies. They have been reported to cross react with other membrane receptors such as EGFR and RON. To rule out these problems we performed an exhaustive validation of these antibodies and tested in parallel two p-MET antibodies. Finally, our high concordance and the performance of negative and positive controls made, in our opinion, the results reliable. However, p-MET antibodies performance was extremely variable depending on the batch or lot, differences in autostainer process conditions caused by assessment of p-MET, among other variables, making the reproducibility of results difficult to standardize for clinical use. If p-MET antibodies are difficult then to use, an additional and more complex concern was raised: how to define a clinically significant cut-off for the total MET antibody immunoassays that would be able to track MET activation in a tumour. Other issues that will not be easily solved are the heterogeneity of MET expression within a tumour sample and the potential difference of expression with a metastatic site[363]. All this taking into account that the best material we will obtain from a patient is a biopsy of few millimetres.

We have talked here about the prognostic role of MET activation in our series. Another interpretation to our data and in the absence of a controlled arm with no treatment, p-MET can also be interpreted as a predictor of lack of response to platinum and Etoposide combinations, thus explaining our outcome results. This cannot be ruled out by our data and as we will see below could even be a coherent result.

Biomarkers of response to MET inhibitors in SCLC

After these results and with the issues commented above in mind, we sought to evaluate the role of MET inhibitors in SCLC cell line models. To this end, we obtained a specific MET inhibitor, PHA-665752 (Pfizer, Inc) and we tested its molecular and cellular effects in a panel of SCLC cell lines with diverse MET status.

Globally, we observed that the effects of HGF on cell proliferation, colony formation and invasion were detectable in one cell line, H69, harbouring a genetic alteration in the MET gene, the mutation R988C. Other cell lines with similar morphologic and molecular characteristics and the same molecular behaviour upon HGF short stimulation, but with wild type MET, were not affected by HGF stimulation or MET inhibition. In contrast, cells harbouring the R988C mutation, H69 and its isogenic chemoresistant H69AR, were sensitive to HGF stimulation and MET inhibition by PHA. The R988C mutation was first described in SCLC[47] in cell lines and patients as an oncogenic mutation, but was later classified as a polymorphism[183]. The R988C mutation was a potential predictive factor of response to MET inhibition. Therefore, we explored the prevalence of MET mutations in a subset of SCLC patients (37 samples). We found no mutation/polymorphisms in our limited series. It remains to be demonstrated if this aberration in the MET gene is relevant in SCLC patients and if it identifies responsiveness to MET inhibition. Recently a paper on NSCLC patients with ALK translocation has demonstrated the presence of this mutation in this setting[364]. Further analysis is warranted.

The major problem when treating SCLC patients is the chemoresistance disease we face at relapse/progression. One of the mechanisms, among many, that has been postulated as a cause of resistance to treatment in

cancer is epithelial to mesenchymal transition (EMT)[296,365,366]. HGF has also been demonstrated to be inductor of EMT[318,367]. We therefore aimed to ascertain possible crosstalk between these two phenomenons in SCLC models and tumours.

MET inhibitors targeting HGF induced EMT

To this end we explored if HGF stimulation was able to induce EMT in our cell line models. Again we found that H69 cells were the only ones who under HGF prolonged stimulation showed scattering activity and attachment to the plate. This was correlated at the molecular level with an upregulation of Snail1 and downregulation of E-cadherin. We performed this experiment repeatedly with similar results, demonstrating that this was a robust and reproducible effect. We then obtained from Pfizer a new MET inhibitor, derived from PHA-665752, which is currently in clinical studies, PF-2341066. This drug is an orally available MET and ALK inhibitor that has been approved for the treatment of ALK+ tumours. We first characterized ALK in all our SCLC cell lines and found no translocation or overexpression of ALK in any of them. In our experiments, we observed that treatment with PF-2341066 was able to inhibit MET phosphorylation at specific doses and that it was able to prevent HGF induced EMT. We then confirmed that it was not only able to prevent this process but also revert it when already established. This was correlated at the molecular level with inhibition of Snail1. As Snail1 is a principal player in EMT in many tumour models, we evaluated if knock out of this transcription factor in H69 would prevent HGF induced EMT and this was demonstrated by our experiments, suggesting that HGF induction of EMT could be associated with Snail1 modulation.

Mesenchymal features: association with biological effects by HGF

One interesting observation in this experiment was that when cells were treated with HGF and suffered EMT, a subpopulation of cells with mesenchymal characteristics (fibroblastic morphology) could be distinguished. We were able to isolate these cells and performed a thorough characterization of them. We could demonstrate that this cell line expressed mesenchymal markers (Snail1, Fibronectin, Vimentin, SPARC) by different techniques and we also observed downregulation of epithelial markers. We ruled out a contamination of the parental H69 cell line, performing a karyotype study. However, the most intriguing finding of this mesenchymal H69M cell was that it showed high levels of basal phosphorylation of MET. We investigated the mechanism of this basal phosphorylation and we observed no genetic alteration explaining this finding. What we observed was higher levels of HGF expression and excretion of H69M cells when compared to H69, suggesting an autocrine stimulation explaining this basal pathway activation.

In vivo, H69M xenografted tumours grew faster, were more locally invasive and were more chemoresistant compared to H69. Histological studies showed that they were able to recapitulate the original small cell morphology, but immunohistochemical studies revealed the expression of mesenchymal and angiogenesis markers, not present in tumours derived from H69. As mesenchymal features are typical also of tumour initiating cells[355] we explored the potential of tumorigenesis of H69M cells with injection of low number of cells (100-500). H69M cells were able to form tumours in all cases under these experimental conditions. This reveals a potential stemness capacity of this mesenchymal cells, that would perfectly correlate with their resistance to chemotherapy[368].

We then wanted to evaluate the role of MET inhibition in reverting this chemoresistance via prevention of EMT. Our *in vivo* experiments demonstrated that in chemoresistant-mesenchymal cells the addition of PF to chemotherapy was able to arrest tumour growth that was not achieved by either drug. One of the most interesting findings in these experiments was that PF alone was able to downregulate p-MET and mesenchymal markers, however, no effect on tumour growth observed. In contrast, in the combination of PF and Etoposide, these molecular effects were in the same direction although more profound and derived in tumour arrest. This suggests that the effects of MET inhibition in this setting does not act as in the setting of oncogenic addiction (seen for example in cases with *MET* amplification). The role of MET in this case is closely associated with morphologic changes, invasion, angiogenesis and protection of cells from apoptosis, all effects well characterized for the HGF/MET pathway[67,76,317].

One of the most relevant findings, however, is that mice tumours were not cured by the combination of treatment with the MET inhibitor and chemotherapy. When we retired treatment, tumours regrew rapidly leading to deterioration of mice. Maintenance of treatment with PF slowed down this process, but ultimately tumours increased their volume progressively. These findings might not be exportable to patients because treatment schedules are not exactly the same to the ones used in patients, regarding dosing and timing. This question will only be answered by a controlled clinical trial testing this hypothesis.

MET and EMT in SCLC patients

Observing this association between HGF/MET and EMT in SCLC models we assessed MET status and EMT markers in a series of SCLC

patients with annotated clinical history. We confirmed our previous findings of expression of MET in the majority of cases and p-MET in 34%. Again this MET activation was independently associated with poor survival. MET phosphorylation has been linked to poor survival in many tumour models[115,363,369-371] and this is coherent with its biological functions[62,69,317]. Furthermore, our study demonstrated that mesenchymal markers were associated with p-MET expression and that they were also independently associated with worse survival. More importantly, we were able to demonstrate that p-MET expression was observed in the same tumour cells where Snail1 and vimentin was expressed, suggesting a mechanistic link between these proteins as suggested by our preclinical findings.

Returning to the issue on prognostic and/or predictive significance of MET activation, the association of p-MET with mesenchymal markers in this disease could explain the shorter survival by decreased efficacy of chemotherapy to eradicate these "mesenchymal, MET activated" subset of cells. MET phosphorylation in our set of diagnostic samples is not associated in our series with response to chemotherapy, because the vast majority of patients respond to first line treatment. However, in tumours with a chemorefractory subpopulation of cells, these could survive to the effects of chemotherapy and then take over the more sensitive cells at relapse, explaining the shorter survival of the patients with these markers upfront. This is consistent with the "stem cell" theory and some groups have argued in favour of combining treatment of the bulk tumour with chemotherapy adding a stem cell inhibitor to eradicate this subpopulation of chemorefractory mesenchymal cells[372]. In our case, MET would be a marker of this more stem subpopulation and the MET inhibitor could contribute to the growth arrest of these cells. This theory of MET as a

marker of stemness has been postulated by others and is currently being validated by many works[373,374].

Some studies have demonstrated that tumours change over the course of progression, especially in response to treatment[375]. And this might be specifically relevant in SCLC as this tumour's behaviour changes remarkably after first line chemotherapy. We were able to collect samples at relapse/progression from some patients that were subsequently treated with chemotherapy. Globally we observed that MET phosphorylation and "mesenchymality" was increased in these rebiopsies compared to the primary tumours and that this correlated with lack of response to second line chemotherapy. These findings emerged from few cases and although consistent with our hypothesis need further validation in larger series.

HGF levels and SCLC evolution

Finally, and to further characterize the HGF/MET pathway in SCLC we wanted to evaluate HGF levels in these patients at diagnosis and during follow-up. Ideally HGF expression in the tumour samples (stroma or tumour cells) would be a good marker of tumour exposition to this cytokine. However, in our hands the HGF antibodies that are commercially available did not have a consistent performance in IHC assays. We then explored the meaning of HGF levels in serum in this patient set prospectively. We used a commercially available ELISA-based kit (used frequently in clinical investigations). Our first finding was that patients have higher baseline HGF levels when compared to healthy volunteers. Then we found that HGF levels correlated with higher risk of death when increased. In addition, and in a limited number of samples we observed that mean levels of HGF in serum of patients at response was lower and increased again at progression.

Some questions still remain open:

1. The possible association between the HGF serum levels and MET status in SCLC tumours.
2. The possible association between HGF levels in serum and in the tumour microenvironment.
3. Other serum biomarkers associated with tumour evolution and/or response to therapy.

Some may argue that HGF serum levels are not representative of HGF levels in the tumour environment. However, our hypothesis suggests that tumour cells are able to secrete HGF and stimulate their MET receptors in an autocrine fashion. So in this case, HGF in the serum could be a consequence of the process more than a cause and this could explain the lower HGF levels observed in patients with tumour shrinkage and the increased HGF levels at chemorefractory relapse.

Traslational relevance

Improvements in treatments for SCLC are urgently needed. Although its incidence is going down in Western countries, it still represents 15% of all lung cancers, which means around 2000 patients a year in Spain.

Our work identifies a subset of patients (probably around one third) whose tumours are partly driven by the HGF/MET pathway that may be inducing early EMT and associated chemoresistance in these patients. MET inhibitors, that are currently being tested in the clinic with good tolerability profiles and convenient schedules might be an option to improve the effectiveness of chemotherapy in patients with chemoresistant disease with MET induced EMT. We believe our results need to be validated in a prospective clinical trial evaluating MET inhibitors in this molecularly selected population of SCLC patients.

CONCLUSIONS

CONCLUSIONS

1. SCLC cell lines show different patterns of MET protein expression, mutational status of the *MET* gene and response to HGF stimulation.
2. MET phosphorylation is found in approximately 40% of SCLC patients and is associated with decreased survival in MET-positive SCLC.
3. Serum HGF levels are significantly higher in SCLC patients than in healthy volunteers and show a decrease during chemotherapy response. In addition, increased HGF serum levels in SCLC patients correlate with higher risk of death.
4. HGF stimulation, via MET activation, induces EMT and the appearance of a mesenchymal, chemoresistant and tumorigenic subpopulation in SCLC cell lines.
5. Treatment with MET inhibitors is able to block the HGF-induced MET activation, proliferation, colony formation and invasion in SCLC cells.
6. MET inhibition is able to prevent and reverse the HGF-induced EMT in SCLC cell lines.
7. MET inhibition is able to resensitise SCLC cells to chemotherapy *in vitro* and *in vivo*.
8. Mesenchymal markers are associated with MET phosphorylation and with worse prognosis in SCLC patients.
9. Relapsed human SCLC enhanced mesenchymal features when compared to initial chemosensitive disease.

MATERIAL AND METHODS

M.1. CELL LINES AND CELL CULTURE

A panel of 10 SCLC cell lines: H69, H69AR, H187, SHP-77, H345, H740, H748, H865, H524 and H1688, and the NSCLC H1993 cell line were obtained from the American Type Culture Collection (ATCC) (Rockville, MD). All cells were maintained in RPMI 1640 media from Invitrogen. All media were supplemented with 10% Foetal Bovine Serum (FBS), 2 nM L-Glutamine, 100 units/ml Penicillin and 100 μg/ml Streptomycin. All cell lines were cultured in a humidified atmosphere of 95% air and 5% CO_2 at 37ºC.

M.2. DRUGS AND GROWTH FACTORS

Cisplatin was purchased from Sigma-Aldrich (St. Louis, MO) and dissolved to a stock concentration of 5000 μg/ml in DMSO. The stock solution was diluted for instant use in our experiments.

Etoposide was obtained from Calbiochem (La Jolla, CA) and was resuspended in DMSO and stored at a stock concentration of 10 mM at -20ºC.

Doxorubicin was purchased from Sigma-Aldrich and was resuspended in water and stored at a stock concentration of 10 mM at 4ºC.

PHA-665752,(3Z)-5-[(2,6-dichlorobenzyl)sulfonyl]-3-[(3,5-dimethyl-4 -1H-pyrrol-2-yl)methylene]-1,3-dihydro-2H-indol-2-one (obtained from Pfizer Inc., San Diego, CA) was dissolved to a stock concentration of 10 mM in DMSO and stored at -80ºC.

PF-2341066, (R)-3-[1-(2,6-dichloro-3-fluoro-phenyl)-ethoxy]-5-(1-piperidin-4-yl-1H-pyrazol-4-yl)-pyridin-2-ylamine (obtained from Pfizer

Inc., San Diego, CA) was dissolved to a stock concentration of 20 mM in DMSO and stored at -80ºC.

Recombinant human HGF was purchased from Calbiochem (La Jolla, CA) and was resuspended in sterile PBS containing 0.1 % BSA and stored at a stock concentration of 100µg/mL at -80ºC. Treatments (unless otherwise indicated) were done at 40 ng/ml as final concentration in culture medium.

M.3. CELL PROLIFERATION AND VIABILITY

Several approaches were used to asses the effects of different treatments on cell proliferation and viability.

M.3.1. MTS assay

Cell proliferation and viability was studied using the colorimetric method provided by the MTS-CellTiter96 Aqueous Non-Radioactive Cell Proliferation Assay Kit (Promega, Madison, WI). MTS assay is a modification from MTT assay and depends on two solutions: a tetrazolium compound (MTS) and an electron coupling reagent (phenazine methosulfate; PMS). MTS is bioreduced by cells into a formazan product. Cells that are metabolically active can accomplish by dehydrogenase enzymes the conversion of MTS into aqueous, soluble formazan product. The quantity of formazan product measured by the amount of 490nm absorbance is directly proportional to the number of living cells in the culture. We performed this viability assay in 96- well flat-bottomed plates. Approximately $1x10^4$ cells were seeded in 100µl of culture media in each well and incubated during 24h before drug

treatment. 100µl of 2x drug containing media was added in each well. After 72h, 40µL of MTS/PMS were added to each well and the cells were further incubated from 2 to 4 hours more. The amount of soluble formazan was measured on a microplate spectrophotometer at 490nm (test wavelength) and 690nm (reference wavelength). The percentage of surviving cells to each treatment was estimated by dividing the A490nm-A690nm of treated cells with the A490nm- A690nm of control cells.

M.3.2. Manual cell counting

Cell proliferation and viability was alternatively studied by manual counting of the cells. Approximately $3x10^5$ cells/well were seeded in a six-well plate with culture medium containing 10% FBS. After 24 hours HGF, PHA-665752 or the combination were added at 40 ng/ml or 0.5 µM respectively and incubated during 72 hours. The number of viable cells in each condition was determined by counting the cells stained with Trypan Blue die solution in a hemocytometer chamber. The number of viable cells in each treatment was plotted as percentage of control.

M.3.3. Automatic cell counting

Scepter Automated Cell Counter (Millipore, Billerica, MA) was used to measure PF-2341066 effects on cell proliferation in H69 and H69M cells. Cells were seeded in triplicate in 24-well plates at a density of 8000 cells per well and incubated during 24 hours before drug treatment. Then, cells were treated with or without 200 nM PF-2341066 for 0, 3, 6 and 10 days in the appropriate culture media. Cells were then harvested and counted

using Scepter Automated Cell Counter. The number of viable cells in each treatment was plotted as percentage of control.

M.3.4. Anchorage-dependent clonogenic assay

Clonogenic assay is an *in vitro* cell survival assay based on the ability of a single cell to grow into a colony attached on a plastic surface.
For measuring clonogenic capacity of SCLC cell lines $6x10^3$ cells/well were seeded in a 6-well plate with culture medium containing 10% FBS. After 24 hours of attachment period, cells were continuously exposed to different concentrations of drugs or solvent from 10 to 15 days. Every 3 days media was removed and fresh culture media containing the corresponding drug or solvent was added to the plates. Cells were grown since clones were observed in control plates. At the end of the experiment, cells were washed with PBS and fixed and stained with Crystal Violet (61135, Sigma) solution in 10% acetic acid during 1 hour. The plates were scanned and the number of colonies was quantified using the Java ImageJ software. The percentage of growth was calculated by dividing the mean value of treated cells by the mean value of control cells.

M.3.5. Anchorage-independent soft agar colony formation assay

Anchorage-independent growth is one of the hallmarks of malignant cell transformation. In general tumour cells have the ability to grow unattached. To determine the capacity of SCLC cell lines to grow independently of anchorage, single cell suspensions ($2x10^4$cells in 35mm

plates) were grown in 0.3% top agar layer containing RPMI 1640 medium in the presence and absence of HGF (40 ng/ml) and PHA-665752 (0.5μM) on top of 0.5% bottom agar layer. The plates were incubated (37ºC, 5% CO_2) and cells were fed every three days with 0.5 ml of culture medium containing the above mentioned treatments. The number and size of colonies were evaluated at 20X magnification on a light microscope at each condition after 21 days.

M.4. CELL INVASION ASSAY

Invasion through the extracellular matrix (ECM) is an important step in tumour metastasis. Invasion of tumour cells into ECMatrix is widely used to study the metastatic potential of tumour cells. The invasion capacity of SCLC cell lines was assessed using QCM ECMatrix Cell Invasion Colorimetric Assay (Millipore, Billerica, MA). This kit consists of invasion chambers formed by an insert with 8 μm pore size polycarbonate membrane that is covered with a thin layer of dried ECMatrix™. This ECMatrix blocks the migration of non-invasive cells, whereas the invasive cells can migrate through this layer and arrives to the outside of the insert. To evaluate the invasiveness of SCLC cell lines, cell suspensions were prepared in serum-free media and $2.5x10^4$ adherent cells or $1x10^6$ cells growing in suspension were seeded into the inserts of 24-well invasion chamber and treated with PHA-665752 (0.5 μM) or PF-2341066 (200 nM), concentrations that does not have a significant effect on cell viability. Inserts were placed into Falcon companion plates containing media with 10% FBS and 40 ng/ml HGF and incubated for 24 h at 37ºC and 5% CO_2 atmosphere.

Following incubation non-invaded cells were removed from the top chamber using cotton swabs and the invasive cells of the outside of the insert was gently rinsed with PBS, stained with 0.25% crystal violet for 20 min, and rinsed again. Acetic acid (10%, 200 μl/well) was applied to dissolve the stained cells, and then the dye/solute mixture was transferred to a 96-well plate for colorimetric reading of optical density (OD) at 560 nm. The OD value represents the invasive ability. All experiments were performed in triplicate.

M.5. PROTEIN DETECTION

M.5.1. Total protein extraction

For whole-cell protein extracts, cells were cultured in plates and lysed in ice-cold Nonidet P-40 buffer (Tris-HCL (pH = 7.4) 50mM, NaCl 150mM, 1 % NP40, EDTA 5mM, NaF 5mM, Na3VO4 2mM, PMSF 1mM, Leupeptin 5μg/mL and Aprotinin 5μg/mL) mechanically with the help of an scrapper. After shaking during 30min at 4ºC, the samples were centrifuged 10min at 13200rpm and the supernatant was aliquoted and stored at -20ºC.

M.5.2. Western Blot analysis

To determine the expression of specific proteins in different cells or different conditions, the same quantity of protein for each sample (20-40 μg) was adjusted to the same volume with lysis buffer. An equal amount of 2X 5% β-mercaptoethanol Laemmly-sample buffer was added to each sample. Samples were denaturalized by 5 minutes at 95ºC.

Samples (30μg/lane) were subjected to SDS-page and transferred to PDVF membranes. Immunoblotting was carried out according to standard procedure. To block unspecific detection, PDVF membranes were incubated with 5% Milk TBS-T for 1 hour at room temperature. Then, membranes were incubated overnight at 4ºC with the specific primary antibody (listed below). After washing 3 times with TBS-T, horseradish peroxidase-conjugated secondary antibodies (Amersham) were used to detect primary antibodies. Membranes were washed again 3 times with TBS-T and target proteins were visualized after enhanced chemoluminescence treatment (Amersham) of membranes and subsequent exposure to X-ray film.

The following antibodies were purchased from the manufacturers listed below and used for Western blot assay: MET (25H2) mouse monoclonal antibody (mAb), p-MET Y1234/1235 (3D7) rabbit mAb, p-MET Y1349 (130H2) rabbit mAb, p-MET Y1234/35 (D26) XP rabbit mAb, p-GAB1 Y307-rabbit polyclonal antibody (pAb), ERK1/2 rabbit pAb, p-ERK1/2 (Thr202/Tyr204) pAb, CD56 (NCAM) (123C3) mouse mAb were obtained from Cell Signaling (Danvers, MA), MET (SP44) rabbit mAb from Ventana, GAB1(H198) rabbit pAb and ZEB1 (E-20) goat pAb were obtained from Santa Cruz Biotechnology (Santa Cruz, CA), E-Cadherin (36/E-Cadherin) mouse mAb and N-Cadherin (32/N-Cadherin) mouse mAb from BD Biosciences, Fibronectin rabbit pAb obtained from Dako and Snail mouse mAb generously provided by Dr. Antonio Garcia de Herreros.

M.6. MUTATIONAL ANALYSIS OF THE *MET* GENE BY SANGER SEQUENCING

For mutational studies of tumour samples, DNA was extracted from macrodissected tumoural paraffin-embedded tissue using the QIAamp Tissue Kit (QIAGEN GMBH, Hilden, Germany) according to the manufacturer's protocol. The mutational analysis of the MET gene in cell lines and tumour samples (codons E168, R988 and T1010) was performed by direct sequencing. Primers for PCR amplification and sequencing were designed using the Primer Express software (Applied Biosystems, Foster City, CA) and were as follows: 5'-GCAGCAGCAAAGCCAATTTAT-3' and 5'-tGACTTTGGCTCCCAGGGC-3' for the E168 and 5'-ACCCATGAGTTCTGGGCACT-3' and 5'-CAGAACAATAAACTGAAATATACCTTCTGG-3' for the R988 and T1010. PCR conditions were as follows: 95 ºC 10 minutes 1 cycle; 95ºC 1 minute, 55ºC for 1 minute, 72ºC for 1 minute, 40 cycles; and 72ºC 10 minutes, 1 cycle. Sequencing was performed with BigDye v3.1 (Applied Biosystems) following the manufacturer's instructions and analysed on a 3500Dx Genetic Analyzer (Applied Biosystems).

M.7. FLUORESCENCE IN SITU HYBRIDIZATION (FISH) ANALYSIS OF *MET*

To assess the genetic status of the *MET* gene in cell lines, we applied the FISH technique by using the ON·C-MET (7q31)/SE 7 FISH probes (Kreatech Diagnostics, Amsterdam, the Netherlands), labeling the centromeric alpha-satellite region, specific for chromosome 7 (Spectrum

green), and the 7q31 region, that contains the *MET* gene (Spectrum orange).

To assess the genetic status of the *ALK* gene in cell lines, we used the Vysis ALK Break Apart FISH Probe (Abbott Molecular Inc., Des Plaines, IL), labeling the 2p23 region, that contains the *ALK* gene (Spectrum orange) and the centromeric region, specific for chromosome 2 (Spectrum green).

FISH was performed in Carnoy fixed cells (suspension of nuclei and metaphases) obtained from the cell lines after application of a conventional cytogenetic protocol. Samples and the probe were co-denaturated at 75ºC for five minutes and hybridized overnight at 37ºC in a hot plate (Hybrite chamber, Abbot Molecular Inc.). Post-hybridization washes were performed at 45ºC in a series of 50% formamide, 2xSSC and 2xSSC 0.1% NP-40 solutions for 10 minutes. Samples were counterstained with 4, 6-diamino-2-phenilindole (DAPI) (Vysis, Inc.). Results were analyzed in a fluorescent microscope (Olympus, BX51) using the Cytovision software (Applied Imaging, Santa Clara, CA). A minimum of 200 non-overlapping nuclei per case was analyzed.

M.8. CYTOGENETICS STUDIES

M.8.1. Conventional G-banding cytogenetics

Chromosome analyses were carried out on H69 and H69M cells, following standard procedures. Cells were harvested after exposure to the antimitotic colcemid for 4 hours at 37°C. After having cells with hypotonic solution for 2-3 minutes at 37°C, three fixative changes were performed before the slides were prepared. Slides were aged in a slide

warmer at 65°C for 24 hours to obtain G-bands and then stained with Wright's solution. Karyotypes are described according the International System for Human Cytogenetic Nomenclature.

M.8.2. Spectral karyotyping technique

SKY probe kit consists of a set of painting probes for each of the autosomes and sex chromosomes generated from flow sorted human chromosomes.

The SKY method was performed on a slide with metaphases from cell line aged for one night at 65ºC. Spectral karyotyping (SKY-FISH) technique was applied after a pretreatment with pepsin during 1 minute at 37ºC and a further incubation with formaldehide and PBS 1X. Slides were then dehydrated and denatured in 70% formamide at 75ºC. Ten microliters of Skypaint probe (SKYPaint™, Applied Spectral Imagin Ltd., Israel) were applied directly to the slide after a denaturation of 7 minutes at 80ºC. Hybridization was performed for 2 days at 37ºC. Biotinylated probes were detected using avidin conjugated to Cy5.5 (Amersham Life Sciences) and chromosomes were counterstained with 4,6-diamino-2-phenilindole (DAPI). Images were obtained with a 200 Spectralcube (Applied Spectral Imagin, Migdal Ha-Emck, Israel). DNA was counterstained with DAPI II. At least 10 metaphases were analyzed with Nikon Eclipse E800 microscope using a custom designed optical filter (SKY-1) (Chroma Technology, Brattleboro, VT). A minimum of 15 metaphases per case were analyzed.

M.9. EXPRESSION ARRAYS

Microarray technology was used to analyse the expression profiling of thousands of genes in H69 compared to H69M cells.
This technique was performed in the Microarray Analysis Service (SAM) core facility from IMIM, using the Human Exon 1.0 ST GeneChip from Affimetrix and following the manufacturer's protocols.

M.9.1. Quality assessment of RNA samples

Purity and integrity of the RNA were assessed by spectrophotometry and nanoelectrophoresis using the NanoDrop ND-1000 spectrophotometer (NanoDrop Technologies, Wilmington, DE) and the Nano lab-on-a-chip assay for total eukaryotic RNA using Bioanalyzer 2100 (Agilent Technologies, Palo Alto, CA), respectively. Only samples with high purity (A260/280>2.0; A260/230>1.8) and high integrity (RNA integrity number (RIN) >9.4) were subsequently used in microarray experiments.

M.9.2. Generation of gene expression profiles

Microarray expression profiles were obtained using the Affymetrix GeneChip® Human Gene 1.0 ST Array (Affymetrix, Santa Clara, CA).
Amplification, labeling and hybridizations were performed according to protocols from Ambion (Ambion/Applied Biosystems, Foster City, CA, USA) and Affymetrix (Affymetrix Inc., Santa Clara, CA, USA). Briefly, 200 ng of total RNA were amplified using the Ambion® WT Expression Kit (Ambion/Applied Biosystems), labeled using the WT Terminal Labeling Kit (Affymetrix), and then hybridized to Human Gene 1.0 ST Array (Affymetrix) for 16 hours at 45ºC and 60 rpm in a GeneChip®

Hybridization Oven 640. Following hybridization, the array was washed and stained in the Affymetrix GeneChip® Fluidics Station 450. The stained array was scanned using an Affymetrix GeneChip® Scanner 3000 7G, generating CEL files for each array.

M.9.3. Gene expression profile analysis

After quality control of raw data, it was background corrected, quantile-normalized and summarized to a gene-level using the robust multi-chip average (RMA)[376] obtaining a total of 28832 transcript clusters, excluding controls, which roughly correspond to genes. Only transcripts with intensity signal above the 10th percentile and then with a variance higher than the 50th percentile from total resting variance were considered for further analysis, which lead to 13124 transcript clusters. NetAffx 31 annotations, human genome 19 built, were used to summarize data into transcript clusters and to annotate analyzed data. Linear Models for Microarray (LIMMA)[377], a moderated t-statistics model, was used for detecting differentially expressed genes between the conditions. Correction for multiple comparisons was performed using false discovery rate. Genes with an adjusted p-value less than 0.05 and with an absolute logFC value above 2 were selected as significant.

Hierarchical cluster analysis was also performed to see how data aggregate and linear model for regression purposes. K-means was used for cluster analysis. All data analysis was performed in R (version 2.13.1) with packages aroma affymetrix[378], Biobase, Affy, limma and genefilter. Ingenuity Pathway Analysis v 9.0, (Ingenuity® Systems, www.ingenuity.com) was used to perform functional analysis of the results.

M.10. REAL-TIME QUANTITATIVE PCR (RT-PCR)

M.10.1. RNA extraction

To study mRNA expression by RT-PCR, total RNA from culture cells was isolated using RNeasy Mini Kit (Qiagen) according the manufacturer's instructions. The amount of mRNA per sample was quantified using Nanodrop ND-1000 spectrophotometer.

M.10.2. cDNA synthesis

After extraction, the mRNA was reversed transcribed to cDNA using High Capacity cDNA Reverse Transcription Kit (Applied Biosystems, Foster City, CA). The conditions for cDNA reverse transcription performed in the thermal cycler Mastercycler ep (Eppendorf) were 10 minutes at 25ºC, 120 minutes at 37ºC and finally 5 minutes at 85ºC.

M.10.3. Primer design

Primers for selected genes were specifically generated for validating microarray data.

For designing primers for a molecule of interest, in the Universal ProbeLibrary Assay Design Center (Roche) we introduced the GenBank number of the gene of interest to obtain the probe of Roche and the pair of raw primers to optimize. Next, with the DNAstar Primer design software the given primers were improved trying to meet the following characteristics: avoid primer dimer and hairpin formation; length of each primer between 18-23 mer; length of the amplicon between 90-110 base

pairs; melting temperature around 60ºC and equal or similar between primers; preferably ending in "C" or "G" in both 5' and 3' ends; and lack of capacity to bind to other sites in the template. Finally, a BLAST was performed to confirm that the generated primers did not have homology and the capacity to bind inespecifically to other sequences in the human transcriptome and genome.

The following primers were designed using NM_000601.4 (HGF), NM_003380.3 (Vimentin), NM_212482.1 (Fibronectin) and NM_003118.3 (SPARC).

HGF (Roche Probe: #15#)

Fw: 5'-GGGTGACCAAACTCCTGC-3'

Rv: 5'-CTTCTTTTCCTTTGTCCCTCTG-3'

Vimentin (Roche Probe: #56#)

Fw: 5'-CCGCTAGGAGCCCTCAATC-3'

Rv: 5'-GGAGAAGAGGCGAACGAG-3'

Fibronectin (Roche Probe: #23#)

Fw: 5'-GACACTTATGAGCGTCCTAAAG-3'

Rv: 5'-GCGATGGTACAGCTTATTCTC-3'

SPARC (Roche Probe: #4#)

Fw: 5'-GAAGGTGTGCAGCAATGAC-3'

Rv: 5'-CTTGTGGCCCTTCTTGGTG-3'

Specific probes from Universal probe library (Roche) were purchased to recognize each specific DNA product.

M.10.4. RT-PCR

For the DNA amplification we used Lightcycler 408 Probes Master (Roche) and the amplification was performed in the Lighcycle 408 Real Time PCR-System device (Roche) under the following conditions:

1- A denaturation step for 10 minutes at 95ºC
2- 45 cycles consisting of:
    a. 10 seconds at 95ºC
    b. 30 seconds at 60ºC

The relative expression of each gene in each condition was normalized with the expression of the housekeeping gene RPLP0.

M.11. HGF-INDUCED EMT

To evaluate if HGF stimulation induces EMT in H69 cells, we seeded $6.7x10^5$ cells in 60 mm^2 dishes with culture medium containing 10% FBS. After 24 hours, HGF was added at 40 ng/ml. Fresh culture medium containing HGF at the indicated concentration was added every 48 hours during 14 days. A morphological study by light microscopy and molecular study by Western Blot were performed at days 3, 6, 10 and 14 to study if continuous exposure to HGF was able to induce EMT in H69 cells. Fourteen days after HGF stimulation, a small subset of cells with a fibroblastic appearance that grew in adhesion was observed. We isolated this cell subpopulation and was further propagated for cellular and molecular characterization in media containing 10% FBS and without the presence of HGF.

M.12. LENTIVIRAL INFECTION

To stably downmodulate Snail expression in H69 cells we performed lentiviral transduction using MISSION shRNA for Snail (pLKO.1-puro vector) (Sigma-Aldrich). Approximately $3x10^6$ HEK293T packaging cells were seeded in 100 mm^2 dishes with culture medium for producing lentiviral particles. Twenty-four hours later, HEK293T cells were transiently transfected with shSnail or shCT (Scrambled) as well as the three adjuvant vectors: viral envelope vector pVSV-G, the retrotranscriptase vector pRSV and the packaging vector pRRE. Total DNA was added to a volume of 150 mM NaCl and polyethylenimine polymer (PEI). The mixture was incubated 15 minutes at room temperature and added to the medium of HEK293T cells. The transfection medium was replaced with fresh medium after 24 hours in order to concentrate the lentiviral particles produced by the transfected HEK293T cells. In parallel $1.7x10^6$ H69 cells were seeded in 100 mm^2 dishes with culture medium. Viral supernatants were collected 48 and 72 hours post-transfection, clarified by filtration, supplemented with 8 μg/ml of polybrene (Sigma-Aldrich) and added to the medium of H69 to be transduced. H69 transduced cells were selected with puromycin (2.5 μg/ml) for 5 days. The selection ended when no viable H69 cells were in the control non-transduced cells plate. The dose of puromycin needed for the selection of H69 transduced cells was determined previously with a puromycin curve from 0-4 μg/mL in non-transduced cells treated for a week. Snail knockdown was confirmed by determination of Snail protein levels by Western Blot.

M.13. *IN VIVO* STUDIES

M.13.1. Animals

Five-week-old male BALB/c nude mice were purchased from Charles River Laboratories (Wilmington, MA) and hosted in the pathogen-free animal facility at the Barcelona Biomedical Research Park (PRBB). Animal treatments were done according to institution-approved protocols.

M.13.2. Subcutaneous xenograft model in BALB/c nude mice

H69 or H69M cells were harvested, pelleted by centrifugation and resuspended in sterile PBS with 50% Matrigel (BD Biosciences) before injection. The tumorigenicity of these cells was determined by subcutaneous injection of 10 x 10^6 cells into the flank of BALB/c nude mice (Charles River) to produce subcutaneous tumours. Tumour volume was determined from calliper measurements of tumour length (L) and width (W) according to the formula L x $W^2/2$. Both tumour size and body weight were measured three times per week.

M.13.3. Survival study

Tumours were allowed to grow for one week and when tumour volume reached approximately 200 – 300 mm^3 mice were randomized to 4 groups with 10 mice in each group. Treatment groups consisted of control (vehicle), Etoposide (12 mg/kg), PF-2341066 (100 mg/kg) and

combination of both treatments. Etoposide was diluted in 200 µl 0.9 % Sodium Chloride and administered at a dose of 12 mg/kg in one daily intraperitoneal injection on days 1 to 3 of treatment. PF-2341066 was diluted in water and administered daily by oral gavage at a dose of 100 mg/kg daily for 14 days. Control animals received 0.9 % Sodium Chloride and water as vehicle. Both tumour size and body weight were measured three times a week. The mice were euthanized at the indicated times and tumours were measured with digital calipers. A part of the tumours were fixed in 4 % formalin and embedded in paraffin for the H&E staining and immunohistochemical study. Another part of the tumours were embedded in OCT compound for DNA, RNA or protein extraction.

M.14. HGF ELISA IN HUMAN SERUM OR CELL CULTURE SUPERNATANTS

The Quantikine Human HGF Immunoassay (R&D Systems, Minneapolis, MN) was used to measure HGF levels in cell culture supernatants and human serum. This assay employs the quantitative sandwich immunoassay technique. A monoclonal antibody specific for HGF has been pre-coated onto a microplate. Standards and samples are pipetted into the wells and any HGF present is bound by the immobilized antibody.

To analyse HGF levels in human serum, whole-blood samples were obtained from each patient during different disease stages (diagnosis, chemotherapy response and relapses) and also in healthy subjects (control population with similar age and gender). To collect serum, blood samples were centrifuged 10 minutes at 1000 g. Serum was removed and assay immediately or aliquoted and stored at -20ºC. To measure HGF levels in

cell culture supernatants, $1.7x10^6$ cells were seeded in 100 mm^2 dishes with culture medium and incubated during 72 hours at 37ºC and 5% CO_2 atmosphere. Then, the supernatant was centrifuged at 1200 rpm 10 minutes and stored at -80ºC.

HGF levels in human serum or cell culture supernatants were measured by ELISA in accordance with the manufacturer's procedure.

After following the protocol, the optical density of each sample was determined using a microplate reader set at 450 nm. Wavelength correction was set to 540 nm. HGF concentrations were extrapolated from the standard curve generated using the recombinant human HGF of the assay. All samples were run in duplicates.

M.15. TUMOUR SAMPLES AND IMMUNOHISTO-CHEMISTRY

The following antibodies were used for immunohistochemical studies and purchased from the manufactures listed below: MET (SP44) mouse mAb (Ventana-Roche, Tucson, AZ, USA), p-MET Y1349 (130H2) rabbit mAb, p-MET Y1234/35 (D26) XP rabbit mAb (Cell Signaling, Danvers, MA, USA), E-cadherin (NCH-38) mouse mAb (Dako, Carpinteria, CA, USA), NCAM (123C3) mouse mAb (Dako), Snail1 (EC3) mouse mAb (courtesy of Dr. Garcia de Herreros), vimentin (V9) mouse mAb (Dako) and CD31 (SP38) rabbit mAb (Spring Bioscience, Pleasanton, CA, USA).

The study population consisted of 87 patients diagnosed with SCLC at any stage from whom we had clinical and follow-up information. Specimens were retrospectively retrieved from Parc de Salut Mar Biobank (MARBiobanc, Barcelona, Spain) and Fundacion Jimenez Diaz Biobank (Madrid, Spain). This study was approved by the institutional review board of each participating centre. Three um tissue sections from

formalin-fixed and paraffin embedded samples were obtained, mounted onto charged slides and then, deparaffinised in xylene and hydrated.

After heat antigen retrieval performed at high pH solution using PT Link platform (Dako), slides for immunohistochemistry were incubated with primary antibody for 1 h at a dilution of 1:1 for MET mAb, 1:20 for p-MET Y1349 and 1:50 for p-MET Y1234/35, 1:5 for SNAIL1, 1:100 for E-cadherin, 1:100 for NCAM, 1:100 for vimentin and 1:200 for CD31. Then, sections were incubated with the specific polymer EnVision Flex+ (Dako) and revealed with 3–3' diaminobenzidine as chromogen. In situ hybridization was done by deproteinization using proteinase K digestion for 5min at room temperature and incubation with a set of specific digoxigenin-labeled probes for mRNA Sparc (agaaactgtggcagaggtga; aagctccacctggactac at; ctgtgacctggacaatgaca) (Cenbimo, Lugo, Spain) at 62ºC for 1 hour. Reaction was revealed using an anti-digoxigenin rabbit mAb (9H27L19) (Life Technologies, Paisley, UK), anti-rabbit EnVision Flex+ and DAB. Slides were counterstained with haematoxylin. Sections from same specimens above were incubated with normal mouse IgG2 (X0943, Dako) or normal rabbit Ig fraction (X0903, Dako) instead of primary antibodies as negative controls. Stainings were evaluated by two pathologists independently blinded to clinical information on a light microscope (Olympus DX50, Olympus Corp., Tokyo, Japan).

The MET, p-MET, E-cadherin and NCAM were scored when any percentage of tumour cells was stained in the membrane. Snail1 was evaluated in the nucleus of tumour cells. Vimentin and Sparc were quantified when were detected in the cytoplasm of tumour cells. A semiquantitative histoscore (Hscore) was calculated, determined by estimation of the percentage of tumour cells positively stained with low, medium, or high staining intensity for each marker. The final score was determined after applying a weighting factor to each estimate. The

formula used was Hscore = (low %) + 2x(medium %) + 3x(high %), and the results ranged from 0 to 300. Measurement of Microvascular density (MVD) was determined as the mean number of vessels by quantification of the CD31-expressing vascular structures using the ImageJ (NIH) software to recognize contiguous stained tubular vessels, as described previously [379]. Double immunofluorescence for co-localization analysis was performed on tissue sections using same primary antibodies and conditions as described. Snail1, p-MET and vimentin were detected using appropriate Alexa Fluor 568 and 488 conjugated goat anti-rabbit IgG and anti-mouse IgG antibodies (Life Technologies) (diluted 1:700). Sections were counterstained with 4',6-diamidino-2-phenylindole dihydrochloride (DAPI, Abbott Molecular, Des Plaines, IL, USA) to visualize cell nuclei. All incubations were performed at room temperature. Fluorescence assays were performed using a Dako Autostainer. Staining was evaluated by two investigators (FR and SZ) using a Cri Nuance FX Multispectral Imaging System (Perkin-Elmer, Waltham, MA, USA).

M.16. STATISTICAL ANALYSIS

M.16.1. Statistics for *in vitro* and *in vivo* assays

Statistical analysis was carried out with SPSS v12.0 (SPSS IBM). Independent sample t-test was used to compare growth rate and cell invasion in H69 versus H69M cells, as well as to compare the final tumour volumes of H69 versus H69M xenograft. One-way ANOVA was always used to assess differences in cellular effects between combined treatments and each drug alone *in vivo* and *in vitro*. Tukey's and Bonferroni

Post Hoc were used to perform pairwise comparison. All the statistical test were performed at the two-sided 0, 05 level of significance.

M.16.2. Statistics for biomarkers expression in human SCLC specimens

Statistical analysis was carried out with the R program (R project for Statistical computing, http://www.r-project.org/). To analyse correlations between biomarkers and with clinical characteristics we used the Chi-square test (Fisher's exact test). Correlations between positive expression scores for the different biomarkers were calculated by Spearman rho test. Overall survival was analysed by the Kaplan–Meier method. Curves were compared by the log-rank test. Multivariate analysis was performed using the Cox proportional hazards model, including the variables that had reached statistical significance or a trend to significance in the univariate analysis. All the statistical tests were conducted at the two-sided 0.05 level of significance. This work was performed in accordance with Reporting Recommendations for Tumour Marker Prognostic Studies (REMARK) guideline[380].

BIBLIOGRAPHY

1. Jemal, A.*, et al.* Global cancer statistics. *CA Cancer J Clin* **61**, 69-90 (2011).
2. Cooper, S. & Spiro, S.G. Small cell lung cancer: treatment review. *Respirology* **11**, 241-248 (2006).
3. Govindan, R.*, et al.* Changing epidemiology of small-cell lung cancer in the United States over the last 30 years: analysis of the surveillance, epidemiologic, and end results database. *J Clin Oncol* **24**, 4539-4544 (2006).
4. Cheng, S., Evans, W.K., Stys-Norman, D. & Shepherd, F.A. Chemotherapy for relapsed small cell lung cancer: a systematic review and practice guideline. *J Thorac Oncol* **2**, 348-354 (2007).
5. Califano, R., Abidin, A.Z., Peck, R., Faivre-Finn, C. & Lorigan, P. Management of small cell lung cancer: recent developments for optimal care. *Drugs* **72**, 471-490 (2012).
6. Puglisi, M.*, et al.* Treatment options for small cell lung cancer - do we have more choice? *Br J Cancer* **102**, 629-638 (2010).
7. Lally, B.E., Urbanic, J.J., Blackstock, A.W., Miller, A.A. & Perry, M.C. Small cell lung cancer: have we made any progress over the last 25 years? *Oncologist* **12**, 1096-1104 (2007).
8. Vallieres, E.*, et al.* The IASLC Lung Cancer Staging Project: proposals regarding the relevance of TNM in the pathologic staging of small cell lung cancer in the forthcoming (seventh) edition of the TNM classification for lung cancer. *J Thorac Oncol* **4**, 1049-1059 (2009).
9. Shepherd, F.A.*, et al.* The International Association for the Study of Lung Cancer lung cancer staging project: proposals regarding the clinical staging of small cell lung cancer in the forthcoming (seventh) edition of the tumor, node, metastasis classification for lung cancer. *J Thorac Oncol* **2**, 1067-1077 (2007).
10. Spira, A. & Ettinger, D.S. Multidisciplinary management of lung cancer. *N Engl J Med* **350**, 379-392 (2004).
11. Brahmer, J.R. & Ettinger, D.S. Carboplatin in the Treatment of Small Cell Lung Cancer. *Oncologist* **3**, 143-154 (1998).
12. Eckardt, J.R.*, et al.* Open-label, multicenter, randomized, phase III study comparing oral topotecan/cisplatin versus etoposide/cisplatin as treatment for chemotherapy-naive patients with extensive-disease small-cell lung cancer. *J Clin Oncol* **24**, 2044-2051 (2006).
13. Seifart, U.*, et al.* Randomised phase II study comparing topotecan/carboplatin administration for 5 versus 3 days in the treatment of extensive-stage small-cell lung cancer. *Ann Oncol* **18**, 104-109 (2007).

14. Niell, H.B., *et al.* Randomized phase III intergroup trial of etoposide and cisplatin with or without paclitaxel and granulocyte colony-stimulating factor in patients with extensive-stage small-cell lung cancer: Cancer and Leukemia Group B Trial 9732. *J Clin Oncol* **23**, 3752-3759 (2005).
15. Lara, P.N., Jr., *et al.* Phase III trial of irinotecan/cisplatin compared with etoposide/cisplatin in extensive-stage small-cell lung cancer: clinical and pharmacogenomic results from SWOG S0124. *J Clin Oncol* **27**, 2530-2535 (2009).
16. Asakuma, M., *et al.* Phase I trial of irinotecan and amrubicin with granulocyte colony-stimulating factor support in extensive-stage small-cell lung cancer. *Cancer Chemother Pharmacol* **69**, 1529-1536 (2012).
17. Auperin, A., *et al.* Prophylactic cranial irradiation for patients with small-cell lung cancer in complete remission. Prophylactic Cranial Irradiation Overview Collaborative Group. *N Engl J Med* **341**, 476-484 (1999).
18. Miura, I., Graziano, S.L., Cheng, J.Q., Doyle, L.A. & Testa, J.R. Chromosome alterations in human small cell lung cancer: frequent involvement of 5q. *Cancer Res* **52**, 1322-1328 (1992).
19. Sozzi, G., *et al.* Chromosomal abnormalities in a primary small cell lung cancer. *Cancer Genet Cytogenet* **27**, 45-50 (1987).
20. Testa, J.R. & Graziano, S.L. Molecular implications of recurrent cytogenetic alterations in human small cell lung cancer. *Cancer Detect Prev* **17**, 267-277 (1993).
21. Testa, J.R., *et al.* Advances in the analysis of chromosome alterations in human lung carcinomas. *Cancer Genet Cytogenet* **95**, 20-32 (1997).
22. Naylor, S.L., Johnson, B.E., Minna, J.D. & Sakaguchi, A.Y. Loss of heterozygosity of chromosome 3p markers in small-cell lung cancer. *Nature* **329**, 451-454 (1987).
23. Levin, N.A., Brzoska, P.M., Warnock, M.L., Gray, J.W. & Christman, M.F. Identification of novel regions of altered DNA copy number in small cell lung tumors. *Genes Chromosomes Cancer* **13**, 175-185 (1995).
24. Ried, T., *et al.* Mapping of multiple DNA gains and losses in primary small cell lung carcinomas by comparative genomic hybridization. *Cancer Res* **54**, 1801-1806 (1994).
25. Brauch, H., *et al.* Molecular analysis of the short arm of chromosome 3 in small-cell and non-small-cell carcinoma of the lung. *N Engl J Med* **317**, 1109-1113 (1987).
26. Kim, Y.H., *et al.* Combined microarray analysis of small cell lung cancer reveals altered apoptotic balance and distinct expression

signatures of MYC family gene amplification. *Oncogene* **25**, 130-138 (2006).
27. Wistuba, II, Gazdar, A.F. & Minna, J.D. Molecular genetics of small cell lung carcinoma. *Semin Oncol* **28**, 3-13 (2001).
28. Mirski, S.E., Evans, C.D., Almquist, K.C., Slovak, M.L. & Cole, S.P. Altered topoisomerase II alpha in a drug-resistant small cell lung cancer cell line selected in VP-16. *Cancer Res* **53**, 4866-4873 (1993).
29. Cole, S.P., Chanda, E.R., Dicke, F.P., Gerlach, J.H. & Mirski, S.E. Non-P-glycoprotein-mediated multidrug resistance in a small cell lung cancer cell line: evidence for decreased susceptibility to drug-induced DNA damage and reduced levels of topoisomerase II. *Cancer Res* **51**, 3345-3352 (1991).
30. Kubo, A.*, et al.* Point mutations of the topoisomerase IIalpha gene in patients with small cell lung cancer treated with etoposide. *Cancer Res* **56**, 1232-1236 (1996).
31. Pedersen, N.*, et al.* Transcriptional gene expression profiling of small cell lung cancer cells. *Cancer Res* **63**, 1943-1953 (2003).
32. Sugita, M.*, et al.* Combined use of oligonucleotide and tissue microarrays identifies cancer/testis antigens as biomarkers in lung carcinoma. *Cancer Res* **62**, 3971-3979 (2002).
33. Virtanen, C.*, et al.* Integrated classification of lung tumors and cell lines by expression profiling. *Proc Natl Acad Sci U S A* **99**, 12357-12362 (2002).
34. Bhattacharjee, A.*, et al.* Classification of human lung carcinomas by mRNA expression profiling reveals distinct adenocarcinoma subclasses. *Proc Natl Acad Sci U S A* **98**, 13790-13795 (2001).
35. Westerman, B.A.*, et al.* Quantitative reverse transcription-polymerase chain reaction measurement of HASH1 (ASCL1), a marker for small cell lung carcinomas with neuroendocrine features. *Clin Cancer Res* **8**, 1082-1086 (2002).
36. Pedersen, N., Pedersen, M.W., Lan, M.S., Breslin, M.B. & Poulsen, H.S. The insulinoma-associated 1: a novel promoter for targeted cancer gene therapy for small-cell lung cancer. *Cancer Gene Ther* **13**, 375-384 (2006).
37. Esquela-Kerscher, A. & Slack, F.J. Oncomirs - microRNAs with a role in cancer. *Nat Rev Cancer* **6**, 259-269 (2006).
38. Hayashita, Y.*, et al.* A polycistronic microRNA cluster, miR-17-92, is overexpressed in human lung cancers and enhances cell proliferation. *Cancer Res* **65**, 9628-9632 (2005).
39. Angeloni, D.*, et al.* Analysis of a new homozygous deletion in the tumor suppressor region at 3p12.3 reveals two novel intronic

noncoding RNA genes. *Genes Chromosomes Cancer* **45**, 676-691 (2006).

40. ter Elst, A.*, et al.* Functional analysis of lung tumor suppressor activity at 3p21.3. *Genes Chromosomes Cancer* **45**, 1077-1093 (2006).
41. Sekido, Y., Fong, K.M. & Minna, J.D. Progress in understanding the molecular pathogenesis of human lung cancer. *Biochim Biophys Acta* **1378**, F21-59 (1998).
42. Zakowski, M.F., Ladanyi, M. & Kris, M.G. EGFR mutations in small-cell lung cancers in patients who have never smoked. *N Engl J Med* **355**, 213-215 (2006).
43. Macaulay, V.M.*, et al.* Autocrine function for insulin-like growth factor I in human small cell lung cancer cell lines and fresh tumor cells. *Cancer Res* **50**, 2511-2517 (1990).
44. Fontanini, G.*, et al.* A high vascular count and overexpression of vascular endothelial growth factor are associated with unfavourable prognosis in operated small cell lung carcinoma. *Br J Cancer* **86**, 558-563 (2002).
45. Ruotsalainen, T., Joensuu, H., Mattson, K. & Salven, P. High pretreatment serum concentration of basic fibroblast growth factor is a predictor of poor prognosis in small cell lung cancer. *Cancer Epidemiol Biomarkers Prev* **11**, 1492-1495 (2002).
46. Maulik, G.*, et al.* Modulation of the c-Met/hepatocyte growth factor pathway in small cell lung cancer. *Clin Cancer Res* **8**, 620-627 (2002).
47. Ma, P.C.*, et al.* c-MET mutational analysis in small cell lung cancer: novel juxtamembrane domain mutations regulating cytoskeletal functions. *Cancer Res* **63**, 6272-6281 (2003).
48. Rygaard, K., Nakamura, T. & Spang-Thomsen, M. Expression of the proto-oncogenes c-met and c-kit and their ligands, hepatocyte growth factor/scatter factor and stem cell factor, in SCLC cell lines and xenografts. *Br J Cancer* **67**, 37-46 (1993).
49. Doria, M.I., Jr., Montag, A.G. & Franklin, W.A. Immunophenotype of small cell lung carcinoma. Expression of NKH-1 and transferrin receptor and absence of most myeloid antigens. *Cancer* **62**, 1939-1945 (1988).
50. Antonia, S.J.*, et al.* Combination of p53 cancer vaccine with chemotherapy in patients with extensive stage small cell lung cancer. *Clin Cancer Res* **12**, 878-887 (2006).
51. Cagle, P.T., el-Naggar, A.K., Xu, H.J., Hu, S.X. & Benedict, W.F. Differential retinoblastoma protein expression in neuroendocrine tumors of the lung. Potential diagnostic implications. *Am J Pathol* **150**, 393-400 (1997).

52. Sartorius, U.A. & Krammer, P.H. Upregulation of Bcl-2 is involved in the mediation of chemotherapy resistance in human small cell lung cancer cell lines. *Int J Cancer* **97**, 584-592 (2002).
53. Moore, S.M.*, et al.* The presence of a constitutively active phosphoinositide 3-kinase in small cell lung cancer cells mediates anchorage-independent proliferation via a protein kinase B and p70s6k-dependent pathway. *Cancer Res* **58**, 5239-5247 (1998).
54. Wu, C.*, et al.* Overcoming cisplatin resistance by mTOR inhibitor in lung cancer. *Mol Cancer* **4**, 25 (2005).
55. Mahmoud, S.*, et al.* [Psi 13,14] bombesin analogues inhibit growth of small cell lung cancerin vitro and in vivo. *Cancer Res* **51**, 1798-1802 (1991).
56. Corjay, M.H.*, et al.* Two distinct bombesin receptor subtypes are expressed and functional in human lung carcinoma cells. *J Biol Chem* **266**, 18771-18779 (1991).
57. Dingemans, A.M.*, et al.* Expression of DNA topoisomerase IIalpha and topoisomerase IIbeta genes predicts survival and response to chemotherapy in patients with small cell lung cancer. *Clin Cancer Res* **5**, 2048-2058 (1999).
58. Trusolino, L. & Comoglio, P.M. Scatter-factor and semaphorin receptors: cell signalling for invasive growth. *Nat Rev Cancer* **2**, 289-300 (2002).
59. Peschard, P.*, et al.* Mutation of the c-Cbl TKB domain binding site on the Met receptor tyrosine kinase converts it into a transforming protein. *Mol Cell* **8**, 995-1004 (2001).
60. Abella, J.V.*, et al.* Met/Hepatocyte growth factor receptor ubiquitination suppresses transformation and is required for Hrs phosphorylation. *Mol Cell Biol* **25**, 9632-9645 (2005).
61. Benvenuti, S. & Comoglio, P.M. The MET receptor tyrosine kinase in invasion and metastasis. *J Cell Physiol* **213**, 316-325 (2007).
62. Birchmeier, C., Birchmeier, W., Gherardi, E. & Vande Woude, G.F. Met, metastasis, motility and more. *Nat Rev Mol Cell Biol* **4**, 915-925 (2003).
63. Stoker, M., Gherardi, E., Perryman, M. & Gray, J. Scatter factor is a fibroblast-derived modulator of epithelial cell mobility. *Nature* **327**, 239-242 (1987).
64. Gherardi, E., Gray, J., Stoker, M., Perryman, M. & Furlong, R. Purification of scatter factor, a fibroblast-derived basic protein that modulates epithelial interactions and movement. *Proc Natl Acad Sci U S A* **86**, 5844-5848 (1989).
65. Nakamura, T., Teramoto, H. & Ichihara, A. Purification and characterization of a growth factor from rat platelets for mature

parenchymal hepatocytes in primary cultures. *Proc Natl Acad Sci U S A* **83**, 6489-6493 (1986).

66. Naldini, L.*, et al.* Scatter factor and hepatocyte growth factor are indistinguishable ligands for the MET receptor. *EMBO J* **10**, 2867-2878 (1991).
67. Comoglio, P.M., Giordano, S. & Trusolino, L. Drug development of MET inhibitors: targeting oncogene addiction and expedience. *Nat Rev Drug Discov* **7**, 504-516 (2008).
68. Stamos, J., Lazarus, R.A., Yao, X., Kirchhofer, D. & Wiesmann, C. Crystal structure of the HGF beta-chain in complex with the Sema domain of the Met receptor. *EMBO J* **23**, 2325-2335 (2004).
69. Trusolino, L., Bertotti, A. & Comoglio, P.M. MET signalling: principles and functions in development, organ regeneration and cancer. *Nat Rev Mol Cell Biol* **11**, 834-848 (2010).
70. Lyon, M., Deakin, J.A., Mizuno, K., Nakamura, T. & Gallagher, J.T. Interaction of hepatocyte growth factor with heparan sulfate. Elucidation of the major heparan sulfate structural determinants. *J Biol Chem* **269**, 11216-11223 (1994).
71. Sonnenberg, E., Meyer, D., Weidner, K.M. & Birchmeier, C. Scatter factor/hepatocyte growth factor and its receptor, the c-met tyrosine kinase, can mediate a signal exchange between mesenchyme and epithelia during mouse development. *J Cell Biol* **123**, 223-235 (1993).
72. Bhowmick, N.A., Neilson, E.G. & Moses, H.L. Stromal fibroblasts in cancer initiation and progression. *Nature* **432**, 332-337 (2004).
73. Owen, K.A.*, et al.* Pericellular activation of hepatocyte growth factor by the transmembrane serine proteases matriptase and hepsin, but not by the membrane-associated protease uPA. *Biochem J* **426**, 219-228 (2010).
74. Zhang, Y.W. & Vande Woude, G.F. HGF/SF-met signaling in the control of branching morphogenesis and invasion. *J Cell Biochem* **88**, 408-417 (2003).
75. Corso, S., Comoglio, P.M. & Giordano, S. Cancer therapy: can the challenge be MET? *Trends Mol Med* **11**, 284-292 (2005).
76. Gherardi, E., Birchmeier, W., Birchmeier, C. & Woude, G.V. Targeting MET in cancer: rationale and progress. *Nat Rev Cancer* **12**, 89-103 (2012).
77. Liu, Z.X., Yu, C.F., Nickel, C., Thomas, S. & Cantley, L.G. Hepatocyte growth factor induces ERK-dependent paxillin phosphorylation and regulates paxillin-focal adhesion kinase association. *J Biol Chem* **277**, 10452-10458 (2002).

78. Kermorgant, S. & Parker, P.J. Receptor trafficking controls weak signal delivery: a strategy used by c-Met for STAT3 nuclear accumulation. *J Cell Biol* **182**, 855-863 (2008).
79. Kermorgant, S., Zicha, D. & Parker, P.J. PKC controls HGF-dependent c-Met traffic, signalling and cell migration. *EMBO J* **23**, 3721-3734 (2004).
80. Hammond, D.E., Urbe, S., Vande Woude, G.F. & Clague, M.J. Down-regulation of MET, the receptor for hepatocyte growth factor. *Oncogene* **20**, 2761-2770 (2001).
81. Carter, S., Urbe, S. & Clague, M.J. The met receptor degradation pathway: requirement for Lys48-linked polyubiquitin independent of proteasome activity. *J Biol Chem* **279**, 52835-52839 (2004).
82. Conrotto, P., Corso, S., Gamberini, S., Comoglio, P.M. & Giordano, S. Interplay between scatter factor receptors and B plexins controls invasive growth. *Oncogene* **23**, 5131-5137 (2004).
83. Foveau, B.*, et al.* Down-regulation of the met receptor tyrosine kinase by presenilin-dependent regulated intramembrane proteolysis. *Mol Biol Cell* **20**, 2495-2507 (2009).
84. Birchmeier, C. & Gherardi, E. Developmental roles of HGF/SF and its receptor, the c-Met tyrosine kinase. *Trends Cell Biol* **8**, 404-410 (1998).
85. Schmidt, L.*, et al.* Germline and somatic mutations in the tyrosine kinase domain of the MET proto-oncogene in papillary renal carcinomas. *Nat Genet* **16**, 68-73 (1997).
86. Maina, F.*, et al.* Uncoupling of Grb2 from the Met receptor in vivo reveals complex roles in muscle development. *Cell* **87**, 531-542 (1996).
87. Borowiak, M.*, et al.* Met provides essential signals for liver regeneration. *Proc Natl Acad Sci U S A* **101**, 10608-10613 (2004).
88. Huh, C.G.*, et al.* Hepatocyte growth factor/c-met signaling pathway is required for efficient liver regeneration and repair. *Proc Natl Acad Sci U S A* **101**, 4477-4482 (2004).
89. Chmielowiec, J.*, et al.* c-Met is essential for wound healing in the skin. *J Cell Biol* **177**, 151-162 (2007).
90. Iyer, A.*, et al.* Structure, tissue-specific expression, and transforming activity of the mouse met protooncogene. *Cell Growth Differ* **1**, 87-95 (1990).
91. Christensen, J.G., Burrows, J. & Salgia, R. c-Met as a target for human cancer and characterization of inhibitors for therapeutic intervention. *Cancer Lett* **225**, 1-26 (2005).
92. Zhang, Y.W., Su, Y., Volpert, O.V. & Vande Woude, G.F. Hepatocyte growth factor/scatter factor mediates angiogenesis

through positive VEGF and negative thrombospondin 1 regulation. *Proc Natl Acad Sci U S A* **100**, 12718-12723 (2003).

93. Cooper, C.S.*, et al.* Molecular cloning of a new transforming gene from a chemically transformed human cell line. *Nature* **311**, 29-33 (1984).
94. Liang, T.J., Reid, A.E., Xavier, R., Cardiff, R.D. & Wang, T.C. Transgenic expression of tpr-met oncogene leads to development of mammary hyperplasia and tumors. *J Clin Invest* **97**, 2872-2877 (1996).
95. Soman, N.R., Correa, P., Ruiz, B.A. & Wogan, G.N. The TPR-MET oncogenic rearrangement is present and expressed in human gastric carcinoma and precursor lesions. *Proc Natl Acad Sci U S A* **88**, 4892-4896 (1991).
96. Smolen, G.A.*, et al.* Amplification of MET may identify a subset of cancers with extreme sensitivity to the selective tyrosine kinase inhibitor PHA-665752. *Proc Natl Acad Sci U S A* **103**, 2316-2321 (2006).
97. Migliore, C. & Giordano, S. Molecular cancer therapy: can our expectation be MET? *Eur J Cancer* **44**, 641-651 (2008).
98. Engelman, J.A.*, et al.* MET amplification leads to gefitinib resistance in lung cancer by activating ERBB3 signaling. *Science* **316**, 1039-1043 (2007).
99. Carracedo, A.*, et al.* FISH and immunohistochemical status of the hepatocyte growth factor receptor (c-Met) in 184 invasive breast tumors. *Breast Cancer Res* **11**, 402 (2009).
100. Taulli, R.*, et al.* Validation of met as a therapeutic target in alveolar and embryonal rhabdomyosarcoma. *Cancer Res* **66**, 4742-4749 (2006).
101. Houldsworth, J., Cordon-Cardo, C., Ladanyi, M., Kelsen, D.P. & Chaganti, R.S. Gene amplification in gastric and esophageal adenocarcinomas. *Cancer Res* **50**, 6417-6422 (1990).
102. Umeki, K., Shiota, G. & Kawasaki, H. Clinical significance of c-met oncogene alterations in human colorectal cancer. *Oncology* **56**, 314-321 (1999).
103. Bean, J.*, et al.* MET amplification occurs with or without T790M mutations in EGFR mutant lung tumors with acquired resistance to gefitinib or erlotinib. *Proc Natl Acad Sci U S A* **104**, 20932-20937 (2007).
104. Tong, C.Y.*, et al.* Detection of oncogene amplifications in medulloblastomas by comparative genomic hybridization and array-based comparative genomic hybridization. *J Neurosurg* **100**, 187-193 (2004).

105. Beroukhim, R.*, et al.* Assessing the significance of chromosomal aberrations in cancer: methodology and application to glioma. *Proc Natl Acad Sci U S A* **104**, 20007-20012 (2007).
106. Cappuzzo, F.*, et al.* Increased MET gene copy number negatively affects survival of surgically resected non-small-cell lung cancer patients. *J Clin Oncol* **27**, 1667-1674 (2009).
107. Go, H.*, et al.* High MET Gene Copy Number Leads to Shorter Survival in Patients with Non-small Cell Lung Cancer. *J Thorac Oncol* **5,** 305-313 (2010).
108. Zeng, Z.S.*, et al.* c-Met gene amplification is associated with advanced stage colorectal cancer and liver metastases. *Cancer Lett* **265**, 258-269 (2008).
109. Park, W.S.*, et al.* Somatic mutations in the kinase domain of the Met/hepatocyte growth factor receptor gene in childhood hepatocellular carcinomas. *Cancer Res* **59**, 307-310 (1999).
110. Lee, J.H.*, et al.* A novel germ line juxtamembrane Met mutation in human gastric cancer. *Oncogene* **19**, 4947-4953 (2000).
111. Seiwert, T.Y.*, et al.* The MET receptor tyrosine kinase is a potential novel therapeutic target for head and neck squamous cell carcinoma. *Cancer Res* **69**, 3021-3031 (2009).
112. Sattler, M. & Salgia, R. c-Met and hepatocyte growth factor: potential as novel targets in cancer therapy. *Curr Oncol Rep* **9**, 102-108 (2007).
113. Ma, P.C.*, et al.* Functional expression and mutations of c-Met and its therapeutic inhibition with SU11274 and small interfering RNA in non-small cell lung cancer. *Cancer Res* **65**, 1479-1488 (2005).
114. Jagadeeswaran, R.*, et al.* Functional analysis of c-Met/hepatocyte growth factor pathway in malignant pleural mesothelioma. *Cancer Res* **66**, 352-361 (2006).
115. Puri, N.*, et al.* c-Met is a potentially new therapeutic target for treatment of human melanoma. *Clin Cancer Res* **13**, 2246-2253 (2007).
116. Puri, N.*, et al.* A selective small molecule inhibitor of c-Met, PHA665752, inhibits tumorigenicity and angiogenesis in mouse lung cancer xenografts. *Cancer Res* **67**, 3529-3534 (2007).
117. Jeffers, M.*, et al.* Activating mutations for the met tyrosine kinase receptor in human cancer. *Proc Natl Acad Sci U S A* **94**, 11445-11450 (1997).
118. Kong-Beltran, M.*, et al.* Somatic mutations lead to an oncogenic deletion of met in lung cancer. *Cancer Res* **66**, 283-289 (2006).

119. Graveel, C., *et al.* Activating Met mutations produce unique tumor profiles in mice with selective duplication of the mutant allele. *Proc Natl Acad Sci U S A* **101**, 17198-17203 (2004).
120. Di Renzo, M.F., *et al.* Somatic mutations of the MET oncogene are selected during metastatic spread of human HNSC carcinomas. *Oncogene* **19**, 1547-1555 (2000).
121. Aebersold, D.M., *et al.* Prevalence and clinical impact of Met Y1253D-activating point mutation in radiotherapy-treated squamous cell cancer of the oropharynx. *Oncogene* **22**, 8519-8523 (2003).
122. Lorenzato, A., *et al.* Novel somatic mutations of the MET oncogene in human carcinoma metastases activating cell motility and invasion. *Cancer Res* **62**, 7025-7030 (2002).
123. Pennacchietti, S., *et al.* Hypoxia promotes invasive growth by transcriptional activation of the met protooncogene. *Cancer Cell* **3**, 347-361 (2003).
124. Wang, R., Ferrell, L.D., Faouzi, S., Maher, J.J. & Bishop, J.M. Activation of the Met receptor by cell attachment induces and sustains hepatocellular carcinomas in transgenic mice. *J Cell Biol* **153**, 1023-1034 (2001).
125. Danilkovitch-Miagkova, A. & Zbar, B. Dysregulation of Met receptor tyrosine kinase activity in invasive tumors. *J Clin Invest* **109**, 863-867 (2002).
126. Ichimura, E., Maeshima, A., Nakajima, T. & Nakamura, T. Expression of c-met/HGF receptor in human non-small cell lung carcinomas in vitro and in vivo and its prognostic significance. *Jpn J Cancer Res* **87**, 1063-1069 (1996).
127. Cipriani, N.A., Abidoye, O.O., Vokes, E. & Salgia, R. MET as a target for treatment of chest tumors. *Lung Cancer* **63**, 169-179 (2009).
128. Garcia, S., *et al.* Poor prognosis in breast carcinomas correlates with increased expression of targetable CD146 and c-Met and with proteomic basal-like phenotype. *Hum Pathol* **38**, 830-841 (2007).
129. Olivero, M., *et al.* Overexpression and activation of hepatocyte growth factor/scatter factor in human non-small-cell lung carcinomas. *Br J Cancer* **74**, 1862-1868 (1996).
130. Takanami, I., *et al.* Hepatocyte growth factor and c-Met/hepatocyte growth factor receptor in pulmonary adenocarcinomas: an evaluation of their expression as prognostic markers. *Oncology* **53**, 392-397 (1996).

131. Tsao, M.S., *et al.* Differential expression of Met/hepatocyte growth factor receptor in subtypes of non-small cell lung cancers. *Lung Cancer* **20**, 1-16 (1998).
132. Natali, P.G., *et al.* Overexpression of the met/HGF receptor in renal cell carcinomas. *Int J Cancer* **69**, 212-217 (1996).
133. Di Renzo, M.F., *et al.* Overexpression of the Met/HGF receptor in ovarian cancer. *Int J Cancer* **58**, 658-662 (1994).
134. Wong, A.S., *et al.* Coexpression of hepatocyte growth factor-Met: an early step in ovarian carcinogenesis? *Oncogene* **20**, 1318-1328 (2001).
135. Garcia, S., *et al.* c-Met overexpression in inflammatory breast carcinomas: automated quantification on tissue microarrays. *Br J Cancer* **96**, 329-335 (2007).
136. Takeuchi, H., *et al.* c-MET expression level in primary colon cancer: a predictor of tumor invasion and lymph node metastases. *Clin Cancer Res* **9**, 1480-1488 (2003).
137. Sawada, K., *et al.* c-Met overexpression is a prognostic factor in ovarian cancer and an effective target for inhibition of peritoneal dissemination and invasion. *Cancer Res* **67**, 1670-1679 (2007).
138. Tolgay Ocal, I., Dolled-Filhart, M., D'Aquila, T.G., Camp, R.L. & Rimm, D.L. Tissue microarray-based studies of patients with lymph node negative breast carcinoma show that met expression is associated with worse outcome but is not correlated with epidermal growth factor family receptors. *Cancer* **97**, 1841-1848 (2003).
139. Gentile, A., Trusolino, L. & Comoglio, P.M. The Met tyrosine kinase receptor in development and cancer. *Cancer Metastasis Rev* **27**, 85-94 (2008).
140. Boccaccio, C., Gaudino, G., Gambarotta, G., Galimi, F. & Comoglio, P.M. Hepatocyte growth factor (HGF) receptor expression is inducible and is part of the delayed-early response to HGF. *J Biol Chem* **269**, 12846-12851 (1994).
141. Aguirre Ghiso, J.A., Alonso, D.F., Farias, E.F., Gomez, D.E. & de Kier Joffe, E.B. Deregulation of the signaling pathways controlling urokinase production. Its relationship with the invasive phenotype. *Eur J Biochem* **263**, 295-304 (1999).
142. Wojcik, E.J., *et al.* A novel activating function of c-Src and Stat3 on HGF transcription in mammary carcinoma cells. *Oncogene* **25**, 2773-2784 (2006).
143. Kankuri, E., Cholujova, D., Comajova, M., Vaheri, A. & Bizik, J. Induction of hepatocyte growth factor/scatter factor by fibroblast clustering directly promotes tumor cell invasiveness. *Cancer Res* **65**, 9914-9922 (2005).

144. Michieli, P., *et al.* Mutant Met-mediated transformation is ligand-dependent and can be inhibited by HGF antagonists. *Oncogene* **18**, 5221-5231 (1999).
145. Koochekpour, S., *et al.* Met and hepatocyte growth factor/scatter factor expression in human gliomas. *Cancer Res* **57**, 5391-5398 (1997).
146. Tuck, A.B., Park, M., Sterns, E.E., Boag, A. & Elliott, B.E. Coexpression of hepatocyte growth factor and receptor (Met) in human breast carcinoma. *Am J Pathol* **148**, 225-232 (1996).
147. Ferracini, R., *et al.* Retrogenic expression of the MET proto-oncogene correlates with the invasive phenotype of human rhabdomyosarcomas. *Oncogene* **12**, 1697-1705 (1996).
148. Ferracini, R., *et al.* The Met/HGF receptor is over-expressed in human osteosarcomas and is activated by either a paracrine or an autocrine circuit. *Oncogene* **10**, 739-749 (1995).
149. Rong, S., Segal, S., Anver, M., Resau, J.H. & Vande Woude, G.F. Invasiveness and metastasis of NIH 3T3 cells induced by Met-hepatocyte growth factor/scatter factor autocrine stimulation. *Proc Natl Acad Sci U S A* **91**, 4731-4735 (1994).
150. Mak, H.H., *et al.* Oncogenic activation of the Met receptor tyrosine kinase fusion protein, Tpr-Met, involves exclusion from the endocytic degradative pathway. *Oncogene* **26**, 7213-7221 (2007).
151. Ishibe, S., *et al.* Met and the epidermal growth factor receptor act cooperatively to regulate final nephron number and maintain collecting duct morphology. *Development* **136**, 337-345 (2009).
152. Liska, D., Chen, C.T., Bachleitner-Hofmann, T., Christensen, J.G. & Weiser, M.R. HGF rescues colorectal cancer cells from EGFR inhibition via MET activation. *Clin Cancer Res* **17**, 472-482 (2011).
153. Tang, Z., *et al.* Dual MET-EGFR combinatorial inhibition against T790M-EGFR-mediated erlotinib-resistant lung cancer. *Br J Cancer* **99**, 911-922 (2008).
154. Guo, A., *et al.* Signaling networks assembled by oncogenic EGFR and c-Met. *Proc Natl Acad Sci U S A* **105**, 692-697 (2008).
155. Fischer, O.M., Giordano, S., Comoglio, P.M. & Ullrich, A. Reactive oxygen species mediate Met receptor transactivation by G protein-coupled receptors and the epidermal growth factor receptor in human carcinoma cells. *J Biol Chem* **279**, 28970-28978 (2004).
156. Khoury, H., *et al.* HGF converts ErbB2/Neu epithelial morphogenesis to cell invasion. *Mol Biol Cell* **16**, 550-561 (2005).

157. Follenzi, A., *et al.* Cross-talk between the proto-oncogenes Met and Ron. *Oncogene* **19**, 3041-3049 (2000).
158. Benvenuti, S., *et al.* Ron kinase transphosphorylation sustains MET oncogene addiction. *Cancer Res* **71**, 1945-1955 (2011).
159. Orian-Rousseau, V., Chen, L., Sleeman, J.P., Herrlich, P. & Ponta, H. CD44 is required for two consecutive steps in HGF/c-Met signaling. *Genes Dev* **16**, 3074-3086 (2002).
160. Orian-Rousseau, V., *et al.* Hepatocyte growth factor-induced Ras activation requires ERM proteins linked to both CD44v6 and F-actin. *Mol Biol Cell* **18**, 76-83 (2007).
161. Trusolino, L., Bertotti, A. & Comoglio, P.M. A signaling adapter function for alpha6beta4 integrin in the control of HGF-dependent invasive growth. *Cell* **107**, 643-654 (2001).
162. Wang, X., *et al.* A mechanism of cell survival: sequestration of Fas by the HGF receptor Met. *Mol Cell* **9**, 411-421 (2002).
163. Klaus, A. & Birchmeier, W. Wnt signalling and its impact on development and cancer. *Nat Rev Cancer* **8**, 387-398 (2008).
164. Boon, E.M., van der Neut, R., van de Wetering, M., Clevers, H. & Pals, S.T. Wnt signaling regulates expression of the receptor tyrosine kinase met in colorectal cancer. *Cancer Res* **62**, 5126-5128 (2002).
165. Liu, Y., *et al.* Coordinate integrin and c-Met signaling regulate Wnt gene expression during epithelial morphogenesis. *Development* **136**, 843-853 (2009).
166. Monga, S.P., *et al.* Hepatocyte growth factor induces Wnt-independent nuclear translocation of beta-catenin after Met-beta-catenin dissociation in hepatocytes. *Cancer Res* **62**, 2064-2071 (2002).
167. Brembeck, F.H., *et al.* Essential role of BCL9-2 in the switch between beta-catenin's adhesive and transcriptional functions. *Genes Dev* **18**, 2225-2230 (2004).
168. Bhowmick, N.A., *et al.* TGF-beta signaling in fibroblasts modulates the oncogenic potential of adjacent epithelia. *Science* **303**, 848-851 (2004).
169. Sulpice, E., *et al.* Cross-talk between the VEGF-A and HGF signalling pathways in endothelial cells. *Biol Cell* **101**, 525-539 (2009).
170. Bussolino, F., *et al.* Hepatocyte growth factor is a potent angiogenic factor which stimulates endothelial cell motility and growth. *J Cell Biol* **119**, 629-641 (1992).
171. Grant, D.S., *et al.* Scatter factor induces blood vessel formation in vivo. *Proc Natl Acad Sci U S A* **90**, 1937-1941 (1993).

172. Silvagno, F.*, et al.* In vivo activation of met tyrosine kinase by heterodimeric hepatocyte growth factor molecule promotes angiogenesis. *Arterioscler Thromb Vasc Biol* **15**, 1857-1865 (1995).
173. Van Belle, E.*, et al.* Potentiated angiogenic effect of scatter factor/hepatocyte growth factor via induction of vascular endothelial growth factor: the case for paracrine amplification of angiogenesis. *Circulation* **97**, 381-390 (1998).
174. Wojta, J.*, et al.* Hepatocyte growth factor increases expression of vascular endothelial growth factor and plasminogen activator inhibitor-1 in human keratinocytes and the vascular endothelial growth factor receptor flk-1 in human endothelial cells. *Lab Invest* **79**, 427-438 (1999).
175. Gerritsen, M.E., Tomlinson, J.E., Zlot, C., Ziman, M. & Hwang, S. Using gene expression profiling to identify the molecular basis of the synergistic actions of hepatocyte growth factor and vascular endothelial growth factor in human endothelial cells. *Br J Pharmacol* **140**, 595-610 (2003).
176. Ma, P.C.*, et al.* Expression and mutational analysis of MET in human solid cancers. *Genes Chromosomes Cancer* **47**, 1025-1037 (2008).
177. Rikova, K.*, et al.* Global survey of phosphotyrosine signaling identifies oncogenic kinases in lung cancer. *Cell* **131**, 1190-1203 (2007).
178. Beau-Faller, M.*, et al.* MET gene copy number in non-small cell lung cancer: molecular analysis in a targeted tyrosine kinase inhibitor naive cohort. *J Thorac Oncol* **3**, 331-339 (2008).
179. Kanteti, R., Yala, S., Ferguson, M.K. & Salgia, R. MET, HGF, EGFR, and PXN gene copy number in lung cancer using DNA extracts from FFPE archival samples and prognostic significance. *J Environ Pathol Toxicol Oncol* **28**, 89-98 (2009).
180. Onitsuka, T.*, et al.* Comprehensive molecular analyses of lung adenocarcinoma with regard to the epidermal growth factor receptor, K-ras, MET, and hepatocyte growth factor status. *J Thorac Oncol* **5**, 591-596 (2010).
181. Onozato, R.*, et al.* Activation of MET by gene amplification or by splice mutations deleting the juxtamembrane domain in primary resected lung cancers. *J Thorac Oncol* **4**, 5-11 (2009).
182. Camacho LH, M.S., LoRusso PM, et al. First in human phase I study of MK-2461, a small molecule inhibitor of c-Met, for patients with advanced solid tumors. in *American Society of Clinical Oncology (ASCO), Annual Meeting; Chicago, IL; 2008*.

183. Tyner, J.W.*, et al.* MET receptor sequence variants R970C and T992I lack transforming capacity. *Cancer Res* **70**, 6233-6237 (2010).
184. Lokker, N.A.*, et al.* Structure-function analysis of hepatocyte growth factor: identification of variants that lack mitogenic activity yet retain high affinity receptor binding. *EMBO J* **11**, 2503-2510 (1992).
185. Lietha, D., Chirgadze, D.Y., Mulloy, B., Blundell, T.L. & Gherardi, E. Crystal structures of NK1-heparin complexes reveal the basis for NK1 activity and enable engineering of potent agonists of the MET receptor. *EMBO J* **20**, 5543-5555 (2001).
186. Matsumoto, K., Kataoka, H., Date, K. & Nakamura, T. Cooperative interaction between alpha- and beta-chains of hepatocyte growth factor on c-Met receptor confers ligand-induced receptor tyrosine phosphorylation and multiple biological responses. *J Biol Chem* **273**, 22913-22920 (1998).
187. Trusolino, L., Pugliese, L. & Comoglio, P.M. Interactions between scatter factors and their receptors: hints for therapeutic applications. *FASEB J* **12**, 1267-1280 (1998).
188. Martens, T.*, et al.* A novel one-armed anti-c-Met antibody inhibits glioblastoma growth in vivo. *Clin Cancer Res* **12**, 6144-6152 (2006).
189. Jin, H.*, et al.* MetMAb, the one-armed 5D5 anti-c-Met antibody, inhibits orthotopic pancreatic tumor growth and improves survival. *Cancer Res* **68**, 4360-4368 (2008).
190. Wu, H.C., Wu, C.K., Liao, J.W., Chang, L.H. & T, I.C. Coping strategies of hospitalized people with psychiatric disabilities in Taiwan. *Psychiatr Q* **81**, 23-34 (2010).
191. Urick, T.*, et al.* The pnhA gene of Pasteurella multocida encodes a dinucleoside oligophosphate pyrophosphatase member of the Nudix hydrolase superfamily. *J Bacteriol* **187**, 5809-5817 (2005).
192. Jun, H.T.*, et al.* AMG 102, a fully human anti-hepatocyte growth factor/scatter factor neutralizing antibody, enhances the efficacy of temozolomide or docetaxel in U-87 MG cells and xenografts. *Clin Cancer Res* **13**, 6735-6742 (2007).
193. Giordano, S. Rilotumumab, a mAb against human hepatocyte growth factor for the treatment of cancer. *Curr Opin Mol Ther* **11**, 448-455 (2009).
194. Gordon, M.S.*, et al.* Safety, pharmacokinetics, and pharmacodynamics of AMG 102, a fully human hepatocyte growth factor-neutralizing monoclonal antibody, in a first-in-human study of patients with advanced solid tumors. *Clin Cancer Res* **16**, 699-710 (2010).

195. Wen, P.Y., *et al.* A phase II study evaluating the efficacy and safety of AMG 102 (rilotumumab) in patients with recurrent glioblastoma. *Neuro Oncol* **13**, 437-446 (2011).
196. Schoffski, P., *et al.* A phase II study of the efficacy and safety of AMG 102 in patients with metastatic renal cell carcinoma. *BJU Int* **108**, 679-686 (2011).
197. Okamoto, W., *et al.* TAK-701, a humanized monoclonal antibody to hepatocyte growth factor, reverses gefitinib resistance induced by tumor-derived HGF in non-small cell lung cancer with an EGFR mutation. *Mol Cancer Ther* **9**, 2785-2792 (2010).
198. i Cancho, R.F., Riordan, O. & Bollobas, B. The consequences of Zipf's law for syntax and symbolic reference. *Proc Biol Sci* **272**, 561-565 (2005).
199. Li-Chun, C., L, I.C., Bi-Ying, H., Wan-En, C. & Shu-Feng, L. A preliminary survey of the health behaviors of community leaders. *J Nurs Res* **12**, 92-102 (2004).
200. Li-chun, C. & L, I.c. Patterns of complementary therapy use by homebound cancer patients in Taiwan. *Appl Nurs Res* **17**, 41-47 (2004).
201. LY, I.C. & Tan, C.L. Use of intravenous midazolam for sedation in children undergoing ward procedures. *J Singapore Paediatr Soc* **34**, 30-33 (1992).
202. Cui, J.J., *et al.* Structure based drug design of crizotinib (PF-02341066), a potent and selective dual inhibitor of mesenchymal-epithelial transition factor (c-MET) kinase and anaplastic lymphoma kinase (ALK). *J Med Chem* **54**, 6342-6363 (2011).
203. Camidge, D.R., *et al.* Activity and safety of crizotinib in patients with ALK-positive non-small-cell lung cancer: updated results from a phase 1 study. *Lancet Oncol* **13**, 1011-1019 (2012).
204. Lennerz, J.K., *et al.* MET amplification identifies a small and aggressive subgroup of esophagogastric adenocarcinoma with evidence of responsiveness to crizotinib. *J Clin Oncol* **29**, 4803-4810 (2011).
205. Zou, H.Y., *et al.* An orally available small-molecule inhibitor of c-Met, PF-2341066, exhibits cytoreductive antitumor efficacy through antiproliferative and antiangiogenic mechanisms. *Cancer Res* **67**, 4408-4417 (2007).
206. Tanizaki, J., *et al.* MET tyrosine kinase inhibitor crizotinib (PF-02341066) shows differential antitumor effects in non-small cell lung cancer according to MET alterations. *J Thorac Oncol* **6**, 1624-1631 (2011).
207. Zillhardt, M., Christensen, J.G. & Lengyel, E. An orally available small-molecule inhibitor of c-Met, PF-2341066, reduces tumor

burden and metastasis in a preclinical model of ovarian cancer metastasis. *Neoplasia* **12**, 1-10 (2010).
208. Kwak, E.L.*, et al.* Anaplastic lymphoma kinase inhibition in non-small-cell lung cancer. *N Engl J Med* **363**, 1693-1703 (2010).
209. Shaw, A.T.*, et al.* Effect of crizotinib on overall survival in patients with advanced non-small-cell lung cancer harbouring ALK gene rearrangement: a retrospective analysis. *Lancet Oncol* **12**, 1004-1012 (2011).
210. Ou, S.H.*, et al.* Activity of crizotinib (PF02341066), a dual mesenchymal-epithelial transition (MET) and anaplastic lymphoma kinase (ALK) inhibitor, in a non-small cell lung cancer patient with de novo MET amplification. *J Thorac Oncol* **6**, 942-946 (2011).
211. Chi, A.S.*, et al.* Rapid radiographic and clinical improvement after treatment of a MET-amplified recurrent glioblastoma with a mesenchymal-epithelial transition inhibitor. *J Clin Oncol* **30**, e30-33 (2012).
212. Zou, H.Y.*, et al.* Sensitivity of Selected Human Tumor Models to PF-04217903, a Novel Selective c-Met Kinase Inhibitor. *Mol Cancer Ther* **11**, 1036-1047 (2012).
213. Munshi, N.*, et al.* ARQ 197, a novel and selective inhibitor of the human c-Met receptor tyrosine kinase with antitumor activity. *Mol Cancer Ther* **9**, 1544-1553 (2010).
214. Yap, T.A.*, et al.* Phase I trial of a selective c-MET inhibitor ARQ 197 incorporating proof of mechanism pharmacodynamic studies. *J Clin Oncol* **29**, 1271-1279 (2011).
215. Sierra, J.R. & Tsao, M.S. c-MET as a potential therapeutic target and biomarker in cancer. *Ther Adv Med Oncol* **3**, S21-35 (2011).
216. Feng, Y., Thiagarajan, P.S. & Ma, P.C. MET signaling: novel targeted inhibition and its clinical development in lung cancer. *J Thorac Oncol* **7**, 459-467 (2012).
217. Sequist, L.V.*, et al.* Randomized phase II study of erlotinib plus tivantinib versus erlotinib plus placebo in previously treated non-small-cell lung cancer. *J Clin Oncol* **29**, 3307-3315 (2011).
218. Qian, F.*, et al.* Inhibition of tumor cell growth, invasion, and metastasis by EXEL-2880 (XL880, GSK1363089), a novel inhibitor of HGF and VEGF receptor tyrosine kinases. *Cancer Res* **69**, 8009-8016 (2009).
219. Eder, J.P.*, et al.* A phase I study of foretinib, a multi-targeted inhibitor of c-Met and vascular endothelial growth factor receptor 2. *Clin Cancer Res* **16**, 3507-3516 (2010).

220. Liu, L.*, et al.* Synergistic effects of foretinib with HER-targeted agents in MET and HER1- or HER2-coactivated tumor cells. *Mol Cancer Ther* **10**, 518-530 (2011).
221. Seiwert, T.*, et al.* Phase II trial of single-agent foretinib (GSK1363089) in patients with recurrent or metastatic squamous cell carcinoma of the head and neck. *Invest New Drugs* **31**, 417-424 (2012).
222. Yakes, F.M.*, et al.* Cabozantinib (XL184), a novel MET and VEGFR2 inhibitor, simultaneously suppresses metastasis, angiogenesis, and tumor growth. *Mol Cancer Ther* **10**, 2298-2308 (2011).
223. Zhang, Y., Guessous, F., Kofman, A., Schiff, D. & Abounader, R. XL-184, a MET, VEGFR-2 and RET kinase inhibitor for the treatment of thyroid cancer, glioblastoma multiforme and NSCLC. *IDrugs* **13**, 112-121 (2012).
224. Rider, R.V., Harper, P.A., Chow, L.P. & C, I.c. [Comparison of 4 methods of determining the incidence of induced abortion]. *Estud Poblac* **4**, 41-60 (1979).
225. www.clinicaltrials.gorv
226. Wang, W.*, et al.* Met kinase inhibitor E7050 reverses three different mechanisms of hepatocyte growth factor-induced tyrosine kinase inhibitor resistance in EGFR mutant lung cancer. *Clinical cancer research : an official journal of the American Association for Cancer Research* **18**, 1663-1671 (2012).
227. Daniele G, R.M., Blanco-Codesido M, et al. Phase I dose-finding study of golvatinib (E7050), a c-Met and Eph receptor targeted multi-kinase inhibitor, administered orally QD to patients with advanced solid tumors. in *J Clin Oncol 2012;30:abstr 3030*.
228. Welsh, J.W.*, et al.* The c-Met receptor tyrosine kinase inhibitor MP470 radiosensitizes glioblastoma cells. *Radiat Oncol* **4**, 69 (2009).
229. Eder, J.P., Vande Woude, G.F., Boerner, S.A. & LoRusso, P.M. Novel therapeutic inhibitors of the c-Met signaling pathway in cancer. *Clin Cancer Res* **15**, 2207-2214 (2009).
230. Ma, P.C.*, et al.* Downstream signalling and specific inhibition of c-MET/HGF pathway in small cell lung cancer: implications for tumour invasion. *Br J Cancer* **97**, 368-377 (2007).
231. Jagadeeswaran, R., Jagadeeswaran, S., Bindokas, V.P. & Salgia, R. Activation of HGF/c-Met pathway contributes to the reactive oxygen species generation and motility of small cell lung cancer cells. *Am J Physiol Lung Cell Mol Physiol* **292**, L1488-1494 (2007).

232. Shook, D. & Keller, R. Mechanisms, mechanics and function of epithelial-mesenchymal transitions in early development. *Mech Dev* **120**, 1351-1383 (2003).
233. Christiansen, J.J. & Rajasekaran, A.K. Reassessing epithelial to mesenchymal transition as a prerequisite for carcinoma invasion and metastasis. *Cancer Res* **66**, 8319-8326 (2006).
234. Tarin, D., Thompson, E.W. & Newgreen, D.F. The fallacy of epithelial mesenchymal transition in neoplasia. *Cancer Res* **65**, 5996-6000; discussion 6000-6001 (2005).
235. Miyoshi, J. & Takai, Y. Structural and functional associations of apical junctions with cytoskeleton. *Biochim Biophys Acta* **1778**, 670-691 (2008).
236. Conacci-Sorrell, M., Zhurinsky, J. & Ben-Ze'ev, A. The cadherin-catenin adhesion system in signaling and cancer. *J Clin Invest* **109**, 987-991 (2002).
237. Adams, C.L. & Nelson, W.J. Cytomechanics of cadherin-mediated cell-cell adhesion. *Curr Opin Cell Biol* **10**, 572-577 (1998).
238. Garrod, D., Chidgey, M. & North, A. Desmosomes: differentiation, development, dynamics and disease. *Curr Opin Cell Biol* **8**, 670-678 (1996).
239. Byers, S.W., Sommers, C.L., Hoxter, B., Mercurio, A.M. & Tozeren, A. Role of E-cadherin in the response of tumor cell aggregates to lymphatic, venous and arterial flow: measurement of cell-cell adhesion strength. *J Cell Sci* **108**, 2053-2064 (1995).
240. Li, S., Guan, J.L. & Chien, S. Biochemistry and biomechanics of cell motility. *Annu Rev Biomed Eng* **7**, 105-150 (2005).
241. Seiki, M. Membrane-type 1 matrix metalloproteinase: a key enzyme for tumor invasion. *Cancer Lett* **194**, 1-11 (2003).
242. Lang, S.H.*, et al.* Enhanced expression of vimentin in motile prostate cell lines and in poorly differentiated and metastatic prostate carcinoma. *Prostate* **52**, 253-263 (2002).
243. LaGamba, D., Nawshad, A. & Hay, E.D. Microarray analysis of gene expression during epithelial-mesenchymal transformation. *Dev Dyn* **234**, 132-142 (2005).
244. Peinado, H., Olmeda, D. & Cano, A. Snail, Zeb and bHLH factors in tumour progression: an alliance against the epithelial phenotype? *Nat Rev Cancer* **7**, 415-428 (2007).
245. Kalluri, R. & Neilson, E.G. Epithelial-mesenchymal transition and its implications for fibrosis. *J Clin Invest* **112**, 1776-1784 (2003).
246. Thiery, J.P. Epithelial-mesenchymal transitions in tumour progression. *Nat Rev Cancer* **2**, 442-454 (2002).

247. Thiery, J.P. Epithelial-mesenchymal transitions in development and pathologies. *Curr Opin Cell Biol* **15**, 740-746 (2003).
248. Thiery, J.P. & Sleeman, J.P. Complex networks orchestrate epithelial-mesenchymal transitions. *Nat Rev Mol Cell Biol* **7**, 131-142 (2006).
249. Nieto, M.A. The snail superfamily of zinc-finger transcription factors. *Nat Rev Mol Cell Biol* **3**, 155-166 (2002).
250. Kemler, R. From cadherins to catenins: cytoplasmic protein interactions and regulation of cell adhesion. *Trends Genet* **9**, 317-321 (1993).
251. Zheng, Z.H.*, et al.* Analysis of metastasis suppressing function of E-cadherin in gastric cancer cells by RNAi. *World J Gastroenterol* **11**, 2000-2003 (2005).
252. Behrens, J., Mareel, M.M., Van Roy, F.M. & Birchmeier, W. Dissecting tumor cell invasion: epithelial cells acquire invasive properties after the loss of uvomorulin-mediated cell-cell adhesion. *J Cell Biol* **108**, 2435-2447 (1989).
253. Burdsal, C.A., Damsky, C.H. & Pedersen, R.A. The role of E-cadherin and integrins in mesoderm differentiation and migration at the mammalian primitive streak. *Development* **118**, 829-844 (1993).
254. Perl, A.K., Wilgenbus, P., Dahl, U., Semb, H. & Christofori, G. A causal role for E-cadherin in the transition from adenoma to carcinoma. *Nature* **392**, 190-193 (1998).
255. Frixen, U.H.*, et al.* E-cadherin-mediated cell-cell adhesion prevents invasiveness of human carcinoma cells. *J Cell Biol* **113**, 173-185 (1991).
256. Hajra, K.M. & Fearon, E.R. Cadherin and catenin alterations in human cancer. *Genes Chromosomes Cancer* **34**, 255-268 (2002).
257. Kowalski, P.J., Rubin, M.A. & Kleer, C.G. E-cadherin expression in primary carcinomas of the breast and its distant metastases. *Breast Cancer Res* **5**, R217-222 (2003).
258. Chan, A.O.*, et al.* Soluble E-cadherin is an independent pretherapeutic factor for long-term survival in gastric cancer. *J Clin Oncol* **21**, 2288-2293 (2003).
259. Gould Rothberg, B.E. & Bracken, M.B. E-cadherin immunohistochemical expression as a prognostic factor in infiltrating ductal carcinoma of the breast: a systematic review and meta-analysis. *Breast Cancer Res Treat* **100**, 139-148 (2006).
260. Wijnhoven, B.P., Dinjens, W.N. & Pignatelli, M. E-cadherin-catenin cell-cell adhesion complex and human cancer. *Br J Surg* **87**, 992-1005 (2000).

261. Birchmeier, W. & Behrens, J. Cadherin expression in carcinomas: role in the formation of cell junctions and the prevention of invasiveness. *Biochim Biophys Acta* **1198**, 11-26 (1994).
262. Guilford, P. E-cadherin downregulation in cancer: fuel on the fire? *Mol Med Today* **5**, 172-177 (1999).
263. Dorudi, S., Hanby, A.M., Poulsom, R., Northover, J. & Hart, I.R. Level of expression of E-cadherin mRNA in colorectal cancer correlates with clinical outcome. *Br J Cancer* **71**, 614-616 (1995).
264. Peinado, H., Portillo, F. & Cano, A. Transcriptional regulation of cadherins during development and carcinogenesis. *Int J Dev Biol* **48**, 365-375 (2004).
265. Christofori, G. Changing neighbours, changing behaviour: cell adhesion molecule-mediated signalling during tumour progression. *EMBO J* **22**, 2318-2323 (2003).
266. Isobe, Y.*, et al.* Neural cell adhesion molecule (CD56)-positive B-cell lymphoma. *Eur J Haematol* **79**, 166-169 (2007).
267. Perl, A.K.*, et al.* Reduced expression of neural cell adhesion molecule induces metastatic dissemination of pancreatic beta tumor cells. *Nat Med* **5**, 286-291 (1999).
268. Fogar, P.*, et al.* Neural cell adhesion molecule (N-CAM) in gastrointestinal neoplasias. *Anticancer Res* **17**, 1227-1230 (1997).
269. Roesler, J., Srivatsan, E., Moatamed, F., Peters, J. & Livingston, E.H. Tumor suppressor activity of neural cell adhesion molecule in colon carcinoma. *Am J Surg* **174**, 251-257 (1997).
270. Tezel, E., Kawase, Y., Takeda, S., Oshima, K. & Nakao, A. Expression of neural cell adhesion molecule in pancreatic cancer. *Pancreas* **22**, 122-125 (2001).
271. Thomas, P.A.*, et al.* Association between keratin and vimentin expression, malignant phenotype, and survival in postmenopausal breast cancer patients. *Clin Cancer Res* **5**, 2698-2703 (1999).
272. Al-Saad, S.*, et al.* The prognostic impact of NF-kappaB p105, vimentin, E-cadherin and Par6 expression in epithelial and stromal compartment in non-small-cell lung cancer. *Br J Cancer* **99**, 1476-1483 (2008).
273. Utsunomiya, T., Yao, T., Masuda, K. & Tsuneyoshi, M. Vimentin-positive adenocarcinomas of the stomach: co-expression of vimentin and cytokeratin. *Histopathology* **29**, 507-516 (1996).
274. Mutlu, N., Turkeri, L. & Emerk, K. Analytical and clinical evaluation of a new urinary tumor marker: bladder tumor fibronectin in diagnosis and follow-up of bladder cancer. *Clin Chem Lab Med* **41**, 1069-1074 (2003).

275. Inufusa, H., *et al.* Localization of oncofetal and normal fibronectin in colorectal cancer. Correlation with histologic grade, liver metastasis, and prognosis. *Cancer* **75**, 2802-2808 (1995).
276. Franke, F.E., Von Georgi, R., Zygmunt, M. & Munstedt, K. Association between fibronectin expression and prognosis in ovarian carcinoma. *Anticancer Res* **23**, 4261-4267 (2003).
277. Yoshinaga, K., *et al.* N-cadherin is regulated by activin A and associated with tumor aggressiveness in esophageal carcinoma. *Clin Cancer Res* **10**, 5702-5707 (2004).
278. Nakashima, T., *et al.* Neural-cadherin expression associated with angiogenesis in non-small-cell lung cancer patients. *Br J Cancer* **88**, 1727-1733 (2003).
279. Lascombe, I., *et al.* N-cadherin as a novel prognostic marker of progression in superficial urothelial tumors. *Clin Cancer Res* **12**, 2780-2787 (2006).
280. Batlle, E., *et al.* The transcription factor snail is a repressor of E-cadherin gene expression in epithelial tumour cells. *Nat Cell Biol* **2**, 84-89 (2000).
281. Cano, A., *et al.* The transcription factor snail controls epithelial-mesenchymal transitions by repressing E-cadherin expression. *Nat Cell Biol* **2**, 76-83 (2000).
282. Blanco, M.J., *et al.* Correlation of Snail expression with histological grade and lymph node status in breast carcinomas. *Oncogene* **21**, 3241-3246 (2002).
283. Cheng, C.W., *et al.* Mechanisms of inactivation of E-cadherin in breast carcinoma: modification of the two-hit hypothesis of tumor suppressor gene. *Oncogene* **20**, 3814-3823 (2001).
284. Come, C., *et al.* Snail and slug play distinct roles during breast carcinoma progression. *Clin Cancer Res* **12**, 5395-5402 (2006).
285. Roy, H.K., Smyrk, T.C., Koetsier, J., Victor, T.A. & Wali, R.K. The transcriptional repressor SNAIL is overexpressed in human colon cancer. *Dig Dis Sci* **50**, 42-46 (2005).
286. Takeno, S., *et al.* E-cadherin expression in patients with esophageal squamous cell carcinoma: promoter hypermethylation, Snail overexpression, and clinicopathologic implications. *Am J Clin Pathol* **122**, 78-84 (2004).
287. Miyoshi, A., *et al.* Snail accelerates cancer invasion by upregulating MMP expression and is associated with poor prognosis of hepatocellular carcinoma. *Br J Cancer* **92**, 252-258 (2005).
288. Sugimachi, K., *et al.* Transcriptional repressor snail and progression of human hepatocellular carcinoma. *Clin Cancer Res* **9**, 2657-2664 (2003).

289. Imai, T.*, et al.* Hypoxia attenuates the expression of E-cadherin via up-regulation of SNAIL in ovarian carcinoma cells. *Am J Pathol* **163**, 1437-1447 (2003).
290. Saito, T.*, et al.* E-cadherin mutation and Snail overexpression as alternative mechanisms of E-cadherin inactivation in synovial sarcoma. *Oncogene* **23**, 8629-8638 (2004).
291. Elloul, S.*, et al.* Snail, Slug, and Smad-interacting protein 1 as novel parameters of disease aggressiveness in metastatic ovarian and breast carcinoma. *Cancer* **103**, 1631-1643 (2005).
292. Martin, T.A., Goyal, A., Watkins, G. & Jiang, W.G. Expression of the transcription factors snail, slug, and twist and their clinical significance in human breast cancer. *Ann Surg Oncol* **12**, 488-496 (2005).
293. Shioiri, M.*, et al.* Slug expression is an independent prognostic parameter for poor survival in colorectal carcinoma patients. *Br J Cancer* **94**, 1816-1822 (2006).
294. Uchikado, Y.*, et al.* Slug Expression in the E-cadherin preserved tumors is related to prognosis in patients with esophageal squamous cell carcinoma. *Clin Cancer Res* **11**, 1174-1180 (2005).
295. Shih, J.Y.*, et al.* Transcription repressor slug promotes carcinoma invasion and predicts outcome of patients with lung adenocarcinoma. *Clin Cancer Res* **11**, 8070-8078 (2005).
296. Yauch, R.L.*, et al.* Epithelial versus mesenchymal phenotype determines in vitro sensitivity and predicts clinical activity of erlotinib in lung cancer patients. *Clin Cancer Res* **11**, 8686-8698 (2005).
297. Thomson, S.*, et al.* Epithelial to mesenchymal transition is a determinant of sensitivity of non-small-cell lung carcinoma cell lines and xenografts to epidermal growth factor receptor inhibition. *Cancer Res* **65**, 9455-9462 (2005).
298. Frederick, B.A.*, et al.* Epithelial to mesenchymal transition predicts gefitinib resistance in cell lines of head and neck squamous cell carcinoma and non-small cell lung carcinoma. *Mol Cancer Ther* **6**, 1683-1691 (2007).
299. Fuchs, B.C.*, et al.* Epithelial-to-mesenchymal transition and integrin-linked kinase mediate sensitivity to epidermal growth factor receptor inhibition in human hepatoma cells. *Cancer Res* **68**, 2391-2399 (2008).
300. Black, P.C.*, et al.* Sensitivity to epidermal growth factor receptor inhibitor requires E-cadherin expression in urothelial carcinoma cells. *Clin Cancer Res* **14**, 1478-1486 (2008).

301. Wang, X., *et al.* Identification of a novel function of TWIST, a bHLH protein, in the development of acquired taxol resistance in human cancer cells. *Oncogene* **23**, 474-482 (2004).
302. Cheng, G.Z., *et al.* Twist transcriptionally up-regulates AKT2 in breast cancer cells leading to increased migration, invasion, and resistance to paclitaxel. *Cancer Res* **67**, 1979-1987 (2007).
303. Li, Q.Q., *et al.* Twist1-mediated adriamycin-induced epithelial-mesenchymal transition relates to multidrug resistance and invasive potential in breast cancer cells. *Clin Cancer Res* **15**, 2657-2665 (2009).
304. Kurrey, N.K., *et al.* Snail and slug mediate radioresistance and chemoresistance by antagonizing p53-mediated apoptosis and acquiring a stem-like phenotype in ovarian cancer cells. *Stem Cells* **27**, 2059-2068 (2009).
305. Kajita, M., McClinic, K.N. & Wade, P.A. Aberrant expression of the transcription factors snail and slug alters the response to genotoxic stress. *Mol Cell Biol* **24**, 7559-7566 (2004).
306. Hoshino, H., *et al.* Epithelial-mesenchymal transition with expression of SNAI1-induced chemoresistance in colorectal cancer. *Biochem Biophys Res Commun* **390**, 1061-1065 (2009).
307. Yang, A.D., *et al.* Chronic oxaliplatin resistance induces epithelial-to-mesenchymal transition in colorectal cancer cell lines. *Clin Cancer Res* **12**, 4147-4153 (2006).
308. Kajiyama, H., *et al.* Chemoresistance to paclitaxel induces epithelial-mesenchymal transition and enhances metastatic potential for epithelial ovarian carcinoma cells. *Int J Oncol* **31**, 277-283 (2007).
309. Shah, A.N., *et al.* Development and characterization of gemcitabine-resistant pancreatic tumor cells. *Ann Surg Oncol* **14**, 3629-3637 (2007).
310. Wang, Z., *et al.* Acquisition of epithelial-mesenchymal transition phenotype of gemcitabine-resistant pancreatic cancer cells is linked with activation of the notch signaling pathway. *Cancer Res* **69**, 2400-2407 (2009).
311. Shi, Y. & Massague, J. Mechanisms of TGF-beta signaling from cell membrane to the nucleus. *Cell* **113**, 685-700 (2003).
312. Siegel, P.M. & Massague, J. Cytostatic and apoptotic actions of TGF-beta in homeostasis and cancer. *Nat Rev Cancer* **3**, 807-821 (2003).
313. Xie, W., *et al.* Alterations of Smad signaling in human breast carcinoma are associated with poor outcome: a tissue microarray study. *Cancer Res* **62**, 497-505 (2002).
314. Massague, J. TGFbeta in Cancer. *Cell* **134**, 215-230 (2008).

315. Huber, M.A., Kraut, N. & Beug, H. Molecular requirements for epithelial-mesenchymal transition during tumor progression. *Curr Opin Cell Biol* **17**, 548-558 (2005).
316. Boyer, B., Roche, S., Denoyelle, M. & Thiery, J.P. Src and Ras are involved in separate pathways in epithelial cell scattering. *EMBO J* **16**, 5904-5913 (1997).
317. Boccaccio, C. & Comoglio, P.M. Invasive growth: a MET-driven genetic programme for cancer and stem cells. *Nat Rev Cancer* **6**, 637-645 (2006).
318. Grotegut, S., von Schweinitz, D., Christofori, G. & Lehembre, F. Hepatocyte growth factor induces cell scattering through MAPK/Egr-1-mediated upregulation of Snail. *EMBO J* **25**, 3534-3545 (2006).
319. Togawa, A.*, et al.* Hepatocyte Growth Factor stimulated cell scattering requires ERK and Cdc42-dependent tight junction disassembly. *Biochem Biophys Res Commun* **400**, 271-277 (2010).
320. Nagai, T.*, et al.* Sorafenib inhibits the hepatocyte growth factor-mediated epithelial mesenchymal transition in hepatocellular carcinoma. *Mol Cancer Ther* **10**, 169-177 (2011).
321. Pan, F.Y.*, et al.* Beta-catenin signaling involves HGF-enhanced HepG2 scattering through activating MMP-7 transcription. *Histochem Cell Biol* **134**, 285-295 (2010).
322. Savagner, P., Yamada, K.M. & Thiery, J.P. The zinc-finger protein slug causes desmosome dissociation, an initial and necessary step for growth factor-induced epithelial-mesenchymal transition. *J Cell Biol* **137**, 1403-1419 (1997).
323. Leroy, P. & Mostov, K.E. Slug is required for cell survival during partial epithelial-mesenchymal transition of HGF-induced tubulogenesis. *Mol Biol Cell* **18**, 1943-1952 (2007).
324. Han, S.U.*, et al.* Modulation of E-cadherin by hepatocyte growth factor induces aggressiveness of gastric carcinoma. *Ann Surg* **242**, 676-683 (2005).
325. Mitra, A.K.*, et al.* Ligand-independent activation of c-Met by fibronectin and alpha(5)beta(1)-integrin regulates ovarian cancer invasion and metastasis. *Oncogene* **30**, 1566-1576 (2011).
326. Sato, M., Shames, D.S. & Hasegawa, Y. Emerging evidence of Epithelial-to-Mesenchymal Transition in lung carcinogenesis. *Respirology* **17**, 1048-1059 (2012).
327. Hung, J.J.*, et al.* Prognostic significance of hypoxia-inducible factor-1alpha, TWIST1 and Snail expression in resectable non-small cell lung cancer. *Thorax* **64**, 1082-1089 (2009).

328. Schmalhofer, O., Brabletz, S. & Brabletz, T. E-cadherin, beta-catenin, and ZEB1 in malignant progression of cancer. *Cancer Metastasis Rev* **28**, 151-166 (2009).
329. Prudkin, L.*, et al.* Epithelial-to-mesenchymal transition in the development and progression of adenocarcinoma and squamous cell carcinoma of the lung. *Mod Pathol* **22**, 668-678 (2009).
330. Bremnes, R.M., Veve, R., Hirsch, F.R. & Franklin, W.A. The E-cadherin cell-cell adhesion complex and lung cancer invasion, metastasis, and prognosis. *Lung Cancer* **36**, 115-124 (2002).
331. Tischler, V.*, et al.* L1CAM protein expression is associated with poor prognosis in non-small cell lung cancer. *Mol Cancer* **10**, 127 (2011).
332. Kase, S.*, et al.* Expression of E-cadherin and beta-catenin in human non-small cell lung cancer and the clinical significance. *Clin Cancer Res* **6**, 4789-4796 (2000).
333. Nakata, S.*, et al.* The methylation status and protein expression of CDH1, p16(INK4A), and fragile histidine triad in nonsmall cell lung carcinoma: epigenetic silencing, clinical features, and prognostic significance. *Cancer* **106**, 2190-2199 (2006).
334. Yanagawa, J.*, et al.* Snail promotes CXCR2 ligand-dependent tumor progression in non-small cell lung carcinoma. *Clin Cancer Res* **15**, 6820-6829 (2009).
335. Hasegawa, Y.*, et al.* Transforming growth factor-beta1 level correlates with angiogenesis, tumor progression, and prognosis in patients with nonsmall cell lung carcinoma. *Cancer* **91**, 964-971 (2001).
336. Kasai, H., Allen, J.T., Mason, R.M., Kamimura, T. & Zhang, Z. TGF-beta1 induces human alveolar epithelial to mesenchymal cell transition (EMT). *Respir Res* **6**, 56 (2005).
337. Shintani, Y., Maeda, M., Chaika, N., Johnson, K.R. & Wheelock, M.J. Collagen I promotes epithelial-to-mesenchymal transition in lung cancer cells via transforming growth factor-beta signaling. *Am J Respir Cell Mol Biol* **38**, 95-104 (2008).
338. Sequist, L.V.*, et al.* Genotypic and histological evolution of lung cancers acquiring resistance to EGFR inhibitors. *Sci Transl Med* **3**, 75ra26 (2011).
339. Salido, M.*, et al.* Cytogenetic characterization of NCI-H69 and NCI-H69AR small cell lung cancer cell lines by spectral karyotyping. *Cancer Genet Cytogenet* **191**, 97-101 (2009).
340. Mirski, S.E., Gerlach, J.H. & Cole, S.P. Multidrug resistance in a human small cell lung cancer cell line selected in adriamycin. *Cancer Res* **47**, 2594-2598 (1987).

341. Whang-Peng, J.*, et al.* A nonrandom chromosomal abnormality, del 3p(14-23), in human small cell lung cancer (SCLC). *Cancer Genet Cytogenet* **6**, 119-134 (1982).
342. Salido, M.*, et al.* Cytogenetic characterization of NCI-H69 and NCI-H69AR small cell lung cancer cell lines by spectral karyotyping. *Cancer Genet Cytogenet* **191**, 97-101 (2009).
343. Lutterbach, B.*, et al.* Lung cancer cell lines harboring MET gene amplification are dependent on Met for growth and survival. *Cancer Res* **67**, 2081-2088 (2007).
344. Christensen, J.G.*, et al.* A selective small molecule inhibitor of c-Met kinase inhibits c-Met-dependent phenotypes in vitro and exhibits cytoreductive antitumor activity in vivo. *Cancer Res* **63**, 7345-7355 (2003).
345. Travis, W.D. Update on small cell carcinoma and its differentiation from squamous cell carcinoma and other non-small cell carcinomas. *Mod Pathol* **25 Suppl 1**, S18-30 (2012).
346. Xie, L.*, et al.* Activation of the Erk pathway is required for TGF-beta1-induced EMT in vitro. *Neoplasia* **6**, 603-610 (2004).
347. Tanizaki, J.*, et al.* MET Tyrosine Kinase Inhibitor Crizotinib (PF-02341066) Shows Differential Antitumor Effects in Non-small Cell Lung Cancer According to MET Alterations. *J Thorac Oncol* **6**, 1624-1631 (2011).
348. Christensen, J.G.*, et al.* Cytoreductive antitumor activity of PF-2341066, a novel inhibitor of anaplastic lymphoma kinase and c-Met, in experimental models of anaplastic large-cell lymphoma. *Mol Cancer Ther* **6**, 3314-3322 (2007).
349. Li, X.*, et al.* Intrinsic resistance of tumorigenic breast cancer cells to chemotherapy. *J Natl Cancer Inst* **100**, 672-679 (2008).
350. Sayan, A.E.*, et al.* SIP1 protein protects cells from DNA damage-induced apoptosis and has independent prognostic value in bladder cancer. *Proc Natl Acad Sci U S A* **106**, 14884-14889 (2009).
351. Sharma, S.V.*, et al.* A chromatin-mediated reversible drug-tolerant state in cancer cell subpopulations. *Cell* **141**, 69-80 (2010).
352. Voulgari, A. & Pintzas, A. Epithelial-mesenchymal transition in cancer metastasis: mechanisms, markers and strategies to overcome drug resistance in the clinic. *Biochim Biophys Acta* **1796**, 75-90 (2009).
353. Witta, S.E.*, et al.* Restoring E-cadherin expression increases sensitivity to epidermal growth factor receptor inhibitors in lung cancer cell lines. *Cancer Res* **66**, 944-950 (2006).

354. Comijn, J.*, et al.* The two-handed E box binding zinc finger protein SIP1 downregulates E-cadherin and induces invasion. *Mol Cell* **7**, 1267-1278 (2001).
355. Mani, S.A.*, et al.* The epithelial-mesenchymal transition generates cells with properties of stem cells. *Cell* **133**, 704-715 (2008).
356. Corso, S.*, et al.* Silencing the MET oncogene leads to regression of experimental tumors and metastases. *Oncogene* **27**, 684-693 (2008).
357. Gutekunst, M.*, et al.* Cisplatin hypersensitivity of testicular germ cell tumors is determined by high constitutive noxa levels mediated by oct-4. *Cancer Res* **73**, 1460-1469 (2013).
358. Pleasance, E.D.*, et al.* A small-cell lung cancer genome with complex signatures of tobacco exposure. *Nature* **463**, 184-190 (2010).
359. Rudin, C.M.*, et al.* Comprehensive genomic analysis identifies SOX2 as a frequently amplified gene in small-cell lung cancer. *Nat Genet* **44**, 1111-1116 (2012).
360. Peifer, M.*, et al.* Integrative genome analyses identify key somatic driver mutations of small-cell lung cancer. *Nat Genet* **44**, 1104-1110 (2012).
361. Kwak, E.L.*, et al.* Anaplastic lymphoma kinase inhibition in non-small-cell lung cancer. *N Engl J Med* **363**, 1693-1703 (2010).
362. Arriola, E.*, et al.* MET phosphorylation predicts poor outcome in small cell lung carcinoma and its inhibition blocks HGF-induced effects in MET mutant cell lines. *Br J Cancer* **105**, 814-823 (2011).
363. Benedettini, E.*, et al.* Met activation in non-small cell lung cancer is associated with de novo resistance to EGFR inhibitors and the development of brain metastasis. *Am J Pathol* **177**, 415-423 (2010).
364. Boland, J.M.*, et al.* MET and EGFR Mutations Identified in ALK-Rearranged Pulmonary Adenocarcinoma: Molecular Analysis of 25 ALK-Positive Cases. *J Thorac Oncol* (2013).
365. Soltermann, A.*, et al.* Prognostic significance of epithelial-mesenchymal and mesenchymal-epithelial transition protein expression in non-small cell lung cancer. *Clin Cancer Res* **14**, 7430-7437 (2008).
366. Vendrell, J.A.*, et al.* ZNF217 is a marker of poor prognosis in breast cancer that drives epithelial-mesenchymal transition and invasion. *Cancer research* **72**, 3593-3606 (2012).
367. Ogunwobi, O.O. & Liu, C. Hepatocyte growth factor upregulation promotes carcinogenesis and epithelial-mesenchymal transition in hepatocellular carcinoma via Akt and COX-2 pathways. *Clin Exp Metastasis* **28**, 721-731 (2011).

368. Zhou, B.B., *et al.* Tumour-initiating cells: challenges and opportunities for anticancer drug discovery. *Nature reviews. Drug discovery* **8**, 806-823 (2009).
369. Belfiore, A., *et al.* Negative/low expression of the Met/hepatocyte growth factor receptor identifies papillary thyroid carcinomas with high risk of distant metastases. *J Clin Endocrinol Metab* **82**, 2322-2328 (1997).
370. Qian, C.N., *et al.* Met protein expression level correlates with survival in patients with late-stage nasopharyngeal carcinoma. *Cancer research* **62**, 589-596 (2002).
371. Tuynman, J.B., Lagarde, S.M., Ten Kate, F.J., Richel, D.J. & van Lanschot, J.J. Met expression is an independent prognostic risk factor in patients with oesophageal adenocarcinoma. *Br J Cancer* **98**, 1102-1108 (2008).
372. Gupta, P.B., *et al.* Identification of selective inhibitors of cancer stem cells by high-throughput screening. *Cell* **138**, 645-659 (2009).
373. Li, Y., *et al.* c-Met signaling induces a reprogramming network and supports the glioblastoma stem-like phenotype. *Proceedings of the National Academy of Sciences of the United States of America* **108**, 9951-9956 (2011).
374. De Bacco, F., *et al.* The MET oncogene is a functional marker of a glioblastoma stem cell subtype. *Cancer Res* **72**, 4537-4550 (2012).
375. Sequist, L.V., *et al.* Genotypic and histological evolution of lung cancers acquiring resistance to EGFR inhibitors. *Sci Transl Med* **3**, 75ra26 (2011).
376. Irizarry, R.A., *et al.* Summaries of Affymetrix GeneChip probe level data. *Nucleic Acids Res* **31**, e15 (2003).
377. Smyth, G.K. Linear models and empirical bayes methods for assessing differential expression in microarray experiments. *Stat Appl Genet Mol Biol* **3**, Article3 (2004).
378. H. Bengtsson, K.S., J. Bullard, K. Hansen. aroma.affymetrix: A generic framework in R for analyzing small to very large Affymetrix data sets in bounded memory. in *Tech Report #745, Department of Statistics, University of California, Berkeley, February 2008*.
379. Moncho-Amor, V., *et al.* DUSP1/MKP1 promotes angiogenesis, invasion and metastasis in non-small-cell lung cancer. *Oncogene* **30**, 668-678 (2011).
380. McShane, L.M., *et al.* Reporting recommendations for tumor marker prognostic studies. *J Clin Oncol* **23**, 9067-9072 (2005).

PUBLICATIONS

PUBLICATIONS PRESENTED IN THIS PhD THESIS

Part of the work presented in this PhD thesis was published in:

Authors: Cañadas I, Rojo F, Taus A, Arpí O, Arumí-Uría M, Dómine M, Bellosillo B, Mojal S, García de Herreros A, Rovira A, Albanell J, Arriola E.
Title: Targeting Epithelial to Mesenchymal Transition with MET inhibitors reverts chemoresistance in Small Cell Lung Cancer.
Journal: Not determined (submitted).

Authors: Arriola E*, **Cañadas I***, Arumí M, Domine M, López-Vilariño JA, Arpí O, Salido M, Menéndez S, Grande E, Hirsch FR, Serrano S, Bellosillo B, Rojo F, Rovira A, Albanell J.
*equal contribution
Title: MET phosphorylation predicts poor outcome in small cell lung carcinoma and its inhibition blocks HGF-induced effects in MET mutant cell lines.
Journal: Br J Cancer 2011; 105(6): 814-823.

Authors: Cañadas I, Rojo F, Arumí M, Rovira A, Albanell J, Arriola E.
Title: C-MET as a new therapeutic target for the development of novel anticancer drugs.
Journal: Clin Transl Oncol 2010; 12(4): 253-260.

Authors: Salido M, Arriola E, Carracedo A, **Cañadas I**, Rovira A, Espinet B, Rojo F, Arumí M, Serrano S, Albanell J, Solé F.
Title: Cytogenetic characterization of NCI-H69 and NCI-H69AR small cell lung cancer cell lines by spectral karyotyping.
Journal: Cancer Genet Cytogenet 2009; 191(2): 97-101.

Authors: Arriola E, **Cañadas I**, Arumí M, Rojo F, Rovira A, Albanell J.
Title: Genetic changes in small cell lung carcinoma.
Journal: Clin Transl Oncol 2008; 10(4): 189-197.

PUBLICATIONS NOT PRESENTED IN THIS PhD THESIS

I have also participated in the following publications during the thesis research period:

Authors: Salido M, Pijuan L, Galvan AB, Gimeno J, **Cañadas I**, Rodríguez M, Rojo F, Albanell J, Solé F, Arriola E.
Title: ALK status in a primary lung tumour and metachronous metastases.
Journal: Histopathology 2012; 60(5): 843-845.

Authors: Salido M, Pijuan L, Martínez-Avilés L, Galvan AB, **Cañadas I**, Rovira A, Zanui M, Martínez A, Longarón R, Solé F, Serrano S, Bellosillo B, Wynes MW, Albanell J, Hirsch FR, Arriola E.
Title: Increased ALK Gene Copy Number and Amplification are Frequent in Non-small Cell Lung Cancer.
Journal: J Thorac Oncol 2011; 6(1): 21-27.

Authors: Montagut C, Iglesias M, Arumí M, Bellosillo B, Gallén M, Martínez-Fernández A, Martínez-Avilés L, **Cañadas I**, Dalmases A, Moragon E, Lema L, Serrano S, Rovira A, Rojo F, Bellmunt J, Albanell J.
Title: Mitogen-activated protein kinase phosphatase-1 (MKP-1) impairs the response to anti-epidermal growth factor receptor (EGFR) antibody cetuximab in metastatic colorectal cancer patients.
Journal: Br J Cancer 2010; 102(7): 1137-1144.